Improved Methods for Structural Wind Engineering

Graham Anthony Knapp, M.Eng M.Sc (Res)

Thesis submitted to the University of Nottingham for the degree of Doctor of Philosophy

October 2007

Abstract

This thesis describes research examining the use of computational fluid dynamics (CFD) in structural wind engineering. It looks in particular at steady and unsteady RANS simulations and Detached Eddy Simulation and their use in the calculation of structural loads on static bluff building structures. Previous research across structural wind engineering and CFD is reviewed and critically examined with respect to structural engineering. CFD simulations are performed and compared with published flow data for simple cubes. Loading studies are performed for a complex building and the results compared with wind tunnel studies used in the structural design of the building.

Some important local pressure and design forces are found to be highly dependent upon simulation parameters including the spatial discretisation used. In particular, local forces and pressures in the separation and reattachment regions cannot be consistently predicted. Standard industrial CFD methods for improving simulation accuracy including mesh refinement and increasing discretisation accuracy do not necessarily improve prediction of structural loads and explanations are given for this. Results for overall structural loads are found to be sufficiently settled and repeatable for comparison with experimental values, while some local forces and pressures cannot be predicted consistently.

Recommendations are made for the appropriate use of CFD in structural engineering and for the future development of CFD techniques. In particular, improved representation of multiple turbulent scales in the free stream and separation regions is required.

Acknowledgements

I would like to take this opportunity to put my thanks to numerous people into print.

Firstly, thanks to my supervisors, colleagues and friends at the University of Nottingham. In particular Nigel Wright, John Owen, David Hargreaves and Hervé Morvan for their academic support. Thanks also to my fellow students in the CFD group, plus Rob, Adam, Dilan and Jo.

I must also thank all at Buro Happold, who provided industrial experience and insight throughout, particularly Garry Palmer, Bernardo Vazquez and Paul Shepherd. Thanks go also to BMT Fluid Mechanics Ltd and Silsoe Research Institute for providing data and advice.

Looking further back, I would not have embarked on this venture without the sense of inquiry inspired by Ian Burgess of Sheffield University.

And endless support has come throughout from my family, friends and most of all from my partner Gwenaëlle.

Contents

Figures

Tables

1. Introduction

1.1. Background

Wind engineering is a diverse field, drawing on the skills of meteorologists, structural and mechanical engineers, physicists and aerodynamicists, amongst others, to predict the effects of wind on the built environment and its inhabitants. Pedestrian comfort, pollutant dispersal, structural loading and dynamic behaviour all fall within the field of wind engineering. This work is concerned with the interface between wind action and structural response, structural wind engineering.

Traditional wind engineering tools include meteorological records, full-scale testing and model-scale testing in a wind tunnel. In recent decades interest has grown in the use of computational fluid dynamics (CFD) in wind engineering. This computational tool has been developed largely for use in the aerospace and motor industries where it is used to predict the flow of air around aircraft, involving mostly attached flow over streamlined bodies with relatively small areas of separation and turbulent length scales smaller than the body under investigation.

1.2. Identification of problem

Wind engineering for the built environment involves complex turbulent flow around bluff bodies. It involves areas of separation which may be larger than the bluff body and turbulent length scales which can be many times the body size. As with wind tunnel testing, when CFD technology was first applied here, much work was required to achieve an acceptable level of accuracy. Thus far, most of this work has concentrated on the prediction of mean wind speeds for the purposes of human comfort and the dispersion of atmospheric pollution. Far less work has been done on the more challenging problem of predicting the fluctuating surface pressures on buildings.

Where pressures have been predicted, they are generally considered as isolated point values and compared with point values from an experiment.

This neglects the importance of area and time-averaged forces used in structural design and can place great importance on local detailed effects which may not be significant to the design.

1.3. Aims and Objectives

This document describes a research project investigating the use of CFD in structural wind engineering. The purpose of this research is to critically assess the extent to which CFD can be used in predicting wind loads on structures. Whereas previous studies have concentrated on predicting wind speeds and comparing the predictions with full-scale results and wind tunnel tests, this study looks at what parameters are important in predicting wind effects on structures. In particular, unsteadiness in the flow around bluff bodies is investigated and the implications for CFD modelling of this unsteadiness is demonstrated.

It is necessary to compare the type of information given by different methods and how much of this information is required for different types of study. For instance, RANS methods will give time-averaged results while LES methods and wind tunnel studies will give fluctuating values. The strengths and weaknesses of each method must be assessed qualitatively and, where possible, quantitatively. To achieve this, the following aims were set:

1. To compare CFD results for simple cubes with both full-scale and model-scale test results, assessing the velocity and pressure results in terms of their effect on the accuracy of prediction of structural loads.

2. Based on the result of these studies, to run CFD simulations for a complex building and comparing these with the results of model-scale testing in a boundary layer wind tunnel.

3. To critically assess the ability of CFD simulation to predict structural loads for static bluff bodies relative to traditional design tools including codes of practice and wind tunnels.

1.4. Thesis structure

This thesis is structured as follows:

Chapter 1 reviews structural wind engineering practice and research, boundary layer wind theory and experimental and computational methods. The aim is to provide the reader with sufficient information to understand the subsequent results and discussion.

Chapter 2 discusses the computational techniques used in this research. Previous studies are critically discussed to determine which methods should be adopted in this research and the key parameters investigated are highlighted.

Chapter 3 presents initial results for a model-scale cube in a channel and discusses these with reference to the Silsoe 6m Cube results and with regard to the application of CFD to structural engineering

Chapter 4 presents results for the Silsoe 6m Cube and discusses them in the context of structural design. The limitations of these studies are discussed and areas of interest highlighted. Investigations are made into the source of the unstable asymmetric flow observed.

Chapter 5 discusses a series of CFD simulations representing a complex full-scale building, the new Ascot Grandstand. The wind tunnel tests used in the structural design of the building are discussed and the results interpreted. Details are given of the new CFD simulations and the results compared with the wind tunnel output both qualitatively and quantitatively.

Chapter 6 discusses the implications of these 3 studies for the use of CFD in structural engineering. Conclusions are drawn in section 7.3 and recommendations for future work are made in Chapter 8, including suggestions for the development of CFD techniques, software improvements and ways of using CFD data in design.

2. Literature Review

This chapter gives an introduction to the subject of computational wind engineering and of structural wind engineering more generally. Relevant background theory in atmospheric flow, structural engineering and CFD is discussed. A history of the subject of structural wind engineering is presented and a critical examination is made of the key literature relating to this project.

2.1. Background

Air flow over man made structures involves complex flow patterns. Flow usually separates from the surface, creating zones of recirculating air. These flow patterns are generally unsteady and as they repeatedly form and break down, vortices are shed from the structure. On a larger scale, these unsteady vortices combine and superpose to create the complex turbulent environment in which we spend our lives and construct our environment. This section discusses the source of these fluctuations and ways to describe and interpret them.

2.1.1. Boundary Layer Flow

Turbulence can be viewed as an apparently random motion of a fluid, superimposed on the average fluid motion. In wind engineering terms this fluctuation can be described as gusting and may exist in a range of sizes and durations, from large sustained gusts to small eddies.

Atmospheric turbulence is generated by the shearing of air against a rough surface and unstable flow and vortex shedding from structures and obstacles on the ground. This turbulence is transmitted upwards through shear (Reynolds stresses) and vertical movement of air and then transported downwind so the turbulence develops first on the surface and then progressively deeper into the flow. The thickness of this boundary layer and the intensity of the turbulence within it depend upon the velocity and viscosity of the fluid and on the roughness of the surface.

In the United Kingdom (UK), by the time any weather system has developed enough to cause strong winds, the boundary layer will be highly developed with a thickness of several kilometres.

In many other parts of the world, particularly in tropical climates, thunderstorms and tornadoes both cause damaging winds that do not fit into the pattern of atmospheric boundary layer flow. Thunderstorms in the UK rarely cause significant structural damage and although the phenomenon of stingjets is now being investigated in the UK (Browning 2004), it is not yet clear whether these cause significant structural damage, nor has guidance been developed on how to design for their effects. Such weather systems are outside the scope of this work.

In the atmospheric boundary layer, large-scale turbulence is formed by atmospheric instabilities and by flow around bluff bodies. These large vortices generate smaller vortices around them and so on. The large scale eddies feed energy into the smaller ones in an 'energy cascade' with the size of the smallest eddies depending upon the following relationship:

$$\eta = \left[\frac{\nu^3}{\varepsilon}\right]^{\frac{1}{4}} \qquad \textit{[equation 2-1]}$$

Where:

η = Kolmogorov length scale, the ratio of the largest eddy size to the smallest eddy size

ν = Kinematic viscosity

ε = Rate of energy dissipation

The rate of energy dissipation, ε scales as u^3/L where L is the length scale, meaning that the Kolmogorov length scale is proportional to the Reynolds number raised to the power 9/4. For typical wind engineering flows with Reynolds numbers in the range 10^6 and above this implies a need for more than 10^{13} grid points to fully resolve the turbulent structures.

Although turbulence has a strong random element, it contains identifiable coherent structures. Recent work (e.g. Sterling et al. 2005) has

attempted to give a fuller understanding of the structure of turbulent eddies with the aim of developing models of vortices for use in engineering design. While a wide range of eddy structures has been identified, the significance of this specifically for structural design has yet to be investigated.

Log Law Profile

The atmospheric boundary layer in the UK is approximately 2.5km deep as shown in Figure 2-1 and changes dependent upon the wind conditions and the roughness of the ground beneath. Typical boundary layers are shown here for open country and town terrain as well as the transition between the two. The transition typically takes many hundreds of kilometres to propagate through the entire height of the boundary layer, so the boundary layer at most sites is in a period of transition between two or more equilibrium profiles.

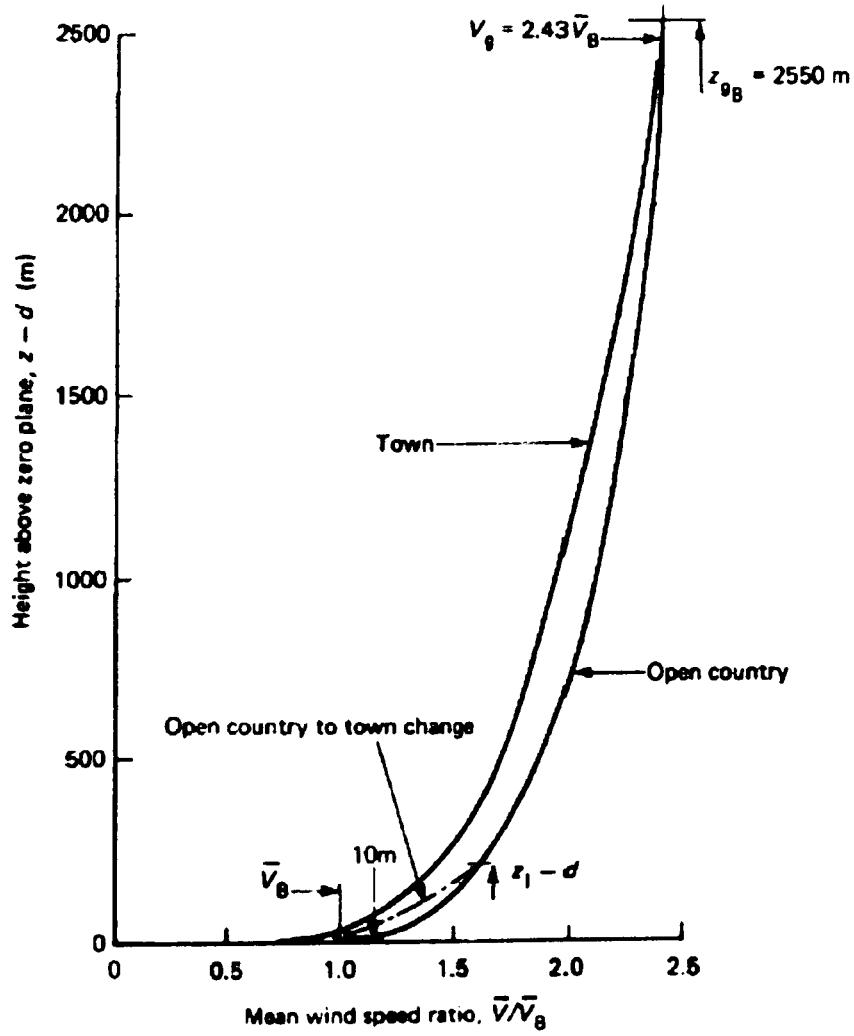

Figure 2-1: The turbulent boundary layer in open country and towns (Cook 1985)

The boundary layer can be closely approximated with a log-function in the region near to the ground with a profile as follows:

$$\overline{V} = \frac{1}{\mathrm{K}} u_* \ln[(z-d)/z_0] \qquad \textit{[equation 2-2]}$$

Where:

K = von Karman's constant, equal to 0.40

$\overline{V}$ = Mean velocity at height z

u_* = friction velocity

z = Height above zero plane

d = Height of zero plane

z_0 = Aerodynamic roughness length

This log law approximation becomes less accurate at altitudes of more than about 100-200m, where a power law is more appropriate, but the log law is suitable for all but the tallest of buildings. The profile is dependent upon the ground roughness, expressed in terms of the aerodynamic roughness height, z_0, measured in metres.

Velocity and turbulence vary considerably through the boundary layer and a number of distinct areas can be identified. For idealised surfaces with homogenous roughness, very near to the ground the flow velocity is very low and viscous forces dominate. There is very little vertical velocity in this layer of flow named the 'laminar sub-layer'. Above this layer is the log region described above, containing turbulence on a great many scales. The laminar sub-layer is important to the understanding of near-wall behaviour and turbulence modelling, discussed in section 2.2.

For real urban surfaces, where the roughness consists of buildings and other obstructions much thicker than the laminar sub-layer, the majority of the turbulence is generated in the unsteady separation regions around these obstructions.

The typical approach to dealing with very rough surfaces is to assume that the point of zero velocity is displaced upwards from the ground. This is represented by the zero plane of height d in [equation 2-2].

The size of the largest eddies may be the full depth of the boundary layer, extending towards the gradient height.

Deaves and Harris Model

The log law approximation applies to ground with constant roughness but cannot describe the change in velocity profile from areas of one surface roughness to another. The Deaves and Harris model (Deaves and Harris 1978) was developed to deal with this problem and allows the calculation of velocity profiles downwind of changes in roughness profile. This is essential in cities where a full transition from the country profile to the city profile has not generally been achieved.

Within 300m of the surface the velocity profile is given by:

$$\overline{V} = \frac{1}{K} u_* \left\langle \ln[(z-d)/z_0] + 5.75(z/d)/z_g \right\rangle \qquad \textit{[equation 2-3]}$$

Where

z_g is the gradient height, which varies between approximately 1km and 2km around the earth.

This is the model adopted by the Engineering Sciences Data Unit (ESDU 1993) and is widely used in wind engineering for temperate regions around the world.

Turbulence Spectra

As has been commented, atmospheric turbulence exists at a huge range of length scales, from large weather systems to brief gusts and vortices. This variation in length (and therefore time) scales can be represented with the spectrum of turbulence, displaying the relative turbulent content

at different frequencies. A typical plot is shown in Figure 2-2. The large macrometeorological peak corresponds to large scale weather systems with a period of a few days, with a smaller peak representing night/day effects (around 12 hours). The micrometeorological peak refers to boundary layer turbulence, generated by atmospheric instability and roughness effects.

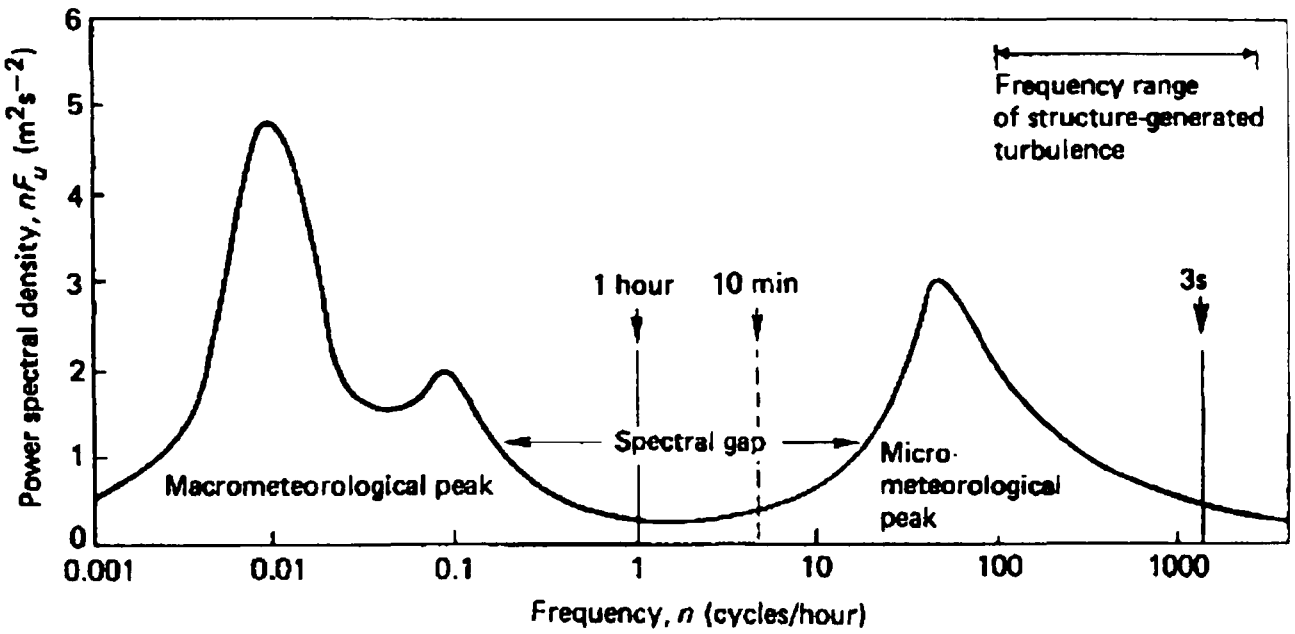

Figure 2-2, Wind spectrum, after van der Hoven, from (Cook 1985)

The spectral gap between these two sources of turbulence allows separate treatment of weather conditions and atmospheric turbulence. Weather conditions are usually considered from meteorological records, generally recorded in terms of 10-60 minute averages. The atmospheric turbulence is more complex, itself containing a huge range of length scales, with a combination of coherent 2D and 3D structures and higher frequency isotropic turbulence.

Recent work by Richards et al. (2004) examines the treatment of this atmospheric turbulence in wind tunnels and CFD and recommends that:

- Turbulence spectra should be normalised by using the mean velocity and that in general plotting $nS(n)/U^2$ against reduced frequency $f=nz/U$ should be preferred over $nS(n)/\sigma^2$ against nL_{ux}/U, as the latter approach obscures differences, where:

n = frequency

U = mean velocity

z = height above ground

σ = standard deviation of turbulent fluctuations

L_{ux} = streamwise turbulent length scale

- Care should be taken to model the mid to high frequency levels even if this means that the turbulence intensity and integral length scales are less than the full-scale value.

In other words, the isotropic high frequency turbulence should be modelled while the lower frequency 2D and 3D turbulence should be simulated directly or considered by other means. The paper suggests that the quasi-steady assumption is appropriate for this lower frequency turbulence.

2.1.2. Forces and Pressures on Structures

As air moves past ground-based structures it generates pressures across them, generally causing positive relative pressure on the windward surface(s) and negative relative pressure on the sides and leeward surfaces. Non-streamlined or 'bluff' bodies create complex flow structures resulting in the separation of the air flow from the surface of the body and the generation of one or more areas of circulating flow. These flows will be altered by the motion of the turbulent air past the body and may be unstable in themselves, giving rise to constantly varying pressures and forces.

The flow structures and therefore the pattern of pressures across the body will be dependent on the oncoming turbulence and therefore even predicting the mean forces on a building requires an understanding of the magnitude, scales and structures of turbulence in the flow and their significance.

2.1.3. Aerodynamic Phenomena

Aerodynamics covers all classes of dynamic air movement, including gusting of winds and flow instability around bluff bodies. Aeroelasticity describes the interaction between fluid and structure and is particularly significant in the case of large structures with a high degree of flexibility. Long span bridges, membrane structures and tall buildings are all examples of buildings where aeroelastic effects are likely to be a significant design consideration.

Aerodynamic phenomena can be divided into 3 classes, described below. The first one relates to externally driven dynamic loading while the latter two relate to true aeroelastic phenomena:

Extraneously Induced Excitation

This class of phenomena covers varying or periodic loading from an external source, commonly called "buffeting". This includes:

- Atmospheric turbulence– Inherent unsteadiness of the airflow approaching the structure.
- Vortices shed from identifiable upstream structures or terrain features. This will generally be present at a smaller range of frequencies than the above but may be highly coherent in time and space.

Instability-Induced Excitation

This covers unstable flow around the structure and includes vortex shedding from the structure. This is a particular problem for long span bridges, which often generate vortices as wind blows across the deck. For bluff bodies this includes body-generated turbulence created in the separation zones to the sides and rear of the structure.

Movement-Induced Excitation

This third classification covers fluid forces caused by deflection of the body, typically involving a feedback effect between structural movement and wind loads. It includes the following:

- Galloping, or cross-wind deflection. This can be seen in cables supporting suspension and cable-stay bridges, and has often been observed following ovalisation of the cross-section due to ice formation. It has not been observed for bridge decks or other large engineering structures.

- Flutter. This can occur in aerofoils when the torsional and translational modes of vibration have similar frequencies and are coupled, although for bridges it mainly involves the torsional mode. Flutter was responsible for the famous collapse of the Tacoma Narrows Bridge (Bilah and Scanlan 1991).

This third class of unsteady phenomena is in practice only seen for highly flexible structures such as long-span suspension bridges, cables, masts and tall buildings. For the type of low bluff building considered in this study we are only concerned with the first two classes of unsteady flow.

2.2. Computational Fluid Dynamics

Computational Fluid Dynamics (CFD) has developed with the decreasing cost and increasing power of computer processing, as well as developments in the algorithms and software used. The technique involves the discretisation of a fluid into a continuous array of smaller volumes bounded by a set of known conditions and the application of a form of the Navier-Stokes Equations for fluid flow. The most commonly used techniques are described below. More detail is given on all the techniques by Versteeg and Malalaskera (1995) and Ferziger and Peric (2002).

2.2.1. Direct Numerical Simulation

The purest form of CFD is the direct solution of the Navier-Stokes equations. The fluid domain is divided into volume elements, and the Navier-Stokes (N-S) equations written for each element. To accurately model all of the turbulent effects, the size of the elements must be smaller than the smallest of the turbulent eddies in the flow. They must therefore be smaller than the Kolmogorov length scale, η. In practice this means that Direct Numerical Simulation (DNS) is only possible for small scale simulations with relatively low Reynolds numbers. Even with current advances in computer power it will be many decades or centuries before DNS will be possible for the modelling of the smallest of practical wind engineering problems.

2.2.2. Turbulence Modelling

For practical wind engineering problems it is necessary to simplify the flow using elements that are larger than the smallest turbulent eddies, and to artificially model the effects of some or all of the turbulence.

RANS Models

One method is to simulate the mean fluid flow using the time-averaged versions of the Navier Stokes equations, the Reynolds Averaged Navier Stokes (RANS) equations.

Time-averaging removes the turbulent terms but introduces an extra set of terms to the N-S equations. This means that the RANS equations cannot be solved directly and some extra equations are needed to describe the extra terms. A large number of methods exist for this, with industrial practice generally favouring two-equation models such as the RNG k-ε formulation (Easom 2000). The Shear Stress Transport (SST) k-ω model (Menter 1993) is gaining popularity due to its greater accuracy in predicting the onset of separation under adverse pressure gradients but convergence can be hard to achieve with this model. Academic discussion continues over which models are most appropriate for wind engineering

problems (Franke et al. (2004), Miles and Westbury (2002), Oliveira and Younis (2000)).

In the transient or unsteady RANS (URANS) formulation, time-dependent terms are retained, allowing transient simulations to be run predicting longer-term variations in the flow.

Large Eddy Simulation (LES)

Large eddy simulation uses the spatially averaged Navier-Stokes equations. The full treatment is described in some detail by Layton (2002). The method involves resolving the domain in sufficient detail to simulate the larger eddies directly whilst modelling the effects of small-scale turbulence. This clearly involves a transient simulation, whilst resolving the eddies requires a large number of cells. To obtain settled (stationary) mean and standard deviation point pressure values from the transient simulation requires a very large number of timesteps, typically of the order of 10,000 steps for published studies of bluff body flows. This makes the LES method very computationally expensive in comparison with RANS methods.

An advantage of LES over RANS methods is that as the grid is refined and more turbulent scales are directly represented the solution approaches the strict DNS solution. Therefore grid refinement studies should show whether the results have reached an acceptable level of accuracy. However as discussed above it is not possible to come close to this level of refinement for practical wind engineering problems.

Furthermore, refining the grid in an LES simulation changes the filter scale for direct simulation of turbulence resulting in the direct simulation of smaller turbulent scales. Grid refinement therefore alters what is being modelled and this can obscure or counter any improvement in numerical accuracy from the finer grid.

The process of averaging out turbulent scales smaller than the grid size again introduces extra terms in the Navier-Stokes equations and closure in this case is achieved via an eddy-viscosity model. The most common of

these is the Smagorinsky model, although a number of other models have been proposed.

Through this more accurate treatment of turbulence, LES simulates a portion of the range of turbulent frequencies involved. In terms of structural loads this translates into some of the range of gust durations, allowing more accurate treatment of peak wind speeds than that allowed by RANS modelling. This requires a more detailed simulation of the oncoming atmospheric boundary layer, accounting for the full-scale turbulence spectrum and the presence of coherent structures in the oncoming flow, a topic discussed by (Thomas and Williams 1999) who propose that CFD practitioners should develop a library of standard atmospheric flows generated by LES simulation of an empty domain with realistic roughness elements.

Detached Eddy Simulation (DES)

The detached eddy simulation method (Spalart et al. 1997) is a combination of the RANS and LES methods, intended to combine useful features from both. The simpler RANS equations are used to simulate the majority of the fluid flow, while the grid is refined and a more accurate LES method is used in regions of separation. As with most CFD methods, DES was developed in the field of aeronautics. In aeronautical flows it is particularly appropriate as the majority of the flow field is considered to be laminar, with attached flow around much of the aeroplane and small zones of separation which can be resolved with the LES portion. The method does not yet appear to have been applied to buffeting of bluff-bodies in wind engineering, where the entire flow field is highly turbulent, but may prove useful in predicting flow in the separation and wake regions. It could be particularly useful where one structure is subject to buffeting in the wake of another structure.

Where the cell size is smaller than the turbulent eddy scale, predicted by the RANS model, the solution switches to LES. Where this is not the case, the RANS model is employed.

The DES method has been investigated for surface-mounted cubes (Schmidt and Thiele 2002), investigating flow speeds and temperature (but not surface pressures) for a single cube in laminar flow (Lyn et al. 1995) and a series of cubes, generating turbulent flow (Meinders 1998). In each case, comparisons were made between experimental results and RANS, LES and DES simulations.

The case of a single cube used a coarse approximation of the spanwise behaviour, in one case using only 2 grid points in the spanwise direction, increasing to 20 for other studies. This clearly limits the ability of the method to predict 3-D flow and prevents resolution of turbulent eddies in the spanwise direction. Given that turbulence is a fully three-dimensional phenomenon with a high degree of interaction between turbulent eddies in all three directions, great care must be taken if one dimension is to be ignored. The paper did not comment on the possible effects of this assumption.

The multiple-cube experiments are illustrated in Figure 2-3 and consisted of a series of cubes in initially laminar oncoming flow with flow velocities measured using Laser Doppler Velocimetry. The simulations used periodic boundary conditions so that only one cube was simulated and the outlet boundary condition was applied as the inlet boundary condition for the next iteration. It was noted that insufficient iterations were used to obtain settled time-averaged statistics.

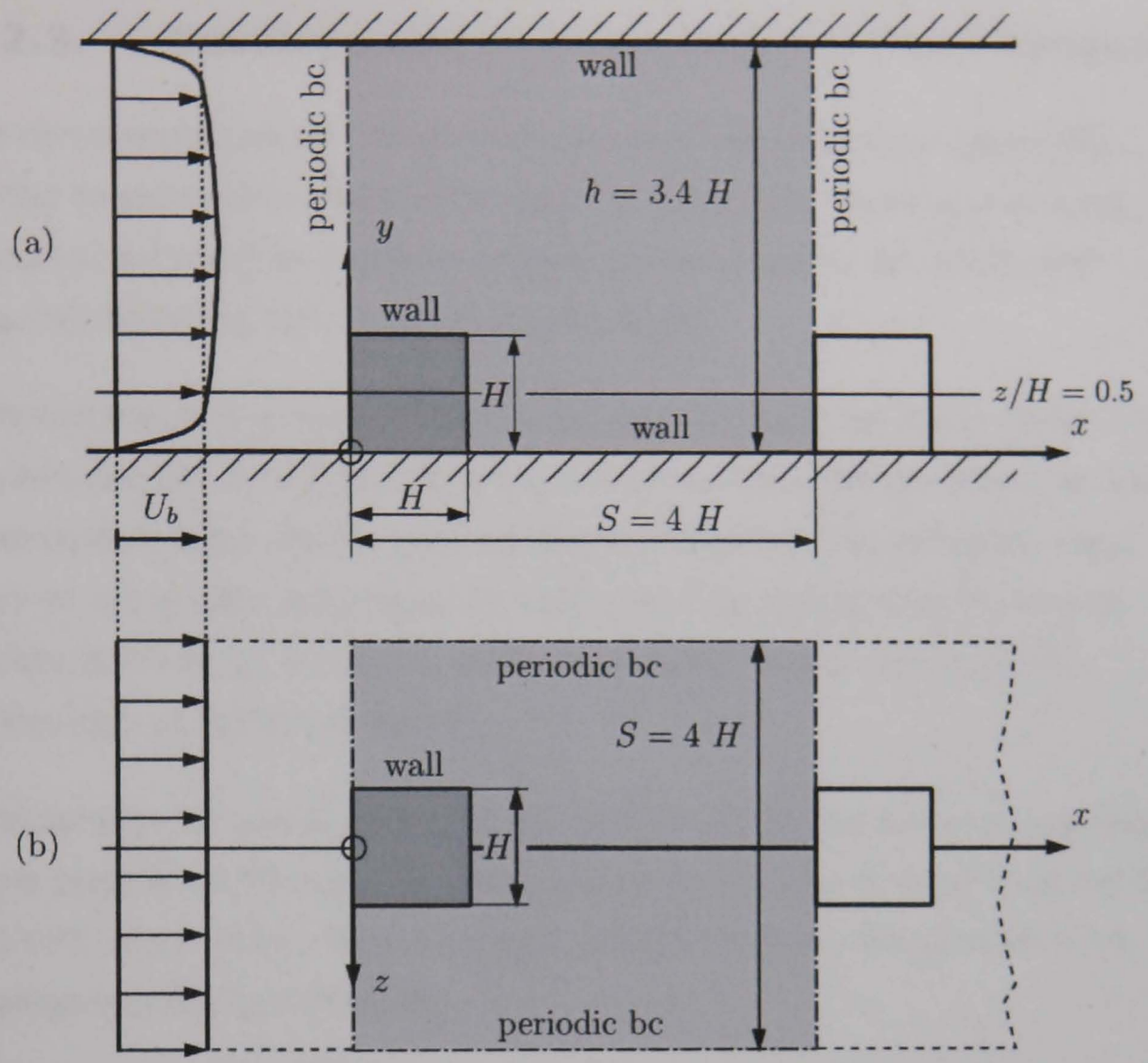

Figure 2-3 Experimental and computational setup for flow over an array of cubes (Schmidt and Thiele 2002)

The authors concluded that DES has a great deal of potential in modelling external flows as it allows RANS methods to be used in the near-wall region and in the laminar flow region, with LES employed in the separation and wake regions. This conclusion would not hold for complex external flows in cities, in which the majority of the flow is highly complex and significantly affected by surrounding buildings. The method may be more useful in the case of large buildings, where the effects of neighbouring buildings are less important, and flow instability due to the building is important. This would include long-span bridges and tall buildings subject to flutter and/or galloping, as well as investigations into the effect of one structure on other downstream structures.

2.3. Development of Computational Fluid Dynamics

The commercial use of CFD software in wind engineering is generally limited to examining mean wind speed at pedestrian level and around balconies for comfort modelling, grass growth studies for stadia and thermal modelling for buoyancy-driven flows.

In structural engineering, CFD may be used to examine the general wind environment around a building: the atmospheric boundary layer, as well as to complement wind tunnel modelling. Engineers have rightly been wary of using CFD technology for safety-critical issues such as overall structural loads on a building and a number of issues remain to be addressed, as described below.

Ferziger gives a useful review of the factors of interest to wind engineers more generally and the differences between CFD use in wind engineering and CFD use in other fields (Ferziger 1993). The key features of wind engineering are described as:

- Complex geometry.
- Medium accuracy requirement.
- Requires prediction of average force on an object and the distribution of force.
- Requires prediction of peak force and frequency of fluctuation.
- Involves complex unsteady approach flow that may not be well characterised.

Stathopoulos has twice reviewed the subject of CFD modelling for the construction industry (Stathopoulos 1997; Stathopoulos 2002), finding that results have been reasonable in terms of pressure on the front and back face. He advises that 'practitioners should be warned about the uncertainties of the numerical wind tunnel results and urged to exercise caution in their utilisation'. However, he also states that the potential of CWE 'is extremely high and its progress should be monitored carefully'.

The picture is similar in terms of commercial wind engineering consultants. One wind engineering consultant (Hansford 2002) states "the difficulty with flow effects is that you can always think of a post-rational explanation for what may, in fact, be a wrong result" and "with a wind tunnel, what you see is what you get. With CFD it is much more difficult to see the difference between model errors and physical actions". These criticisms are equally valid for wind tunnel results, however, and the quality of modern CFD post-processors allows clear visualisation of flow results, often in greater detail than is possible in the wind tunnel.

Both commercially and practically CFD has a number of potential advantages over wind tunnel testing as it can be integrated with modern computer aided design tools and performed as quickly as the available computational power allows.

A great deal of research in recent years has centred on the issue of validation of CFD models against wind tunnel measurements and against full-scale measurements. Less work has been seen on the verification of the CFD solution in terms of checking the effects of changing grid resolution and numerical scheme.

Meroney et al. (2002) claim good agreement between physical model testing and CFD results for a tall building. They conclude that "similar pressure and wind flow presentations were produced by the physical model measurements and CFD calculations... the general character of flow about the building produced by the two modelling alternatives is very similar. Regions of flow acceleration, separation, reattachment, and evidence for rooftop and ground level vortices are evident" and "mean pressure coefficients calculated by the two modelling alternatives are very similar. Regions of positive pressure and negative suction are coincident in both models."

Morteza et al. (2002) have modelled a 40-storey building using the finite element code ETABS with a pseudo-turbulent wind model, representing winds with harmonic load functions. They concluded that the angle of approach of the wind was very important, as were the building damping

ratio and the torsional behaviour of the building. The torsional stiffness was particularly significant where gust frequencies were close to the natural torsional frequency of the building.

Oliveira and Younis (2000) compared the mean loading of greenhouses in full-scale tests and RANS modelling, based on full-scale experiments (Hoxey and Moran 1991). They examined the effects of using a 2-D approximation for the building geometry, varying domain size and grid density, different turbulence models (k-ε and RSM-SSG). The inlet boundary was obtained in a separate simulation with the SSG model based on the work of Hoxey and Richards (1993).

LES models appear to give much closer approximation to mean surface pressures on bluff bodies than can be achieved using the RANS equations (Stathopoulos 1997) but adequate representation of fluctuating pressures is yet to be achieved and even mean predictions are challenging. The use of LES requires that the grid be refined to a much greater degree than that generally used in RANS simulations and this, coupled with the need to run for thousands or tens of thousands of timesteps to get settled flow statistics, puts the use of LES in the built environment beyond the computational resources of all but a few research centres.

Where aeroelastic effects are significant, for instance long span bridges and tall buildings, a coupled structural finite element / CFD simulation may be required to examine structural behaviour. This involves a further step increase in computer power, and current efforts in this field have largely been limited to 2-D behaviour of bridge cross sections, although some results have recently been published using LES for 3D bridge deck sections (Sun et al. 2005).

More progress has been made coupling CFD with finite-element analysis in the field of biology, where the flow in a single organ is much simpler than that seen in wind engineering. The BLOODSIM project (Staples and Penrose 2000) has developed a loose coupled solution method combining the CFD analysis capabilities of the commercial CFD package CFX with the finite-element analysis software ANSYS. The BLOODSIM coupling

software manages the CFD and FE packages. Pressures from CFX are passed to ANSYS, which then calculates the deflection characteristics of the boundary. This boundary movement is then fed back into the CFD solution, changing the pressures exerted on the boundary. The process is repeated until a solution is found for both the fluid and the solid boundary. The fluid mesh and finite element mesh are not necessarily coincident so results must be interpolated between nodes by the BLOODSIM software. Progress in this field is likely to feed into future work in the built environment where the methods must deal with larger flow problems, higher Reynolds numbers and more complex boundary flows.

2.3.1.CWE 2000 Competition

A competition was launched leading up to the 2000 Computational Wind Engineering conference in which experienced CFD users were challenged to predict the results of the Silsoe study (see section 2.5.2) using commercial or academic CFD software. The challenge was in three parts:

1. Boundary layer modelling in the absence of any obstruction: closeness of fit to the defined inlet and its stability through the solution domain with no building present.

2. Model the flow around the cube with the wind perpendicular to one face.

3. Model the flow around the cube with the wind at 45° to the faces.

Three computational solutions were presented (Richards et al. 2002), two of which were performed by modellers with more than 5 years experience and one by a relative novice with less than 1 year of CFD experience. The modellers chose different turbulence models, grid sizes, grid structures, differencing schemes and near-wall treatments. One modeller forced symmetry in the solutions by only modelling half of the cube while the others did not. Differences between the solutions were largely attributed to differences between turbulence models, although the large number of variables changing and the small number of solutions presented makes it hard to be confident of the conclusions.

However, a separate study (Easom 2000) showed a similar trend in results varying only the turbulence model, leading to the authors' conclusion that the turbulence model employed was the main source of the difference between the solutions. The trend observed was that the k-ε solution underpredicted separation and the MMK overpredicted separation while the RNG k-ε solution was much closer to the full-scale results.

The competition entries were also compared with wind tunnel studies on a variety of cuboid buildings (Hoxey et al. 2002) and mean pressures from the CFD predictions generally fell within the same margin of error as the wind tunnel results. The results showed that both wind tunnel testing and CFD tended to underpredict pressures on the roof of the cube. It was not possible to make a full comparison for pressures in the corner of the roof and velocities around the cube due to the lack of detailed information from the published wind tunnel results.

These results suggest that CFD can reasonably be used to predict mean pressure coefficients for simple buildings, as used in the design of building ventilation systems. The study does not address more complex shapes or the fluctuating component of pressure, the latter being beyond the scope of RANS studies. Nor does it consider the additional steps necessary to move from predicting mean pressure coefficients to performing the structural design.

2.3.2.Cube in a Channel

Another standard test case for air flow around a surface mounted cube is the case of a cube in a fully-enclosed channel (Larousse et al. 1991; Martinuzzi and Tropea 1993). This was selected as a CFD validation case by the Network for Quality and Trust in the Industrial Application of Computational Fluid Dynamics, QNET (QNET 2002).

The experiment consists of a thin slot or channel of dimensions 3900 x 600 x50 mm with a 25mm high bluff object mounted on the bottom surface. The high degree of vertical containment makes this a rather

different case from the Silsoe cube in the atmospheric boundary layer, but it exhibits separation and reattachment in turbulent flow and is therefore a useful reference flow case. It has the additional advantage of being small enough to allow detailed refinement of the computational grid and has proved amenable to analysis using LES simulation.

The experiment involved wind tunnel simulation of three-dimensional flow around surface mounted rectangular prisms with width to height ratios varying from 1 (cube) to 24 (rib).

The cube results formed the basis for an LES workshop (Rodi 1997) in which 3 LES and 4 RANS simulations were compared with the experimental values. In this study the RANS simulations consistently over-predicted the wake reattachment length, whereas LES simulations gave good prediction of overall flow features.

In the same paper, LES results were found to be better in predicting flow over the surface mounted cube than they were predicting vortex shedding past a square cylinder. This was attributed to the fact that the flow was already fully turbulent before it arrived at the cylinder, damping out vortex shedding oscillations.

The LES simulations were run with 160,000 time steps in order to provide sufficient data for averaging and spectral analysis. At the time this required 160 hours on an SNI S600/20 vector computer.

Calculation Method		x_{FI}	x_T	x_{R1}	Grid
LES	UKAHY3, Smag	1.29		1.70	165 × 65 × 97
	UKAHY4. Dyn	1.00		1.43	165 × 65 ×97
	UBWM2, Smag	0.81	0.837	1.72	144 × 58 × 88
RANS	Std. k-ε; WF	0.65	0.43	2.18	110 × 32 × 32
	KL-k-ε;-WF	0.64		2.73	110 × 32 × 32
	TL- k-ε	0.95		2.68	142 × 84 × 64
	TL-KL- k-ε	0.95		3.40	142 × 84 × 64
Experiment		1.04	1.61		

x_{FI} = Upstream separation point

x_T = Roof reattachment point

x_{R1} = Downstream reattachment point

Table 2-1: Results of LES Workshop on Martinuzzi Cube (Rodi 1997)

The cube was also used as one of three validation cases for the implementation of the DES method in the commercial CFD package CFX-5 (Menter and Kuntz 2003).

The DES method implemented is the SST-DES method proposed by Strelets (Strelets 2001), modified to prevent grid-induced separation in the boundary layer. The numerical scheme employed is a blend between a second order upwind scheme for RANS regions and a second order central difference scheme for DES regions.

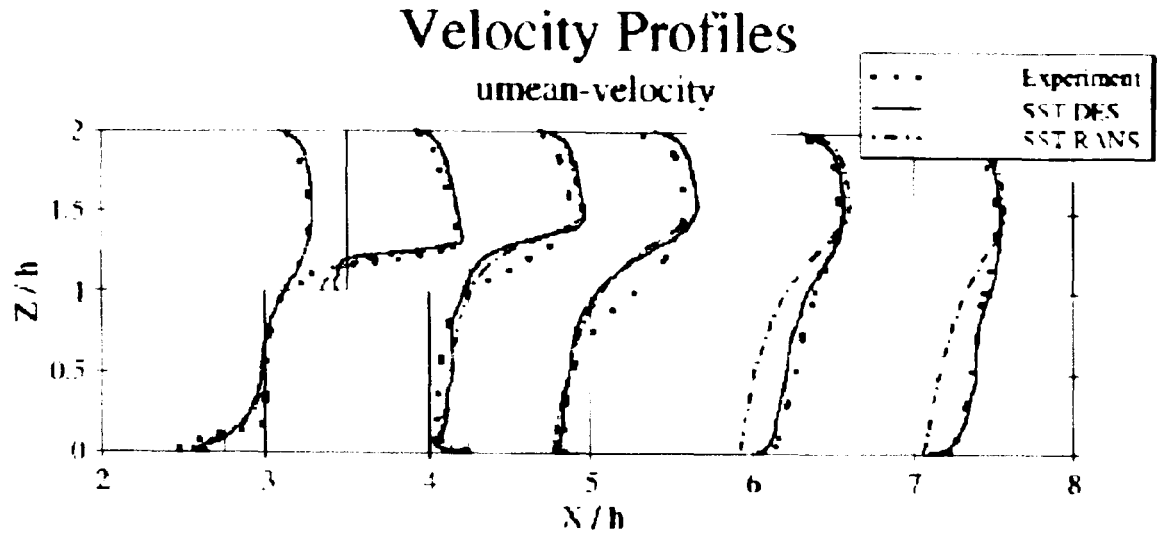

Comparison of RANS and DES simulations with experimental results for the Martinuzzi cube (Menter and Kuntz 2003)

The cube was further investigated in an LES study of coherent structures around the cube by Alfonsi et al. (2003). The POD method was used to extract information on the coherent structures observed in an LES study. Comparisons of centreline velocity components are presented for the LES study and the experiment but no comparisons of turbulence intensity are shown. The comparisons are plotted on a small scale but show reasonable agreement upstream of the cube and deteriorating quality alongside and downstream of the cube. No comparison is presented for positions other than the centreline and no comment made on the sensitivity of the results to grid resolution or on the criteria used in judging convergence.

The paper goes on to examine the energy present in different modes of the fluctuating kinetic energy within the channel but with no comparison shown with the experimental results it is hard to judge the value of these studies.

One recent study (Cremona and Amandolese 2005) on flow loading on bridges uses CFD to predict mean pressure coefficients around aerodynamically profiled bridge decks and finds that the CFD consistently underpredicts the negative pressure in regions of separated and reattaching flow. Interestingly, the dynamic behaviour is well represented in these studies, suggesting that in some cases mean values may be harder to predict than fluctuation frequencies.

2.4. Other Wind Engineering Disciplines

The field of wind engineering also covers pedestrian level wind speeds, dispersion of pollutants, natural ventilation, wind power generation, crop damage and a number of other related disciplines. A brief review of some of these is given and their relevance to this work discussed.

2.4.1. Pedestrian-Level Wind Speeds

Large buildings significantly affect airflow and influence ground level wind speeds around their base. This can lead to the development of very high wind speeds around the base of a building, rendering certain areas unsafe for pedestrians. On a smaller scale, moderately increased wind speeds may make areas less comfortable and therefore unsuitable for a street café or park bench.

A number of methods exist for assessing human comfort, many developed independently by different researchers during the 1970s. Melbourne (Melbourne 1978) found that there was remarkable agreement between them. The BRE have performed a review of this area and BRE Digest 390 (BRE 1994) summarises the techniques used to assess wind speed and methods for relating wind speed to human comfort. They found that people generally accept occasional high wind speeds as a fact of life, but object to suddenly experiencing particularly strong winds at specific locations. Commercial wind speed consultancy therefore concentrates on calculating how much the new building will accelerate wind speeds rather than predicting absolute values of wind speed.

For certain activities, such as sitting at a café, the absolute wind speed is more important and in these cases the number of days during which a critical wind speed will be exceeded may be more useful.

The technique that is most commonly employed at present is wind tunnel testing in a Boundary Layer Wind Tunnel. Pitot tubes, anemometers and/or flow visualisation techniques (most commonly scouring methods) are used to assess wind speeds and identify areas where the wind speed is acceptable for different activities.

Consultants are now starting to turn to CFD techniques for this work. The BRE assessed the potential of CFD for prediction of wind speeds around a complicated urban environment, comparing the results of CFD simulation with wind tunnel testing (Miles and Westbury 2002). The CFD package used was CFX 5.5 with an unstructured mesh of tetrahedral and prismatic elements. They compared results for the standard k-ε, RNG k-ε and k-ω models, finding that the RNG k-ε model gave the best results.

This work using CFD to predict wind speeds around buildings is a useful first step towards predicting surface pressure upon buildings. Correct prediction of mean wind speeds around a building will be necessary for the correct prediction of surface pressures, although it will not be sufficient to guarantee this as local turbulence levels will influence the fluctuating pressure values. Thus, computational structural wind engineering can be seen as a significantly greater challenge than pedestrian level wind-speed analysis.

2.4.2. Environmental Health Modelling

Another key area of concern for wind engineers is the spread of pollutants from industrial facilities as well as plant emissions from conventional buildings. Full scale testing, model scale testing in the wind tunnel and now CFD have all been applied to this problem, and some sensitive sites now have continuously updated CFD models showing what would happen if a leak were to occur, given current meteorological conditions (Morvan 2005). Transient RANS simulations are generally employed to show the movement of pollutants with time.

There has been a great deal of interest in the use of CFD for the modelling of pollutant spread from industrial facilities as well as plant emissions from conventional buildings. A number of researchers have looked at this subject, including recently Fothergill et al. (2002). They investigated flow dispersion around rectangular and circular storage tanks. They compared results using both the k-ε and RSM turbulence models with wind tunnel test results and found that "The CFD simulations are very good qualitatively and, in many cases, quantitatively". The inlet velocity and

turbulence parameters were well matched in the CFD simulation. The effects of using an expanded hexahedral surface mesh were investigated and it was concluded that the expanded mesh improved prediction of flow, turbulence and separation more accurately, especially for curved surfaces.

Scanlon modelled pollutant dispersion around a cube using the first order accurate HYBRID-UPWIND scheme and the second order accurate QUICK scheme (Scanlon 1997). Velocity profile predictions for both schemes compared well with wind tunnel test results by Robins and Castro (Robins and Castro 1977a), (Robins and Castro 1977b). Turbulence intensity predictions were similar qualitatively but very different quantitatively, giving approximately 100% under-prediction.

Montavon et al. have reviewed the use of the CFX software in environmental flow modelling (Montavon et al. 2000), including case studies demonstrating:

1 Furnace modelling and prediction of NOx emissions, on the scale of metres.

2 Modelling of interactions between the atmosphere and buildings, including diesel particulate transport, on the scale of hundreds of metres.

3 Meso-scale atmospheric modelling, on the scale of tens of kilometres.

This work demonstrates the capabilities of CFD software in tackling practical wind engineering problems, combining wind and buoyancy effects. However it does not provide validation data for the wind pressures or velocity fields predicted.

2.4.3. Natural Ventilation

The majority of natural ventilation strategies used in the UK are dependent upon buoyancy-driven flow. Wind may have either a positive or a negative impact on this, and a number of researchers are looking at using wind tunnels and/or CFD to quantify this effect. LES simulations for an idealised simple building showed good agreement between calculated

and real ventilation rates when the results were compared with wind tunnel measurements (Jiang et al. 2003). The LES model simulated the wind tunnel rather than simulating the notional equivalent real building however, meaning that the results would be subject to scale effects as well as CFD modelling errors.

Winds capable of causing structural damage are generally far stronger than those caused by buoyancy effects and significantly stronger than those considered in the standard operation of natural ventilation systems. Structural design also requires far greater detail in the distribution and intensity of pressure fluctuations while ventilation studies are usually concerned only with average values. For an exception to this, see Yang (2004) where the effect of fluctuating pressures on ventilation rates are studied.

2.5. History of Structural Wind Engineering

Structural wind engineering aims to quantify the forces a structure will experience due to wind throughout its expected life. In the case of a heavy static structure such as a low masonry building this means predicting the maximum force the building will be subject to. In the case of more flexible structures, which are subject to vibration at certain frequencies, it may be important to know the frequencies of wind excitation the structure may experience. If the structure deflects significantly and regularly in the wind then the effects of fatigue can become important and the quantity and magnitude of oscillations must be calculated.

This section describes the development of structural wind engineering, focusing on how our understanding of pressure on the surface of bluff bodies has developed. For a more extensive review of this subject see the *Designers Guide to Wind Loading on Structures Volume 2* (Cook 1990). For a brief history of the related field of industrial aerodynamics the reader is directed to Morgenthal and McRobie (2002).

2.5.1. Early Structural Design Experience

As is the case with most engineering disciplines, the history of structural wind engineering is marked with great successes and great failures. Failures can often lead to further advances as modes of behaviour that were previously ignored or misunderstood receive great investigation. The earliest structural failures occurred in bridges as the use of steel allowed spans to became longer and lighter.

The collapse of the Tay Bridge in 1879 due to high winds caused a great deal of engineering interest in wind loading for bridge structures (Martin and MacLeod 1995). Before this, wind load calculations were rarely performed for bridges as the effect of gravity on masonry arch bridges always outweighed the loading due to wind. The failure was carefully investigated, leading directly to Baker's tests on the site of the Forth Bridge, described in section 2.5.2.

Figure 2-4: The Tay Bridge After Collapse in 1879 (Martin and MacLeod 1995)

The failure of Brighton chain pier in 1836, the Menai Strait Bridge in 1839 and the Tacoma Narrows Bridge in 1940 alerted the engineering community to the susceptibility of long-span bridges to the dynamic effects of the wind. The infamous and well-documented case of the Tacoma Narrows bridge in particular (Bilah and Scanlan 1991) showed that pseudo-static analysis could not be used to predict the behaviour of

such structures. Again, a step change in construction technology highlighted an area where understanding was limited.

These dramatic failures of bridge structure highlight a wider problem of damage or destruction of property in strong winds. (Cook 1985) provides a review of structural damage to buildings in the UK and overseas.

2.5.2. Full-Scale Testing

Early developments in structural wind engineering involved the use of full-scale tests to measure wind pressures on sample objects or real structures. Cook discusses a series of early load tests in his Designer's Guide to Wind Loading of Building Structures: Volume 2 (Cook 1990).

In 1884, Baker performed a series of wind load tests at the site of his proposed Forth Rail Bridge measuring the force on a 300 square-foot board and two 1.5 square-foot boards mounted on spring balances. He concluded that forces were not steady and that small areas were more susceptible to peak loading by gusts than large areas.

In 1900, Gustave Eiffel measured the displacement of the Eiffel Tower in Paris using a vertically mounted telescope at the base. The results were compared with simultaneous wind speed and direction measurements.

In the 1960s, full-scale tests were performed by the Building Research Station (Newberry et al. 1968) on an 18-storey office block in central London. These tests identified the significance of building porosity, due to openings around doors and windows, in determining the internal pressure and therefore the net load across the faces of the building.

Silsoe 6m Cube

The Silsoe 6m Cube (Hoxey et al. 2002), Figure 2-5 is situated in an open field in the UK with 600m of open fetch, consisting of regularly cut grass. Nearby buildings are set at a distance of 16-20m or approximately 3 cube heights (Figure 2-6), while a reference mast was used for some of the time to characterise the oncoming wind. This was set four cube heights

upwind of the cube to minimise the effect of the cube and the other buildings on flow at the mast position. At the same position, wind velocity and static pressure (Moran and Hoxey 1979) were measured at 6m height throughout the experiment.

5-10 taps were available on the centre line of each face to characterise the overall pressure profile (Figure 2-5) and a cluster of 27 pressure taps were available to characterise the pressure zones in one quadrant of the roof. A total of 32 of these taps could be used at any one time. The building was rotated so this one quadrant could be displaced to any position relative to the wind.

Richards et al. (2002) compare the results of the full-scale tests with a number of wind tunnel tests on cuboidal buildings. The wind tunnel results vary significantly, although the majority of these were intended to represent significantly larger buildings in different flow conditions.

Figure 2-5: The Silsoe 6m Cube and Silsoe Structures Building. Pressure tapping locations are visible highlighted in white

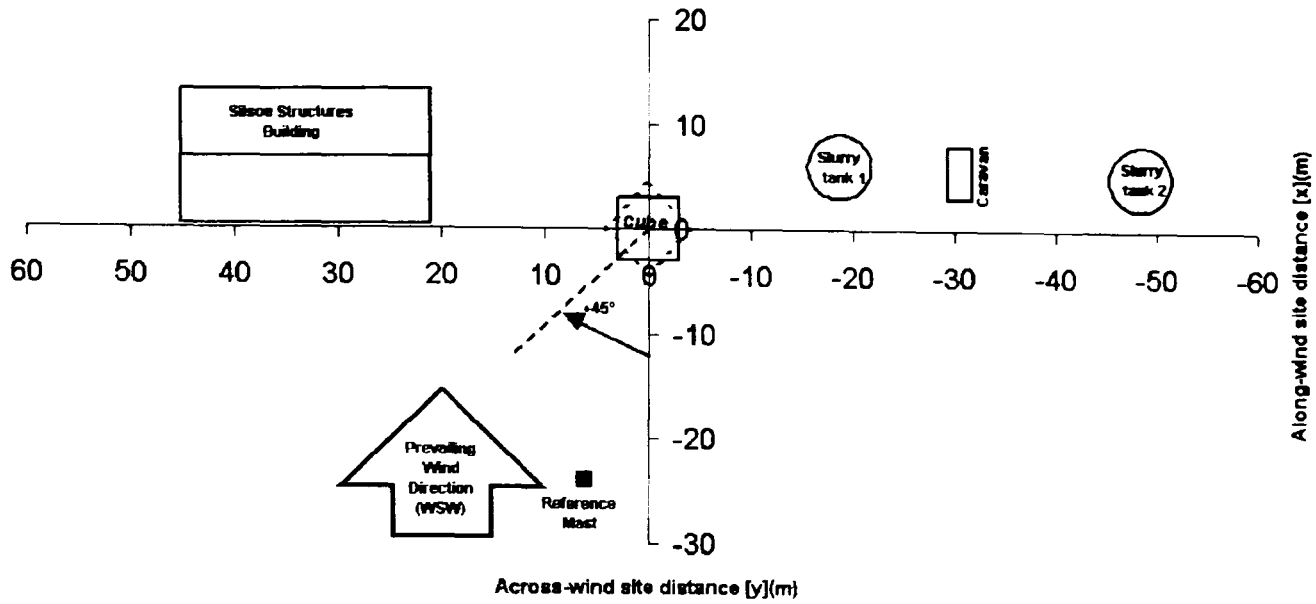

Figure 2-6: The Silsoe 6m Cube site (Hoxey et al. 2002)

2.5.3. Model-Scale Testing in Wind Tunnels

By the 1930s, wind tunnels were in use for model-scale testing and full-scale tests were rarely used to provide load information for individual projects (Cook 1990). Full-scale testing was reserved for testing theories and developing design techniques, as well as to investigate the results of model-scale tests and, later, CFD simulations.

Empirical rules provided by codes of practice can only ever provide design information suitable for a number of standard building types. More complicated or unusual building forms require an approach that is tailored to that particular form. Small-scale testing in a wind tunnel can give valuable design information to the engineer and if performed appropriately can predict many of the flow phenomena experienced at full scale.

Wind tunnel testing is generally performed by specialist testing laboratories based on a specification developed with the design team and in particular with the structural engineer, who may have limited understanding of aerodynamics.

Blackmore (Blackmore 1997) provides a useful general review of the use of wind tunnel testing in structural design. A more detailed study of the science behind wind tunnel testing is made in chapter 7 of 'Wind Effects

on Structures' (Simiu and Scanlan 1996). For a more recent review of applications to civil engineering, the interested reader is directed towards a review by Cermak (2003) which gives a particularly comprehensive summary of the development of wind tunnel testing.

The method is to build a scale model of the building within a wind tunnel facility. Pressure taps at key points measure pressure on the faces of the test model. Total force and overturning moment may be separately measured at the base of the model. Where aeroelastic phenomena are significant, the physical model must have appropriately scaled dimensions and stiffness. Turbulence is generated using a combination of grids and screens with scaled roughness elements at the inlet.

In early studies it was found that the floor and wall boundary layer varied from wind tunnel to wind tunnel, affecting the results. Attempts were initially made to remove this effect by suspending the model in the wind tunnel but later work showed that accurate wind tunnel modelling required a well-developed turbulent boundary layer representative of the atmospheric boundary layer.

Modern boundary layer wind tunnel design can be traced back to 1958 when it was shown that accurate modelling of the atmospheric boundary layer is vital if model-scale tests are to give a good representation of full-scale behaviour (Jensen 1958). This invalidated much previous work, where the significance of this effect had not been recognised.

Understanding scaling effects is vital to obtaining a realistic representation of loading on the real structure. It is theoretically impossible to accurately simulate all aspects of flow at small scale. As stated by Simiu and Scanlan (1996), "normal wind tunnel testing in air under standard gravity and atmospheric conditions entails fundamental scale violations of the Reynolds and of the Rossby number". This is due to the fact that it is not practical in the laboratory to scale the effect of gravity and that air is used for almost all wind tunnel simulations, and therefore density and viscosity are not scaled.

A further complication in the application of wind-tunnel test results comes in the derivation of load effects from surface pressures. Peak pressures from the wind tunnel cannot be directly scaled into full-scale peaks and a number of techniques have been developed to make the conversion (Holmes 2002). For ease of use by structural engineers, the peak wind loads are generally converted into equivalent static loads, accounting for both the mean and the fluctuating component of the load.

When resonant structural response is negligible, the Load-Response-Correlation (LRC) method (Kasperski and Niemann 1992) can be used to calculate the equivalent static load from the fluctuating wind tunnel results. This produces an equivalent pressure distribution which represents the fluctuating loading.

Despite these limitations, well-performed wind tunnel testing shows reasonable agreement with full-scale measurements. Reynolds number does not significantly affect most structural wind engineering flows, with the important exception of separation from a smooth surface. Demonstrations of Reynolds number independence combined with the success of wind tunnel techniques over many years have made wind tunnels the design tool of choice for most unusual buildings.

2.5.4. Analytical Methods

The response of an individual building to the wind is too complex a system to be represented by a single closed form solution (CFS). However, analytical methods are extensively used in research as a tool to increasing understanding of structural response, wind behaviour and in developing standard solutions for simple classical structural forms such as a thin cantilever. A review of this field is available to the interested reader in Solari (2002).

2.5.5. Calculation of Structural Loads

The process by which fluctuations in the oncoming wind translate into fluctuating structural loads is complex, but can be though of in the following hierarchical steps.

1. Parent wind as described in section 2.1.1 above

2. Local wind conditions. These are a result of the parent wind, modified by local orography and adjacent structures.

3. Point surface pressures. Point pressures on the windward surface of a structure are chiefly a result of the attenuation of wind pressure fluctuations in the upwind stagnation / separation region. This is discussed in some detail in (Sharma and Richards 2004). Point pressures on the side and rear faces of the structure are strongly affected by separation patterns and body generated turbulence.

4. Area averaged pressures. Area pressure admittance is the result of spatial averaging of the point pressures over a single building element such as a cladding panel or group of panels. Large scale fluctuations are not attenuated while very small high frequency fluctuations are highly attenuated.

5. Internal pressure fluctuations. These are a product of the surface pressure fluctuations and the number, size and positions of openings (Sharma and Richards 2004). The response of internal pressures to changes in external pressures is complex and dependent on a number of variables including window and door positions which may be expected to change during the life of the building. Therefore a constant internal pressure coefficient is frequently assumed in design, chosen to represent the worst case for each design calculation.

6. Structural response. This is a result of the response time and dynamic behaviour of the structure. Response will be further attenuated due to the response time of the structure and non-simultaneous loading of different parts of the structure. Conversely the response may be increased due to dynamic excitation of the structure. Small stiff components of the building will be affected by shorter gusts while larger more flexible members will respond to load more slowly. Brittle cladding panels are often designed

assuming a 1 to 3 second gust, while large components of the main structure may be designed assuming gust times of 10-20s.

The structural designer is directly interested only in the last of these, in the forces which must be resisted by the structure and the resulting movement which must be accommodated in the design. These forces and deflections occur on a number of different scales – cladding panels and their supports must resist loading on a small area. Beams and columns supporting these may be loaded by a number of different cladding panels. The foundations and stability system will support the whole or a large part of the building and must respond to the sum of all these forces.

In order to account for this accumulation of structural loading, a load path must be identified through the building allowing the summing of forces. In most standard regular buildings, a simple hierarchy will be assumed by the structural designer with purlins and cladding rails supported by secondary beams, fixed to primary beams which themselves lead to a grid of columns and back to the shear cores or walls which form the stability system. In more complex or unusual buildings the load path may be less clear and a finite element analysis may be required to trace the route taken from the point of loading down to the foundations. In either event, this process must be followed for all buildings if the engineer is to prove that the building can safely resist the forces it may be subjected to.

The aim of the engineer is to prove that the building will not collapse or fail due to rain penetration or excessive movement under loading which may be expected in the building's lifetime. At the time of designing, all these loads are uncertain, whether due to the weight of the structure itself, imposed loading from occupants and furniture, snow loading, or extreme winds. It is impossible to precisely know how strong is the worst storm that will hit a building in its life, or to predict whether the building will be fully occupied and otherwise loaded at the time.

When calculating loads from wind tunnel or full-scale measurements, load effects may be calculated directly from the integration of surface pressures across the building. In practice this is often not possible as

historically it has been impossible to retain full sets of wind tunnel loading information for every wind direction and the wind tunnel specialist is unlikely to perform the structural design. Additionally, the structural layout and load path are not necessarily known at the time of planning the wind tunnel tests and the pressure tap locations may not map exactly to structural members. For this reason, loads may be conveyed to the designer as maps of mean pressures and standard deviations, with peak loads calculated by applying an appropriate gust factor to the standard deviation and adding it to the mean or by taking the mean of an appropriate number of peak events (Cook 1985). The peak load is therefore given by:

$$\hat{L} = \overline{L} + \sqrt{\left(\hat{L}_B\right)^2} \qquad \textit{[equation 2-4]}$$

Where

$\overline{L}$ = Mean load effect

$\hat{L}_B$ = Peak background load effect (Fluctuation from mean)

2.5.6.Codes of Practice for Wind Loading

The British Standard for non-dynamic or mildly dynamic buildings in the UK is BS 6399 part 2(BSI 2002). This was introduced in parallel with the older CP3 Chapter V: Part 2 (BSI 1972), which was withdrawn early in 2002. It will ultimately be superseded by the European standard, EN1991-1-4 (CEN 2002).

The British Standard provides gust peak wind loads for use in static design methods and covers mildly dynamic structures by use of a simple multiplication factor.

For non-standard, large or dynamic structures it recommends the use of wind tunnel testing to examine wind loads. A scale model is built and pressure measurements are taken at critical points around the building. The results of wind tunnel testing are compared with simplified calculations based on BS 6399-2 and a judgement is made on the loads to be applied and the factor of safety to be used.

2.6. Guidance Available to the Wind Engineer

A review of the literature shows no guidance on the use of CFD in predicting structural loads and very little guidance on its use in predicting external flows for other purposes. This section reviews the guidance available on the related subjects of the application of CFD and other computer tools to engineering problems more generally, including verification and validation of results.

Guidelines for the industrial use of CFD are under development by the QNET CFD group, including a short section on external aerodynamics but this can only provide a starting point for those interested in such problems.

2.6.1. Guidance on Use of CFD for External Aerodynamics

The most comprehensive guidance currently available on the application of CFD to wind engineering comes from two recent documents. One is by QNET CFD: a thematic network for quality and trust in the industrial application of CFD and the other is from a COST C14 working group on CFD techniques.

The QNET document (Castro 2003) highlights the importance of accurately modelling the approach flow, including the development of a stable boundary layer flow which is in equilibrium with the CFD boundary conditions. Techniques for this have yet to be developed for LES modelling, while RANS techniques are discussed in the following chapter.

The author states that if average surface pressures can be predicted accurately then it is likely that the average flow regime has been accurately predicted but emphasises the point that fluctuating velocities and pressures may be more important than mean values, as in structural wind engineering.

It is noted that deficiencies exist in current wall-treatments but that these do not generally lead to large errors in mean flow prediction, perhaps because behaviour is dominated by large-scale flow patterns.

At the ERCOFTAC meeting on Urban Scale CFD in September 2004, Castro (2004) further emphasis was placed on the need to resolve unsteady fluctuations around buildings if detailed building-scale results are to be obtained.

The COST recommendations (Franke et al. 2004) concentrate on the choice of turbulence model and the size and resolution of the computational domain. They suggest that the standard k-ε model should be avoided in favour of the RNG k-ε or the realisable k-ε model due to their improved prediction of turbulence production in stagnation regions, or ideally Reynolds stress models although it notes the problems these present in achieving convergence. The RNG k-ε model uses different model constants and a new model function while the realisable k-ε model includes additional constraints on the normal stresses: positive values of normal stress and Schwarz inequality for shear stress. A stable boundary layer should be proven to develop and consideration should be given to how to define convergence, monitoring key variables rather than relying solely on residual values.

The paper also goes into some detail on validation requirements and suggests that wind tunnel measurements are appropriate as they give well-bounded steady state and fluctuating results.

More general advice is given in a recent paper assessing issues of appropriateness and trust in industrial CFD (Wright 2004). This paper highlights the need to consider CFD requirements in terms of:

- Do we need to predict velocity or pressure?
- Are unsteady predictions required?
- What accuracy is required?

The paper goes on to suggest that although CFD is generally appropriate for wind speed predictions for pedestrian comfort, techniques are not yet fully developed for the application of CFD to structural wind engineering.

2.6.2. Use of Computers in the Analysis of Structures

Over the last two decades the availability of computers for structural analysis has increased enormously. Where once they were used only in extremely specialist applications, generally with the input of academics who were specialists in their field, most structural engineers now have access at least to first order linear elastic analysis programs. Engineers are now able to tackle extremely complicated analysis without necessarily understanding the results of their calculations. This has led to the publication of several sets of guidelines for computer analysis. The Steel Construction Institute stresses the importance of fully understanding the structural phenomena involved when preparing the model and provides guidance in assessing one's understanding (SCI 1995).

The Institution of Structural Engineers in a recent publication (IStructE 2002) places more emphasis on the level of checking required for computer analysis, providing methodologies and flow charts for this purpose.

2.6.3. Use of CFD in Other Engineering Disciplines

Guidance is available for Aerospace engineers from the American Institute of Aeronautics and Astronautics (AIAA 1998). Procedures are set out for verification and validation of CFD simulations, and authors in their journals must adhere to these procedures. This guidance distinguishes verification from validation, as well as carefully defining 'prediction'. Verification is defined as "the process of determining that a model implementation accurately represents the developer's conceptual description of the model and the solution to the model". Validation is defined as "the process of determining the degree to which a model is an accurate representation of the real world from the perspective of the intended users of the model". The use of the word prediction is restricted from its general usage and defined as "the use of a CFD model to foretell the state of a physical system under conditions for which the CFD model has not been validated". This covers all use of CFD in engineering design,

as there is no need to perform CFD calculations if past data is available to confirm the answers given.

This guide highlights the fact that not all engineering calculations require the same level of accuracy. For example, for a CFD prediction of wind loads on a tall building, the engineer would accept some inaccuracy but would wish to know how accurate the simulation was. Resistance to wind loads is almost always a critical design case and under-prediction could easily lead to lack of serviceability or to structural failure. By contrast, some under-prediction may be acceptable for CFD predictions of wind speeds around the base of the same tall building. Incorrect results may result in discomfort to pedestrians on windy days but it is unlikely that there would be any loss of life or significant financial loss.

In both cases, a highly accurate solution is desirable but not necessary. If the margin of error is known then an appropriate factor of safety can be used.

Roach (1998) discusses spacial convergence, providing a method for formally estimating discretisation error in CFD simulations. This involves producing a series of grids with a significantly increasing grid refinement, typically a factor of two in each direction, i.e. a factor of 8 overall. A Richardson Extrapolation can then be used to estimate variable values for a fully refined grid (zero spacing).

More general guidance is available on modelling building ventilation from a number of sources (Fawcett 1991), (Setrakian et al. 1991). More recently, the Chartered Institute of Building Services Engineers (CIBSE) have produced a manual on building energy and environmental modelling (CIBSE 1998), as well as including some guidance in CIBSE guide A (CIBSE). The former publication is by far the more comprehensive, covering the use of all manner of building simulation software from simple programs to assist basic calculations to integrated suites of analysis design software, including CFD and dynamic thermal modelling software. The guide describes four main procedures in checking that a piece of software is operating correctly:

- Code Checking: going through the code line-by-line will verify that no mistakes have been made in its implementation, but this is only possible by those writing the code or other expert programmers. This would not be practical for any but the largest engineering consultancies, and even then this would be unlikely.

- Analytical tests: comparing results from a simple study with a solution by analytical methods is a useful test. Problems for which analytical solutions exist will typically be much simpler than those attempted in a real building design. A correct answer to a simplified analytical case is a useful indication that the software is running correctly but does not necessarily prove that it can model can model the complicated behaviour of a real building.

- Inter-program comparisons: if a well-validated program is available for comparison then this can prove a useful additional check.

- Empirical validation: comparison with real building measurements is, in principle, the most powerful validation technique, addressing the central issue 'how well does the program predict reality'. However, variability in experimental data can cloud the results. With most building modelling software, it is possible to vary many factors that affect the final results, and the effects of these must be understood. It is useful for giving confidence in computational simulations that the simulation is performed 'blind' without the option of later adjusting the simulation to match reality.

The guide also highlights the importance of training for software users, both initially and on an ongoing basis and discusses quality assurance procedures, both from a technical point of view and in terms of business development. It goes on to set out in some detail the process of building a building simulation model.

Best practice guidelines have been published by the European Research Community on Flow, Turbulence and Combustion (ERCOFTAC 2000). These give general guidance on planning CFD simulations, modelling turbulence, selecting software and on verification and validation. They

also provide a set of sample cases, which are mainly concerned with internal flow in pipes and engines, and a set of analysis checklists.

The report highlights the need for application procedures in addition to these general guidelines. These would cover individual topics such as external flow over bluff bodies.

2.7. Need for Further Work

CFD is now regularly used in the building industry to model the internal environment and examine natural ventilation schemes. The work discussed earlier in this section has led to its use in the prediction of wind flow around buildings in studies of pedestrian comfort. Similar computational models can be used to predict pressures and therefore structural loads on buildings but serious questions remain about the accuracy of these models. Important flow features, such as separation and recirculation have a significant influence on the pressure distribution and resulting wind loads, and yet they are very sensitive to modelling assumptions. Pressures may therefore be incorrectly predicted, resulting in inaccurate estimates of the wind load.

Furthermore, critical issues such as the importance of turbulence frequency spectra and coherence have not been addressed with respect to CFD studies.

The purpose of this research is to critically assess the extent to which commercially available CFD packages can be used in predicting wind loads on structures. Whereas previous studies have concentrated on predicting wind speeds and comparing the predictions with full-scale results and wind tunnel tests, this study looks at what parameters are important in predicting wind effects on structures. As commercially available software used, the CFD techniques applied are restricted to commonly available turbulence models and meshing techniques. In practice this means steady and unsteady RANS simulations and DES simulations. Full LES simulation of the atmospheric boundary layer is likely to remain beyond the capabilities of most industrial practitioners for many years.

This study compares the level information given by different methods and how much of this information is required for different types of study. For instance, RANS methods give time-averaged results while DES methods and wind tunnel studies give fluctuating values. The strengths and weaknesses of each method are assessed qualitatively and, where possible, quantitatively.

3. CFD Techniques Used

As summarised in the previous chapter, Computational Fluid Dynamics (CFD) is now regularly used in the construction industry to model the internal environment and examine natural ventilation schemes. Its use is increasing for the prediction of wind flow around buildings in studies of pedestrian comfort and environmental pollution. Similar computational models can be used to predict pressures and therefore structural loads on buildings but serious questions remain about the accuracy of these models. Flow features such as separation and recirculation have a significant influence on the pressure distribution and resulting wind loads, and yet simulation of these can be very sensitive to modelling assumptions. The treatment of turbulence through simplified models may be insufficient to allow for all significant turbulent effects. Flow may therefore be predicted incorrectly, resulting in inaccurate estimates of the wind load.

A key challenge in applying CFD to commercial or academic flow studies in the built environment is balancing the spatial and temporal resolution, the sophistication of the turbulence models used and the discretisation schemes employed against the available computer power. This project uses recent advances in computer power and turbulence modelling to examine wind speeds and surface pressures around simple cubes and a complex building. This chapter describes how the studies are performed in terms of the computational methods used, problem definition and how the results are assessed. The key solution parameters are identified for investigation in later chapters.

Commercial wind engineering consultancy in the built environment frequently involves complex building forms which do not lend themselves to simplified code of practice methods and are not easily represented using structured meshes. Design times are typically measured in weeks rather than months, necessitating the use of automatic meshing and minimal repetition of simulation. Standard quality assurance procedures require the use of software which has been thoroughly checked for

accuracy. These requirements of rapid geometry and mesh building, complex geometries and quality assurance generally necessitates the use of commercial software in design practice.

3.1. Computational Model

This study builds on earlier work with CFX-4 (Easom and Wright 2001) by using the latest version of the commercial CFD package, CFX-5 with meshes of several million cells. Structured and unstructured meshes were generated with refinement near boundaries and particularly near areas of flow separation. For the unstructured meshes, an expanded boundary layer mesh of prismatic elements near to the floor and the bluff body was used to improve resolution of the boundary layer near the surface.

Many of the initial simulations were run on a 1.7 GHz Pentium 4 PC with 2 Gb of RAM. Later studies on grids of around 3 million cells and transient simulations of more than 100 timesteps were run in parallel on a set of 12 3GHz PC processors. The CFD code is optimised for efficient parallel processing and there is little computational overhead due to the parallel distribution.

3.1.1. Fluid Models

For turbulent boundary layer flow at wind speeds capable of causing structural damage in temperate regions (synoptic winds), wind speeds are high enough to safely neglect buoyancy effects and yet not so high as to require the calculation of fluid compressibility. A single homogenous fluid is used throughout the calculation domain with air properties as follows:

- Density = 1.284 kg/m^3
- Dynamic viscosity = 1.725×10^{-5} kg/m/s

The basic k-ε turbulence model has become an industry standard turbulence model for turbulent flow modelling in a range of fields (Castro 2003). It suffers, however, from an overprediction of turbulence kinetic energy production in stagnation regions and overpredicts the size of the separation region behind bluff bodies (Easom 2000). The RNG k-ε

turbulence model is widely used in predicting flow around bluff bodies due to its improved prediction of turbulence production and flow separation (Prevezer and Holding 2002; Richards et al. 2002). Its convergence behaviour makes it a preferred option over k-ω type models. It was therefore chosen as the reference turbulence model for these studies. Due to the large scale of these flow cases it is not practicable to refine the mesh near to surfaces down to an appropriate scale for the turbulence model alone. The use of scalable wall functions (CFX 2003) as provided with the software reduces the need for fine resolution of boundary layers.

LES turbulence models, as discussed in section 2.2.2 are widely seen as having great promise for the future of wind engineering but these methods suffer from the inability to transport turbulence quantities on the subgrid scale. This means that all turbulence scales generated in one region must be directly modelled if they are to affect flow in a downstream region. This requires a very fine grid and prohibitively expensive computational resources. As discussed in section 2.2.2, DES methods partially overcome this problem by introducing a RANS model where the grid is not sufficiently refined but still suffer limitations in the transfer of turbulence parameters between the LES and RANS portions of the flow.

The DES method implemented in CFX is the SST-DES method proposed by Strelets (Strelets 2001), modified to prevent grid-induced separation in the boundary layer (Menter and Kuntz 2003). This has the advantage of allowing the RANS method to be used in regions of attached turbulent flow where the Strelets et al. method would require the use of LES. This is important in providing a computational benefit for external aerodynamics cases where the oncoming flow is highly turbulent. The numerical scheme employed is a second order upwind scheme for RANS regions and a second order central difference scheme for LES regions.

This DES implementation combines the SST k-ω RANS model with LES, switching to LES where the local grid resolution is less than the turbulent length scale as calculated using the RANS model.

A limitation of the standard DES model is that near the wall the choice of LES or RANS turbulence model is dependent on grid resolution, resulting in a grid dependent separation point. The DES model implementation in CFX prevents this by enforcing the use of the RANS model in the boundary layer. As the SST k-ω model has been shown to accurately predict the separation point, this model is chosen for the boundary layer region.

3.1.2.Geometry

The fluid domain in a CFD study should be large enough to contain all important flow features and to avoid significantly constraining the flow. This requirement must be balanced against the limit on available computer power. The requirements for the Martinuzzi cube were rather different from those for external flow cases, due to the vertical containment, and are described later. For the external flow cases a domain has been created with a length of 6 times the bluff body height H upstream of, above and to either side of the body and 10H downstream (Figure 3-1), as per recommendations from (Easom 2000) and from the project's industrial partner, Buro Happold. The larger downstream dimension was selected to allow full development of the turbulent wake and recirculation zone behind the body. For the cube studies, these dimensions create a blockage ratio of 100 x (36 / 3276) = 1.1%. This allows the use of standard boundary conditions which constrain the air perpendicular to the direction of flow, similar to the boundaries of a physical wind tunnel.

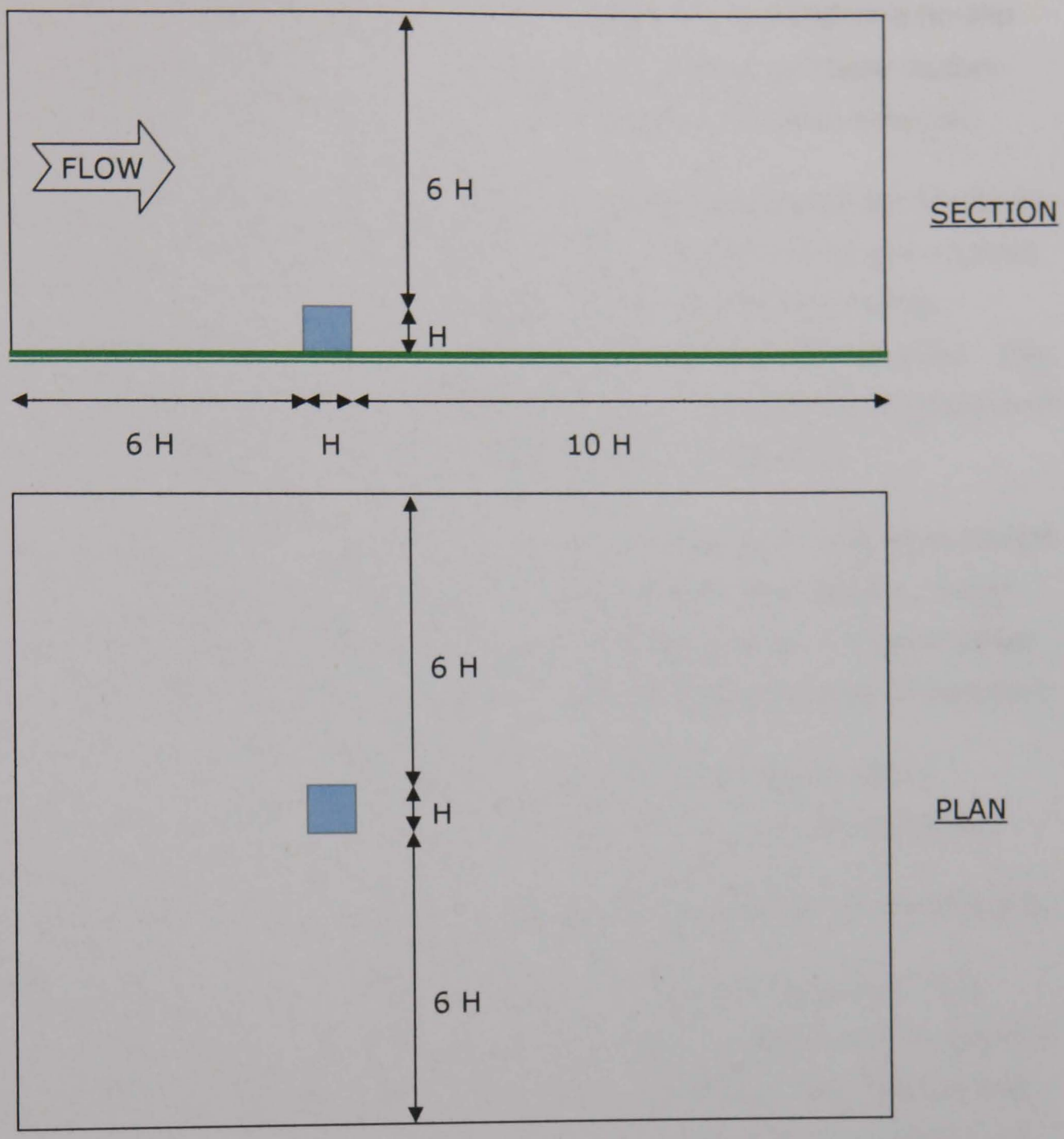

Figure 3-1: Fluid Domain for cube studies

3.1.3. Boundary Conditions

Boundary conditions for the CFD simulations are as shown below. Where the boundary conditions are varied as part of the study, this is indicated.

- Initially, smooth free-slip walls are used above and to either side of the domain. These allow free flow parallel to the wall and no flow across the wall, simulating free stream flow and assuming that the bluff body has no influence on flow at this position. As discussed in section 5.3.1, a velocity and turbulence profile were later added to the boundary to help drive the fluid flow and maintain the turbulence profile.

- The Martinuzzi cube is completely enclosed in a channel so a no-slip wall with an appropriate roughness height is used for these studies. The roughness height is varied as part of the calibration exercise.

- The fetch for the Silsoe cube has an aerodynamic roughness length z_0 of 0.01m (Hoxey et al. 2002). CFX accepts roughness length in terms of the equivalent sand grain roughness height and as an initial estimate, a sand grain height of 0.075, or 7.5 times z_0 was used. This was selected based on the experience of other researchers (Stangroom and Wright 2003) and is further discussed in Chapter 5.

- The faces of the Silsoe cube were given a sand grain roughness height of 0.005m based on the recommendations in Easom (2000). Initial sensitivity analyses show that this value does not have a great effect on surface pressures over the cube, matching the findings of Easom.

- The inlet velocity profile for each simulation was set to match experimental observations, as described in the appropriate section.

- The inlet turbulence intensity is discussed in sections 4.3.1 and 5.3.2.

- A uniform static relative pressure of 0 Pa defines the outlet. This provides a reference static pressure for the simulation and is essential for the simulation not to become over constrained. If a velocity and turbulence profile was specified at the outlet as well as the inlet and the sides then any errors in the mass balance would result in an excess or lack of fluid in the domain, causing an artificial rise or fall in pressure.

3.1.4. Initial Conditions

Initial conditions are set equal to the inlet conditions. For transient and subsequent steady-state analyses a previous steady state results file is used to provide the initial condition. For transient calculations there is an initial set of timesteps during which the periodic solution develops. Results for these initial timesteps are discarded and only the truly periodic results are used.

3.1.5. Mesh Parameters

In any CFD study it is important to demonstrate the degree to which the results are sensitive to the formulation and particularly to the degree of mesh refinement. The aim is to show that significant parameters are not greatly affected by further mesh refinement. Mesh refinement studies for the cube in a channel, Silsoe Cube and Ascot building are described in chapters 4, 5 and 6 respectively.

Structured hexahedral meshes are used for the initial cube studies and unstructured tetrahedral meshes for accurate representation of the more complex building geometry. An inflated boundary layer of thin prismatic cells is used to resolve the boundary with the bluff body without introducing an excessive number of cells. This results in a large aspect ratio but this is reasonable as flow in the first few cells is generally parallel to the walls.

Two options are commonly used in resolving flow in this near wall region. The low Reynolds number approach involves a very fine resolution of the boundary layer (down to a y^+ value of less than 2 for the k-ω model (CFX 2003)). For external flow problems this would be prohibitively expensive in terms of computational cost. The use of wall functions, which has become standard in wind engineering (Franke et al. 2004), allows much coarser resolution (y^+ of less than 100 for scalable wall functions, as used in CFX (CFX 2003)).

Resolving flow further from the wall, Spalart et al. (1997) recommend a stretching ratio $\Delta y_{j+1}/ \Delta y_j$ of 1.25 or less (using no wall functions), and a value of 1.2 has been employed in this work.

Grid spacing parallel to the wall is not constrained by the numerical solution and is varied as part of the mesh refinement studies.

DES Grids

The grid requirements for DES simulations are complicated by the combination of RANS and LES regions, with different grid requirements in

each. This is particularly challenging, as it is not known a priori which areas will use each turbulence model.

The RANS region will have the requirements described above, chiefly requiring y^+ to be controlled near the boundary. The LES region will contain turbulent eddies which must be suitably resolved, requiring finer resolution. The LES region may be very large as the turbulent wake is typically many times the size of the bluff body.

Spalart (2001) discusses the generation of DES grids for aerospace applications, looking at flow over an airfoil, circular cylinder and a landing-gear truck. Although these flow cases are different in some respects to built environment cases, they include separation around bluff bodies and the concepts used by Spalart can be extended to the cases studied here. He uses the concept of a 'Focus Region' in which the fine grid resolution is extended to cover any area in which a particle of fluid may be expected to travel back to the body and interact with it. This is roughly defined as the area where flow reversal is seen. In bluff body flows in the atmospheric boundary layer, this may represent a very large area, with instantaneous flow reversal seen at a considerable length downstream of the building. In the case of detached eddies, this will not result in fluid particles returning to the building and by this method can be ignored. The focus region should therefore be that volume covered by the largest single separation bubble above, behind and around the building, or rather the envelope of all attached separation bubbles behind the building. This cannot be known before the simulation is commenced so a simplified method must be used to estimate the size of this wake. This zone will be considerably smaller than the full turbulent wake, the rest of which (the Departure Region) is modelled using a coarser grid.

There is no standard way to choose the grid size in the focus region and grid refinement tests are still best practice. The aim of the LES filtering should be to model only those turbulence scales which are statistically isotropic. As discussed in section 2.1.1, turbulent structures around the building exist on a great range of length scales. Clearly, major flow structures must be captured – upstream, downstream and other

separation regions, horseshoe vortex, etc. Significant fluctuations in the size and shape of these structures must be captured, as must any smaller turbulent structures directly affecting them. Smaller 3D turbulence can be dealt with by the subgrid scale model. Following recommendations from Richards et al. (2004), the temporal resolution should be sufficient to capture a reduced frequency f=nz/U down to about 1 where n is the frequency and U is the mean speed at height z.

The mesh in the RANS region near the cube is varied as part of the mesh studies, while a coarser mesh is used further out to capture flow in the free stream.

These recommendations can be applied to building studies in the atmospheric boundary layer, except that the free stream is highly turbulent. There is therefore no Euler Region, so the grid spacing in the far field will be governed by the requirement to provide a stable boundary layer using a RANS simulation. Based on discussions with our industrial partner, Buro Happold, unstructured grids are typically used for atmospheric flow simulations as building geometry is an order of magnitude more complex than the simple geometries often studied in vehicle aerodynamics and design times an order of magnitude shorter. This has the dual advantages of allowing tetrahedral cells with near-unity aspect ratios for greater calculation efficiency in the LES region and allowing more mesh coarsening for greater efficiency outside the LES region.

3.1.6. Timestep Selection

Transient RANS simulations were performed for the Silsoe cube and Ascot building, requiring the selection of a timestep. As we are interested in structural loads, this must be less than the typical structural response time of a few seconds but it is not necessary to resolve all turbulent time scales as turbulent pressure fluctuations can be averaged out by the simulation.

For inherently unstable flows, if too large a timestep is used then significant flow instability may be damped out. To capture these instabilities, the timestep must be such that it picks up any required fluctuations, typically with at least 5 timesteps per cycle in order to capture the fluctuations with sufficient resolution. Assuming that 5 timesteps are required to capture one turbulent fluctuation with a reasonable degree of accuracy, this implies a timestep of z/5U. This is further discussed in Chapter 5.

DES simulations require more careful timestep selection and again no universally accepted rules have been developed. Spalart (2001) recommends that provided the grid in the LES region has been sufficiently refined to pick up all significant turbulent structures, the timestep should be selected to give a Courant-Friedrichs-Lewy number (CFL) of near to unity;

$$CFL = \frac{ut}{\Delta_0} \qquad \textit{[equation 3-1]}$$

Where:

U = *velocity*

Δ_0 = Grid spacing in LES region

t = timestep

Run Time

The run time for all unsteady simulations should be sufficient to allow the fluctuating flow conditions to develop and then provide settled mean flow characteristics. Flow simulation results should be assessed for stationarity to show that the flow has settled to its natural state and that the record is long enough to contain all significant frequencies.

The length of record needed for this will depend upon the quantity studied, with mean values typically being obtained more quickly than standard deviation, extreme values or correlation statistics.

One method of testing for stationarity is known as the run test (Bendat and Piersol 1971) and is based on the fact that the sample distribution for samples taken from any arbitrary stationary parent distribution will always be a normal distribution. We can therefore divide our time record into a series of samples, calculate the mean or RMS from those samples and plot them sequentially. Testing the hypothesis *'this data comes from a stationary process'*, the number of runs where the plotted variable value crosses the mean should match standard printed tables. Further details are given by Bendat and Piersol (1971).

3.1.7.Solver Parameters

The solution accuracy of a CFD simulation is usually measured in terms of normalised solver residuals – the local imbalance in each flow equation, normalised by the variable value. As the solver iteratively approaches a solution which satisfies the governing equations, these residuals reduce towards zero.

The initial convergence criteria were to limit RMS mass and momentum residual values to the default value of 1×10^{-4}. However it is important for any CFD simulation to run studies to check whether this achieves settled values of the key variables.

In the case of a transient simulation a number of iterations is performed to achieve convergence at each individual time step.

CFX uses a coupled solver to reduce the number of iterations required for convergence. Two options are available for the advection term, of which the first order Upwind Differencing Scheme (UDS) converges most rapidly, but this is at the expense of introducing numerical diffusion. The second-order accurate Numerical Advection Correction scheme (CFX 2003) is also available, giving greater accuracy at the expense of longer computing time. The second order solution can also introduce non-physical overshoots and undershoots in the solution, particularly following a flow stagnation point or other source of high flow gradients. A number of simulations were performed investigating a blend between 1^{st} and 2^{nd}

order solutions. These simulations and their implications for CFD calculation of structural loads are discussed in section 5.3.4.

The blend described above involves a correction equivalent to a proportion of the second order solution. This is specified in CFX using the following equation:

$$\phi_{ip} = \phi_{up} + \beta \nabla\phi . \Delta_r \qquad \textit{[equation 3-2]}$$

Where:

ϕ_{ip} is the variable value at the integration point.

ϕ_{up} is the value at the upwind node.

$\nabla\phi . \Delta_r$ is a second order correction, removing the numerical diffusion.

β is the 'Blend Factor' between 0 and 1.0 representing the required proportion of the second order correction.

3.2. Assessment of Results

A great deal of research has been performed into the use of CFD in mean predicting flow fields and pedestrian-level wind speeds (see Franke et al. (2005) for a review) or examining point pressures on a bluff body (see Stathopoulos (2002)). These values are useful but structural engineers are primarily interested in the maximum force applied to the building and the distribution of that force across the building. The overall force on the building will be used for stability calculations and foundation design while individual members should be designed for the local pressure, taking into account the fact that smaller members are more susceptible to high local peak pressures and small gusts.

This means that RANS methods may be quite adequate for the design of foundations but not for smaller elements and cladding, where brief fluctuations in pressure are more significant. Design values for these elements would have to be extrapolated from the RANS results by statistical methods, with an appropriate factor of safety.

Load sharing and redistribution between structural members may reduce the significance of local pressures and place a limit on the required refinement of pressure distribution. For large buildings, cladding and glazing panels will generally be of the order of 1m across, supported by purlins, rafters and other structural members of greater size. Unless otherwise stated, it will be assumed in this work that cladding and glazing panels are used. Measurements will therefore be required at approximately 0.1 - 0.5m spacing to adequately represent the forces on an individual element. For smaller buildings, timber boards or slates may be used and so a greater degree of refinement may be needed, but such products are usually judged on past experience or full-scale tests rather than by calculation for each individual building.

It is standard practice in structural wind engineering for static buildings to use time-averaged pressure values from wind tunnel testing and to account for variability by scaling these according to the expected gust wind speed (typically the one in 50 year 3-second gust). If the flow is highly periodic, perhaps due to vortex shedding from an upstream structure, then the engineer may be interested in the variability of the force and the time period of that variation. This would be particularly relevant if the structure receiving this periodic force was highly dynamic.

3.2.1. Comparison of Pressure Results

To compare results for simplified calculation methods, wind tunnel testing and CFD simulations we must be sure that the figures used are mutually compatible.

To remove the effect of the fluctuating wind speed, pressure distribution may be described in terms of a pressure coefficient, non-dimensionalised with respect to a reference pressure. This is acceptable for the structural design of buildings with sharp corners such as the cube, where flow patterns are largely independent of Reynolds Number (Cook 1990). For domes and other curved buildings, separation and reattachment points are generally highly dependent upon Reynolds Number and pressure coefficients will vary with wind speed (Cook 1990).

The reference pressure is typically measured at the eaves height or the top of the roof of the building.

Reference mean dynamic pressure, $q = \frac{1}{2}\rho\overline{V}^2$ *[equation3-3]*

Where:

ρ = density of air = 1.284 kg/m^3

$\overline{V}$ = wind speed at reference height

For the 6m Silsoe cube, the wind velocity upstream of the cube at a height of 6m was used to non-dimensionalise the results (Richards et al. 2002). Similarly, the British Standard BS6399-2 (BSI 2002) and Eurocode (CEN 2002) use the wind velocity at eaves level and wind tunnel tests use wind velocity at eaves level, corrected for scale effects.

3.2.2.Other Significant Results

Although pressure results are of most significance to the structural engineer, other values may be enlightening when considering flow around a structure. Wind velocity around the cube and in particular the sizes of zones of separation are useful when comparing simulations with reality and with wind tunnel results. Separation and reattachment points in particular are extensively reported in the literature and will be used in comparisons made in this study.

4. Cube in Channel

If CFD is to be used to predict structural loads on a building then the pressures on the building must be accurately represented in the computer model. These pressures are directly affected by the flow field around the building, so accurate prediction of the air velocity is a vital first step in predicting the structural loads. This chapter describes studies investigating the flow around a cube in fully-developed channel flow. The clear definition of the boundary conditions and controlled nature of the flow make this an excellent validation case for the use of CFD for turbulent flow around bluff bodies.

The experiment involving a cube in a fully-enclosed channel (Martinuzzi and Tropea 1993) is a standard test case for air flow around a surface mounted cube. It was selected as a CFD validation case by the Network for Quality and Trust in the Industrial Application of Computational Fluid Dynamics, QNET(QNET 2002) and as a validation case for the commercial CFD package CFX (Menter and Kuntz 2003).

The high degree of vertical containment causes significant differences from the case of a cube or building in the atmospheric boundary layer but, as with full-scale structures, it exhibits separation and reattachment in a highly turbulent flow and therefore serves the required purpose. It has the additional advantage of being small enough to allow detailed refinement of the computational grid.

4.1. Description of Experiment

The experiment consists of a channel of 3900mm length × 600mm width × 50mm height with a 25mm cube mounted on the bottom surface. The leading edge of the cube is 52 channel heights or 2600mm from the inlet (Larousse et al. 1991; Martinuzzi and Tropea 1993). The Reynolds number based on channel height was approximately 1×10^5, with an average velocity across the channel of $U_B = 19.81$ m/s for the main tests.

A variety of prismatic obstacles were tested in the same channel flow with different widths in the cross-stream direction but the same height and downstream depth (both 25mm). The cross-stream width was varied in these tests from 25mm (cube) up to 600mm (rib), though the current studies will only use the cube results as these are most directly comparable with the Silsoe cube results. Measurements were taken of velocity and turbulence components in each direction as well as some pressure measurements as described in section 4.1.2.

It is important to note that vertical containment here limits the turbulence length scale to less than the height of the channel. This is in contrast to the atmospheric boundary layer where turbulence scales may be many times the size of a building.

4.1.1. Velocity Data

The original velocity results have been made available in electronic form as part of the Journal of Fluids Engineering databank(JFE 1993). These include components of velocity as well as Reynolds stress terms for numerous points upstream and downstream of the obstruction. Only two components of velocity were measured in any one test so each set of results gives either streamwise and horizontal cross-stream velocity and turbulence values or streamwise and vertical velocity and turbulence values.

Some additional results were presented in the journal paper, including a probability density function for velocity at a point upwind of the front of the cube. This has two peaks, and the paper suggests that these correspond to 'normal' flow with random turbulence and occasional events of intense turbulence production with highly correlated U and V velocity fluctuations. Another possible explanation for this bimodal velocity distribution would be the flow switching between two unstable modes but the accompanying velocity time traces shows signs of some very brief peak events, supporting Martinuzzi's hypothesis. The duration of these peaks is similar to the quoted sample rate of the equipment, suggesting that the magnitude and duration of these peaks may not be accurately

represented, and any turbulence statistics based upon them may be inaccurate.

A trace of turbulence kinetic energy against time for a point adjacent to the cube shows generally very low turbulence with occasional strong peaks. The turbulence intensity is therefore either relatively low or very high. This renders time-averaged values of the local turbulence kinetic energy meaningless, as the mean values represent a state that never actually exists. In such circumstances it would be difficult for a steady RANS simulation to accurately predict the mean turbulence. Time traces are not presented for locations further away from the cube but it is assumed that as channel flow is fully turbulent, this effect diminishes rapidly with distance from the cube.

The boundary layer was tripped at the inlet, leading to a fully developed boundary layer well upstream of the cube. The article describing the original experiment gives only a mean bulk velocity and does not specify the equilibrium profile of velocity and turbulence in the channel. Channel velocities, however, can be seen to settle to an equilibrium profile before reaching the cube, with extremely similar velocity and turbulence profiles at 11.4 cube heights and 5 cube heights upstream of the cube (Figure 4-1). Even just 2H upstream, the velocity and turbulence profiles have changed by less than 5% due to the adverse pressure gradient.

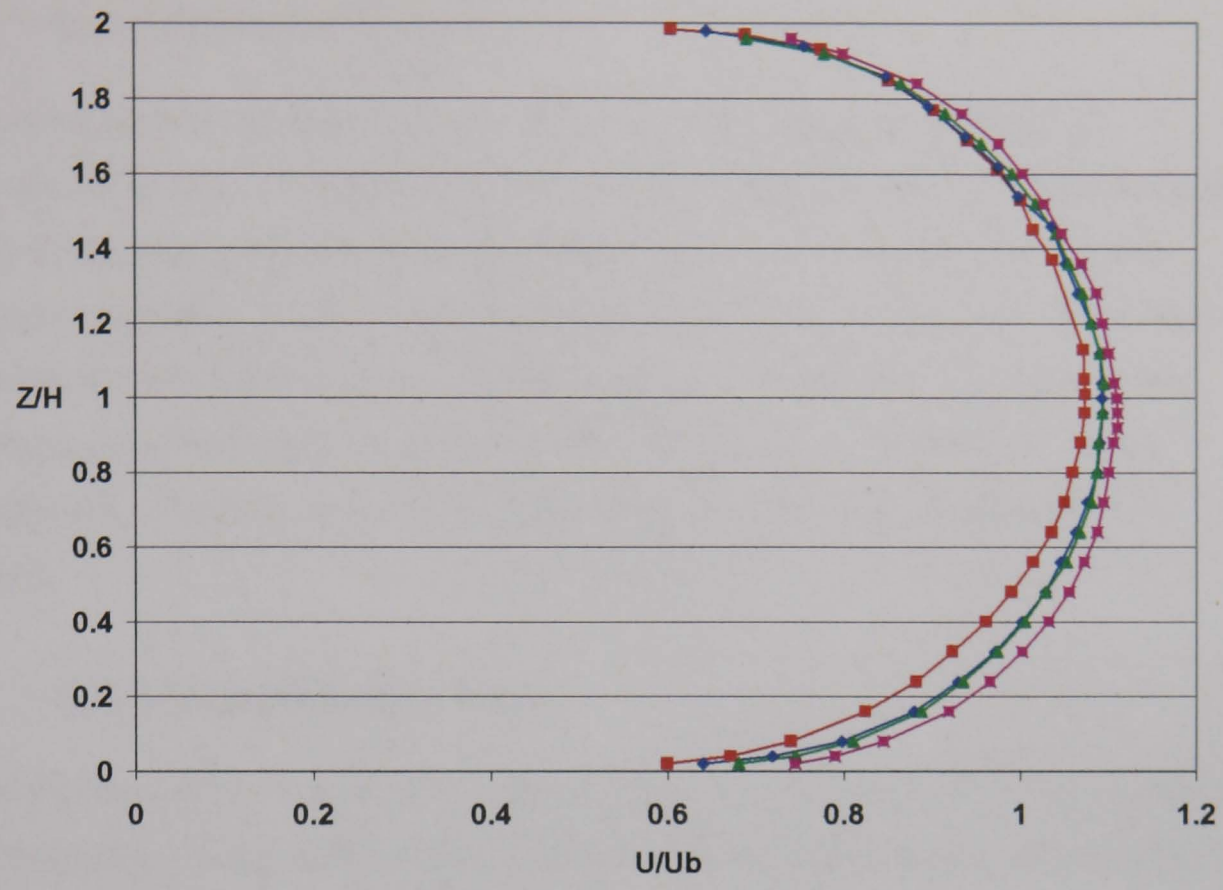

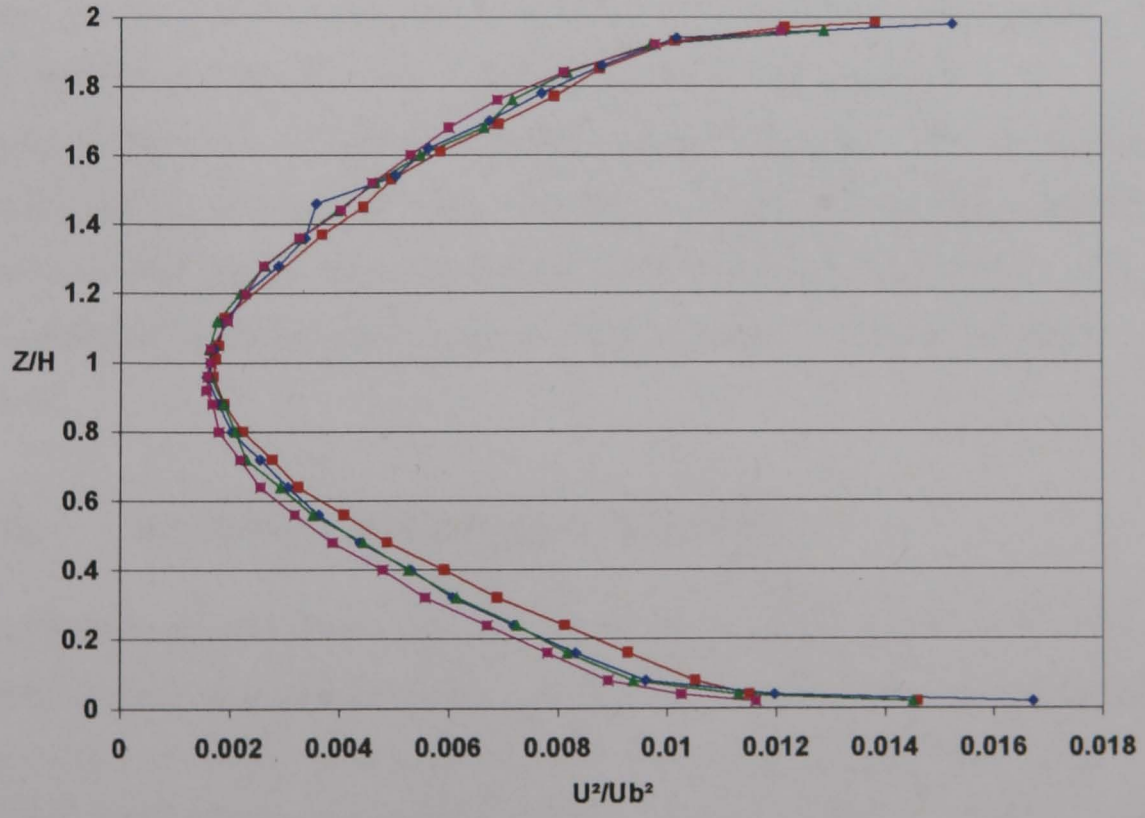

Figure 4-1: Experimental velocity and turbulence profiles upstream of the cube

4.1.2. Pressure Results

In the experiment, pressure was measured on the tunnel floor at numerous points. The measurement points were on the centreline up and downstream of the cube and on horizontal lines perpendicular to the direction of flow. They were recorded in non-dimensionalised form with distances normalised by the cube length and Cp determined using the average channel flow velocity, i.e. $Cp = 0.5 \rho U_b^2$. These results are presented in Figure 4-16 and Figure 4-17 in comparison with the CFD results

4.1.3. Experimental Error

In the case of the pressure measurements, an estimate of the uncertainty in positioning the pressure taps is given as ±0.5mm with an uncertainty of ± 0.02 in the pressure coefficient.

The paper does not comment on the potential experimental error in velocity measurement in this work but the small size of the apparatus presents a significant challenge in placing of measuring equipment. It seems reasonable to assume a similar error to the pressure measurements, i.e. ±0.5mm in measurement location. This could have a significant effect in areas of high velocity and pressure gradient near the cube and in regions of separated flow, where a small change in measurement location would give a large change in velocity and/or pressure.

4.2. Previous Numerical Studies

This cube formed the basis for an LES workshop (Rodi 1997) in which 3 LES and 4 RANS simulations were compared with the experimental values (Table 4-1) . In that study the RANS simulations consistently over-predicted the wake reattachment length, whereas LES simulations gave good prediction of overall flow features.

In the same paper, LES results were found to be better in predicting flow over the surface mounted cube than they were at predicting vortex

shedding past a square cylinder. This was attributed to the fact that the flow was already fully turbulent before it arrived at the cube, and to errors in predicting the evolution of the shear layer for the cylinder case.

The LES simulations were run with 160,000 time steps in order to provide sufficient data for averaging and spectral analysis. At the time this required 160h on an SNI S600/20 vector computer.

Calculation Method		x_{FI}	x_T	x_{R1}	**Grid**
LES	UKAHY3, Smag (Rodi)	1.29		1.70	165 × 65 × 97
	UKAHY4. Dyn (Rodi)	1.00		1.43	165 × 65 × 97
	UBWM2, Smag (Others)	0.81	0.837	1.72	144 × 58 × 88
RANS	Std. k-ε; WF (Rodi)	0.65	0.43	2.18	110 × 32 × 32
	KL- k-ε ;-WF (Rodi)	0.64		2.73	110 × 32 × 32
	TL- k-ε (Rodi)	0.95		2.68	142 × 84 × 64
	TL-KL- k-ε (Rodi)	0.95		3.40	142 × 84 × 64
Experiment	(Martinuzzi)	1.04		1.61	

x_{FI} = Upstream separation point

x_T = Roof reattachment point

x_{R1} = Downstream reattachment point

Table 4-1: Results of LES Workshop on Martinuzzi Cube (Rodi 1997)

The cube was also used as one of three validation cases for the implementation of the DES method in the commercial CFD package CFX-5 (Menter and Kuntz 2003).

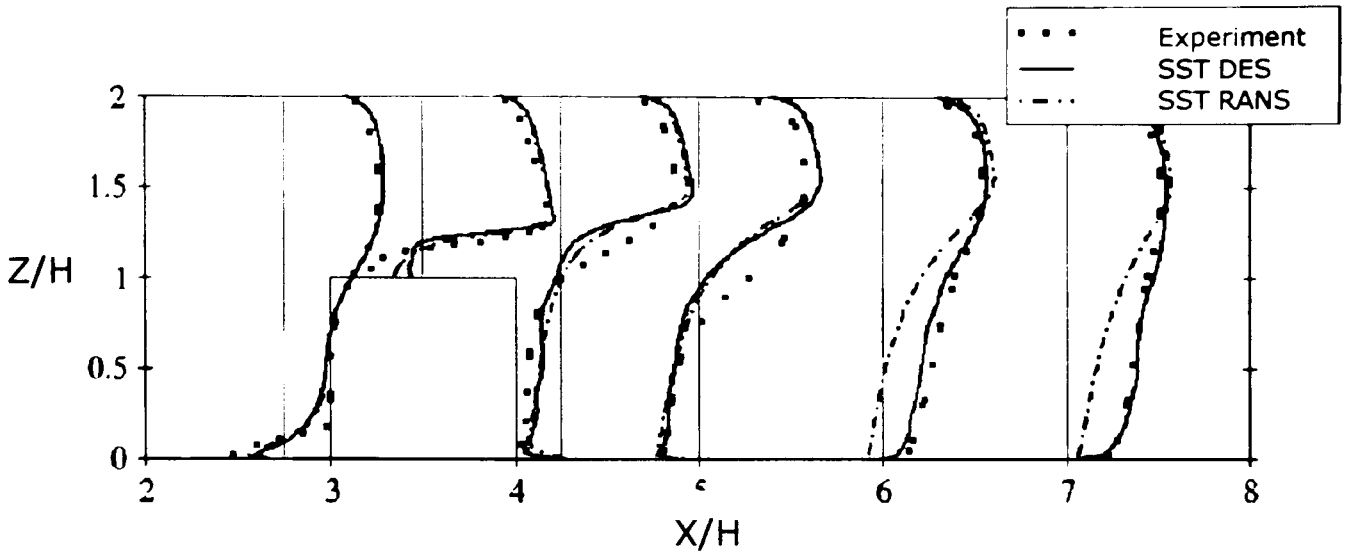

Figure 4-2:Comparison of RANS and DES simulations with experimental results for the Martinuzzi cube: mean streamwise velocity (Menter and Kuntz 2003)

The results presented appear to show that both the SST RANS method and the SST DES method under-predict the zone of re-circulation on top of the cube. This appears to have the knock-on effect of causing an under-prediction of velocity at the height of the cube roof, downstream of the cube. Additionally, the RANS calculations over-predict the reduction in velocity downstream of the cube, apparently over-predicting the size of the wake recirculation region.

No details are given of how many timesteps were performed for averaging in the DES studies. Nor are the full details given of the boundary conditions and fluids models used so it is inadvisable to draw further detailed conclusions from this work.

These studies provide a good starting point for comparison with new results but leave questions in terms of the importance of modelling the boundary layer correctly.

4.3. New Studies

This new set of studies was performed on a section of channel with dimensions 450 x 300 x 50mm, representing part of the full channel. This reduced area was chosen to allow a fine grid resolution around the cube

while still representing a great enough width for the cube studies. The upstream length was sufficient to reach a point where the experimental flow was not significantly affected by the cube. As there is only one target object in this simulation, the wake flow is only of interest in its effect on flow around the cube. The downstream length of 11H can be considered sufficient, however, to give a good representation of the turbulent wake.

As discussed in Chapter 3, initial studies were performed with no cube to establish a consistent turbulence and velocity profile matching those in the experiment. This profile was then used as the inlet boundary condition for the subsequent studies on the cube.

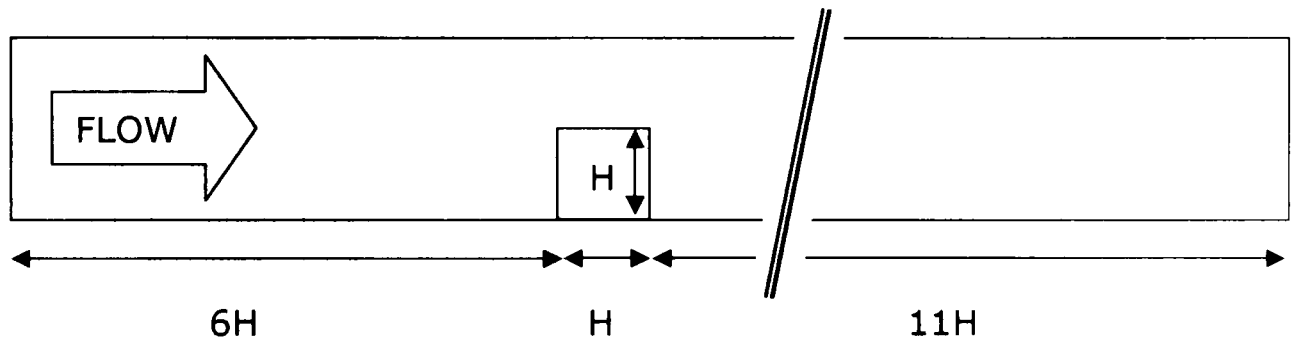

Figure 4-3: Longitudinal section through computational domain

Although the experimental results were symmetrical to within 1-2%, symmetry was not assumed in this study. Asymmetric wake flow has previously been experienced in similar flows (Prevezer and Holding 2002; Knapp et al. 2003) and so it was considered important not to force symmetry. This is considered in more detail in Chapter 5.

Grid dependence studies were performed for the channel, investigating the following features:

1. Required grid density in the channel generally, measured in terms of the effect of further grid refinement on the velocity and turbulence profiles arriving at the cube.

2. Required refinement before, around and after the cube, measured in terms of the effect on velocity and turbulence predictions of further refining the grid in zones around the cube.

The former was investigated for a short length of channel with no cube, while the latter used a slightly larger length of channel with the cube present.

The studies were performed using CFX version 5.6 on a standard desktop PC with 2Gb of RAM and a 1.7GHz processor. Convergence criteria are discussed in 3.1.7 but were initially set to the default values.

4.3.1. Empty Channel Studies

Model Parameters

Mesh Type

A number of mesh types were investigated as an initial study:

- Homogenous unstructured tetrahedral mesh
- Unstructured tetrahedral mesh with hexahedral inflated boundary layer on solid surfaces
- Homogenous structured hexahedral mesh
- Structured hexahedral mesh with progressive refinement towards boundaries.

Results for the homogenous unstructured mesh showed that the results were still highly sensitive to mesh refinement at nearly 2 million cells. Further refinement was not possible with a standard PC and so more efficient mesh designs were sought.

Simulations were then performed with an unstructured mesh but using a structured inflated boundary layer on the top and bottom surface of the channel. These results were compared with those from structured hexahedral meshes. Simulations using the structured hexahedral mesh were found to achieve convergence more quickly. This is to be expected with a flow-aligned grid as there will be fewer problems with diffusion and gradient smearing. As shown in Figure 4-4, problems were experienced at

the interface between the hexahedral mesh in the boundary layer and the tetrahedral mesh in the central region. Turbulence quantities seemed not to pass smoothly between the two regions.

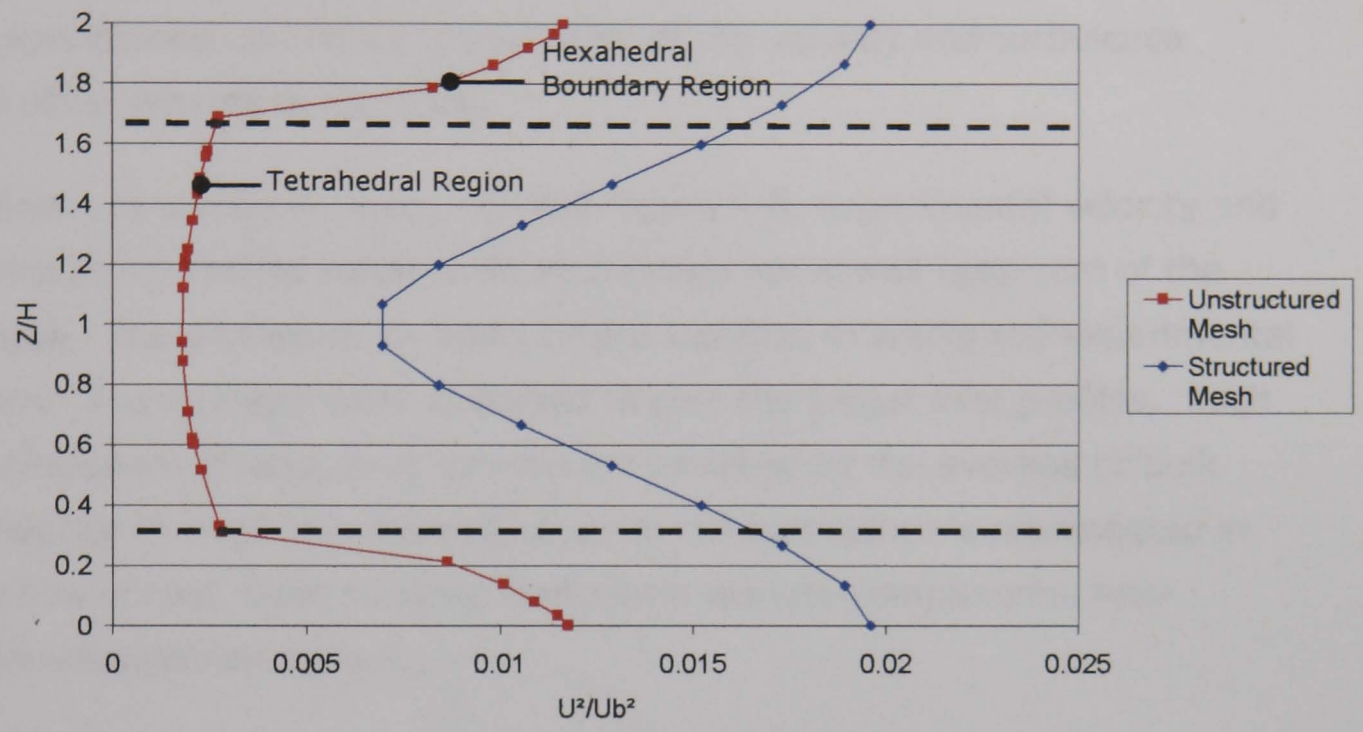

Figure 4-4: Turbulence results for an unstructured and structured mesh with no cube (empty channel)

Structured grids give great computational savings and improved accuracy, particularly where the flow is aligned to the grid, as in the approach region in this case and near the channel walls above and around the cube. Although flow in the stagnation and separation regions near the cube will not be aligned to the grid, convergence should be easier to achieve and mesh quality will be higher with fewer poor quality cells in key locations. A structured hexahedral mesh was therefore chosen for the study.

Previous researchers have used a non-conformal grid interface to allow a greater concentration of cells near the cube and to permit rotation of the far-field for different wind directions (e.g. Stangroom (2004), Morvan et al (2007)). As only one wind direction was used here this was not needed and the additional refinement near the cube was achieved through varying the grid spacing near the cube surface, as described below.

Boundary Conditions

Once these initial mesh studies were completed, a set of boundary conditions was developed which would give a good representation of the experimental conditions, particularly of the velocity and turbulence profiles arriving at the cube.

Inlet: as shown in Figure 4-5 and Figure 4-6, experimental velocity and turbulence results settle to an equilibrium value well upstream of the cube. The profiles at 7h and 11h are identical to within the experimental error and so these were averaged to give the target inlet profiles. Each component of velocity is non-dimensionalised by the average or bulk velocity through the channel, U_b while the turbulence is represented in terms of root mean squared fluctuating velocity components, non-dimensionalised by U_b^2.

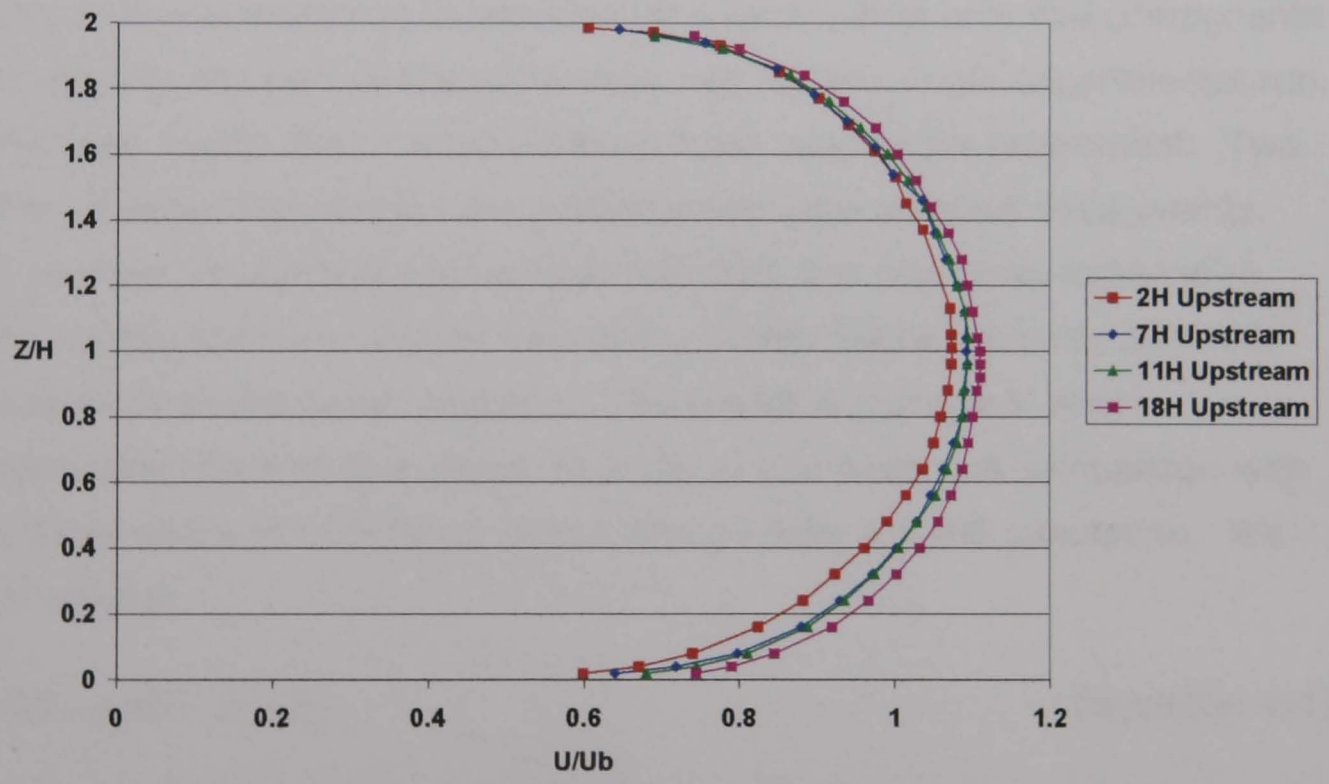

Figure 4-5: Experimental streamwise velocity profiles upstream of the cube

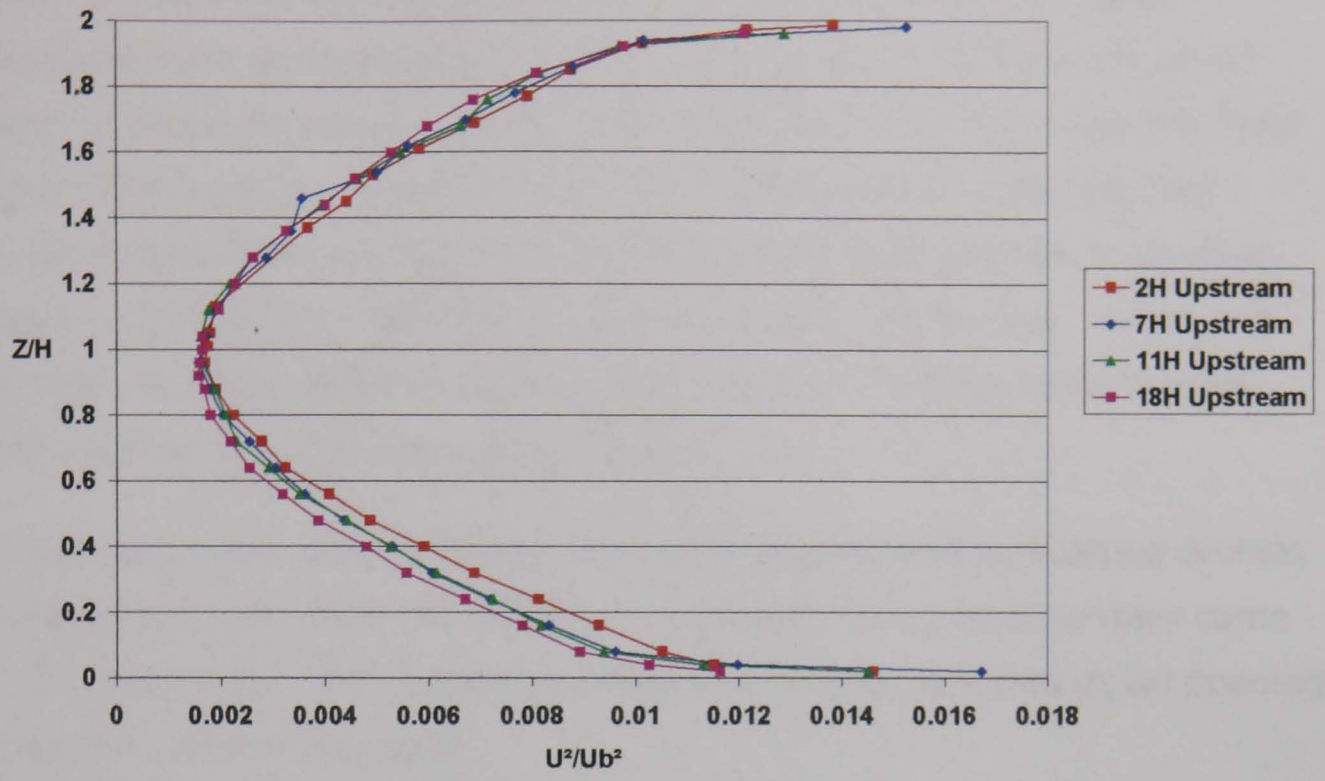

Figure 4-6: Experimental turbulence profiles upstream of the cube

One technical challenge in analysing the data is that only two components of velocity and turbulence were measured for any single experimental run. This was due to the crosswire anemometer used in the experiment. Two sets of experimental data are available from two identical experiments. One gives streamwise and vertical velocities and one gives streamwise and horizontal cross stream velocities. These values were not generally measured at the same locations. This presents a problem when describing the inlet turbulence intensity and in making a comparison with a single value of turbulence kinetic energy from a RANS simulation. We know that:

$$TKE = 0.5(\overline{u'^2} + \overline{v'^2} + \overline{w'^2}) \qquad \textit{[equation 4-1]}$$

Generally, the streamwise turbulence intensity is 2 to 3 times higher than the horizontal and vertical cross stream turbulence intensities. If we assume that the horizontal and vertical turbulence quantities are similar then the equation above becomes:

$$TKE = 0.5(\overline{u'^2} + 2\overline{v'^2}) \qquad \textit{[equation 4-2]}$$

This removes the need to interpolate turbulence intensity between measurement positions but as it ignores the vertical component, it will tend to overestimate the experimental turbulence intensity near the floor where the vertical component reduces to zero. It will underestimate turbulence intensity in areas of high vertical velocity and low horizontal velocity such as the stagnation region upstream of the cube. Given the limitations of the experimental data and of the CFD turbulence models, this method was considered appropriate.

These data were used to provide the inlet velocity and turbulence profiles for the CFX run, while the profile of ε values for the inlet boundary came from initial runs. The outlet boundary was initially specified as an opening with 0Pa relative pressure.

Other CFD Parameters

The turbulence models used were the RNG k-ε model, a popular 2-equation turbulence model for bluff body flows and the SST k-ω model, generally considered superior in modelling separation. Further details on these models are given in section 2.2.2 and their advantages and disadvantages discussed in section 3.1.1. Scalable wall functions were used to represent behaviour near the wall and reduce the flow sensitivity to near-wall grid refinement. This allows the use of coarser near-wall grids than could be achieved with the turbulence model alone. The discretisation was rather strictly set at second order accurate in time and space (CFX Blend factor of 1.0), greatly reducing the numerical diffusion given by first order schemes.

Results

The simulation was run with a uniform flow at the inlet matching the experimental flow rate. The flow conditions were allowed to develop naturally in the tunnel, as they were in the experiment.

Approximately 2m of smooth channel was required before the boundary layer developed properly (Figure 4-8). If this profile was then returned as

the inlet condition for a smooth-channel case, the profile broke down and again took approximately 2m to fully develop again. This suggests that for the cube case, a 2m long inlet would be required to develop the boundary layer. This would require a large number of cells simply to reproduce a known inlet profile, so an alternative method was sought giving the same profile for less computational cost.

Better results were obtained with a sand grain roughness height of 0.1mm on the walls (Figure 4-7). This was found to maintain the turbulence profile if the experimental inlet profiles were used. Higher values of sand grain roughness height resulted in too much turbulence energy production.

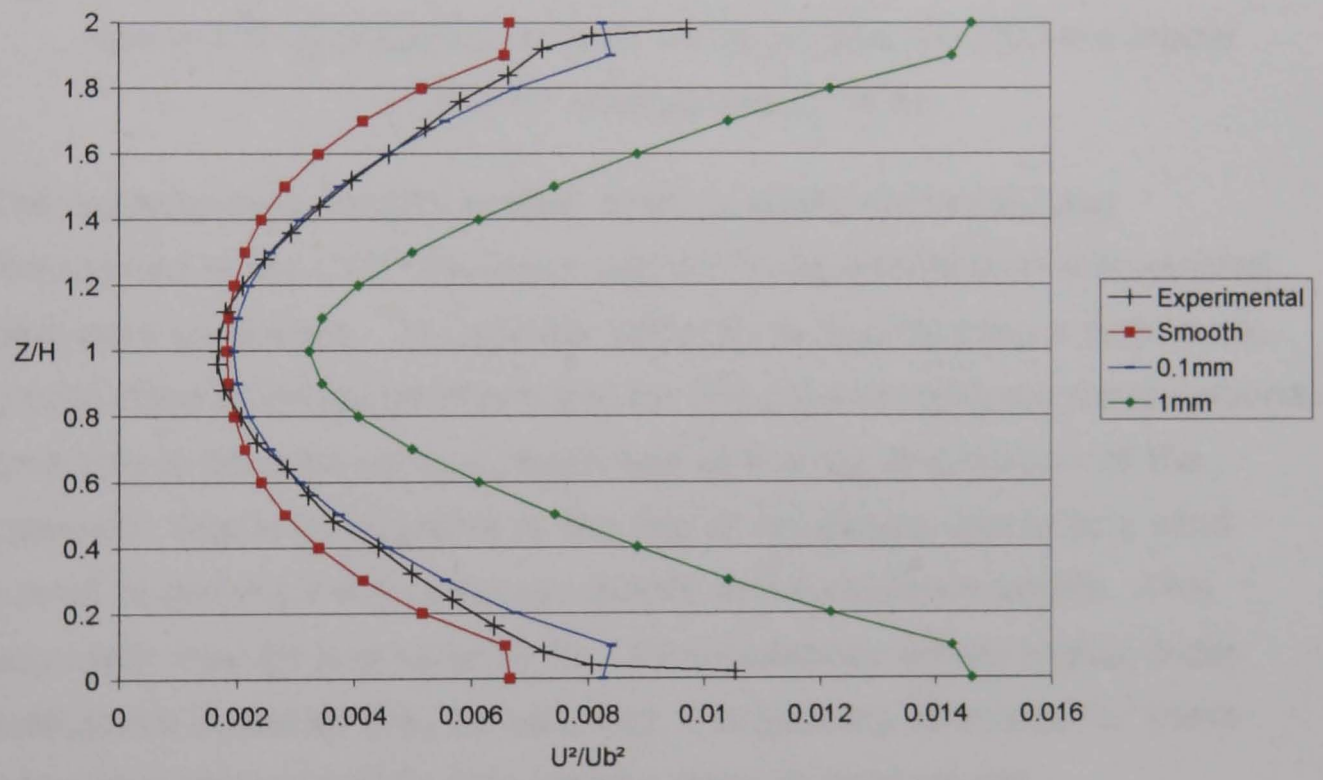

Figure 4-7: Comparison of turbulence profiles for RNG k-ε model (1000mm downstream of inlet)

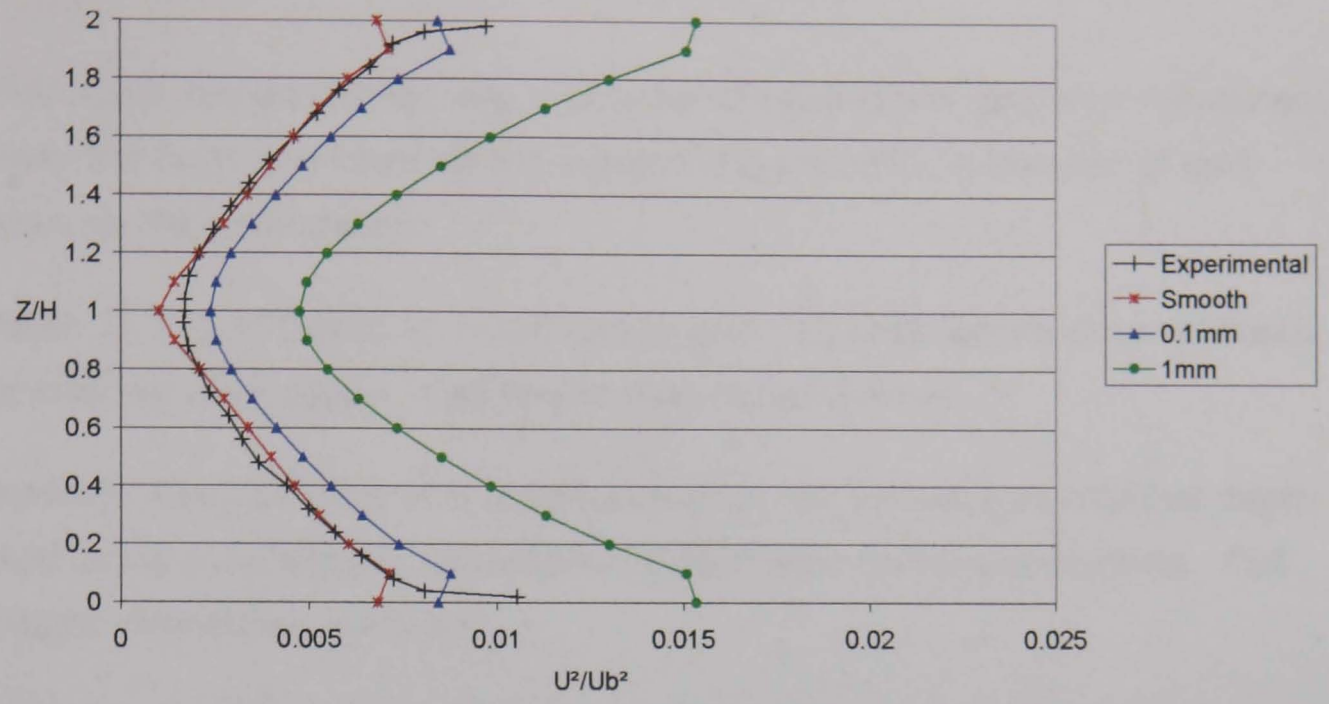

Figure 4-8: Comparison of turbulence profiles for RNG k-ε model (2200mm downstream of inlet)

The experimental velocity profile, then, is easily generated and maintained in the CFD simulation with little dependence on the selected boundary conditions. The greater difficulty is in producing a turbulence profile close to the experiment and for the sake of reducing computational time this is done by using a rough wall at the top and bottom of the channel. This is comparable to the use of roughness blocks in a wind tunnel to generate the required velocity and turbulence profile. This approach may be less suitable for LES simulations where higher order turbulence statistics may be required, but appears adequate for these RANS simulations where only k and ε must be reproduced.

4.3.2. Cube Studies

Once a consistent boundary layer had been developed the studies involving the cube could begin. Boundary conditions were as used previously with a roughness height of 0.1mm.

Mesh Design

The mesh design chosen was a structured hexahedral grid with refinement near the cube and towards the walls of the channel. A number of grid layouts were compared:

Mesh 1: 100,000 cells in a continuous grid. 15 cells across channel depth and along cube edges. Cell height over cube: 2.5mm

Mesh 2: 810,000 cells in a continuous grid. 30 cells across channel depth and along cube edges. Cells concentrated near corners of building. Cell height over cube: <0.5mm

Mesh 3: 725,000 cells in discontinuous grid: 15 cells across channel depth in the upwind portion, changing to 50 cells across depth and along cube edges near the cube. The transition point was 1 cube height upwind of the cube, where the profile was changing significantly in space but the resolution before the transition was considered sufficient to avoid grid dependence problems. Cell height over cube: 0.1mm

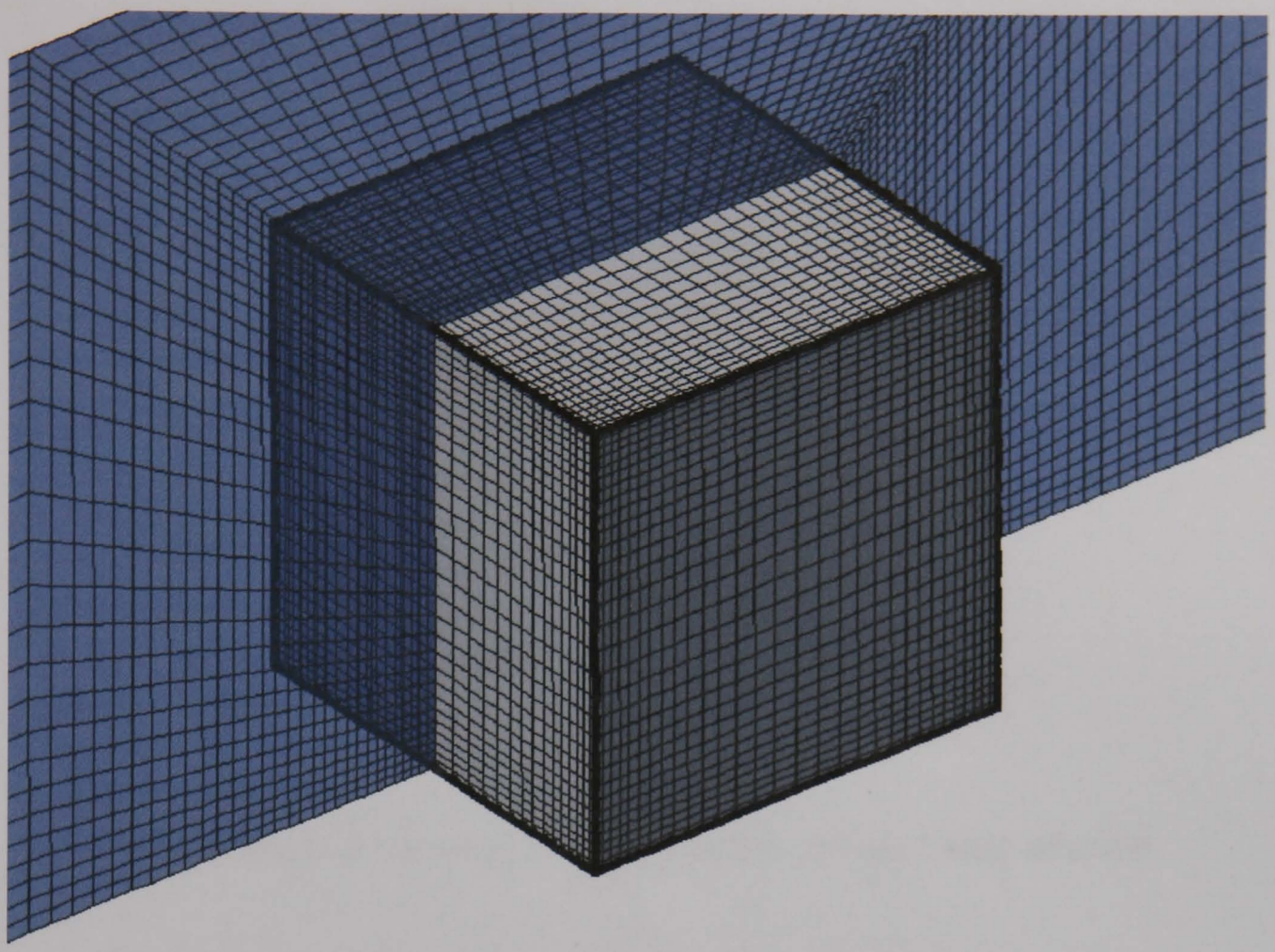

Figure 4-9: Computational Mesh 1, showing refinement near cube

Velocity Results

Velocity results are presented in Figure 4-10 to Figure 4-14. These simulations show good agreement with experimental velocity results upstream of the cube demonstrating accurate prediction of the blockage effect caused by the cube. The finer grids (grids 2 and 3) produce a closer fit to the experiment near the front face and centreline of the cube, better representing the separation region over the cube. In the wake region, velocity results are less accurate and vertical velocity results are generally less accurate than longitudinal results.

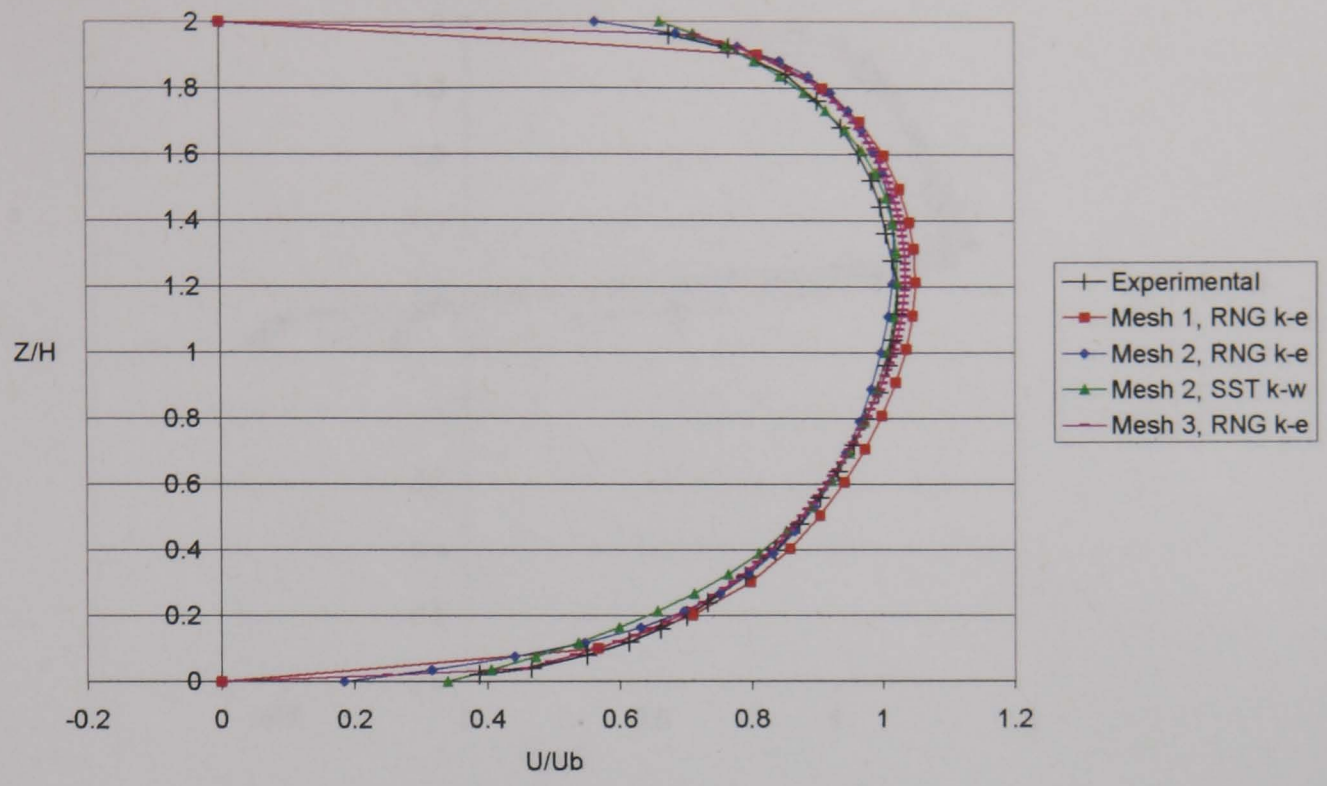

Figure 4-10: Horizontal velocity profiles 1H upstream of cube

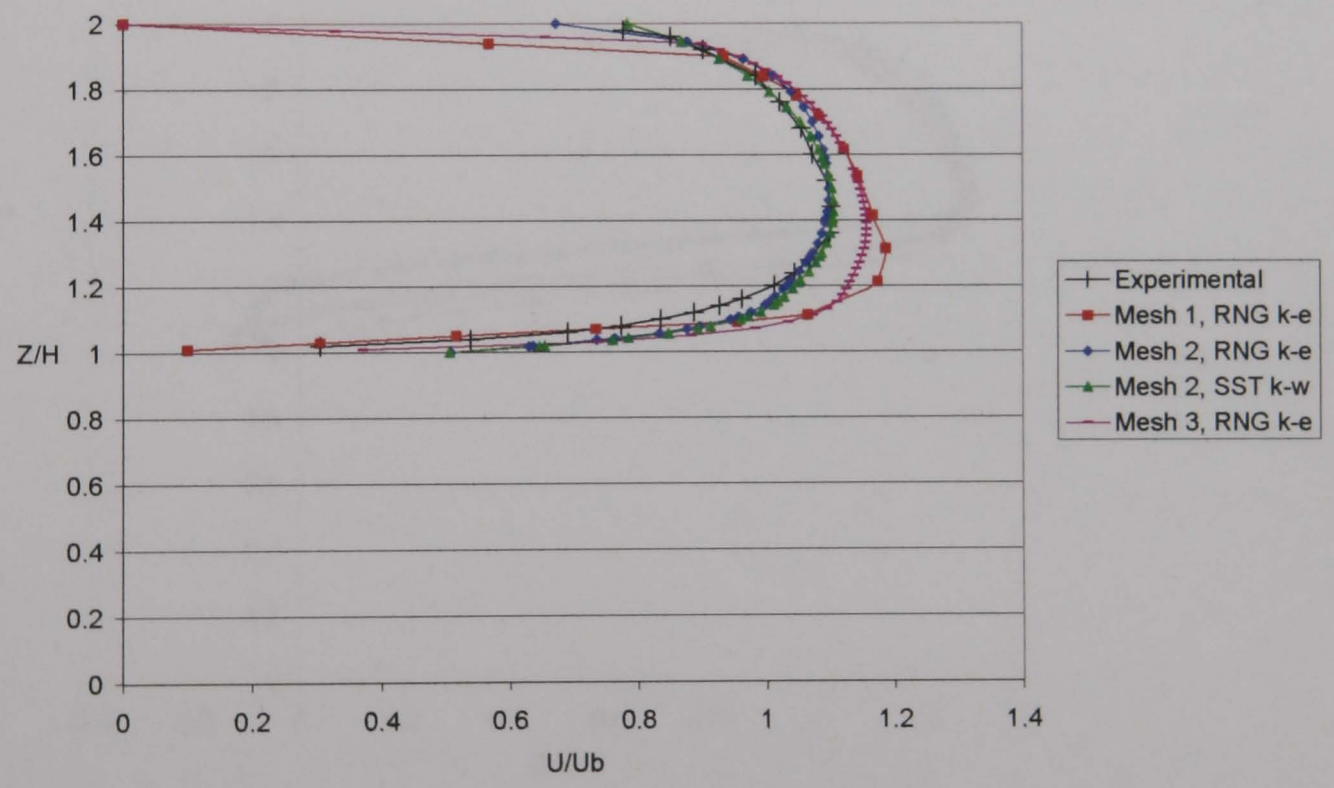

Figure 4-11: Horizontal velocity profiles at upstream face of cube

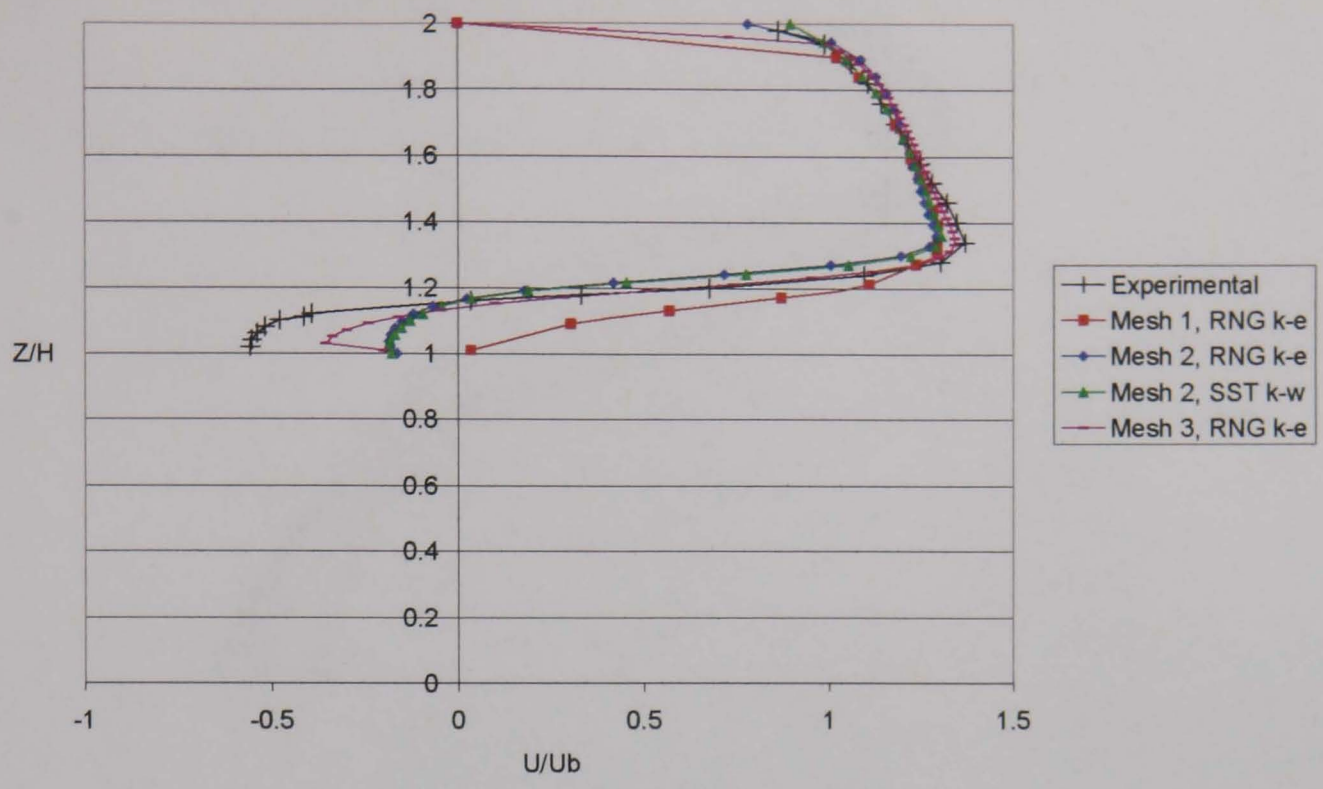

Figure 4-12: Horizontal velocity profiles at centreline of cube

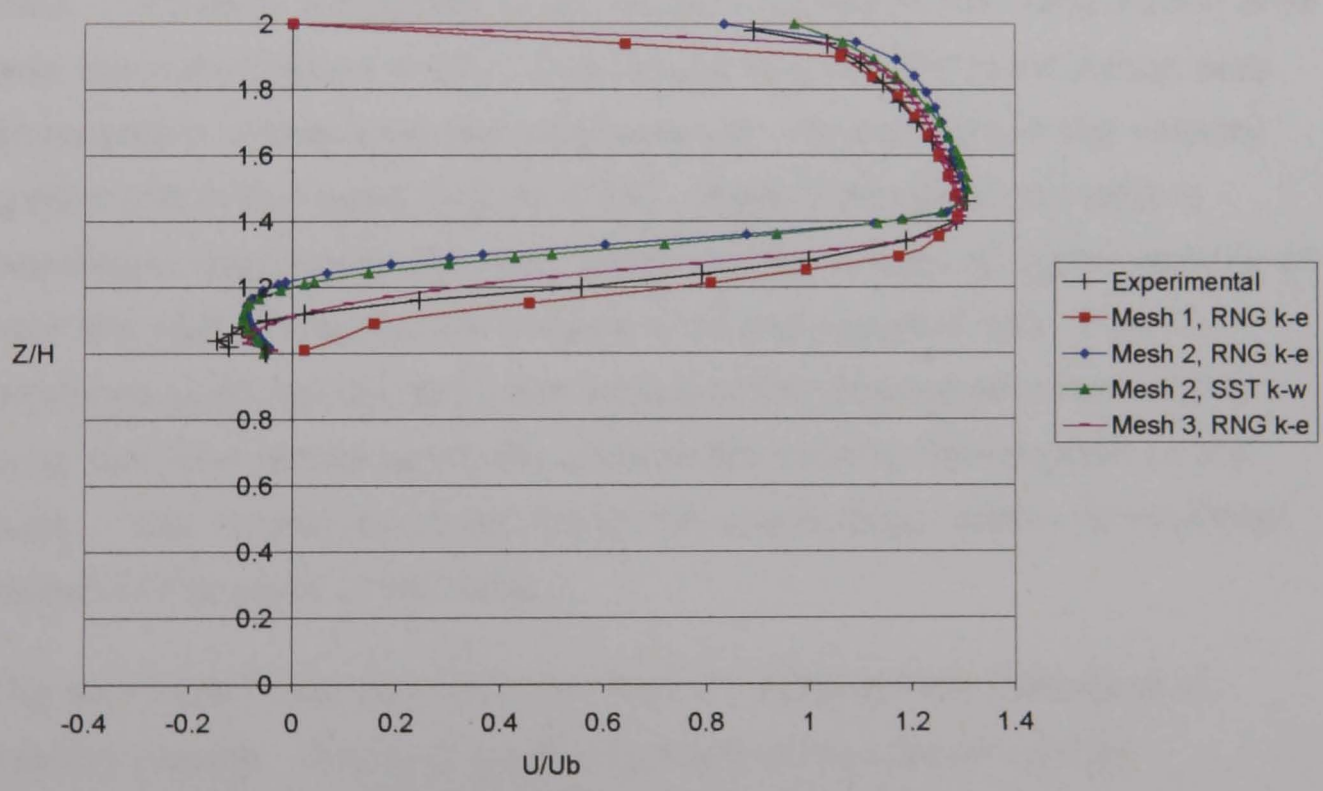

Figure 4-13: Horizontal velocity profiles at downstream face of cube

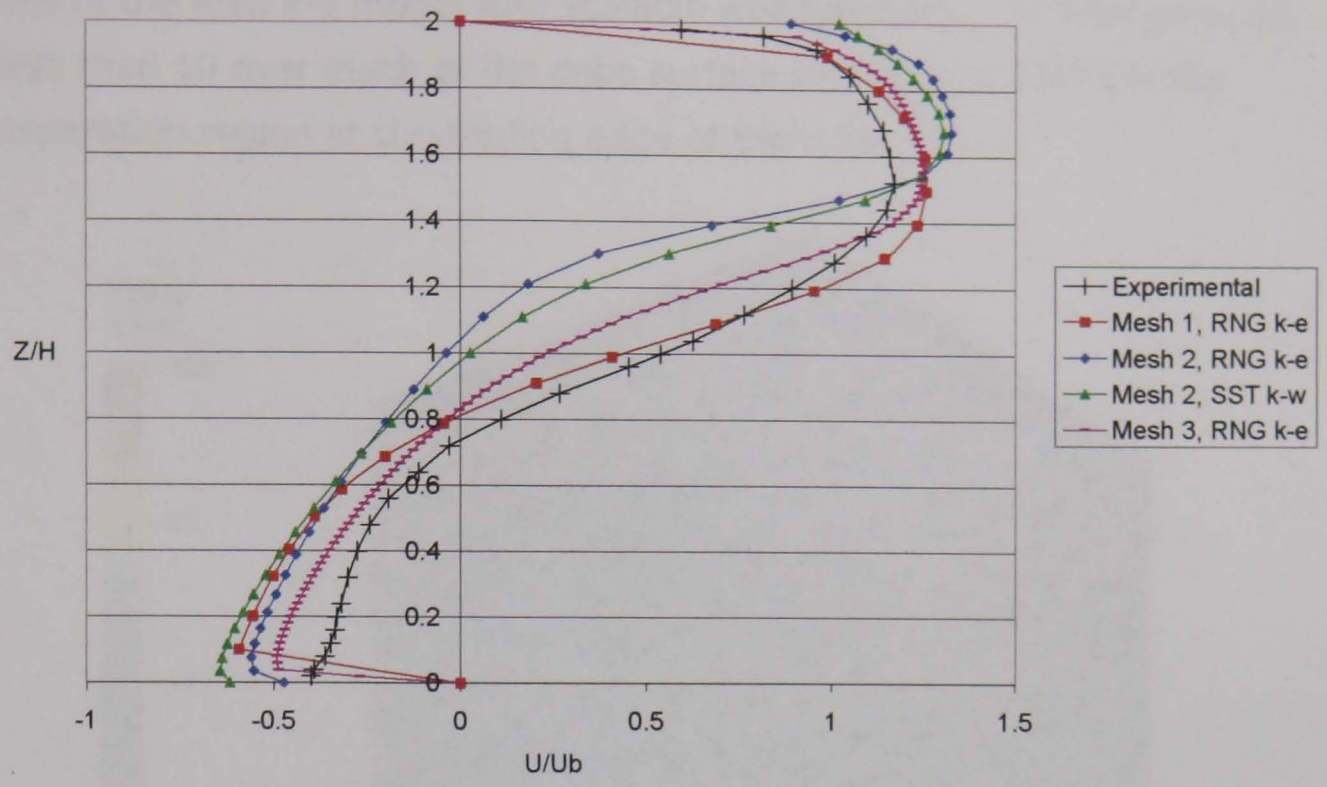

Figure 4-14: Horizontal velocity profiles 1H downstream of cube

Mesh 1 is clearly too coarse to adequately represent the recirculation area over the cube (Figure 4-12). This results in a smaller recirculation area downstream of the cube and a consequent improvement in the velocity predictions in the wake (Figure 4-14). Mesh 2 produces too large a separation region over the roof, which results in a jet of higher velocity air near the roof of the channel (Figure 4-13 and Figure 4-14). Mesh 3 produces good results up to and including the downstream face of the cube but then results gradually deteriorate moving downstream of the cube. This is believed to be due to the overly large, stable recirculation region in the wake of the cube.

The k-ω model was also used for Mesh 2, yielding little difference in velocity results. This may be due to the high degree of vertical confinement and sharp definition of separation points in this study. However, Table 4-2 shows that the k-ω model resulted in improved prediction of the separation region behind the cube, with a smaller separation region compared to the RNG k-ε results.

For Mesh 2, the first cell height on the cube surface was around 0.5mm to give a y^+ value of less than 100 on the cube surface, consistent with the

use of the RNG k-ε model with scalable wall functions. y^+ was generally less than 10 over much of the cube surface and around 50-75 in the separation region at the leading edge of the cube.

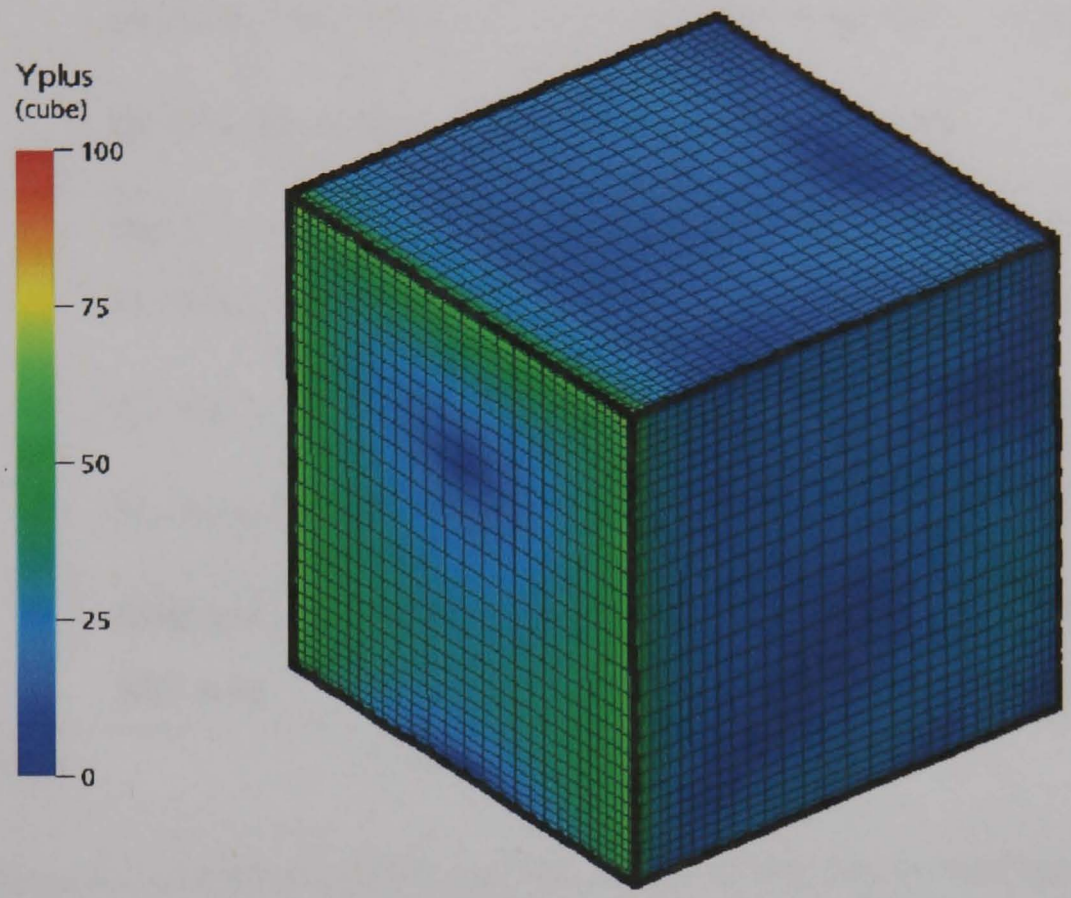

Figure 4-15: y^+ values for Mesh 2 with the RNG k-ε turbulence model

Calculation Method		x_{FI}	x_T	x_{R1}	Grid	Near-wall resolution
LES	UKAHY3, Smag	1.29		1.70	165 × 65 ×97	0.0125H
	UKAHY4. Dyn	1.00		1.43	165 × 65 ×97	0.0125H
	UBWM2, Smag	0.81	0.837	1.72	144 × 58 × 88	
RANS	Std. k-ε; WF	0.65	0.43	2.18	110 × 32 × 32	0.01H
	KL- k-ε ;-WF	0.64		2.73	110 × 32 × 32	0.01H
	TL- k-ε	0.95		2.68	142 × 84 × 64	0.001H
	TL-KL- k-ε	0.95		3.40	142 × 84 × 64	0.001H
	RNG k-ε	**0.76**	**-**	**3.9**	**180 × 130 × 30**	**0.02H**
	SST k-ω	**0.72**	**-**	**3.05**	**180 × 130 × 30**	**0.02H**
Experiment		1.04	-	1.61		

Table 4-2: Comparison with results of LES Workshop on Martinuzzi Cube (Rodi 1997) New results in bold type

The new results shown in Table 4-2 show that these new simulations use a very similar downstream resolution but significantly finer crossstream resolution than previous RANS studies. The near-wall resolution is comparable to the previous standard k-ε studies but due to the use of scalable wall functions it was possible to use a coarser resolution than in the two-layer model (TL) results.

The new RNG k-ε results show an even longer mean wake separation bubble than was seen for the majority of the previous studies. While the k-ω results were better in this respect than the k-ε results, they were still further from the experimental value of 1.61 than previous LES results.

The range of results given in Table 4-2 shows a number of areas where CFD results for bluff bodies are currently formulation dependant. Although the size of the upstream and downstream separation bubbles is not in itself significant for the structural loading of the body, it will affect

neighbouring bodies in more complex urban terrain and the size of the mean separation regions on the roof and sides of the cube will have a direct effect on structural loading in these areas.

The LES results show reduced variation in this respect, although there is a range of ±20-25% in the size of the upstream separation bubble, expressed as a percentage of the experimental value. The RANS results with much greater variation, most notably in the downstream results, suggest that separate validation studies will be required for RANS simulations involving multiple bodies. This is beyond the scope of the present work.

The upstream separation region is larger in these studies than in the standard k-ε results but smaller than was seen in the LES, TL or experimental results. The consequence of this for the pressure values is seen below.

Pressure Results

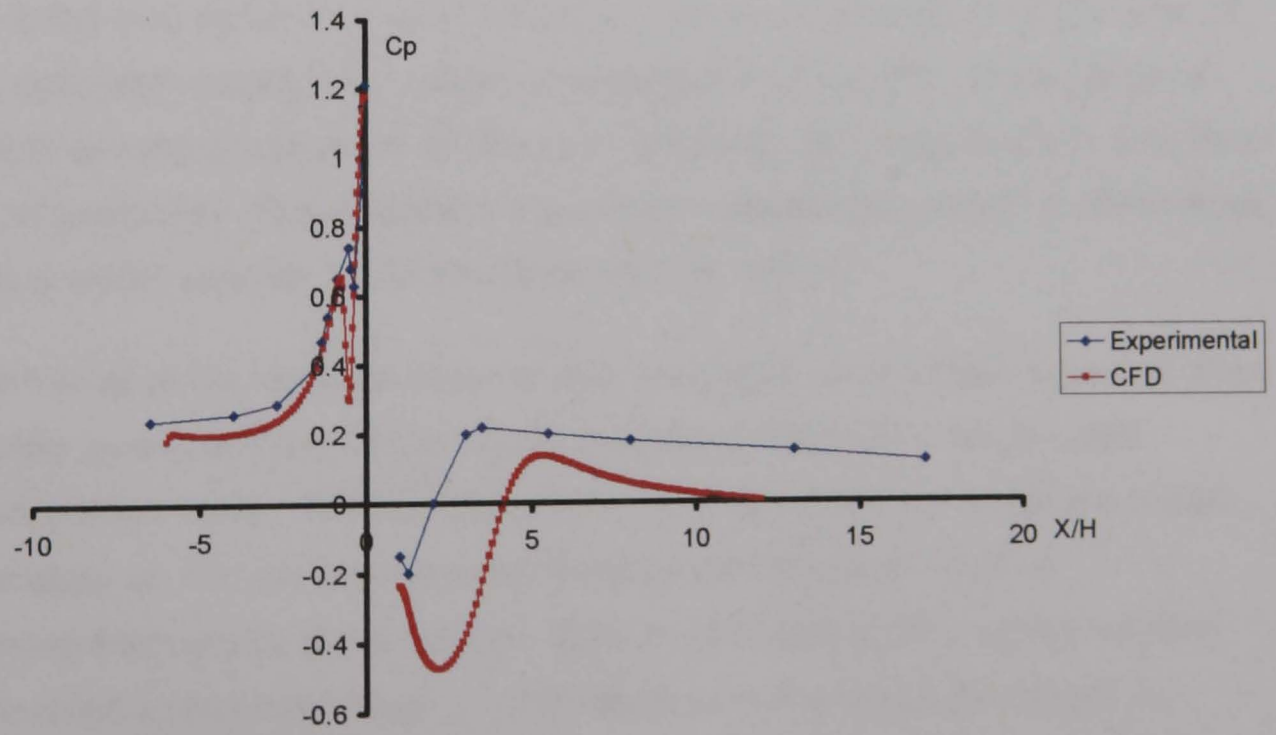

Figure 4-16: Pressure results up- and down-stream of the cube: Mesh 2 with RNG k-ε model

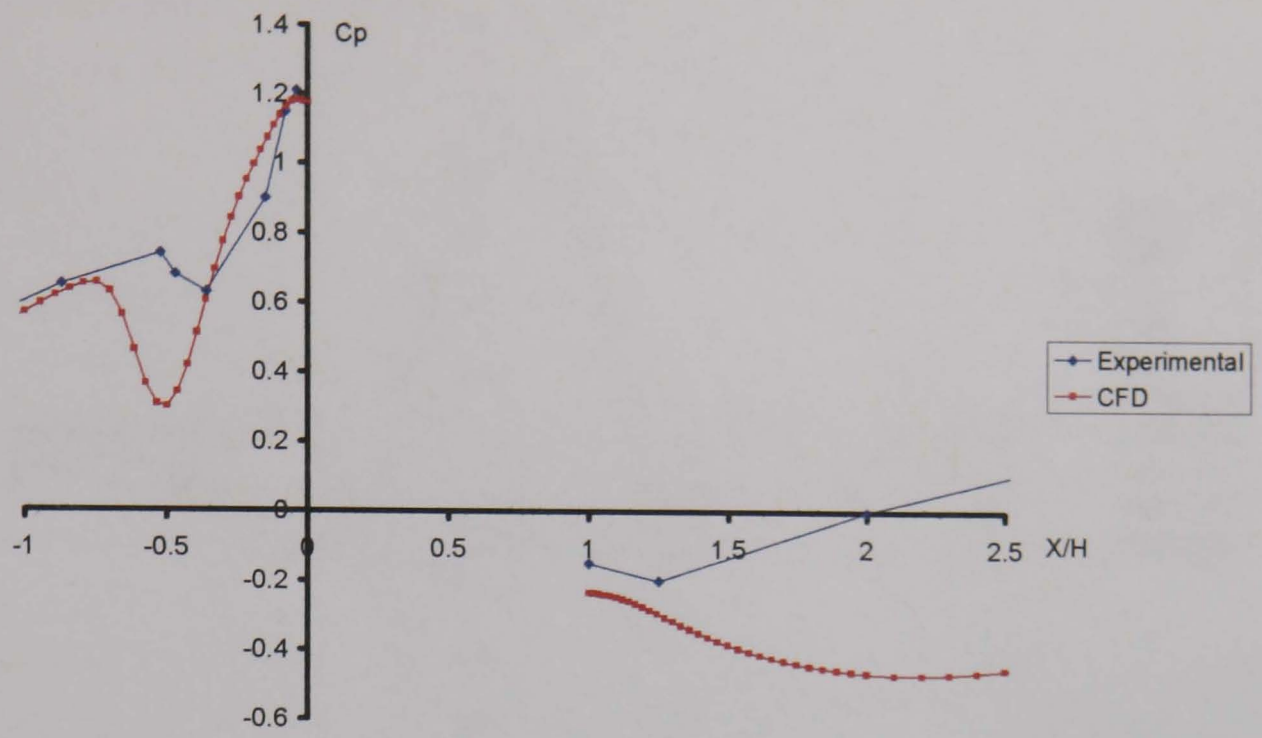

Figure 4-17: Detail of pressure results up- and down-stream of the cube: Mesh 2 with RNG k-ε model

The pressure plots Figure 4-16 and Figure 4-17 show that floor level pressure predictions are remarkably accurate immediately at the foot of the cube and within 0.3 cube heights. The underprediction of the size of the upstream separation region is associated with a shift in the area of lowest pressure upstream of the cube and with the magnitude of this local dip in pressure. This suggests the smaller separation region is associated with a lower velocity of recirculation in that region

Downwind of the cube, suction is overpredicted on the back face and then greatly overpredicted in the wake, indicating the overly large wake recirculation zone. Further downwind, the use of a zero pressure outlet boundary at X=12H results in an incorrect pressure prediction downstream of the wake region. This is well beyond the region we are interested in but may have a small impact on the absolute values of pressure in the wake.

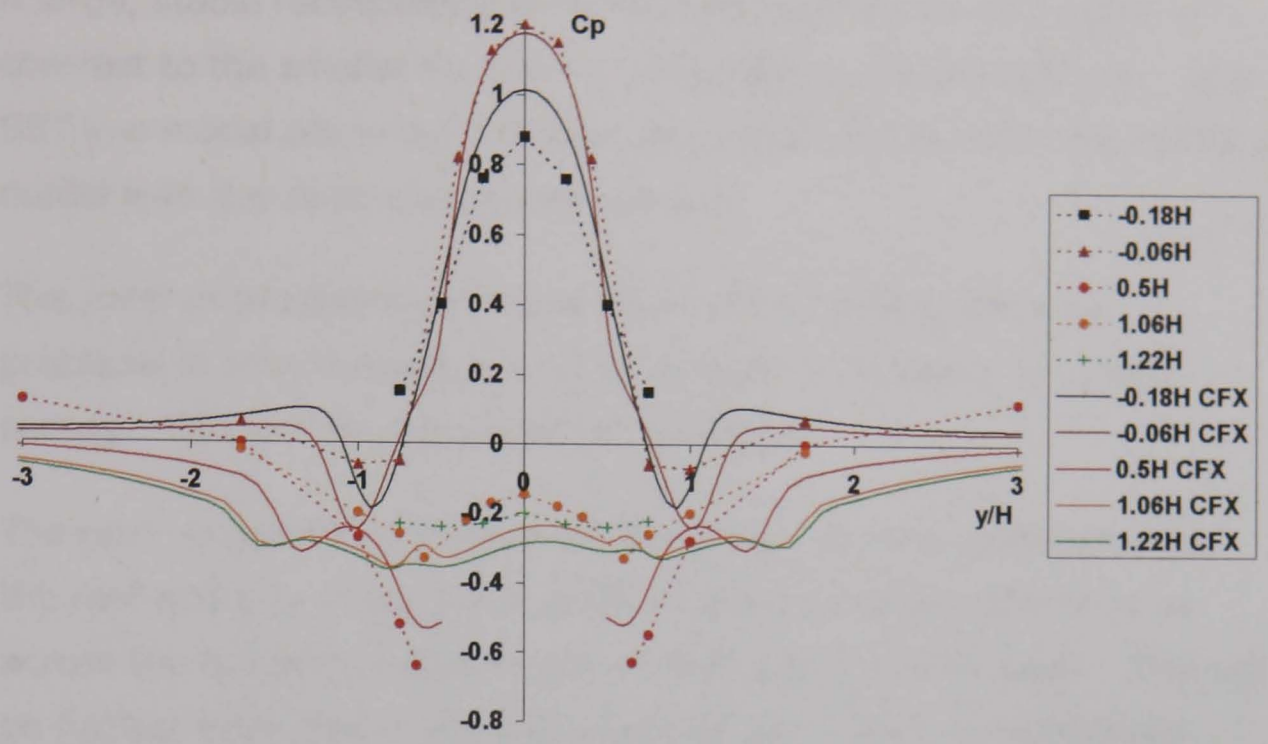

Figure 4-18: Cp at floor level around cube: experimental and computational: Mesh 2 with RNG k-ε model

The cross stream pressure distribution at the tunnel floor is shown in Figure 4-18 for various streamwise positions, in each case measured from the front face of the cube. The agreement is excellent for the front face of the cube and acceptable for the centreline near the cube surface and the rear face. Further from the cube in the cross stream direction suction is overpredicted by the CFD results, suggesting too high a velocity near the floor in these areas caused by overly large separation regions around the cube forcing more air to move around the sides.

4.4. Conclusions

The major points of note when comparing the experimental and RANS results are:

- Overall flow features were reproduced in the RANS results including flow stagnation, separation and reattachment. Average velocity values were well reproduced by the RANS simulations up to and including the back face of the cube. Wake velocities were less well predicted due to the overprediction of the size of the wake separation region.

- A large, stable recirculation zone was produced behind the cube, in contrast to the smaller fluctuating zone seen in the experiments. The SST k-ω model produced a smaller separation bubble than the RNG k-ε model with the same computational grid.

- This error in predicting the wake recirculation zone could pose problems in simulating flow around multiple buildings in an urban setting. This will require separate validation.

- The error in predicting the size of separation regions, particularly on the roof and side walls, will also affect the distribution of pressures across the building surface and therefore the structural loads. This will be further examined in the following chapter, where more detailed surface pressure results are available.

- The upstream recirculation zone was smaller in the CFD results, resulting in local changes in the velocity and pressure results.

- Except for this local error, good predictions were made of pressure upstream and on the front face of the cube.

- Suction pressures at the centre of the side faces were overpredicted.

- Suction pressures at the foot of the back face of the cube were slightly overpredicted. If typical of the whole rear face, this would lead to a small overprediction of the net force on the cube.

- An asymmetric wake was produced, resulting in some asymmetry in the wake pressure and velocity results. This will be further investigated in the next section.

These factors result in an error in prediction of the pressure and velocity field around the cube. Although mean surface pressures on the front and back face of the cube are well predicted, the magnitude and size of the low-pressure regions around the cube are incorrectly predicted. In complex buildings where a number of shapes are combined, errors in predicting the recirculation region from one part of the building will affect adjacent and downwind building parts.

Errors in turbulence production on the cube boundary mean that the CFD turbulence values cannot be used to predict fluctuating pressures on the cube surface. No account has satisfactorily been made of the effects of building-induced turbulence on surface pressures. If these effects are to be accounted for then it must be by empirical methods (e.g. code-based methods) or by an alternative numerical method such as a detailed LES/DES or DVM study of the area of interest.

Although the LES results reviewed by Rodi (Rodi 1997) and shown in Table 4-2 are better in the mean, they still exhibit significant formulation-dependent variation in prediction of mean separation regions, and allowance must be made for this if LES is to be used in design. There is a lack of detailed information on fluctuating velocity and pressure in the published experimental results so it is impossible to draw further conclusions on the validity of LES in predicting fluctuating wind loads.

This study demonstrates the capabilities and limitations in using CFD to predict mean flow velocities around a bluff body in clearly defined conditions. However it lacks the detailed mean and fluctuating pressure information needed for structural design and is not fully representative of full-scale buildings in a thick atmospheric boundary layer.

5. Silsoe Cube

The cube in a channel case allowed detailed study of the velocity field around a bluff body in carefully controlled conditions. It gave detailed velocity and pressure results at a series of points around the cube and allowed comparison with previous computational results. However it lacks the detailed pressure information on the cube surface required for structural engineering. The Silsoe cube experiment included pressure measurements across the cube surface and additionally allows an examination of the steps involved in moving to full-scale flow problems.

Developing a stable oncoming flow and resolving the boundary layer around the body both become more challenging at large scale. The accurate prediction of surface pressures and therefore structural forces is a further challenge and forms the core of this research.

As discussed in section 2.5.2, a number of full-scale tests have been performed to provide reference data on structural wind loads. The Silsoe 6m cube experiment is one of the most recent and was specifically designed to provide a comparison with CFD. Although the geometry is simple, the flow patterns around the cube are complex, and it is therefore chosen for this study.

This chapter discusses the experimental setup and compares new CFD results with experimental and wind tunnel results, codes of practice and published CFD results. Flow instability is investigated in terms of its effect on structural pressures and forces, examining whether traditional ways of dealing with such instabilities can be applied in this field.

5.1. Full Scale Experiment

The experimental layout is described in section 2.5.2 and consists of a 6m cube in an open field with a well defined fetch. Pressure tappings were positioned along the vertical and horizontal centrelines of the cube and in an array of points in the one corner of the roof. The cube could be

rotated through 360°, allowing effectively allowing measurement at any position on the cube with a consistent oncoming fetch.

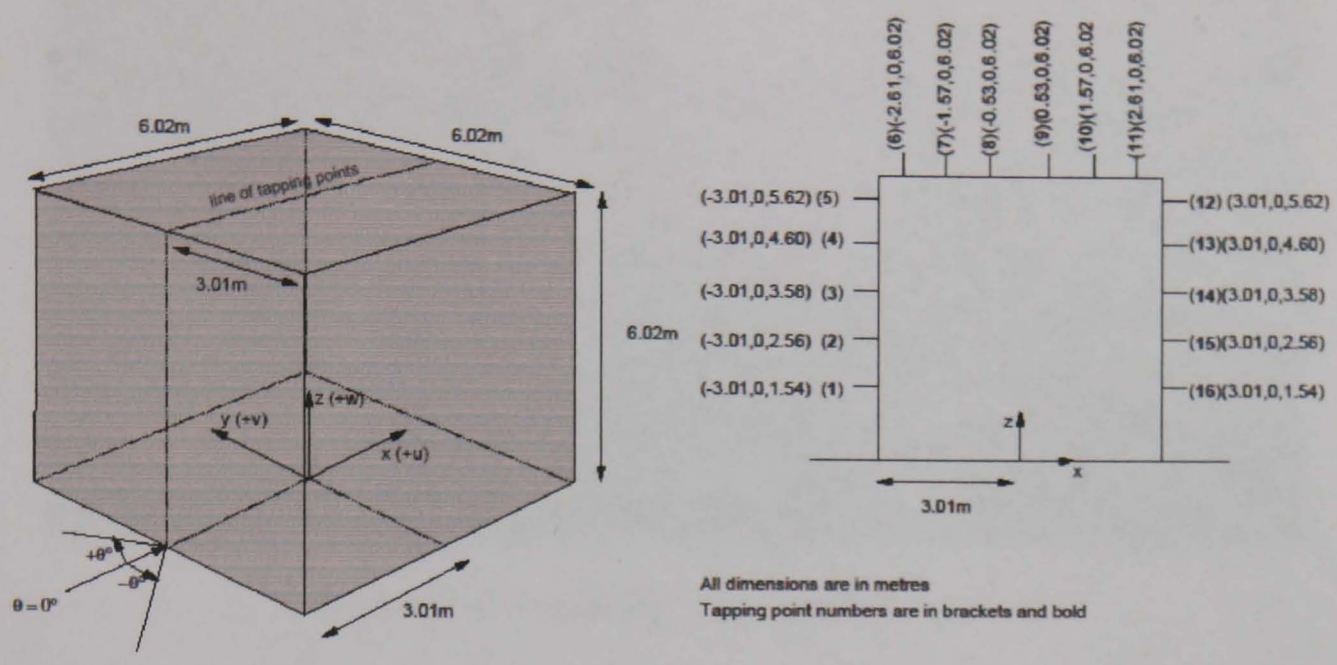

Figure 5-1: Silsoe 6m cube dimensions and pressure tap locations (From CWE2000 competition CD)

Mean and RMS pressures were calculated at all tapping points (Figure 5-1). Velocity was measured at numerous locations around the cube (Figure 5-2) at 1m, 3m and 6m height, at distances of 0.1 cube heights and 1 cube height from the cube faces and 0.1 cube heights above the roof. The local mean and standard deviation were calculated for each point.

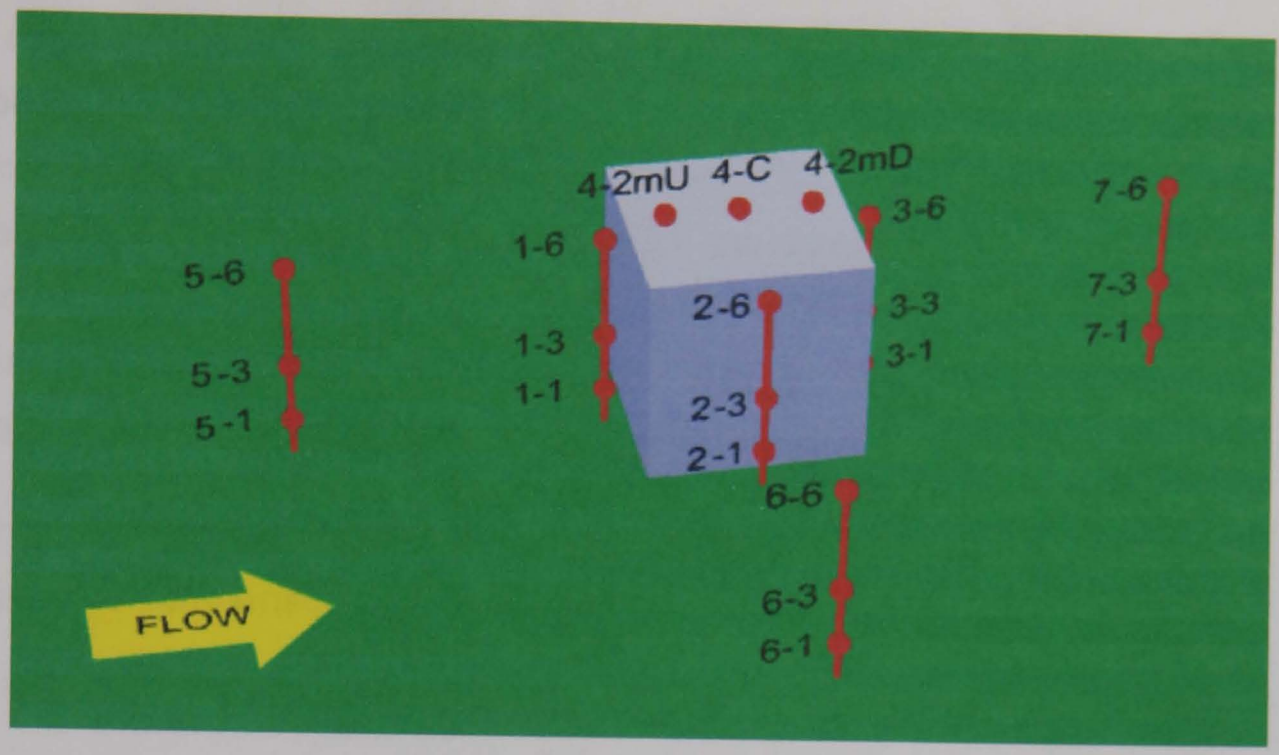

Figure 5-2: Velocity measurement points

5.2. Codes of Practice

For comparison with the CFD and experimental results, design pressures have been calculated using the British and European Standards for wind loading on buildings.

5.2.1. Calculation to BS 6399 Part 2: 1997

Wind loads were calculated according to the current British Standard for wind loads, BS 6399 Part 2:1997(BSI 2002). As a simple building, the 6m cube lends itself well to assessment using this code.

Equivalent quasi-static pressure coefficients are given by the code independent of wind speed. The pressure distribution is simplified into a series of zones, intended to give safe (upper bound) design values for each zone while avoiding excessive conservatism. The size and distribution of the zones depend upon the size and layout of the building. The pressure coefficients specified in BS6399-2 assume a diagonal dimension of 5m, providing a reduction factor for greater loaded areas. No increase is specified for peak local loading on structural or cladding elements smaller than 5m.

A number of options are given by the code for working out pressure coefficients and wind strengths. These range from highly conservative, simplified methods based on wind blowing from any direction to more sophisticated methods which separately calculate pressures for winds blowing in from each of twelve directions, at 30 degree intervals. This more detailed 'directional method' was used for this study, providing equivalent quasi-static pressures assuming a constant wind direction.

The calculations are presented in Appendix A and are summarised in the pressure comparison figures below.

5.2.2. Calculation to Eurocode 1

The structural Eurocodes are currently under development. Eurocode 1 (CEN 2002) has now completed its three year consultation stage and is passing from pre-standard (officially designated ENV) form to draft (prEN) form, for approval by national states. At the time of this research, the conversion process was not complete and the final (EN) version of the code may differ slightly from that used in this study.

Eurocode 1 does not allow calculation for a specific wind direction and the pressure coefficients therein and shown in Appendix B allow for wind from any angle relative to the building. This means the results are more conservative than those given by the British Standard and not directly comparable with CFD and full-scale results for a single wind direction. Another difference between the British Standard and the Eurocode is that the Eurocode gives two sets of pressure coefficients: local coefficients for use on small areas of around $1m^2$ and general pressure coefficients based on an area of $10m^2$.

5.3. CFD Simulations

A series of CFD simulations was run with the aim of assessing the use of standard industrial CFD methods in structural engineering. This involved trying to reproduce the results of the CWE2000 competition and then assessing the improvement possible using more recent CFD codes. The key objective was to extend previous work, which primarily involved

comparing mean pressure coefficients, to look at structural loads and the implications for structural design.

The turbulence models and simulation setup are discussed in section 3 and briefly summarised below. Key simulation parameters are highlighted and their influence on the results is discussed. Recommendations are made for how CFD can best be used in predicting structural loads and remaining areas of uncertainty are set out.

5.3.1.CFD parameters

Boundary Conditions

The cube surface was set as a smooth surface. A study was run to test the effect of changing this to a rough surface with a low roughness height (0.005m) but this was found to have almost no effect on local surface pressures or mean or fluctuating velocity distribution, showing the simulation to be relatively insensitive to the detailed wall treatment.

The inlet boundary was set as a logarithmic velocity profile to match that given for the site (Figure 5-3) as set out in the competition CD (SRI 2000).

$$v = \frac{u_*}{\kappa} \ln\left(\frac{z}{z_0}\right) \qquad \textit{[equation 5-1]}$$

Where u_*/κ was equal to 1.50 m/s.

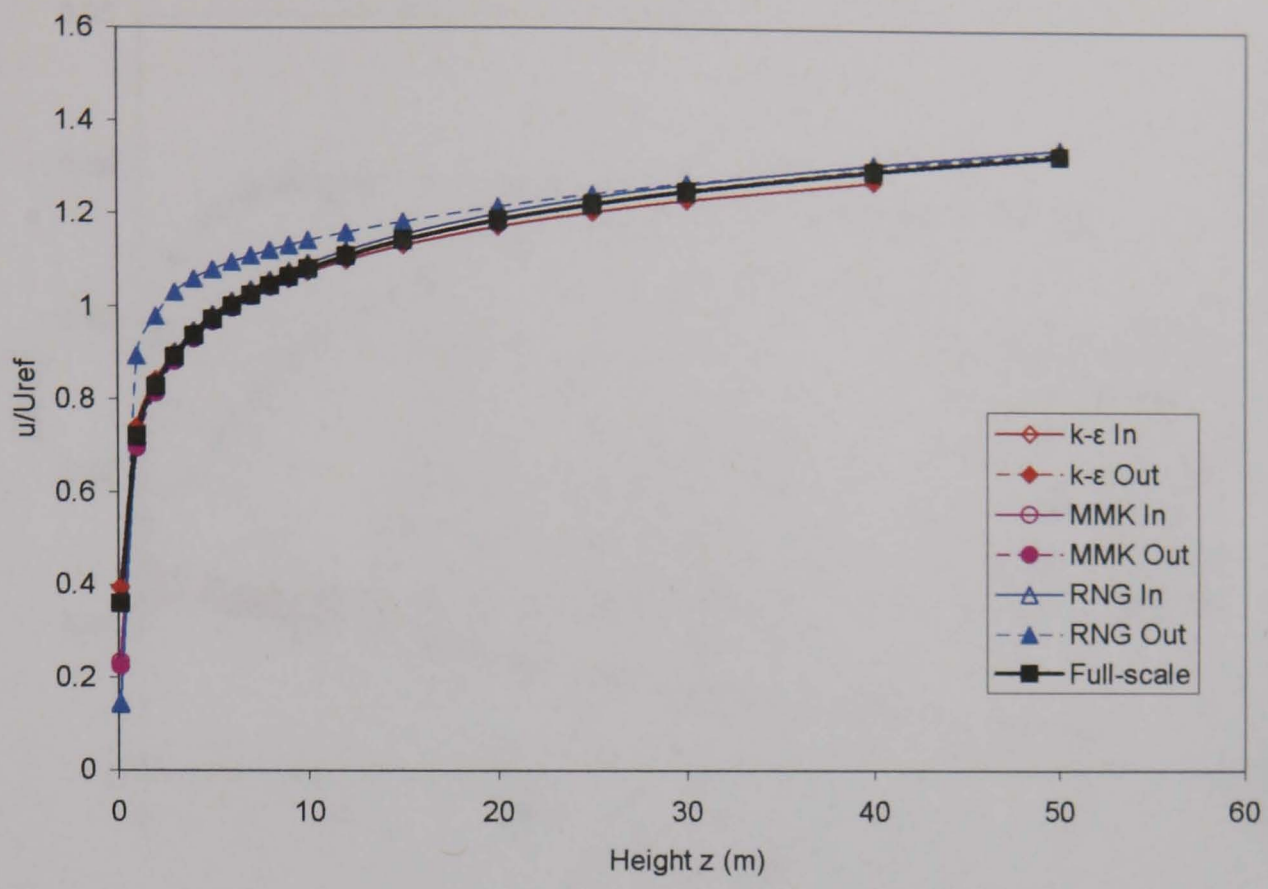

Figure 5-3: Velocity profiles from the CWE 2000 competition (Hoxey et al. 2002)

The average of the site turbulence ratios in the three directions was initially chosen, i.e. $u/U_{ref} = 0.15$. This was revised at a later date to provide a more stable boundary layer. Values used in the CWE competition are shown, together with the full-scale results in *Figure 5-4* below. Details of the revised boundary layer are given in section 5.3.2 below.

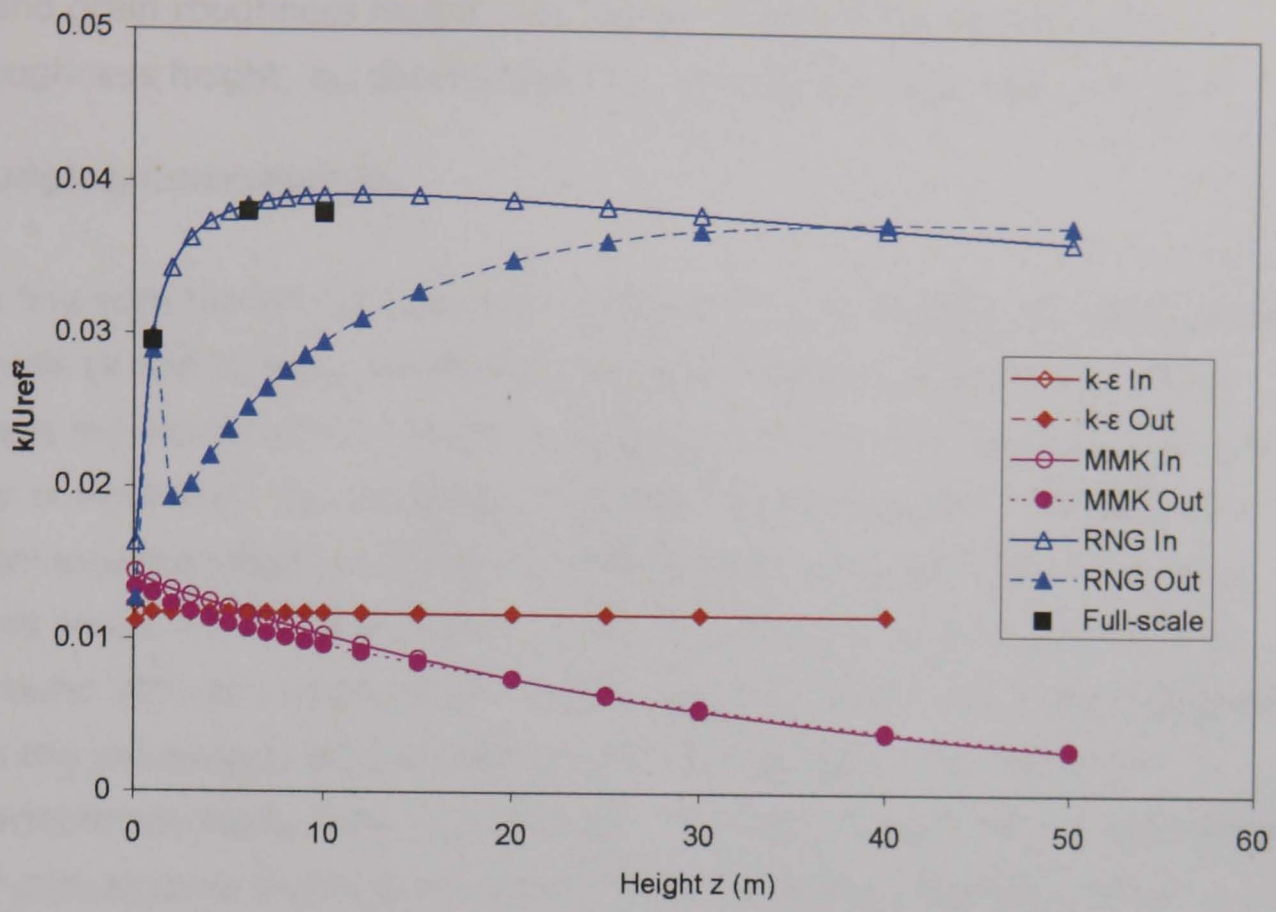

Figure 5-4: Turbulent kinetic energy profiles from the CWE 2000 competition (Hoxey et al. 2002)

5.3.2. Boundary Layer Simulation

Standard turbulence models used in commercial CFD have largely been developed for aerospace and motor industry use representing vehicles moving through previously still or slowly moving air. In these cases turbulence develops in a boundary layer on the surface of the body with length scales limited to the thickness of that boundary layer. The atmospheric boundary layer contains turbulence on a great many scales, bounded by a varying rough surface at the floor and the free stream above. Previous work modelling the atmospheric boundary layer is discussed in section 3.1.3 and shows that although velocity profiles can be accurately represented in CFD simulation, full scale turbulence profiles are more difficult to maintain while the full spectrum of atmospheric turbulent scales cannot be represented by standard turbulence models.

A set of CFD simulations was run to try to improve this prediction by using a more accurate representation of the atmospheric boundary layer. The full domain size was used with no cube. As discussed in section 3.1.3 the

sand grain roughness height was set to 7.5 times the aerodynamic roughness height, z_0, determined from the full-scale data to be 10mm.

Judging Convergence

In line with the aim of this set of simulations, the velocity and turbulence levels (k and ε) were monitored during the solution of each run. They were monitored at the reference height of 6m and also at a height of 1m for comparison. As discussed in section 3.1.7 a standard industrial CFD convergence target would be to achieve RMS residuals of $1x10^{-4}$ or less. This would have led to an error in ε of around 10% and an error in k of around 20% at a distance of 1m from the floor where the error is defined as the percentage difference from the final variable value once the variable had been observed to settle. The RMS residual at this later stage of convergence was approximately $3x10^{-5}$ and this was chosen as a minimum requirement for convergence of further simulations.

Results

Initial studies setting only the target velocity profile at the inlet and a roughness height on the floor only produced a thin turbulent boundary layer with turbulence intensity reducing towards zero at a height of 10m. This is a limitation of the default wall law used in commercial CFD software and presents a challenge in applying this software to atmospheric flows. This generally results in very low turbulence flow in such studies, producing greater instability in the flow and overprediction of separation.

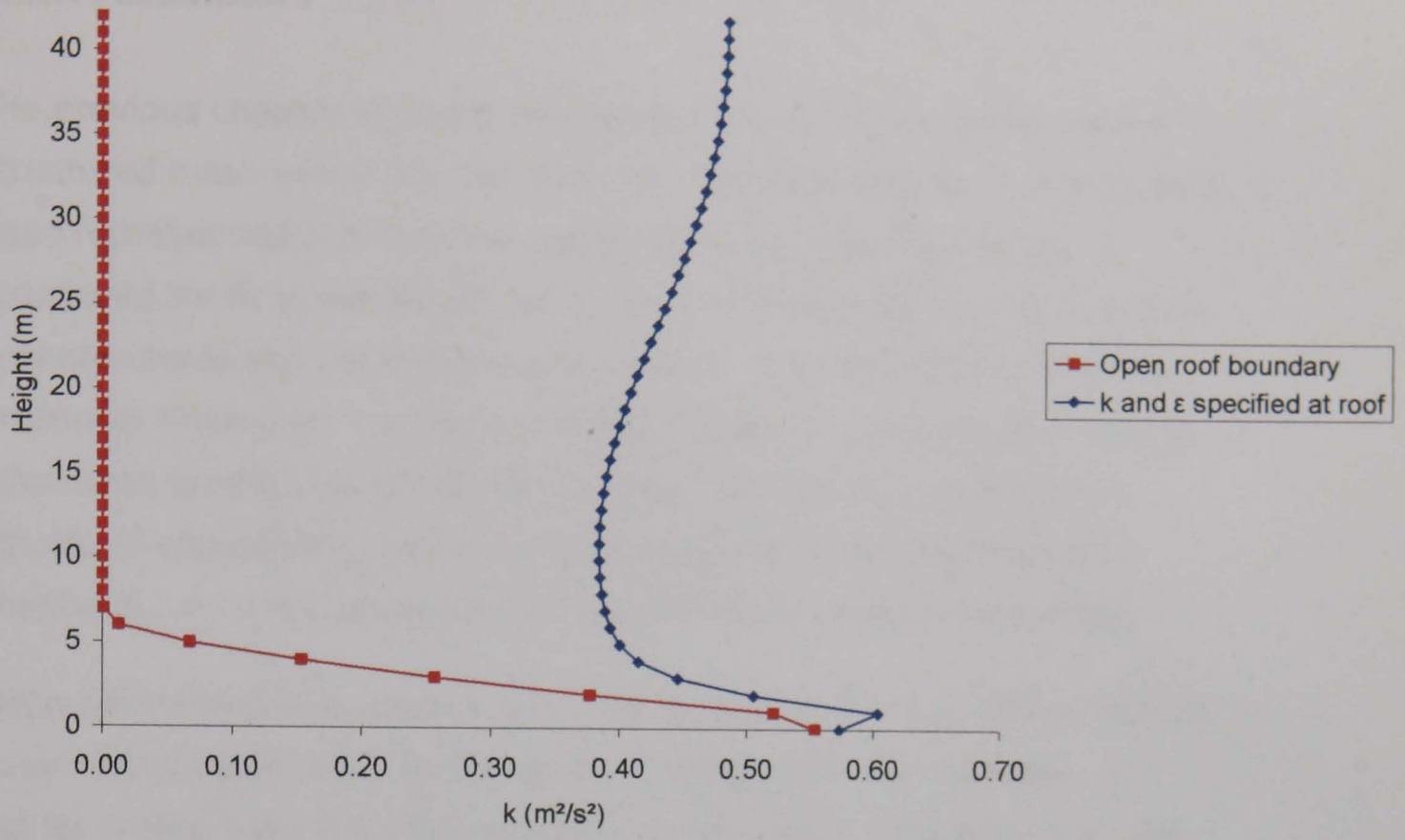

Figure 5-5: Equilibrium turbulence profiles with RNG k-ε model

Using an opening boundary condition with specified values of velocity, k and ε on the sides and roof of the domain better maintains the full turbulent boundary layer. It is not possible (or necessarily desirable) to generate a turbulence boundary layer which matches full-scale turbulence values using standard turbulence models. The aim here is to generate a turbulence profile which is stable and consistent with the roughness length used (Richards et al. 2004).

Starting from a turbulence intensity of 5% at the inlet and sides and then iteratively producing a stable boundary layer produces an improved turbulence profile (Figure 5-5) but there is a significant peak in turbulence intensity in the first cell followed by a significant drop in the next few cells. This is a result of the wall functions used in CFX which generate turbulence in the first cell above the rough surface and will only be improved if new wall functions are implemented in the software.

Mesh Parameters

The previous chapter showing flow around a cube in a channel used a structured mesh which fits well with the rectilinear geometry and gives a good representation of the free stream and attached flow areas. A structured mesh is less beneficial in areas of separated flow as the main flow structures are not aligned to the mesh. Additionally, commercial pressures mean that it is not currently possible to produce good quality structured meshes for the highly complex geometries considered in structural engineering, including the complex building considered in chapter 6. An unstructured mesh was therefore used for this study.

Mesh refinement was used on the cube surface and domain floor with an expanded surface mesh on the floor of the domain and the cube. y^+ values of less than 100 were achieved on the cube, consistent with the use of the wall functions in CFX.

5.3.3.Steady State Simulations

Initial steady state simulations were run to determine appropriate parameters for the later simulations and to investigate key flow effects, notably instability and asymmetry in the flow.

Parameter	**Value**
Simulation type	Steady State
Turbulence model(s)	RNG k-ε with scalable wall functions
Mesh Type	Unstructured
Spatial discretisation	1st Order, 2nd Order and CFX blend factors

Table 5-1, CFD parameters for initial steady state studies

Initial runs were performed using steady-state simulations. These converged to an acceptable level of accuracy when first order discretisation was used but fluctuated when the more accurate second order discretisation was used (see equation 3.2 for a definition of the blend factor used in CFX). Figure 5-6 shows a sample solver residual

trace for the steady state calculations, demonstrating this failure to converge.

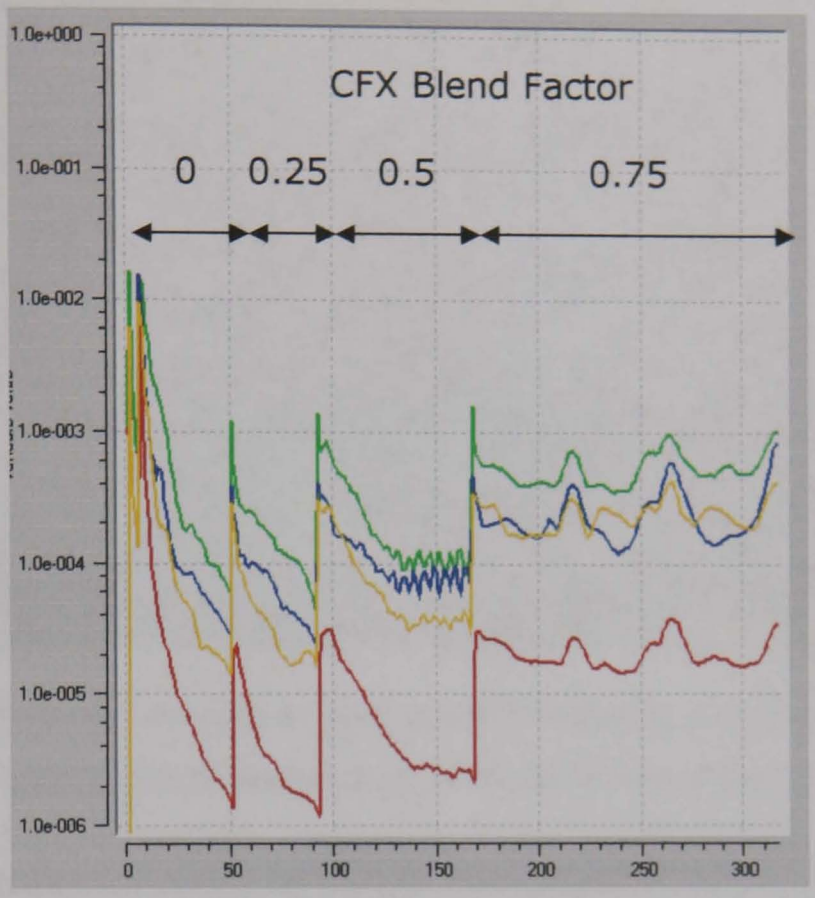

Figure 5-6, RMS solver residuals for steady state calculations showing failure to converge at high blend factor

Simulations with lower order discretisation produced converged results but as the discretisation approached formal second order accuracy, the solution began to oscillate (Figure 5-6).

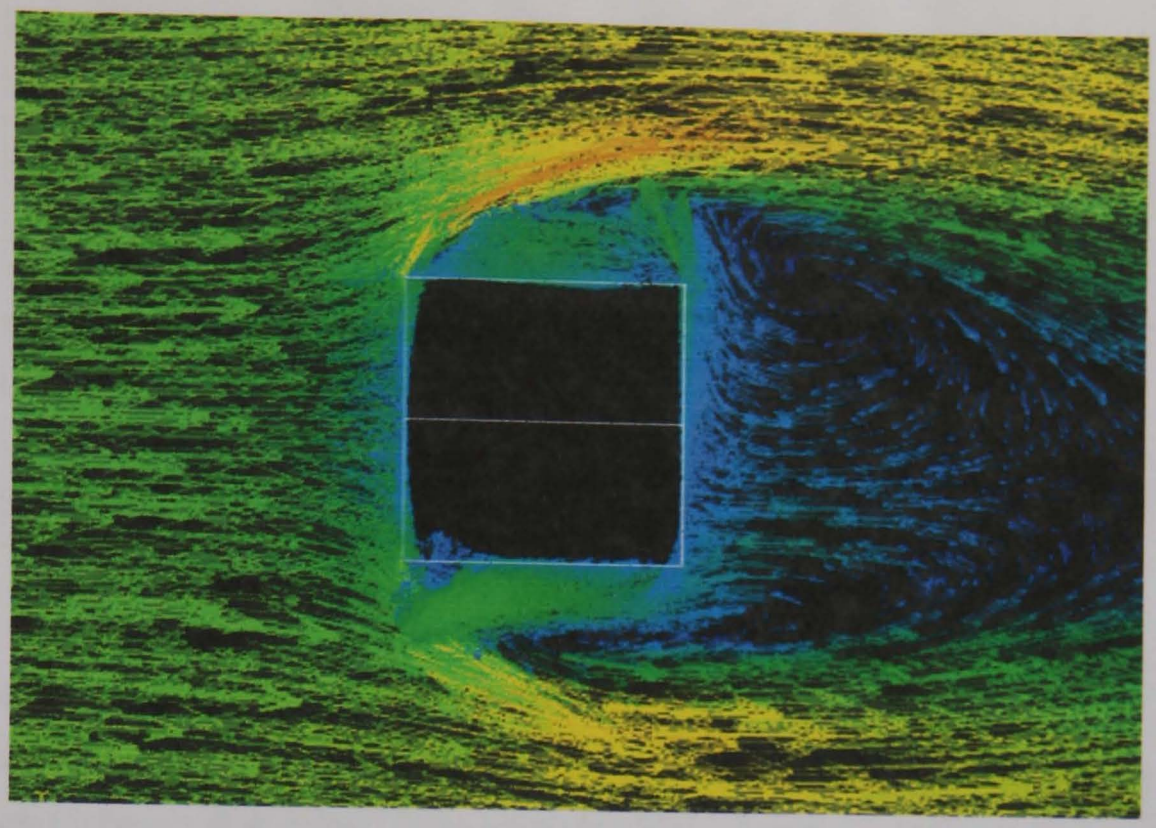

Figure 5-7: Velocity vectors at mid height showing asymmetry in wake: steady state simulation with 75% blend factor

This type of oscillation could be due to non-physical overshoots in the solution at areas of high gradient or due to physical oscillations in the flow. To verify whether this was due to unresolved turbulent unsteadiness in the flow a series of transient simulations was performed.

5.3.4. Transient Simulations – Discretisation studies

When the transient analyses were performed using different spatial discretisation schemes to achieve an acceptable level of convergence, it was again found that with increasing accuracy of discretisation, unsteadiness increased in the flow around the cube and in its wake. The higher order discretisation schemes have the capacity to represent pressure gradients and account for vorticity in the flow better. The timestep was varied to examine the sensitivity of the results to the choice of timestep, the effects of which are shown in Figure 5-10 and Figure 5-11.

Parameter	Value
Simulation type	Transient
Turbulence model(s)	RNG k-ε with scalable wall functions
Mesh Type	Unstructured
Spatial discretisation	1st Order, 2nd Order and CFX blend factors
Temporal discretisation	2nd Order Backward Euler
Timesteps	0.5s

Table 5-2, CFD parameters for initial transient studies

In each case a RMS residual target of 1×10^{-4} was used. This was sufficient to achieve consistent mean values of downstream and cross stream force on the cube. The solution was tested for stationarity of the downstream and cross stream force on the cube.

The effect can be seen in Figure 5-8 and Figure 5-9 showing the net cross stream and down stream force on the cube, non-dimensionalised by the dynamic pressure and cube face area. Here the mean cross stream force on the cube was taken as an indicator of the total degree of asymmetry in the flow. Clearly in the real case there is zero mean cross stream force for a symmetrical flow case.

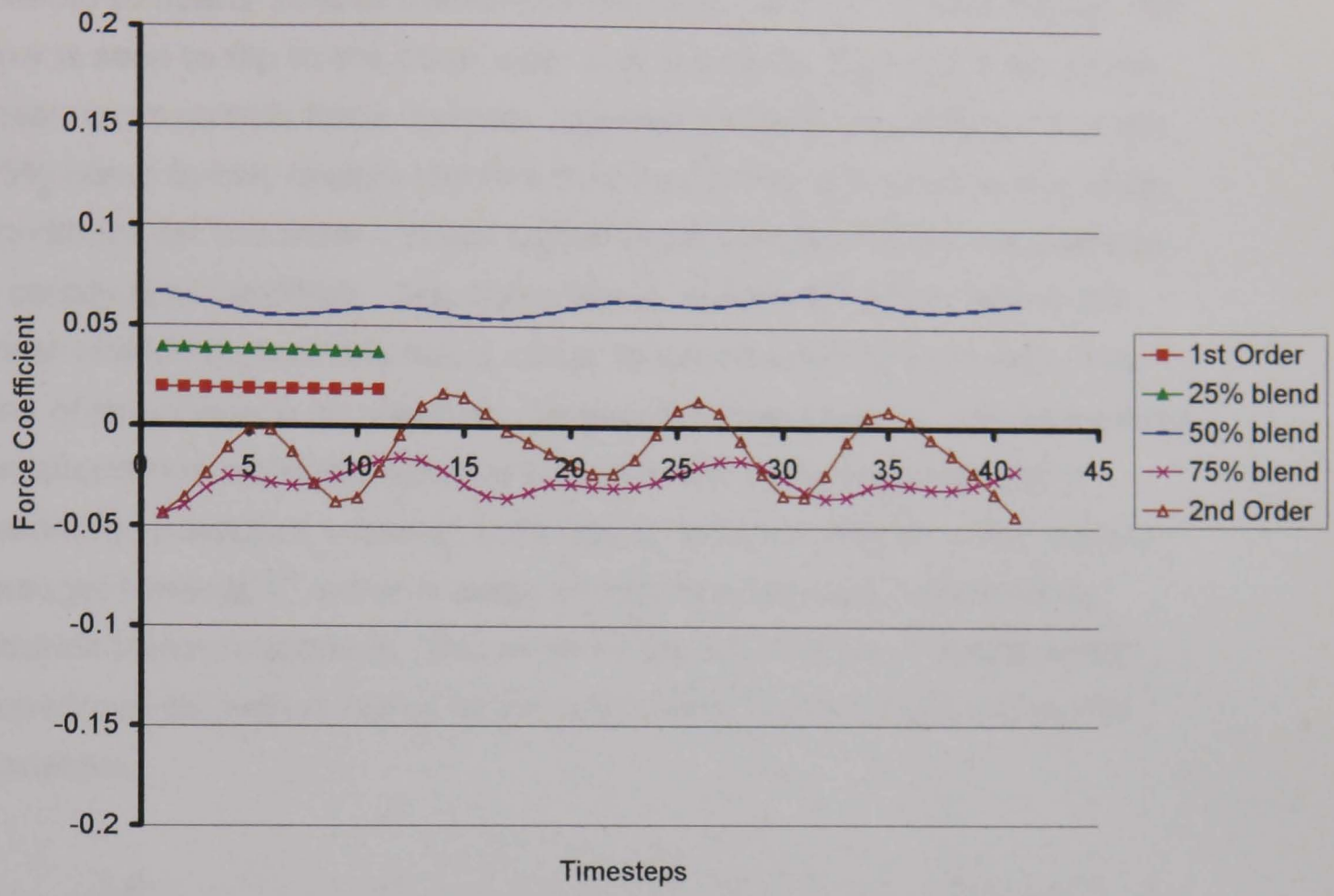

Figure 5-8: Cross-stream force coefficient on cube: sample traces

Discretisation	**Mean cross-stream Force**	**% of 2nd order solution**	**% of downstream force** (From Table 5-4)
Full Scale	0		
1st Order	0.023	-381%	2.4%
25% Blend Factor	0.037	-599%	4.2%
50% Blend Factor	0.078	-1278%	9.8%
75% Blend Factor	-0.014	224%	1.8%
2nd Order	-0.006	100%	0.7%

Table 5-3: Mean cross-stream force on cube from transient simulations

As shown in Table 5-3, first order discretisation produces a converged solution but there is a degree of asymmetry to the results equal to approximately 2.4% of the downstream force. As the solution is blended towards a strictly 2nd order discretisation the asymmetry increases greatly for a 25% or 50% blend with the cross stream force increasing more than

fivefold to nearly 10% of the downwind force. At higher blend factors the flow is seen to flip to the other side. This is seen in Figure 5-8 where the mean cross stream force reverses between the 50% blend factor and the 75% blend factor, despite the fact that the former was used as the initial conditions for the latter. These higher order simulations did not settle to a steady flow condition. The 100% blend, strictly 2nd order, shows the most intense fluctuations but is closer to symmetrical in the mean than any of the previous simulations. To improve convergence, CFX also allows an alternative advection scheme known in the software as the "high resolution advection scheme" (CFX 2003), whereby the 2nd order solution reduces towards 1st order in areas of high flow gradient, maintaining boundedness throughout. This scheme did not produce a satisfactorily converged solution in terms of the residuals achieved or the monitored variables.

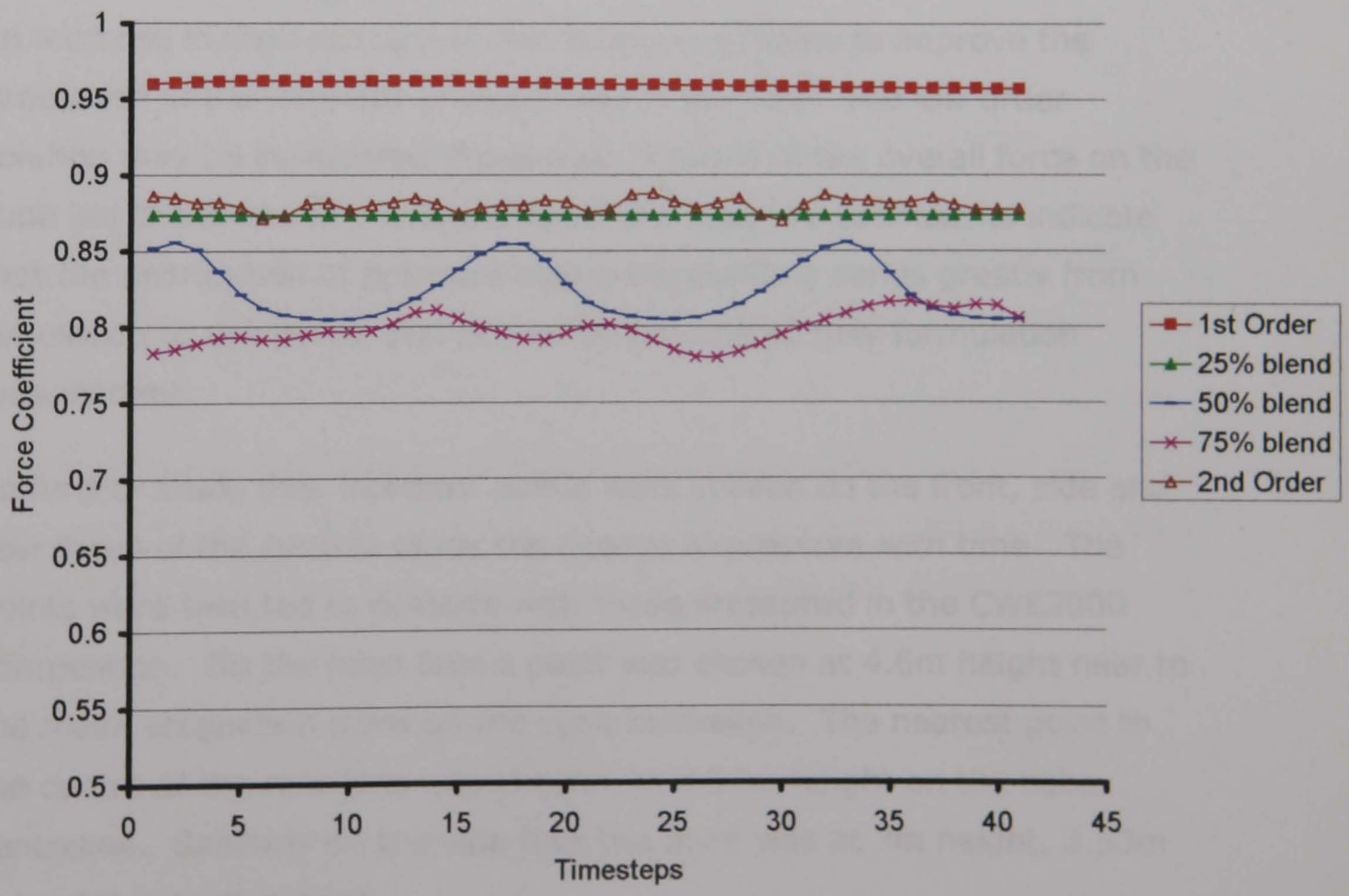

Figure 5-9: Downstream force coefficient on cube: sample traces

Examining the downstream force in Table 5-4 the effect is similar with all results falling within 10% of the formally second order solution. This was

chosen as the reference simulation for comparison with the others as it is the most numerically accurate. The magnitude of variation is similar to that seen in cross stream force but as the downstream force is much larger it equates to a smaller percentage variation.

Discretisation	Mean downstream force	% of 2nd order result
Full scale	0.98	-
1st Order	0.95	108%
25% blend factor	0.874	99%
50% blend factor	0.825	94%
75% blend factor	0.799	91%
2nd Order	0.879	100%

Table 5-4: Mean downstream force for different discretisation schemes

An increase in the accuracy of discretisation appears to improve the simulation of the inherent unsteadiness in the flow. The low order solution may be considered acceptable in terms of the overall force on the cube but the errors in crosswind force and pressure coefficients indicate that the distribution of pressure across the building varies greatly from simulation to simulation and cannot be considered fully formulation independent.

To further study this, indicator points were chosen on the front, side and rear faces of the cube to study the change in pressure with time. The points were selected to coincide with those measured in the CWE2000 competition. On the front face a point was chosen at 4.6m height near to the mean stagnation point on the cube centreline. The nearest point to the centre of the rear face was chosen, at 3.58m height on the cube centreline. Similarly on the side face the point was at 3m height, 3.53m behind the leading edge.

The vortex shedding frequency for this scale of structure may be approximated through the following equation:

$$F = \frac{St \times V}{B}$$ *[equation 5-2]*

Where:

F = Vortex shedding frequency (Hz)
St = Strouhal number
V = wind speed (m/s)
B = Diameter or depth of cross section (m)

Classical vortex shedding is not exhibited for a 3D cube which sheds a variety of coherent vortex structures, however researchers have identified dominant frequencies in experimental studies. A Strouhal number of 0.15 was deduced for the cube in channel flow (Martinuzzi 1991), while weak vortex shedding was also observed for the full scale cube at a frequency of 0.154Hz for a reference velocity of 6.8m/s (Hoxey et al. 2002), equivalent to a Strouhal number of 0.136.

The dominant frequency seen in the wake velocity and side pressure in these new simulations is 8.5s or 0.12Hz, giving a Strouhal number of 0.074. Although of the same order of magnitude as the experimental values, this is not close enough to immediately rule out non-physical overshoots in the CFD solution.

As shown in Figure 5-10, the wake pressure fluctuates at twice the frequency of the variation in pressure on the side face. This supports the suggestion that these fluctuations are caused by vortex shedding from the cube.

Reducing the timestep to 0.1s (Figure 5-11) allows direct simulation of higher frequencies, resulting in a more complex pressure trace. This also has the effect of increasing the negative pressure coefficients, in the wake, decreasing the underprediction of wake pressure. This is discussed further below.

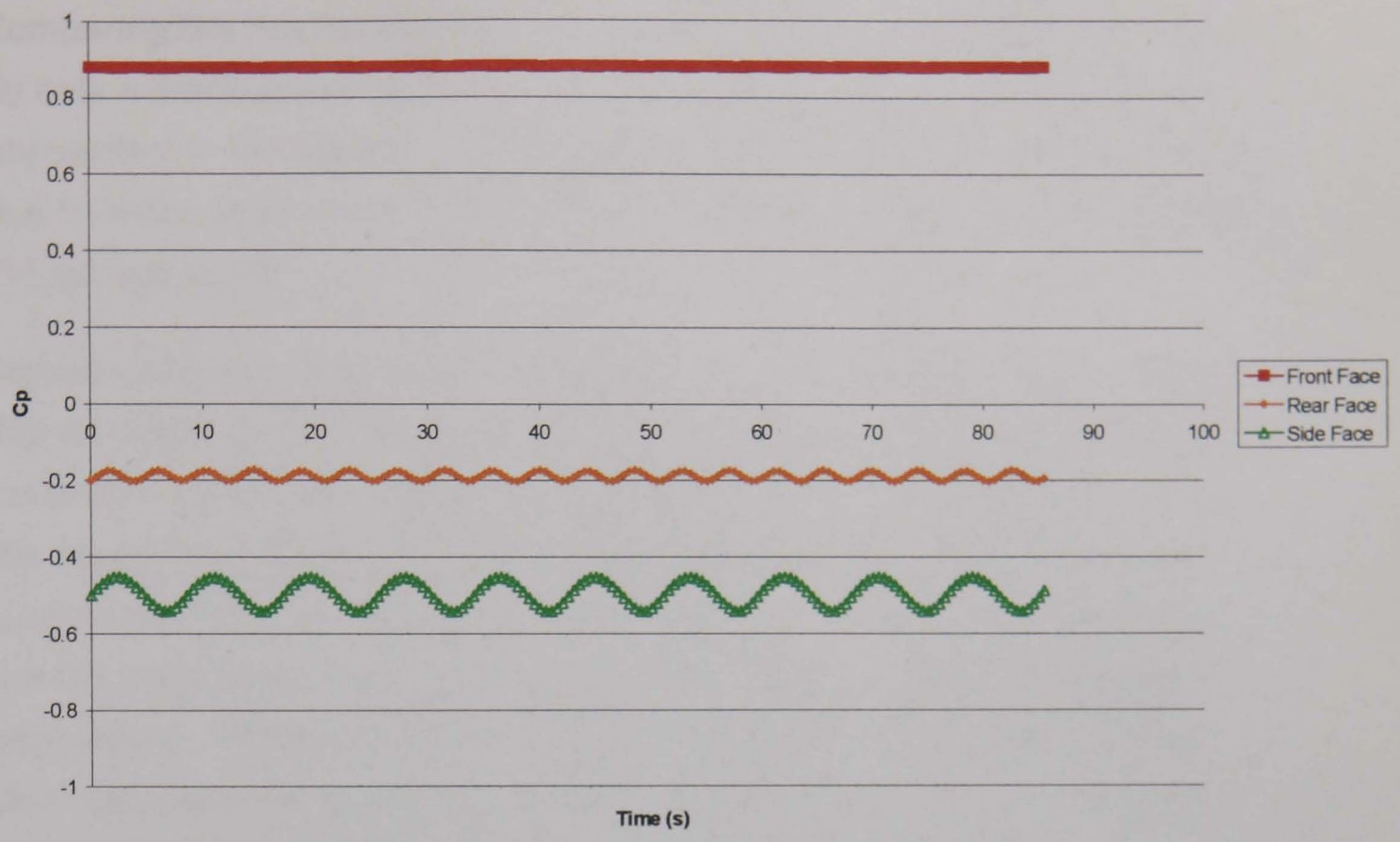

Figure 5-10: Fluctuations in point pressure from unsteady simulations: timestep = 0.5s

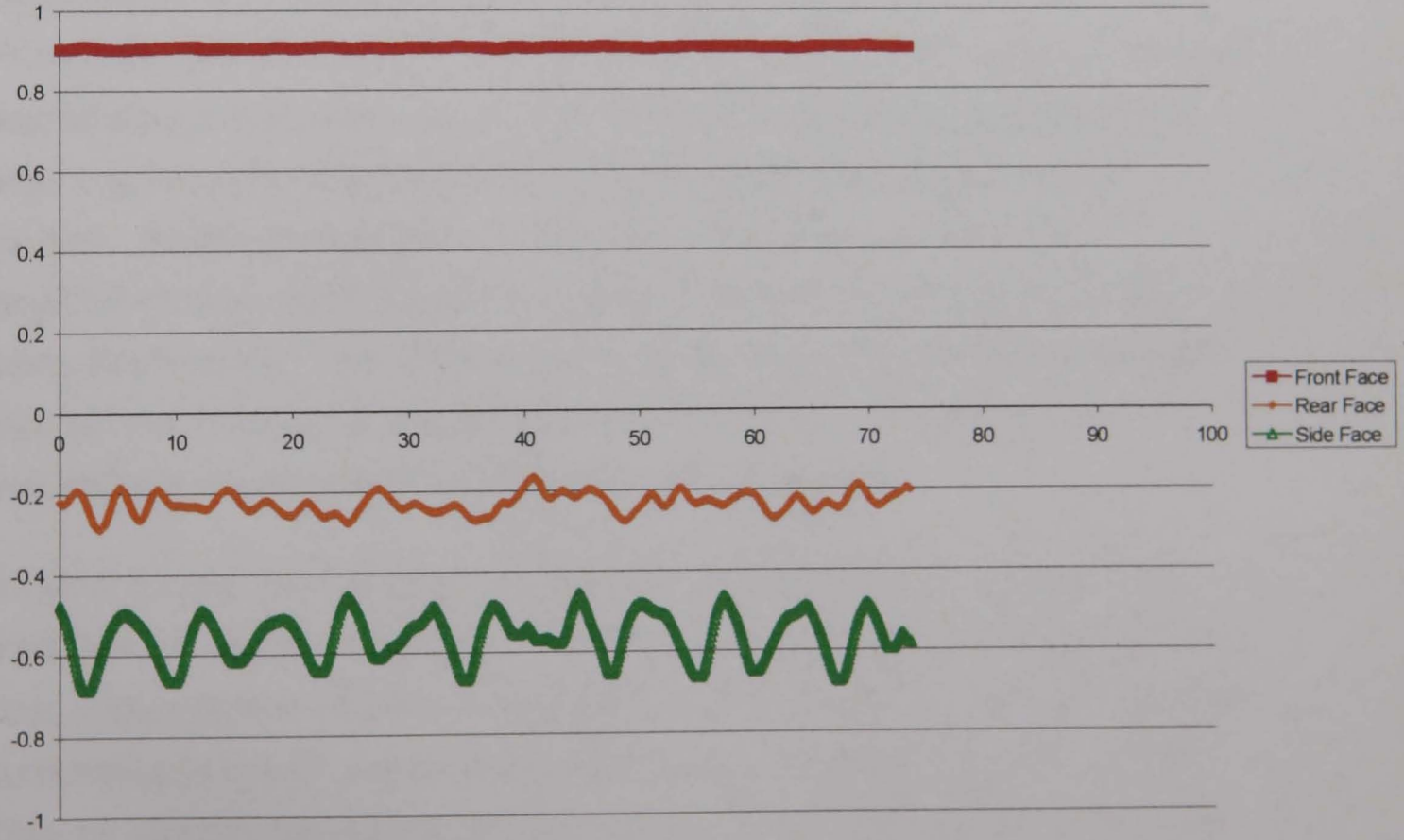

Figure 5-11: Fluctuations in point pressure from unsteady simulations: timestep = 0.1s

Comparing the results with CWE 2000, the MMK solution forced symmetry by only modelling half of the cube. The k-ε and RNG k-ε solutions show asymmetry in the velocity results so the asymmetry does not appear to be due to some gross error in the CFD code or modelling assumptions used in the current study.

Similar unsteady asymmetric results have been found in a previous study, that of a bluff-fronted lorry, both in CFD simulation and in wind-tunnel measurement (Prevezer and Holding 2002). In this case it was found that the asymmetry was only present with more accurate turbulence models such as the RNG k-ε model, with a blend factor of about 0.75 or higher. Simpler turbulence models such as the standard k-ε model did not show asymmetry. The authors found that as well as being asymmetrical, the flow was unsteady and varied with time with the wake separation region fluctuating from side to side. They found that the separation region tended to remain towards one side and not the other. Wind tunnel measurements showed a similar asymmetry, again with a preferential direction of flow, although flow occasionally switched to the other side. This preference for one side can be explained in the wind tunnel by minor asymmetry in the model but in the CFD this is not possible, suggesting asymmetry in the mesh and small numerical imbalances as possible causes. Alternatively a semi-stable flow condition may have been established with small scale flow instabilities superimposed on a large scale asymmetry. The CFD solution may have been sufficiently refined to pick up the small scale instabilities but not to trip the larger scale instability and cause flow to flip fully to the other side.

In wind tunnel and full scale testing, the frequency of vortex shedding frequency is usually modulated by large scale turbulence in the oncoming flow, although the intensity is not diminished. The modelled homogenous turbulence in the CFD simulation clearly does not have the same effect. Only by directly simulating large scales of turbulence could this effect be modelled in CFD, greatly increasing the computational expense.

In the absence of time varying boundary conditions, regular vortex shedding is to be expected for RANS simulations if the solution is

sufficiently accurate to predict structural loads. It is therefore necessary to perform transient analysis.

5.3.5. Further transient analysis

Following on from the investigations into asymmetry and unsteadiness and the boundary layer studies, a new set of simulations was run representing industrial best practice for this case and investigating the effect of mesh design and mesh density on the simulation.

Formal mesh independence can be demonstrated through studies making a significant increase in mesh density and investigating the effect on the key variables. This is a necessary condition in demonstrating that a CFD simulation is a solution to the problem posed and independent of the numerical method. This is rarely achievable for large scale flow studies in the built environment at this point in time.

Previous authors have demonstrated a certain degree of mesh independence in some flow properties, for instance pressure on the front face (Straw 2000) and rear face (Easom, 2000) and the results of these studies were used in setting minimum criteria for this new study. However these authors have highlighted a known mesh dependence in peak pressure values on the roof and sides of the cube and this is discussed further in the relevant sections below.

For these studies, the mesh parameters are clearly set out in the following sections and the results are discussed with reference to the changes in mesh design. However once available computing power permits formal mesh independence studies, these will be required to confirm conclusions drawn herein.

Convergence Criteria

Convergence criteria were again chosen by monitoring the effect of setting increasingly tight convergence limits on both point pressures and area-integrated forces across the cube surface. The value chosen in the boundary layer simulation, 3×10^{-5}, was sufficient to provide settled

structural loads and local pressures. Further tightening the limit had no effect on the mean or fluctuating load and pressure results. All results presented here have achieved this level of convergence.

The boundary layer simulated above was used as the input for the new simulations. Simulations were run transiently with the 0.5s timestep chosen previously and 2nd order spatial discretisation.

The initial mesh was refined around the cube and is shown in Figure 5-12 to Figure 5-14. These figures were produced by creating as solid objects all of the cells which cross the domain centreline and then viewing these objects normally from the centreline. Some cells therefore appear to be very slender as they are viewed from an acute angle. This is inevitable when presenting a 3D mesh in a two dimensional view.

Study	Mesh size	Mesh size on cube surface	Mesh size on leading edge	Number of inflated layers on cube	First inflated cell height
Initial mesh	3000mm	100mm	50mm	0	-
Refined mesh 1	3000mm	100mm	100mm	10	10mm
Refined mesh 2	3000mm	100mm	50mm	10	1mm
Refined mesh 3	3000mm	300mm	300mm	10	1mm

Table 5-5: Mesh details

Additionally, Mesh 3 continued the inflated boundary onto the floor of the domain as described below.

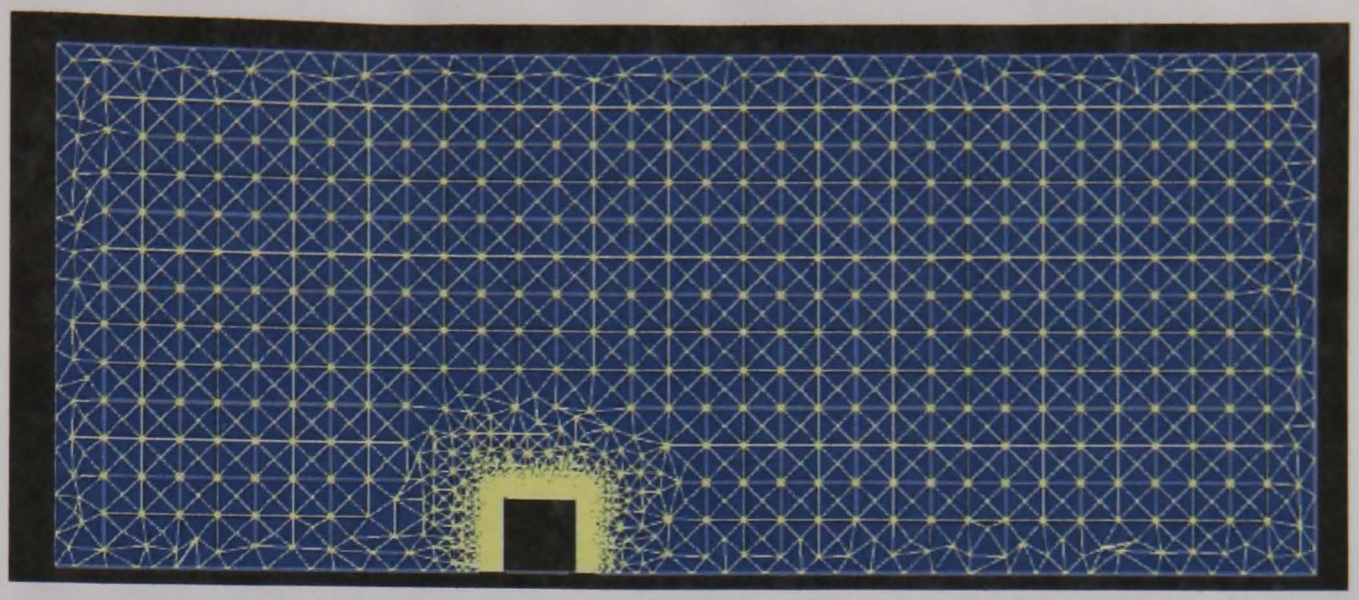

Figure 5-12: Initial mesh: side view (flow is from left to right)

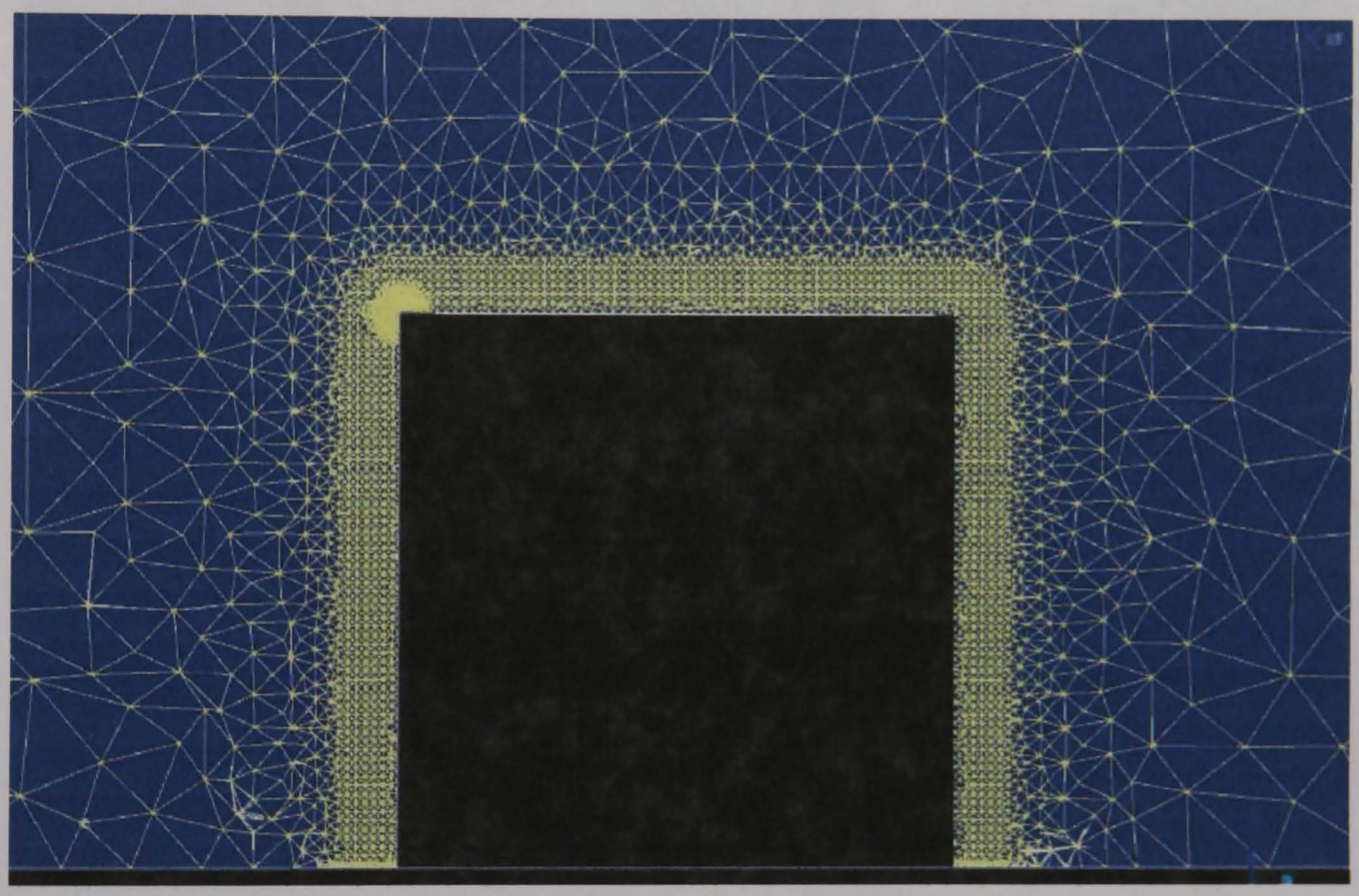

Figure 5-13: Initial mesh: side view on cube

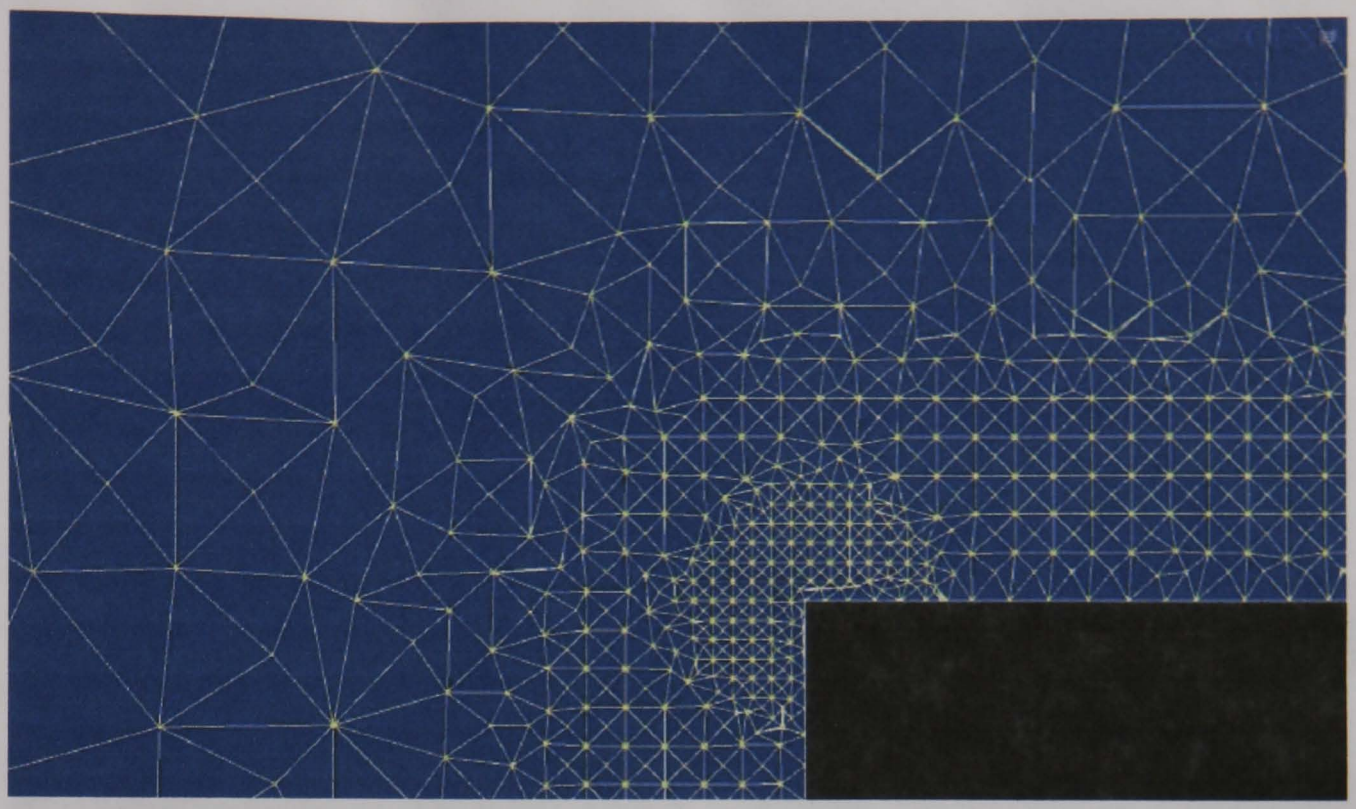

Figure 5-14: Initial mesh: detail at leading edge

This initial mesh used a much finer mesh around the cube but no inflated boundary. This was performed to investigate whether the inflated boundary is required for this type of case or whether a homogenous unstructured mesh provides a better representation given the non grid-aligned flow at areas of high velocity gradient.

This initial mesh uses a coarse mesh in the free field with refinement only near the cube surface. Velocity gradients are relatively low upstream, above and to either side of the cube but in the downstream wake there are much higher velocity gradients and this initial mesh clearly cannot fully resolve the wake.

The first refined mesh is also refined on the cube surface and includes an inflated boundary layer on the cube surface. This mesh was intended mainly to provide a baseline against which to measure further improvements in mesh quality as the aspect ratio of the cells on the cube boundary is a little high to be considered acceptable for industrial CFD work. The thickness of this boundary was chosen to maintain a y^+ value of less than 100 on the cube surface. The mesh refinement at the front edge of the cube was retained to more accurately model flow near the separation point and to maintain a suitable y^+ value here.

A first cell height of approximately 10mm was required to achieve the target y^+ value. Cell edge lengths were limited to 100mm on the cube and 50mm near the leading edge. The mesh took a significant amount of time to build and revise with local refinement required at known points of separation. As the velocity field is not known during initial mesh construction it is not possible to choose the ideal locations to refine the mesh in the wake and side separation zones or to know what first cell height to choose.

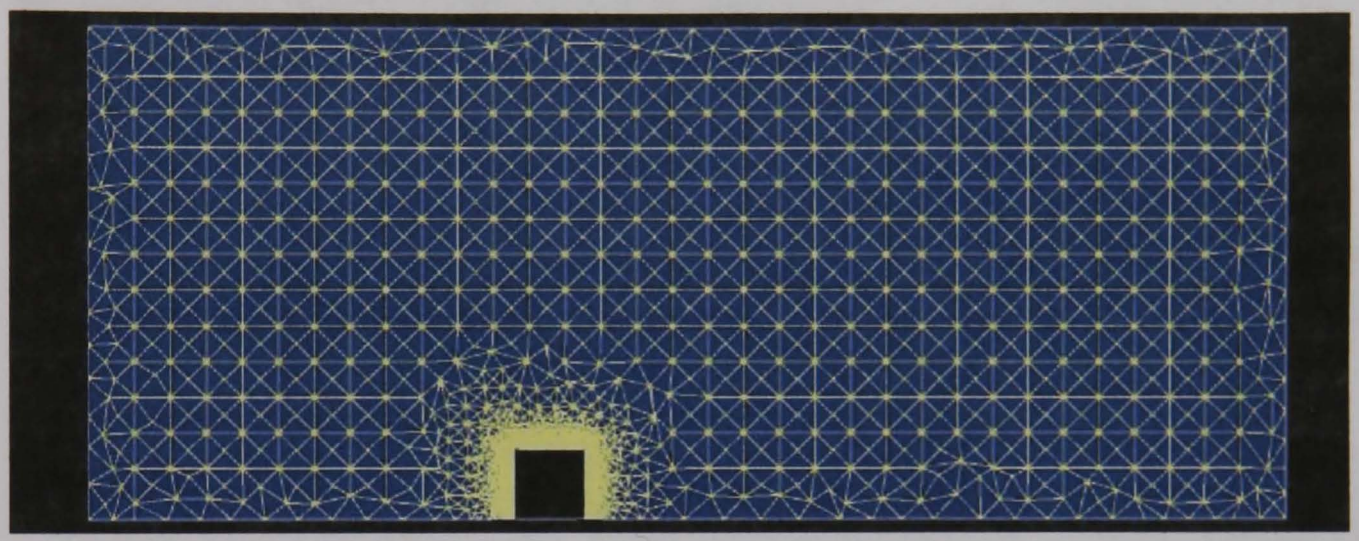

Figure 5-15: Refined mesh 1: side view (flow is from left to right)

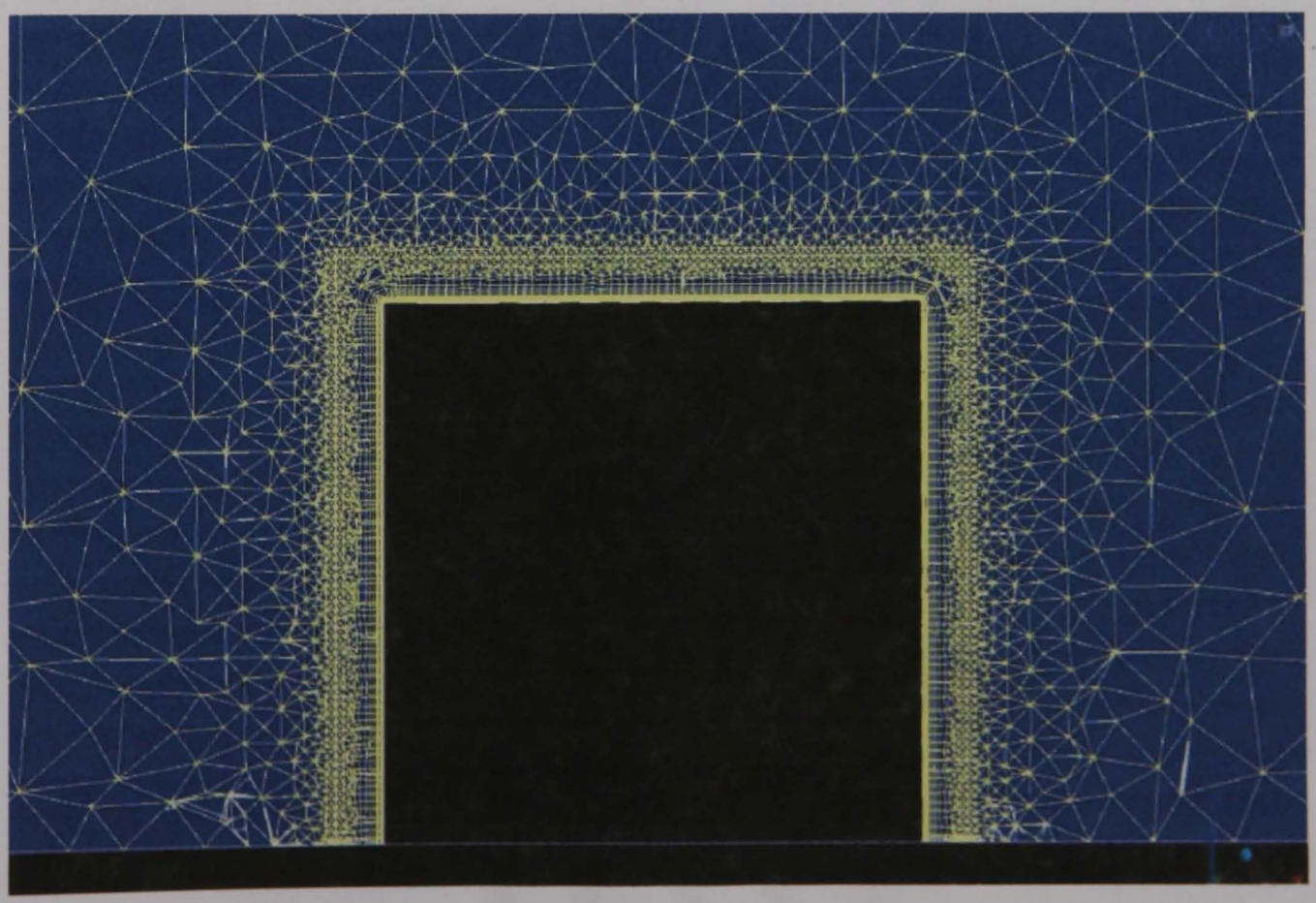

Figure 5-16: Refined mesh 1: side view on cube

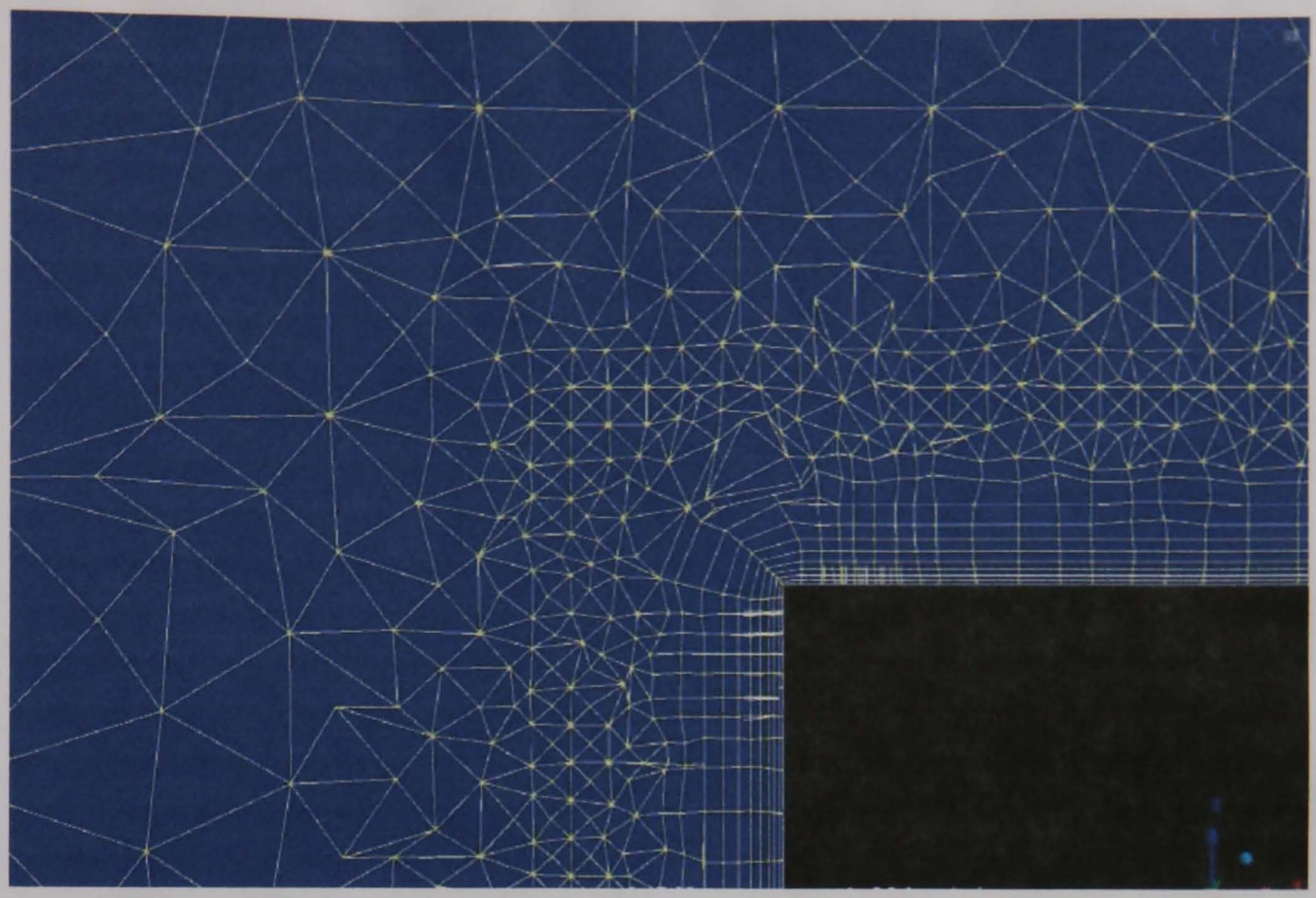

Figure 5-17: Refined mesh 1: leading edge detail

The second refined mesh was intended to further refine the vertical gradient of velocity near the domain floor. The inflated boundary layer was extended from the cube onto the domain floor, improving the boundary layer representation and refining the upwind toe separation region as well as the base of the downwind recirculation region.

This refinement improves representation of the flow field near the cube but necessarily violates the requirement for a first cell height of at least two times the roughness height. This was not considered critical to the results as flow around the cube surface is dominated by flow structures around the cube itself, not by conditions near the upstream wall.

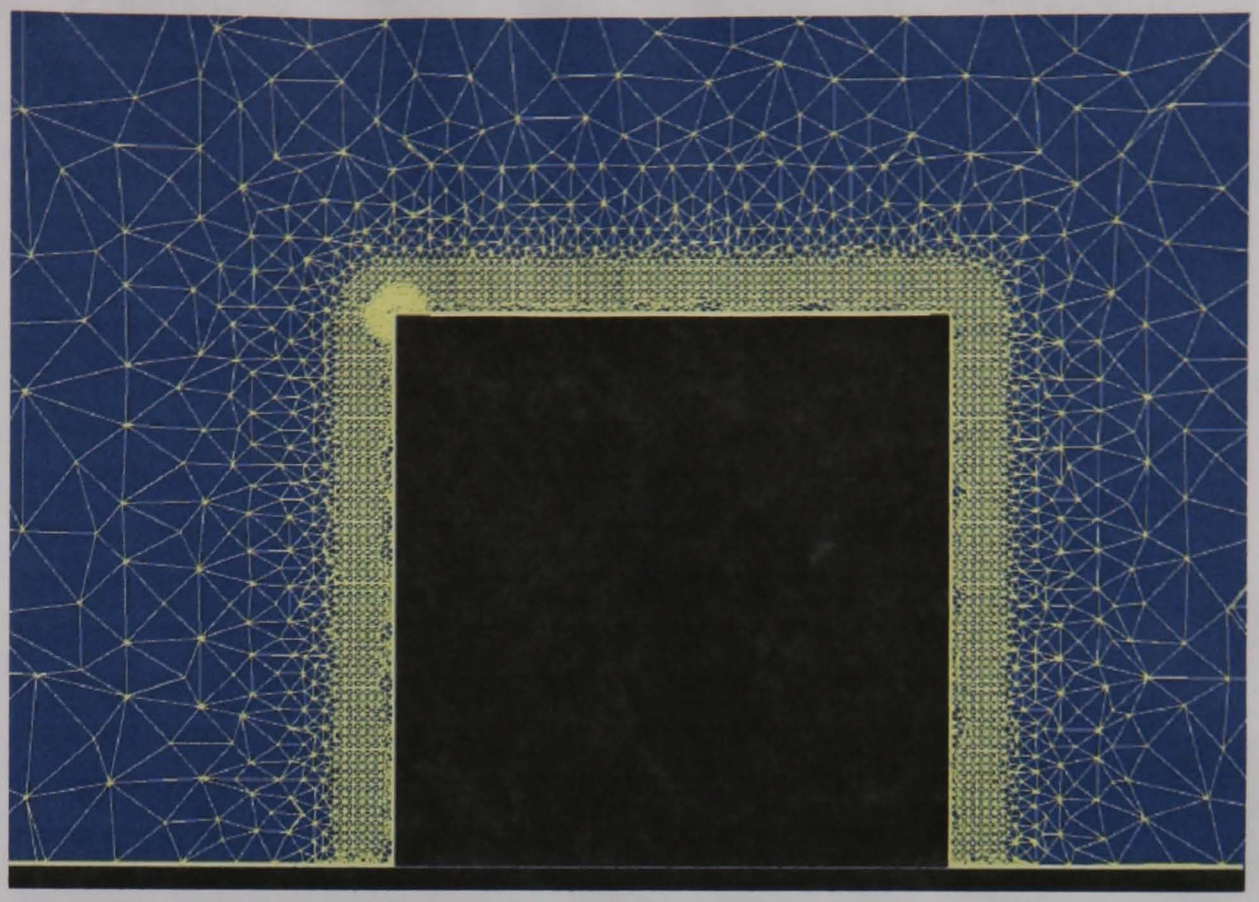

Figure 5-18: Refined mesh 2: side view on cube (flow is from left to right)

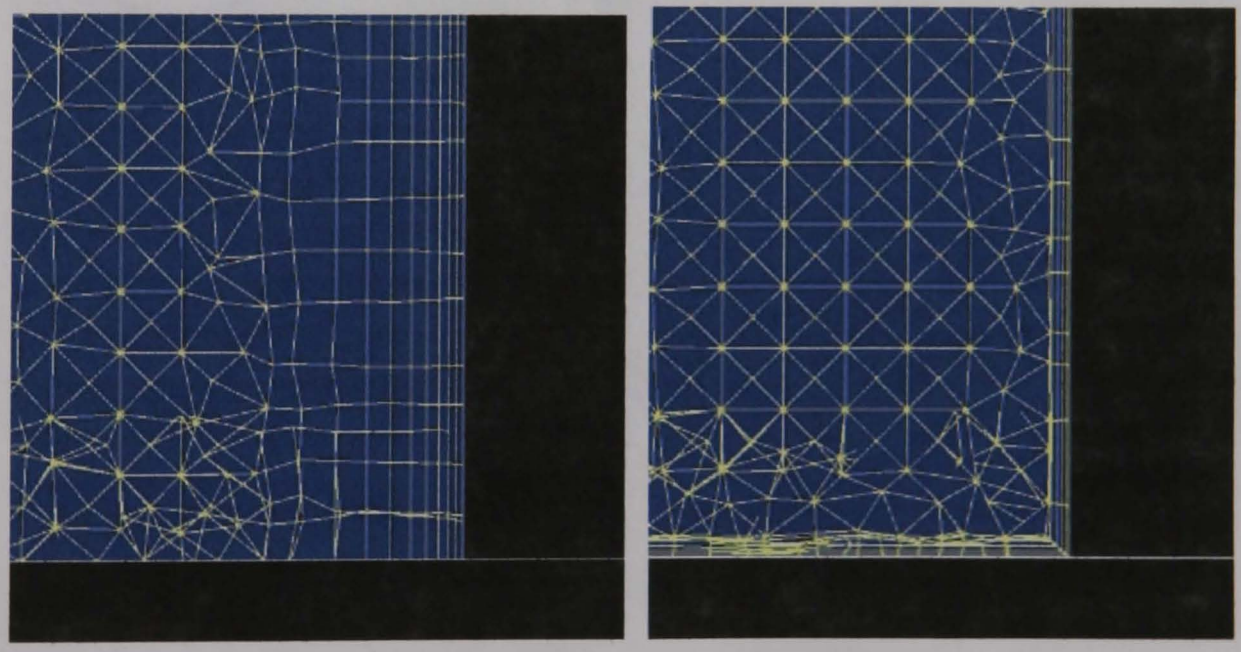

Figure 5-19: Refined mesh 1 and 2: front toe detail

The third refined mesh was selected through discussion with the project industrial partners, Buro Happold. The mesh refinement on the domain floor was improved at the expense of some detail around the cube. This was to better resolve the upstream and downstream separation regions while maintaining a fine grid resolution near the cube. The refined mesh on the floor again violates the first cell height requirement in order to better refine the velocity gradient in these areas.

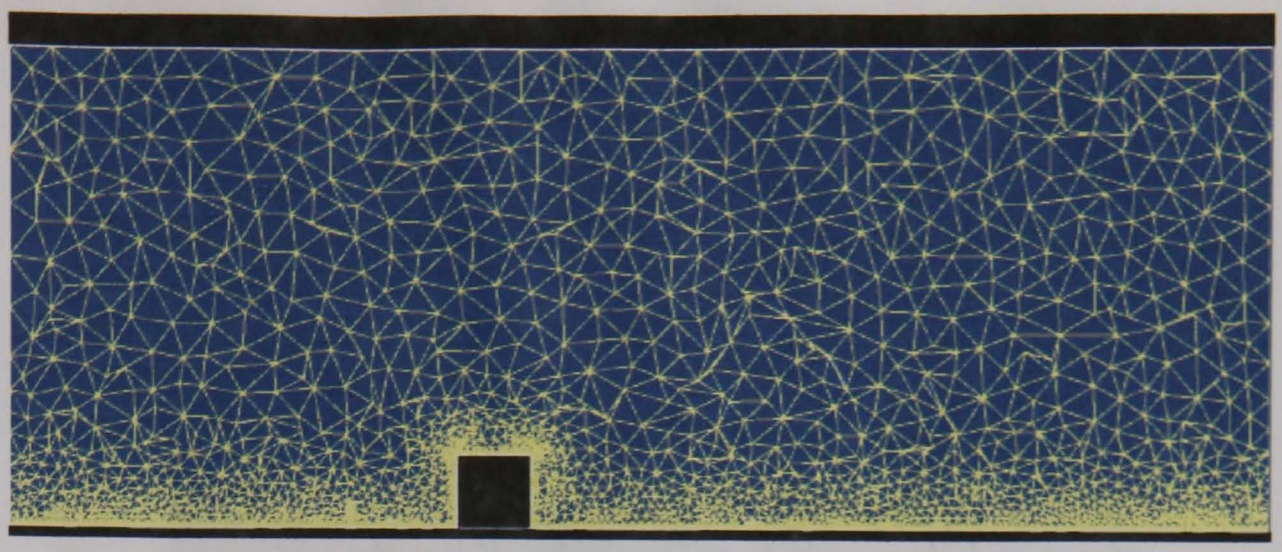

Figure 5-20: Refined mesh 3 (flow is from left to right)

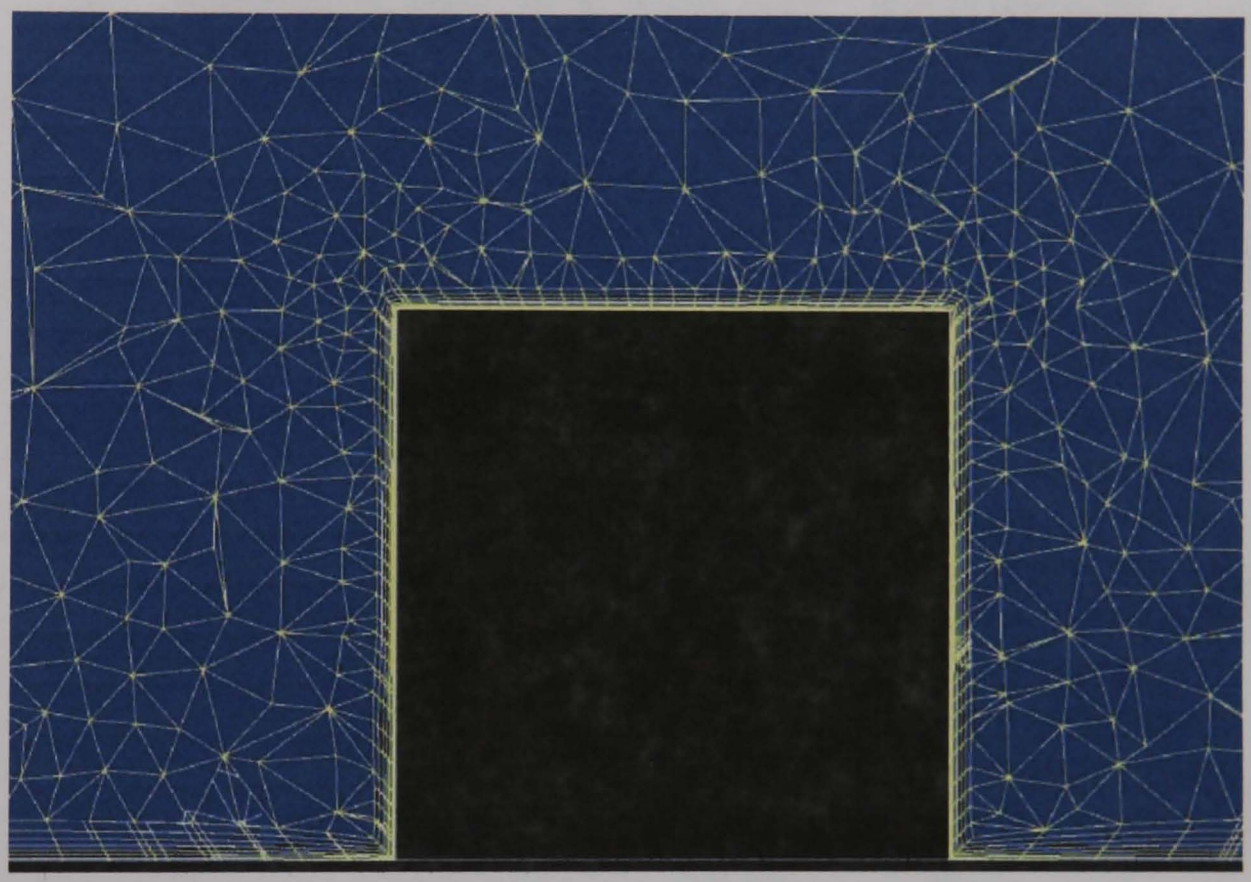

Figure 5-21: Refined mesh 3: Side view on cube

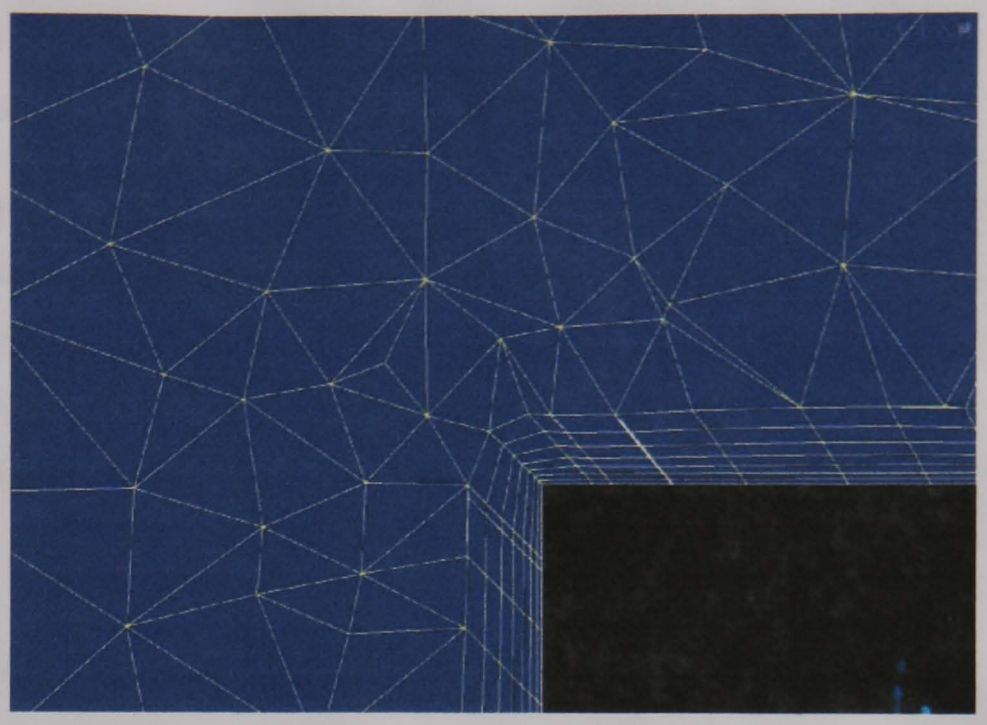

Figure 5-22: Refined mesh 3: Leading edge detail

Mesh Dependence

As discussed previously, it is not currently possible to achieve full mesh independence for complex flow cases such as this. The effect of changing the mesh has been studies for the key variables of force and local pressure and the results are presented below. Firstly the effect on overall building forces is considered.

Study	$\overline{CF_X}$	$\overline{CF_Y}$	$\overline{CF_Z}$
Initial Mesh	0.79	0.022	0.31
Refined Mesh 1	0.80	0.020	0.31
Refined Mesh 2	0.84	0.016	0.35
Refined Mesh 3	0.80	0.006	0.47

Table 5-6: Mesh study: Mean force coefficients

Where

$\overline{CF_X}$, $\overline{CF_Y}$ and $\overline{CF_Z}$ are the mean pressure coefficients in the downstream, cross stream and vertical directions respectively. All

are non-dimensionalised by the reference pressure and the face area.

The mean force coefficients are given in Table 5-6, showing less than 5% variation in mean downstream force. The mean cross-stream force is in all cases less than 1% of the downstream force, and further reduces with mesh refinement. The vertical force or lift increases significantly with mesh refinement however and cannot be considered mesh independent.

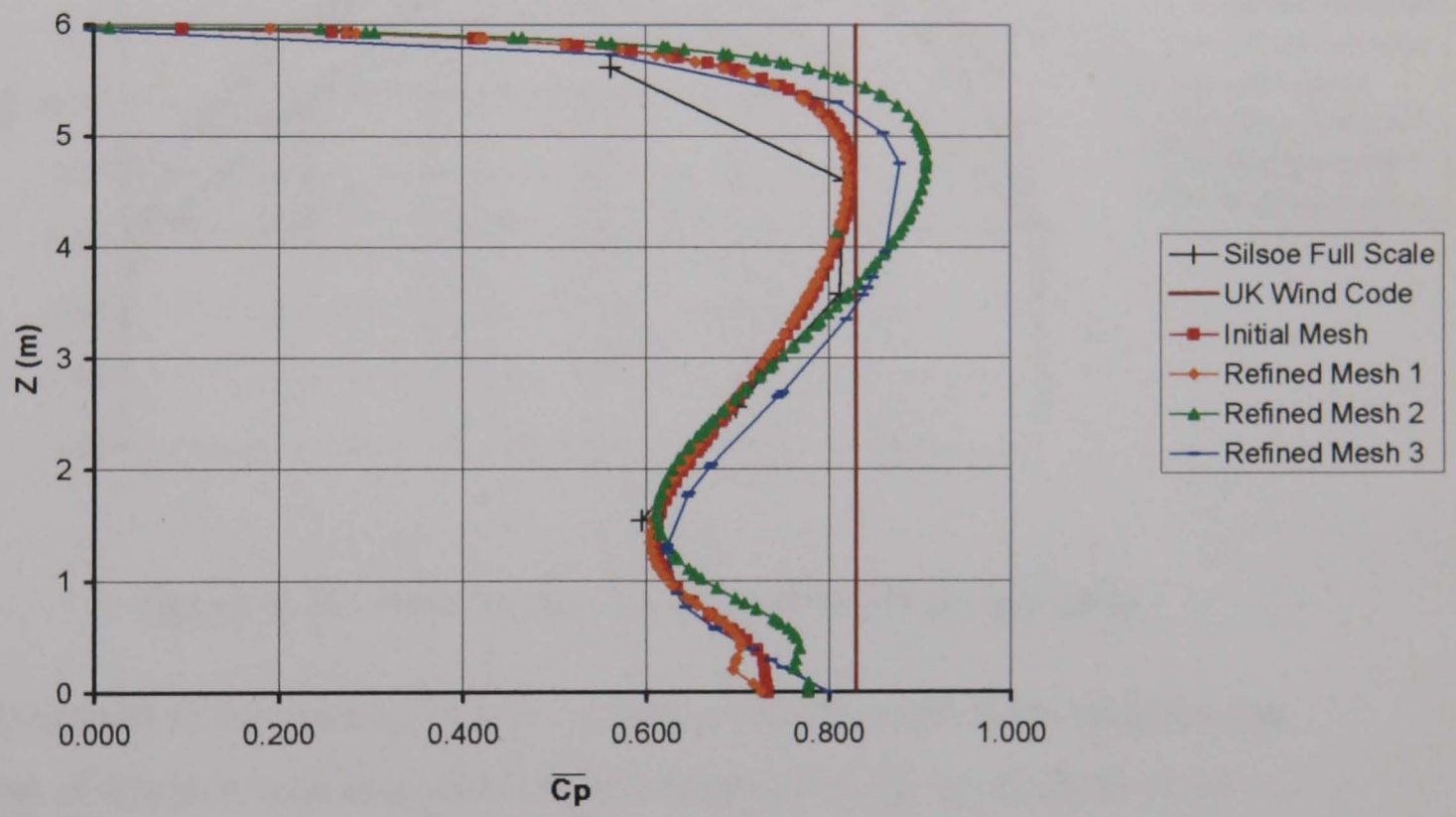

Figure 5-23: Mesh study: $\overline{Cp}$ on front face

As shown in Figure 5-23 The maximum mean pressure coefficient on the vertical centreline on the front face varies by -7% to +3% relative to Refined Mesh 3. The variation at all other points is less than or equal to these values with the exception of the very high gradient region near the top of the face.

Mean pressure coefficients on the rear face are not generally critical for structural loading which is governed by the higher positive pressures on the front face and peak negative pressures on the side faces, however Figure 5-24 shows that the wake pressure coefficients cannot be

considered mesh independent. There is a significant asymmetry in all but the refined mesh 3 results. The reasons for this are further discussed below.

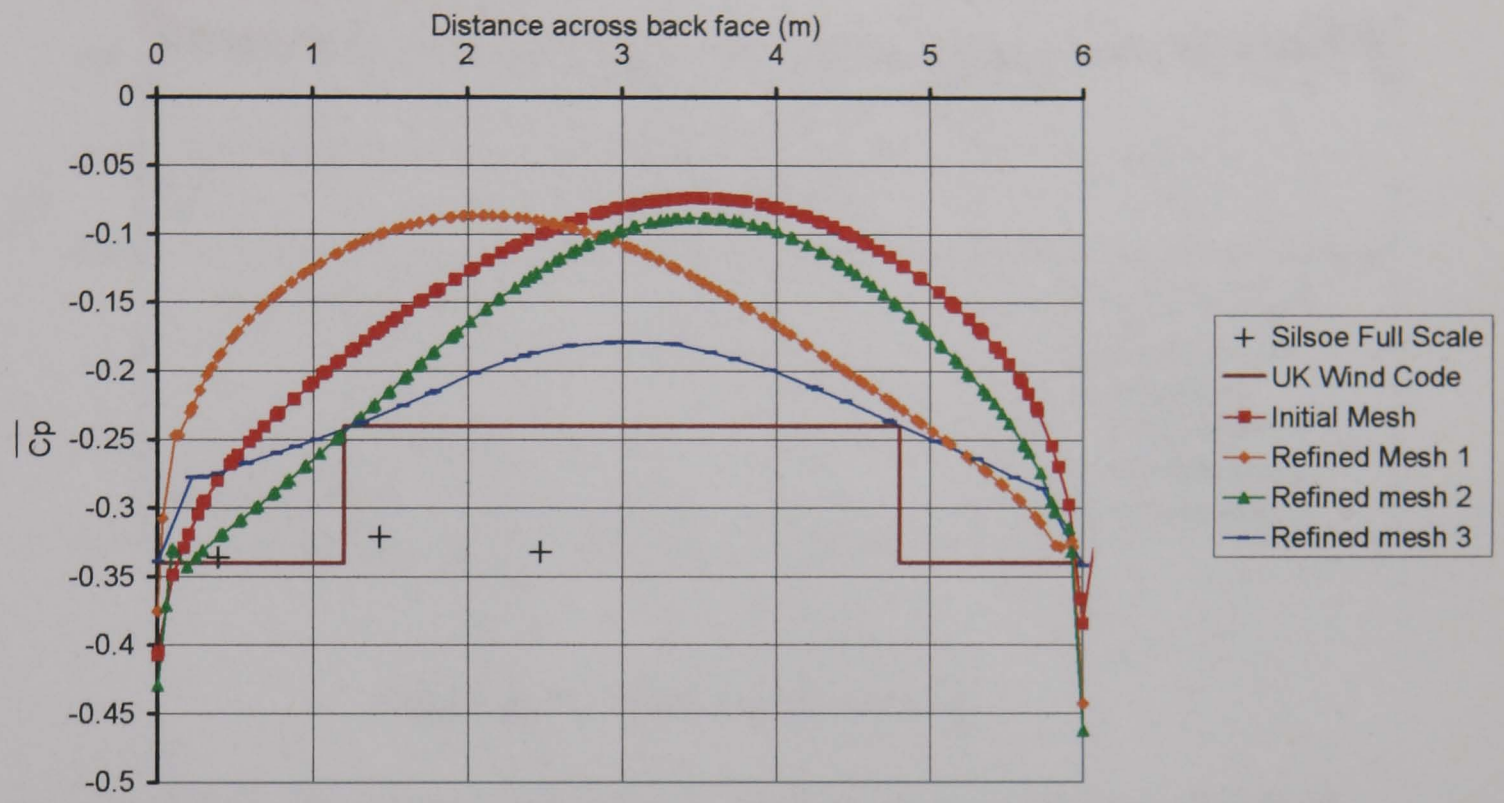

Figure 5-24: Mesh study: $\overline{Cp}$ at mid-height on rear face

Compared to the wake pressure results, pressure coefficients towards the rear of the side face are relatively consistent with $\overline{Cp}$ of -0.32 to -0.43 near the trailing edge. Significant mesh dependence is seen however at the leading edge, with maximum pressure coefficients of -0.34 to -0.73. This is a very significant variation as it could be the governing factor in the design of cladding elements and some structural components.

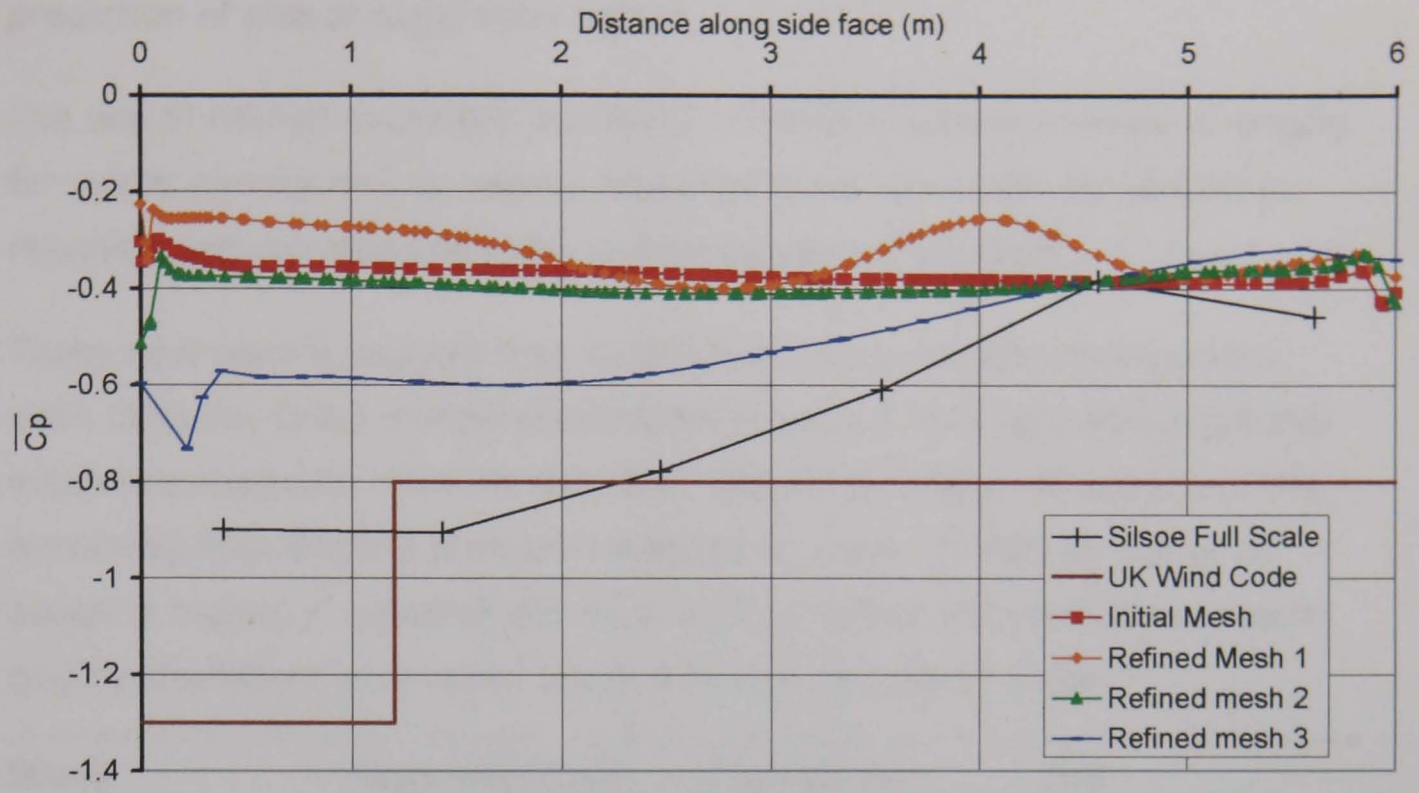

Figure 5-25: Mesh study: side $\overline{Cp}$

Comparing results between the refined meshes with or without an inflated boundary layer and those with the coarser third mesh, the results with refined mesh 3 were far more symmetrical and were a closer match to the full-scale results. This is contrary to standard guidance which recommends mesh refinement near buildings but does not generally comment on the wider flow field and which specifies a first cell height of at least twice the surface roughness height.

The other meshes resulted in far less intense separation from the sides of the cube, greatly underpredicting pressures at these locations. Further mesh refinement did not result in improved pressure predictions, suggesting that mesh refinement studies which concentrate on surface meshing could suggest a grid-independent solution before that had truly been achieved.

Looking at the mesh near the leading edge of the cube, the expanded boundary layer method results in a flow direction diagonally crossing these high aspect ratio cells. This will result in local gradient smearing

with reduced shear stress and may be one source of the errors in prediction of size of separation region.

The use of refined expanded boundary meshes has been developed largely for use in aeronautics to resolve attached flows where the far stream is relatively laminar and the wake is downstream of the body.

These new results suggest that its direct adoption in built environment work does not bring comparable improvements in accuracy and additional mesh requirements must be specified, including careful refinement of the oncoming flow and the upstream stagnation zone. It may be better to accept a higher y^+ value at the cube surface rather than sacrificing mesh quality elsewhere in order to achieve an appropriate y^+ value.

Study	Upstream floor stagnation point (from front of cube)	Downstream floor reattachment length (from rear of cube)	Top reattachment length (from front of cube)
Full-scale	0.748	1.408	0.575
Initial mesh	0.659	3.045	/
Refined mesh 1	0.636	3.045	/
Refined mesh 2	1.205	3.091	/
Refined mesh 3	0.841	1.864	/

/ = no reattachment

Table 5-7: Reattachment lengths for the Silsoe cube given in cube heights

All meshes result in significant overprediction of separation lengths above and behind the cube, with no mean reattachment on the roof or sides of the cube. This is accompanied by significant error in the pressure coefficients here and may be due to the lack of low-frequency turbulence and thus a lack of variation in the mean flow direction.

The earlier meshes used identical convergence targets and yet they resulted in a significantly longer reattachment length behind the cube, more reminiscent of a steady simulation. Only the third mesh, with its improved resolution near the floor and reduced grid resolution at the cube surface, comes close to the full-scale values.

Overall Building Force

The total force on the building is shown below for the time varying case with refined mesh 3:

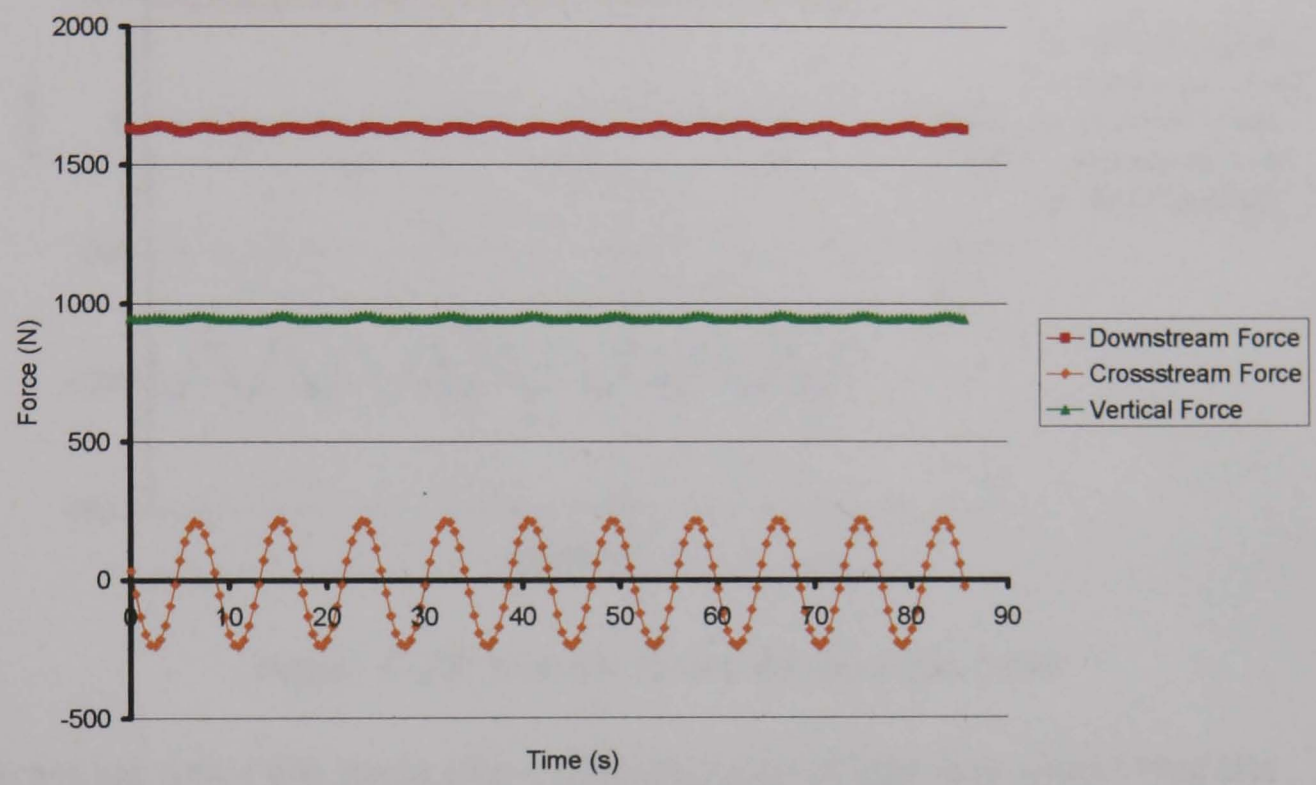

Figure 5-26: Overall load on the cube

The overall downwind force on the cube and vertical uplift vary gradually with time while the crosswind force fluctuates regularly with a time period of 8.5 seconds. These lateral fluctuations have little effect on the net downwind force.

The crosswind force is slightly asymmetrical in the mean, varying between +212N and -240N with a mean of -11N. This asymmetry is significantly lower than was seen for the steady state calculations described previously.

Member Forces

The total force on individual faces and areas were plotted for the time varying case as shown below:

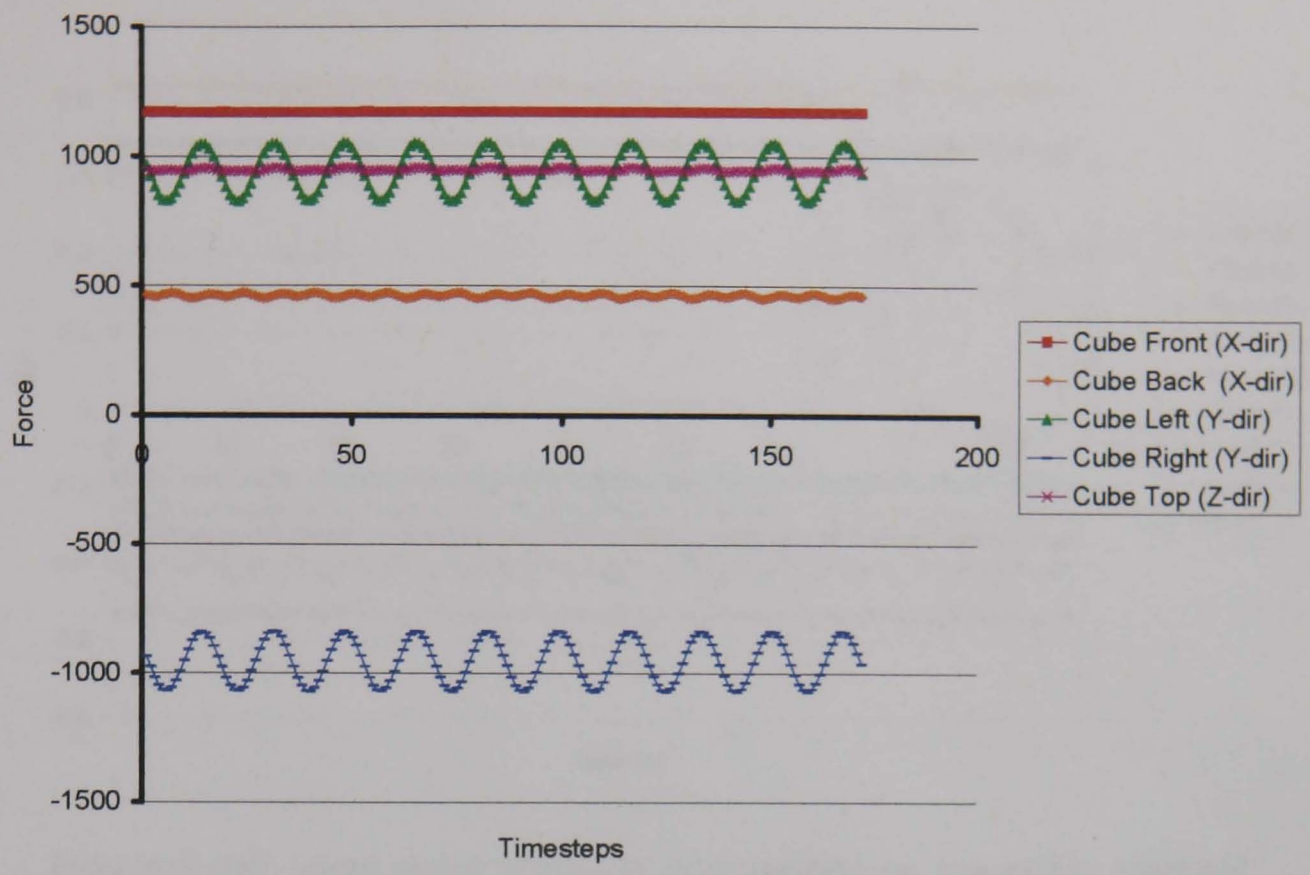

Figure 5-27: Normal forces on the cube faces

Breaking down the loads into individual faces in this way shows that the force on the front of the cube is effectively constant. The force on the back and top faces fluctuate at twice the frequency of the fluctuations in side forces, which are in phase with one another and therefore combine to create the larger crosswind force seen in Figure 5-26. This oscillation in the flow is due to vortex shedding fluctuations, similar to those produced in smooth air flow. It appears that the modelled homogenous turbulence is not sufficient to damp out these fluctuations and allow a mean state to be predicted.

Cladding Pressures

The local pressure at various points on the building was plotted for the time varying case as shown below:

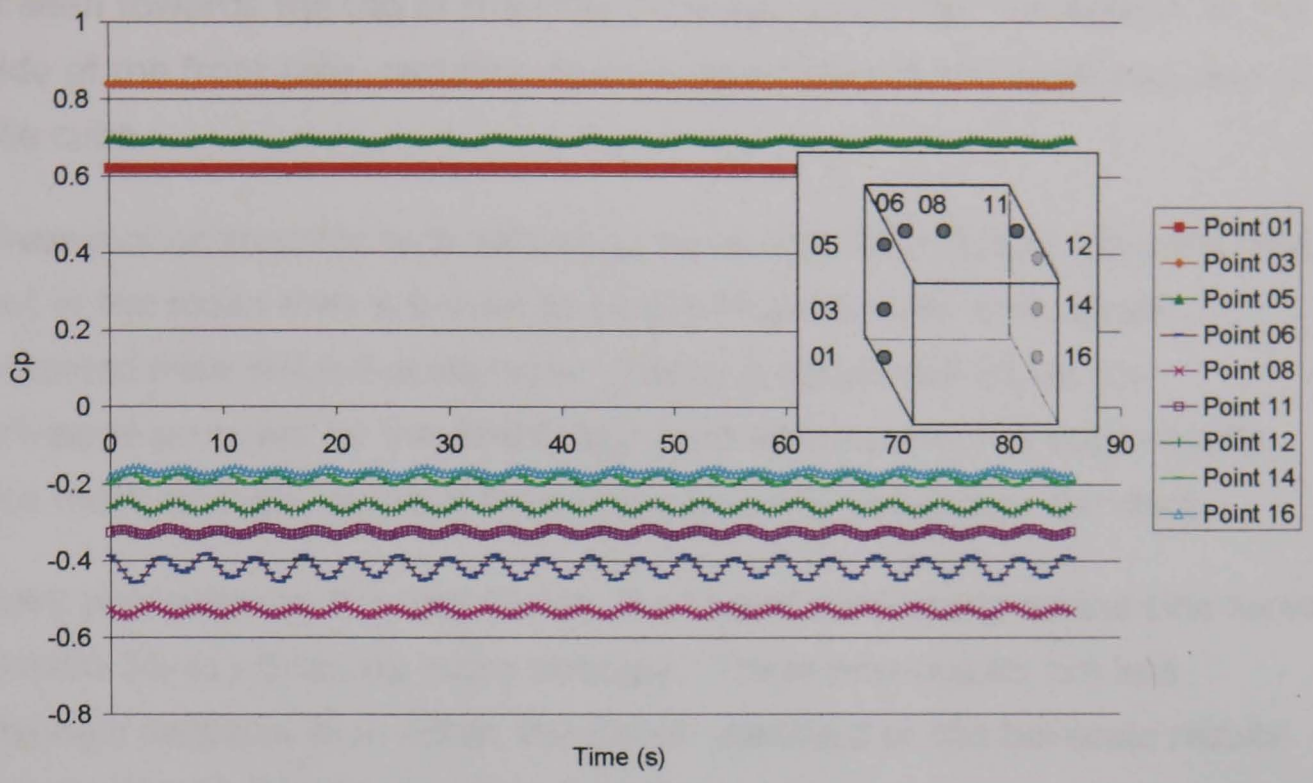

Figure 5-28: Local point pressure fluctuations on the cube: Vertical centreline

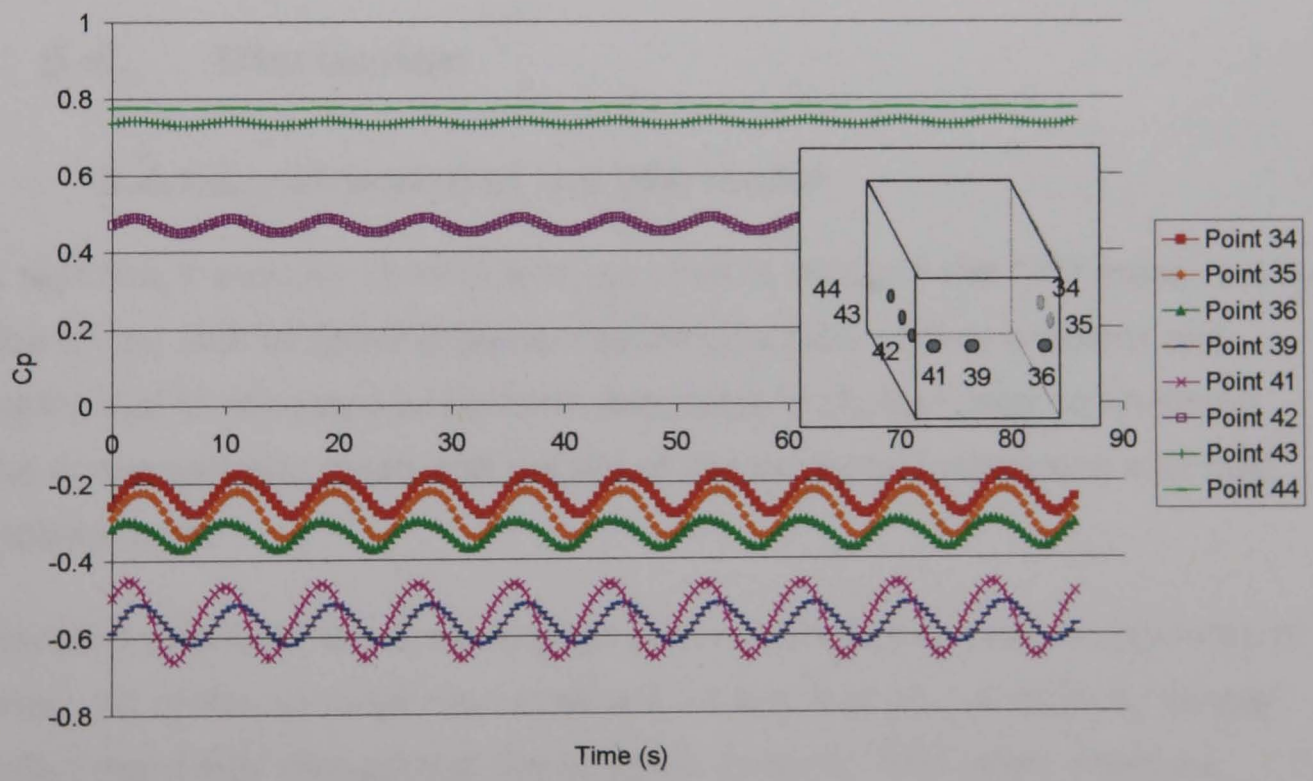

Figure 5-29: Local point pressure fluctuations on the cube: Horizontal centreline at mid-height

Point pressures on the front face (Points 1 to 5 in Figure 5-28 and 42 to 44 in Figure 5-29) are generally steady and match the full-scale results to within a similar degree of accuracy to previous results. A slight variation

is seen towards the top of the front face with a stronger fluctuation at the side of the front face, resulting from unsteadiness at the sides and rear of the cube.

Pressures on the rear face (Points 12 to 16 and 34-35) fluctuate with time but in the mean they are seen to be significantly lower than those obtained from the full-scale tests. The CFD results fall within the envelope provided by the British standard whereas the full-scale results are more strongly negative than those given by the British standard.

Point pressures on the roof (Points 6-11) and particularly on the side faces (Points 36-41) fluctuate more strongly. These new results are less strongly negative than either the British standard or the full-scale results in both the mean and the extreme value.

RMS pressures were not available for the full-scale experiment so a comparison cannot be made here.

5.4. Discussion

5.4.1. Construction of the CFD model

A significant amount of time was required in building the CFD mesh, partly due to the lack of specific guidelines for this type of flow problem and partly due to the need to perform preparatory studies prior to finalising the computational mesh and details of the boundary conditions and fluid models used.

Revising details of the mesh design also requires considerable amounts of time. As computational resources are limited it is not sensible to simply refine the mesh throughout the solution domain. The mesh must be progressively refined at different locations and the effect of the refinement observed at each stage. The mesh in the free stream must be capable of maintaining a stable boundary layer. The mesh near the cube must be sufficiently refined to limit gradient smearing. The separation and recirculation zones must be adequately refined, with particular detail needed on shear layers which will shift in space for a transient run. The

mesh should be refined near points of separation and the near-wall distance should be set appropriately to the turbulence model used.

Industrial CFD codes now allow some degree of automatic dynamic meshing, however in CFX this was only available for steady-state calculations. Improved automatic meshing systems will be needed if complex time-varying flow cases are to be considered. These systems will have to take account of all the above mesh requirements.

The choice of discretisation scheme clearly affects all critical variables, with the possible exception of the mean force on the building. Moving away from the 2nd order discretisation introduced significant errors in structural design values, particularly in cross-stream force on the building and the detailed pressure distribution.

Issues remain around the development of the inlet flow condition and how to maintain a stable boundary layer which accurately represents full-scale atmospheric turbulence. Generally, 10 consecutive empty channel simulations were required to generate a satisfactory boundary profile with a stable velocity and turbulence profile. Even so, the turbulence profile was still changing by up to 20% at cube height between the inlet and the cube location. Further simulation runs did not improve this situation. The velocity profile was much more stable with less than a 2% change between the inlet and the cube at any height.

It is generally accepted that as wind flow is highly complex and relatively difficult to characterise, precise pressure values cannot be predicted (see, for example, Cook (1990) for a discussion of modelling errors in wind tunnel studies). Structural engineers require a result that is sufficiently close to the real value that, once the standard factors of safety are applied, the design load will not normally be exceeded within the design life of the building.

In this context it is vital that broad flow features be predicted including separation and reattachment that determine the size of the zones of high suction pressure at the leading edge of a bluff body. A good approximation must be given to the peak force and pressure values as

well as the general pressure over the rest of the body but any error must be taken in the context of the broader uncertainty over site wind conditions and possible future changes to surrounding buildings.

These results give good predictions of pressure coefficient on the front face with small errors in results on the rear face and on part of the sides and top. However, the high suction pressures around the leading edge of the cube are not predicted in the instantaneous results. This may in part be because the full scale results are grouped by approximate wind direction, with the results for zero angle of attack including winds from several degrees to either side. The effect of lateral turbulence means that instantaneous wind directions sometimes vary significantly from the normal. The CFD results meanwhile only include directly normal flow with a homogenous turbulence. This results in regular vortex shedding oscillations and may affect the mean pressures. This warrants further investigation through the use of time-varying inlet conditions.

5.4.2. Velocity Results

The reattachment lengths detailed in Table 5-7 show that improved grid resolution near the cube does not necessarily improve overall mean flow predictions. The best match to experimental results was provided by a coarser grid on the cube surface combined with a finer grid near the floor of the domain, suggesting that flow patterns near the base of the cube may be instrumental in entraining air from the free stream into the separation bubble. This in turn leads to greater curvature of the separation bubble, earlier reattachment and lower pressure in the separation regions, as seen in the pressure results. This can be seen in Figure 5-30 where surfaces of zero downstream velocity are plotted. Mesh 3 results in flow reattachment on the side walls near the base of the cube and consequently a much smaller recirculation bubble.

Simulations with coarser meshes near the domain floor resulted in significant overprediction of wake size, as highlighted in Table 5-7. This may be partially due to the relatively low turbulence intensity in the simulated flow, which will result in less entrainment of the shear layer

flow into the wake. In full-scale studies, higher turbulence intensity has been shown to result in a decreased radius of curvature in the separation region and therefore lower pressure (Laneville and Williams, 1979).

This mesh also resulted in far more symmetrical flow in the mean, although the flow was still fluctuating, suggesting that this low level flow is instrumental in restabilising the separation bubble and allowing the flow to flip from one side to the other.

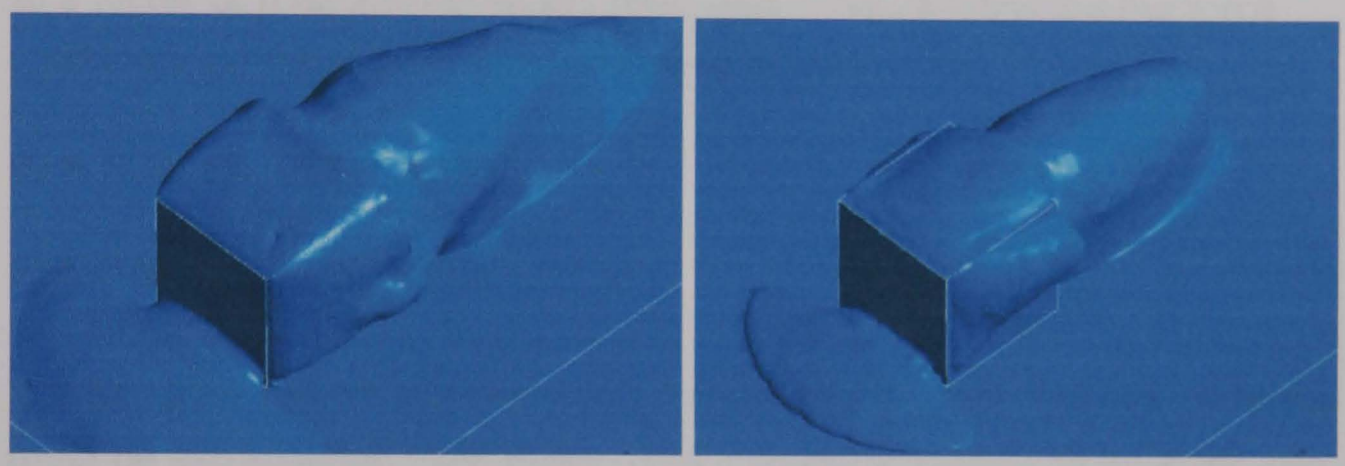

Figure 5-30: Isosurfaces of zero mean streamwise velocity, showing mean separation bubbles with refined mesh 2 (left) and 3 (right).

5.4.3. Overall Structural Loads

The overall structural load on the building will be equal to the net force on the front and back faces. Surface friction is ignored as this only becomes significant for buildings with much longer downwind than crosswind dimensions and buildings with significant surface roughness.

Net loads are presented below for the British Standard, full-scale tests and CFD predictions.

BS6399:2

Front face average pressure coefficient = [(0.7 x 2 x 1.2 x 6) + (0.83 x 3.6 x 6)] / (6 x 6) = 0.778

Rear face average pressure coefficient = [(-0.34 x 2 x 1.2 x 6) + (-0.24 x 3.6 x 6)] / (6 x 6) = -0.28

Net pressure coefficient = 0.778 – (-0.28) = 1.058

However the code also allows for a reduction in this value to allow for the fact that the worst design load on the front face is unlikely to be experienced at exactly the same time as the worst design load on the rear face. The greater the separation between these faces the greater the theoretical reduction in load as the correlation between loads on front and rear face will reduce. This is simplified, however, in the British standard to a factor of 0.85 applied to the total load. This reduces the net force coefficient for calculation of peak overall load to:

$C_F = 0.85 \times 1.058 = 0.899$

Full-Scale

The full-scale results are given only for certain positions and overall forces must be extrapolated from these. This inevitably introduces an error into the prediction.

Front face: Cp = 0.66 by averaging pressures in vertical and horizontal directions

Rear face: $C_p = -0.33$ similarly

Net $C_p = 0.66-(-0.33) = 0.98$

This is similar to the value of 1.058 obtained using the code of practice, which one would expect to be slightly conservative (high). When calculating the peak overall load, the code of practice adjustment could similarly be made here for the non-correlation of peak forces on the front and back faces.

CFX

The overall force on the cube can be monitored throughout the time-dependent simulation by integrating local pressures. Skin friction has again been ignored for consistency with the above results. Only the normal force components are used in the calculation.

Non-dimensionalising by the reference pressure of 56.38 N/m² and frontal area of 36m², the mean net force coefficient was:

$C_F = 0.879$

This is significantly lower than the net force coefficient of 1.058 predicted with the code of practice and 13% below the estimated mean full scale value of 1.01.

The peak force coefficient during the run was only slightly higher than the mean as the instabilities around the cube only significantly affected the crosswind force, with a minimal effect on the negative pressure on the back face. The peak downwind force on the building can therefore be calculated from the mean by quasi-static means with an adjustment for non-correlation across the building face using the code of practice. As RANS studies use modelled point turbulence values, it is not possible for the CFD calculation to allow for lack of correlation of peak loads across the building.

The difference between full-scale, CFD and code of practice results is to be expected when dealing with a complex phenomenon such as extreme wind loading. However, the consistency between the different CFD simulations used suggests a systematic underprediction of mean downwind force, even on simple structures such as this where no external elements interfere. Lower order solutions in some cases underpredicted the net force coefficient by around 20%. This error appears to be caused by the underprediction of suction pressures in the building wake.

For more complex shapes and oblique wind angles it would be advisable to move to a LES based approach, averaging results over a suitable period of timesteps. This should yield a more accurate mean flow pattern and may result in a consequent improvement in pressure predictions. However, it is not yet possible to perform full LES studies for flow problems of this scale, accounting for all significant turbulence scales.

5.4.4.Local Member Forces

The design of the cube did not allow direct measurement of member forces. Full-scale member forces can only be calculated by extrapolating from local pressure results.

A single cube face of 36m² is of the same order of magnitude as a cladding area loading a single structural member on a medium to large building (assuming a typical member spacing of 3 to 6 metres and structural member lengths of 6 to 10 metres). Forces on each of the 5 surfaces of the cube were therefore taken as representative of local member loads.

Forces on the front and back faces of the cube were well represented by the CFD simulation. Significant errors were introduced in calculating forces on the side and top panels due to an underprediction of separation at the leading edge.

Again, the mean load is available through averaging the time varying value in the simulation.

5.4.5.Cladding Pressures

Local pressures were calculated across the cube and compared for the points used in the full-scale experiments.

Mean pressure predictions were significantly more accurate on the front and back face of the cube than in areas of separation on the top and side faces. The magnitude and period of pressure fluctuations was significantly different from those in the full-scale tests.

Although separation and recirculation is predicted on the side and top faces of the cube, the CFD simulations do not correctly calculate the strong suction pressure near the leading edge. This represents the worst case cladding load so errors here will have a significant effect on the design. Cladding materials and cladding supports typically form a larger part of the capital cost of a new building than the structure and therefore

correctly predicting cladding loads has a significant financial incentive attached to it.

Pressure on the side walls in particular is very hard to predict. The vertical gradient of pressure means that any error in predicting the size of the separation bubble will shift the peak pressure locations up or down, with a significant effect on point pressure values. The underprediction of separation intensity meanwhile reduces the peak suction value.

Looking at the reason why the software does not correctly predict these high suction pressures, one possible explanation could be an underprediction of the intensity of separation, possibly due to errors in the near-wall modelling. However the results have been shown to be relatively insensitive to near wall treatment and the overall separation region is too large rather than too small.

The overprediction of separation suggests that the problem comes from a lack of entrainment of the free stream into the wake, weakening the suction in the wake and therefore reducing the overall force on the cube as well as suction pressures in the separation zone.

LES and/or DES methods have been shown to predict mean flow characteristics far more accurately than steady or unsteady RANS methods. They may therefore improve upon the pressure predictions made here as they improve on the entrainment of the free stream into the wake.

5.5. Summary and Conclusions

A new series of CFD simulations has been run to investigate the use of CFD in calculating full-scale structural design loads and pressures. The results have been compared with previous CFD simulations, codes of practice and full-scale results.

These computational studies have demonstrated both the capabilities and the limitations of a traditional RANS approach to calculating wind forces and pressures. The major conclusions are as follows.

- RANS techniques can predict mean pressure coefficients on buildings but introduce systematic errors in the wake region. In order to achieve the level of accuracy described here it is necessary to perform mesh sensitivity studies, apply appropriate turbulence models and monitor all target variables (both forces and pressures) for convergence.

- Current steady RANS techniques are sufficient for the prediction of broad flow features and mean net forces across simple isolated structures. For such simulations, strict convergence cannot be achieved due to inherent unsteadiness in the flow, possibly related to vortex shedding. It is therefore impossible to predict the magnitude of building generated turbulence levels using steady RANS methods. These values have minimal effect on overall building loads but significantly affect local cladding pressure.

- Errors in the size of separation zones and wake prediction suggest that where detailed pressure information is required or where flow around multiple bodies interact, steady RANS methods will not be sufficiently accurate to provide a high level of confidence in the results.

- Inherent unsteadiness in the flow is observed to occur due to vortex shedding oscillations. This unsteadiness prevents satisfactory convergence of steady RANS simulations and necessitates the use of unsteady simulations to obtain settled values of local pressure coefficient.

- Unsteady RANS calculations can extend the application of CFD to more detailed area-averaged load studies and increase the accuracy of overall building force prediction. They are not sufficient to provide detailed pressure information in areas of separation and reattachment and may still significantly overpredict areas of separation and underpredict structural loads and cladding pressures in the wake. LES and DES methods may be capable of solving this problem but they can not yet be applied at full scale.

- Industry standard convergence targets set for mean flow problems are insufficient to provide converged solutions for surface pressures on bluff bodies. Where RMS residuals are used as the convergence criteria, convergence studies should be performed for individual flow problems to determine whether the solution is sufficiently converged.

- Working at full scale, problems of the scale of the Silsoe 6m cube can now be addressed using standard RANS methods. Significant further increases in computer power will be required if larger and more complex problems are to be adequately tackled at full scale using CFD.

- Improved automatic flow-aligned meshing with provision for unstable time-varying flows, automatic surface inflation and tracking of moving shear layers would greatly reduce the time required to build CFD problems and increase solution accuracy by reducing numeric dispersion and allowing limited computer resources to be concentrated on areas of high flow gradient.

6. Ascot Building

The cube studies have illustrated the capabilities and limitations of CFD when simulating complex flow phenomena around simple geometries as well as drawing detailed conclusions about the suitability of RANS methods for structural wind engineering.

Progressing to a large complex building presents a range of new challenges, both in terms of the practicality of building the simulation model and in the complexity of flow considered. This stage of the project tests the previous assumption and critically examines the performance of CFD simulations in predicting structural loading on the Ascot racecourse grandstand, a large and complex new building. This structure has the advantage of being relatively isolated from surrounding buildings and therefore has a clearly defined oncoming fetch. The structural loads were calculated through wind tunnel testing, allowing comparison with the CFD results without the need to run a new set of wind tunnel studies.

This chapter describes the wind tunnel studies (conducted by others) and the CFD simulations representing them and goes on to discuss their relative capabilities and limitations. Conclusions are then drawn about the use of CFD in structural engineering for complex buildings.

This work involved the following major stages:

- Processing the raw wind-tunnel data to produce mean and peak pressure results for each design load case. This provided a full set of building load data, filling in gaps and acting as a quality check on the reported data.

- Simulating the atmospheric boundary layer with no building present to get a sufficiently accurate reproduction of the variation of wind speed and turbulence with height above ground.

- Building a geometric model of the complex grandstand shape in the CFD software. This was performed at model scale (1:300).

- Running simulations of wind flow over the grandstand and calibrating the model (adjusting modelling parameters, roughness of surfaces, etc).

- Predicting building forces and cladding pressures from the CFD results and comparing these with wind tunnel results for mean and peak surface pressures.

- Critically assessing the methods used to predict structural forces using CFD and wind tunnels.

6.1. Building and Surroundings

The building studied is a large grandstand building at the Ascot horse racing track to the west of London in Berkshire, UK (see Figure 6-1). Low-rise developments are present to the east, west and south of the site while the open racetrack lies to the North. A number of low buildings surround the grandstand and these are seen in the wind tunnel model (Figure 6-2).

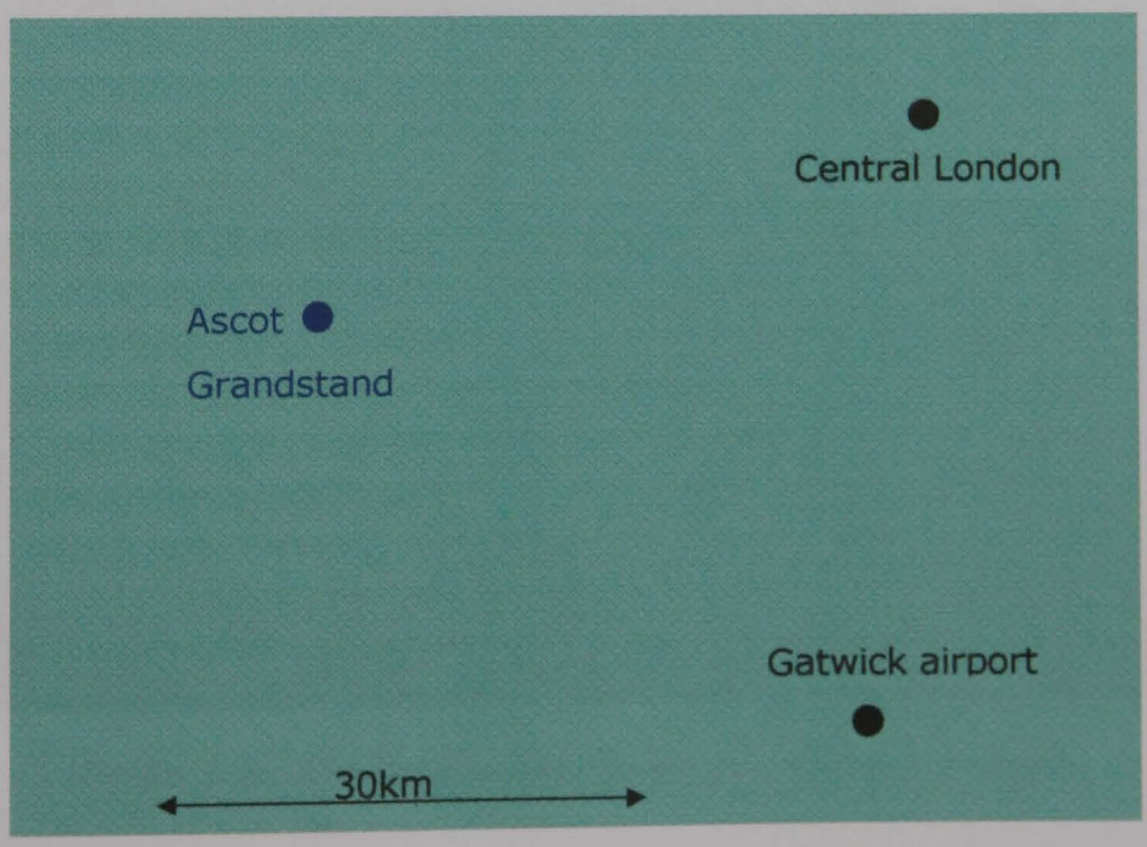

Figure 6-1: Location of Ascot Grandstand relative to Central London

The building itself is approximately 500m long × 60m wide × 40m high. The long axis is gently curved in plan and the building has a complex

shape including a number of projecting balconies and a folded cantilevered roof.

6.2. Wind Tunnel Tests

BMT Fluid Mechanics Ltd, the testing house that performed the wind tunnel study (BMT 2003a - BMT 2003d) provided a full set of data for each wind direction modelled. In their assessment of structural loads for the building they examined 36 different wind directions for two different model configurations. The tests were performed at a scale of 1:300 on a 4.4m diameter revolving baseboard (Figure 6-2). Surrounding buildings and topography were physically modelled up to an equivalent full-scale radius of 450m. Beyond this the orography was represented in the treatment of oncoming flow conditions. The velocity scale was 1:2.5 and the time scale 1:120.

Figure 6-2: Wind tunnel setup viewed from downstream

Pressure readings were taken relative to static pressure and normalised with respect to the dynamic pressure at the reference height, $\rho V_{ref}^2/2$. 584 tappings were placed across the roof top and under the overhanging eave projections and the construction was such that no pressure taps

protruded from the model. 300 point pressures could be measured simultaneously, necessitating two separate tests to measure values at all pressure taps. In each case the whole model was present in the tunnel but measurements were taken from one half each time. The pressure taps were grouped in sets of 8 with a common back pressure attached to the static pressure in the tunnel test section.

BMT Fluid Dynamics has long experience of performing tests of this type and extensive quality control procedures covering instrument calibration, measurement and data processing. The instrumentation and analysis procedures have been developed over many years through a combination of theoretical and empirical research to provide accurate structural loads for buildings.

Pressures were sampled at 600Hz (5Hz full scale) and each test was run for 156 seconds, equivalent to 312 minutes at full scale. This length of time was required to provide suitable extreme values for analysis as described later.

The wind tunnel used was a large boundary layer wind tunnel with a test section 4.8m wide by 2.4m high. The empty tunnel wind speed range is 0.2 – 45m/s and a speed of around 8m/s was used for these tests. The model was constructed of stiff acrylic plastic sheeting and was not susceptible to dynamic excitation within the range of wind speeds considered. The overall roof thickness was 7mm (full-scale equivalent 2.1m).

The configurations tested were an initial design configuration, for which pressure measurements were taken simultaneously across the whole building, and the final design configuration, for which pressures were measured across two-thirds of the building. The former has the advantage of providing a full set of data for each direction and is therefore more suitable for comparison with the CFD analysis.

The wind direction normal to the long face of the building is used for these studies. The building curvature will tend to slightly reduce the stagnation

of flow from the convex side but should not introduce wholly different flow patterns.

The wind profile was determined according to the Deaves and Harris log law description of the atmospheric boundary layer discussed in section 2.1.1 and described in ESDU (1993). The variation of velocity and turbulence intensity with height is given in Figure 6-3 while the variation with direction is shown in Table 6-1.

Figure 6-3: Velocity and turbulence profiles used in the wind tunnel

Wind Direction	Design Wind Speed at 40m height	
° from North	60min	1-s gust
0	20.99	31.85
30	18.9	29.23
60	19.26	29.52
90	18.33	29.43
120	18.23	29.15
150	18.9	31.19
180	21.24	34.14
210	22.1	36.32
240	24.2	39.41
270	23.2	38.34
300	22.89	36.53
330	20.68	32.76

Table 6-1: Design site wind speeds for the wind tunnel study

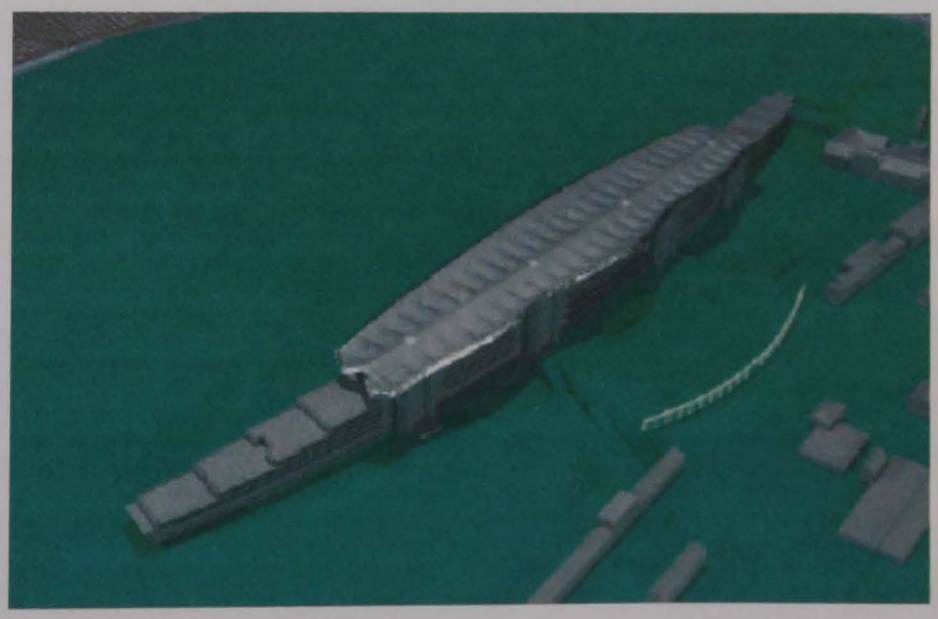

Figure 6-4: Close-up view of the wind tunnel model

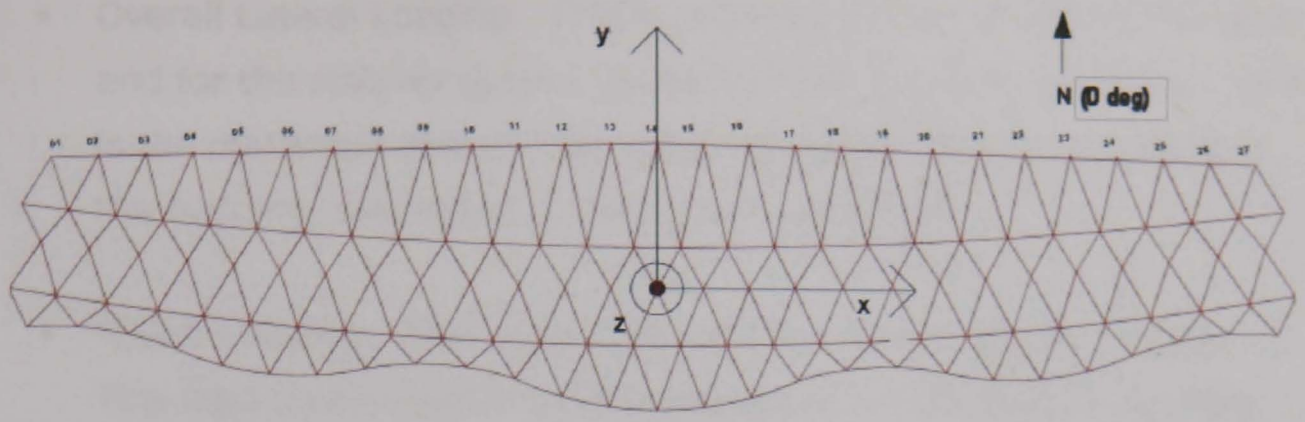

Figure 6-5: Model co-ordinates system used in wind tunnel and CFD studies

6.2.1. Load Effects

The tests were designed to calculate cladding pressures, local structural forces and overall loads for the structural design of the building. They were intended to simulate natural atmospheric turbulence and account for effects of pressure correlation across the building, requiring a suitable length of test and calculation of instantaneous loads as well as pressures. Variation in wind strength and angle were then accounted for statistically.

In order to calculate structural loads from the measured point pressures, the roof was divided into panels, each containing a single pressure tap which was assumed to represent the pressure throughout the panel. The point pressure was multiplied by the panel area, projected in the X, Y and Z directions, to give three orthogonal components for use in design.

For each individual load case, the panels contributing to that case were assigned an influence coefficient, generally ±1 or 0, representing the contribution of a positive force on that panel to a positive load effect. This method can be used for any loading effect although it neglects the effect of lever arm, meaning that it may be unconservative for calculation of bending moments. The analysis here therefore concentrates on direct loading effects.

The overall load effects considered in the wind tunnel tests were:

- Overall Lateral Loading. This is required for the design of the base and for the stability system of each of the 3 building sections. This is the maximum overall load integrated over the entire surface of the building, expressed in Cartesian coordinates.

- 'Twist' Loading. Also used in the design of the stability system. This load case represented the maximum unbalanced or twisting moment about the main axis of the roof trusses. This case is not considered here, although it is analogous to the cases considered.

- Single Bay Loading. For the design of the individual structural frames in each bay.

These effects were all time-averaged over a period of 15 seconds full scale, the appropriate gust period for the structural framing and stability system in accordance with BS6399:2.

A cladding study was performed (BMT 2003c) to assess the local cladding pressures. Results were obtained for averaging periods of 1s and 3s, corresponding to cladding element sizes of the order of 5m and 15m respectively.

Overall Loading Effects and Member Forces

For design of the structural frame we wish to find the peak 15-second load on the structure (see section 2.5.5). In the wind tunnel, this is performed by evaluating the instantaneous net load throughout the test. A specified number of peak load events is chosen and the pressure distribution causing each peak is recorded. At the end of the test, the average is taken of these pressure distributions and this is used to produce an equivalent pressure distribution which gives this average peak load.

An alternative method of calculating the peak overall load on the structure is to use the quasi-steady assumption, multiplying the mean load distribution by a gust factor representing the worst likely gust in the building's design life. This simplified method ignores the effect of non-

correlation of gusts across the building as well as neglecting the effect of body generated turbulence.

Previous results for the cube would suggest that reasonable predictions of the overall loadings should be possible while the more localised load effects will be harder to predict.

Cladding Load

The cladding load can again be evaluated with this simplified approach for a range of different cladding panel sizes. As the panel size approaches zero, the correlation across the panel surface will approach 100% and the quasi-steady assumption can be used alone. In areas of high turbulence production, the quasi-steady assumption breaks down as building-induced turbulence becomes significant.

Wind tunnel data were provided in binary form by BMT Fluid Mechanics Ltd. The data provide a time record of instantaneous pressure values at each tapping point across the structure. The zero degree case for the roof load was chosen for analysis and comparison with the CFD results. This contains 94,200 pressure values for each of 297 tapping points. The samples were taken at 600Hz, i.e. over a testing period of 157 seconds (model scale). The reference wind speed is 20.99m/s, corresponding to a dynamic pressure of 0.27kPa.

The summary data compared for quality checking were plots of mean pressure coefficient for each wind direction and pressure coefficients representing the highest overall building forces (uplift, shear and overturning). These "worst case" plots are intended to provide equivalent static loading for use by structural engineers who are not used to dealing with fluctuating design values. They use a simplified form of the influence coefficient method (Cook 1985), whereby the local influence coefficient is defined as either plus 1.0, minus 1.0 or zero to represent a positive, negative or zero contribution to the load effect respectively. In the final structural design, each of these load cases is considered in turn or in combination to determine the actual design load for individual members.

The load effect chosen for comparison was the highest overall lateral force in the Y - direction. Panels on the bottom surface of the overhanging sections of roof were mapped to panels on the top surface and the sign of the influence coefficient reversed. The results were then multiplied by the area of the panel, projected in the 3 orthogonal directions.

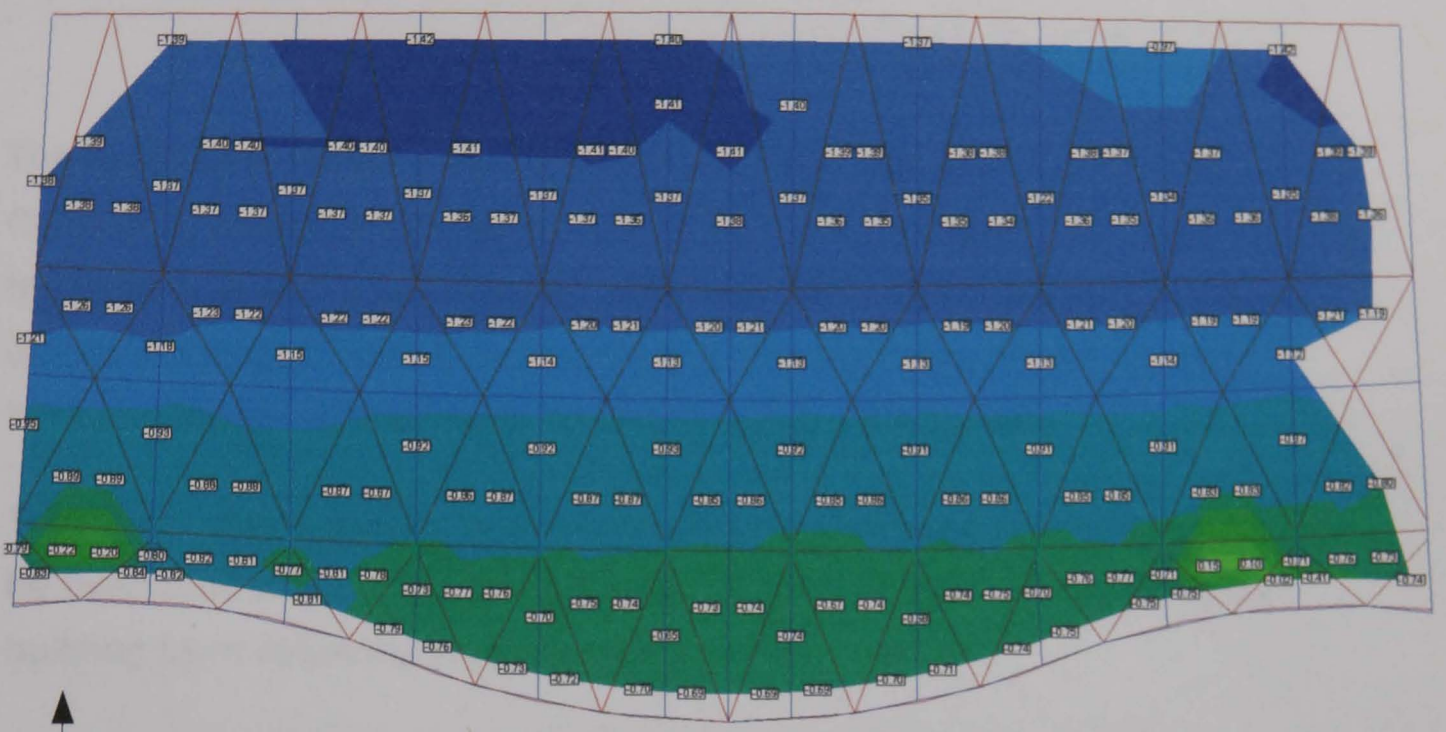

Figure 6-6: Mean pressure coefficient on roof for 180 degree wind

The mean pressure results shown in Figure 6-6 were reproduced from the data provided by averaging the pressure values in the data file.

6.3. CFD Simulations

In order to provide a direct comparison with the wind tunnel, the CFD tests were run at model scale. This has the additional benefit of limiting y^+ values at the building surface.

Parameter	Value
Simulation type	Transient
Turbulence model(s)	RNG k-ε with scalable wall functions and DES model
Mesh Type	Unstructured
Spatial discretisation	2nd Order

Table 6-2, CFD parameters Ascot studies

The Ascot CFD simulations broadly follow the procedures outlined in Chapter 3, except where specified below. While the geometry used in these simulations is significantly more complex than in the cube studies, due to working at wind tunnel scale the physical size of the body falls between the small Martinuzzi cube and the 6m Silsoe cube.

The aim of these studies is to investigate practical and technical issues to be overcome in moving from a simple geometry to the kind of complex building form requiring investigation in a wind tunnel.

The simulations include steady and unsteady RANS as well as DES simulations.

6.3.1. Computational Model

Computational Domain

Previous work on CFD domains for external aerodynamics discussed in section 3.1.2 assumes a cuboidal building and recommends a calculation domain extending 6 to 7 cube heights upstream, above and to either side of the cube and 10 cube heights downstream. In the case of wind perpendicular to the long face of the Ascot building, the crosswind face of the building is much wider than it is tall and an appropriate scaling length must be chosen. Mean flow over the centre of the building will be nearly two-dimensional and will largely be governed by the height of the building. If only 6 building heights were provided over the top of the building then, assuming fully 2-dimensional flow, there would be a blockage ratio of 1/7 and an equivalent artificial local increase in wind

speed. Allowing a width of 6 building widths on either side of the building would clearly have little impact on the local flow conditions over the building centreline.

The domain was therefore enlarged to a height of 18 times the mean building height to match the wind tunnel. Coupled with a width of approximately two building widths (measured in the long direction) this gave an overall blockage ratio of less than 4%. This is in line with standard practice for wind tunnel testing (Cook, 1990), whereby the blockage ratio is limited to prevent the flow from becoming overly constrained and thus artificially accelerated around the building. In the CFD simulation the domain boundaries act to constrain the flow in the same way as the physical walls of a wind tunnel.

The building was set 6 building heights back from the inlet as per previous simulations.

Geometry

The building geometry was taken from a 3D model provided by Buro Happold Limited, the consulting engineer who specified the wind tunnel tests. The roof geometry was carefully compared between the 3D computer model and the wind tunnel test model to ensure that there were no significant discrepancies between the two. The roof geometry was well represented by this method with less than 5% difference between panel surface dimensions from the wind tunnel tests and those in the CFD model. These small differences were accounted for in panel force calculations by scaling the results up or down with panel size.

Whereas the Silsoe and Martinuzzi cubes each required 5 surfaces to define the body plus another 6 to define the boundaries of the computational domain, the Ascot building required 3464 surfaces, each of them unique. Of these, over 600 were in the roof, where the geometry had to be particularly carefully defined to allow confidence in the CFD modelling here. Building the model required approximately 5 days work by a skilled 3D geometry technician and once it had been imported into

the CFD software, several more days were required to remove unneeded details and to group building surfaces together ready to define meshing parameters. This is comparable to the time required to produce a wind tunnel model.

The roof edge detail was specified as shown in Figure 6-7. Care was taken in the wind tunnel model to produce clean sharp edges in order to ensure separation, to avoid Reynolds number effects at model scale.

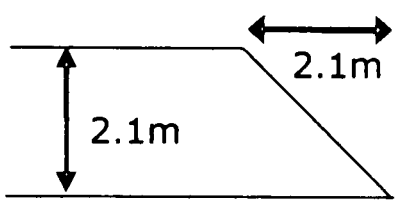

Figure 6-7: Roof edge detail as modelled in the wind tunnel (full-scale dimensions)

Turbulence Models

Initially, steady and unsteady RANS simulations were performed using the RNG k-ε model, as with previous studies. Preparatory studies were performed with the SST k-ω model as a starting point for DES simulations. Later studies were performed using the DES model described in section 2.2.2.

The timestep used for DES simulations was z/0.5U as discussed in section 3.1.6. This equation is height dependent, as shown in Table 6-3 and so an appropriate height must be chosen which is representative of the unsteady fluctuations. In this simulation we are most interested in results at roof level, but as the turbulent fluctuations are mostly present in the wake, 0.6h (24m) was chosen as representative of the wake region. This gives a maximum timestep of 0.02s at model scale, 2.4s at full scale.

Full scale			Wind Tunnel
Ht. (m)	**Velocity (m/s)**	**Timestep (s)**	**Timestep (s)**
10	16.79	1.19	0.00993
15	17.84	1.68	0.01401
20	18.89	2.12	0.01765
25	19.73	2.53	0.02112
30	20.57	2.92	0.02431
35	20.57	3.40	0.02836
40	20.99	3.81	0.03176

Table 6-3, CFX timestep requirements at various heights

To maintain a CFL number of less than 1 (see 3.1.6), this equates to a minimum mesh size Δ_0 of $0.02U_{max}$. Preliminary studies showed the maximum speed to be around 1.5 times the reference speed at eaves level, leading to a minimum value of Δ_0 of 2mm model scale. This is clearly much smaller than the size required to resolve the local geometry and is acceptable as an initial limit on local flow resolution. If the mesh is resolved further then the timestep used will be consequently smaller.

The above method assumes that the wake turbulence has a similar turbulence spectrum to the oncoming wind. If the wake turbulence contains coherent structures at higher frequencies than those in the boundary layer generally then these should be also be captured in the LES region. This may require further mesh refinement based on the observed frequencies.

This mesh size was applied above the building and in the wake of the building to a distance of 2 building heights downstream. As this represents the end of the recirculation zone it was assumed that errors in flow prediction beyond this region would not significantly affect results around the building. The mesh size was therefore gradually increased downstream of this zone.

Boundary Conditions

Boundary conditions were generally developed from the principles established in previous chapters and were thus:

Inlet: The upwind velocity and turbulence profiles were determined from a boundary layer simulation in the absence of the building as described below.

Outlet: This was defined as a zero relative pressure boundary, as used in previous simulations.

Sides + roof: These were specified as openings with identical velocity and turbulence profiles to the inlet, as discussed in section 5.3.2

Floor: The value of z_0 calculated for the site and used in the wind tunnel tests was 0.3m, which equates to 1mm at model scale. A sand grain roughness height of 7.5 times this value was therefore specified for the floor.

Building: All building surfaces were defined as smooth non-slip surfaces.

Meshing

The first cell height in the upwind section of the domain was set to 15mm so that the first calculation point was at 7.5mm from the floor, to match the roughness height. The cell height was allowed to gradually increase moving away from the floor.

The mesh size in the free stream was set to 300mm, reducing to 60mm near the floor. This is sufficient to resolve broad changes in wind direction above and around the building but must be significantly resolved near the building. The mesh size on the building roof was set to 17mm, reducing to 6.7mm on the overhanging edge sections and 3.3mm at the very edge. This was further refined through automatic mesh adaption to pick up the shear layer as flow separated from the leading edge of the roof.

For the DES simulations it was essential to adequately resolve the unsteady fluctuations in the wake. The mesh was therefore resolved as described in the turbulence modelling section above.

6.4. Results

6.4.1. Boundary Layer Simulation

As shown in previous chapters, boundary layer simulations are required to establish a stable equilibrium velocity and turbulence profile for each wind direction and for each turbulence model used. Following the 6m cube work and published recommendations (Richards et al. 2004), a boundary layer was developed which was stable through the domain and consistent with the boundary conditions used rather than aiming to match full-scale turbulence values. This generally results in an underprediction of full-scale turbulence levels but avoids creating a boundary layer which is inconsistent with the CFD boundary conditions.

Convergence

It was found that the default convergence settings did not result in settled values of velocity near the domain floor, so the convergence requirements were tightened until settled values were obtained for the velocity.

For the empty tunnel study, the velocity and turbulence at 0.05m above the floor (equivalent 15m full-scale) was monitored and it was found that normalised RMS residual values of 3×10^{-5} (CFX 2003) were required to obtain satisfactorily settled velocity, k and ε values.

The boundary layer simulations performed were:

- Steady and unsteady RANS simulations with the RNG k-ε model: this required specification of stable profiles for velocity, k and ε at the inlet. These proved identical for the steady and unsteady simulations, as one would expect. y^+ values of between 20 and 100 are recommended for k-ε simulations with scalable wall functions (CFX 2003). The size of the first cell is limited however by the

requirement to have the first calculation point outside of the roughness height. This prevents further grid refinement to reduce y^+ on the domain floor.

- Steady and unsteady RANS simulations with the SST k- ω model: this requires specification of k and ε or the turbulence intensity and eddy length scale at the inlet. Again, separate studies were performed for the steady and unsteady simulations. y^+ values of less than 2 are recommended for k- ω simulations, requiring much greater mesh refinement on the floor. The k- ω models have been developed to give more accurate predictions of separation and should therefore better predict the separation region.

- DES simulations: these avoid the problem of generating a turbulent transient boundary simulation which is self-consistent by using the earlier RANS profiles for the far-field of the flow domain.

RANS Simulations

The RNG k-ε simulations were initially run with a coarse mesh with the aim of developing a stable velocity and turbulence profile. The velocity profile and ground roughness were matched to achieve the wind tunnel velocity profile. The profiles of turbulence parameters k and ε were chosen to be stable and in equilibrium with the boundary conditions rather than to match full-scale conditions.

Velocity Results

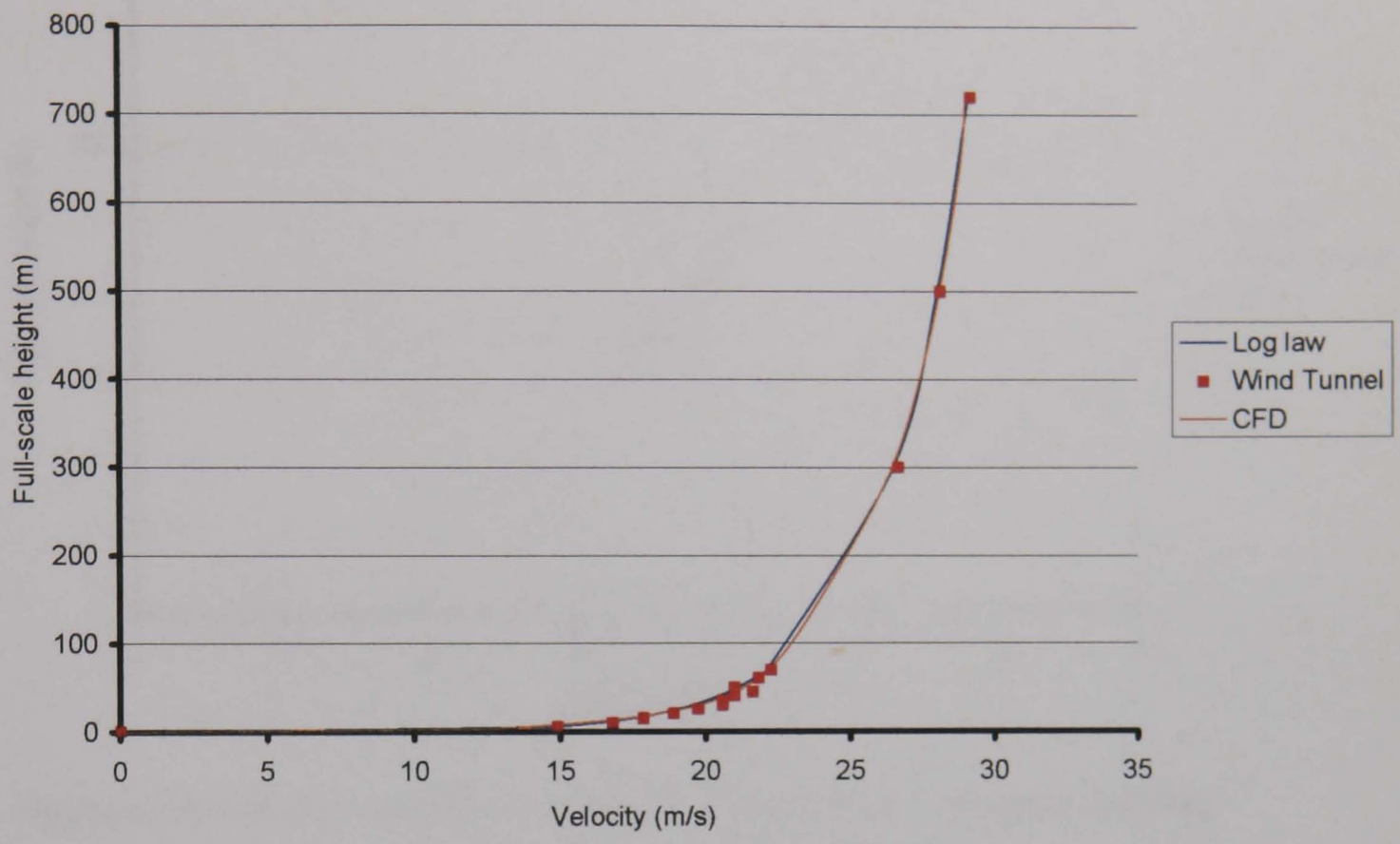

Figure 6-8: Velocity profile from RNG k-ε simulation compared with log law and wind tunnel profile

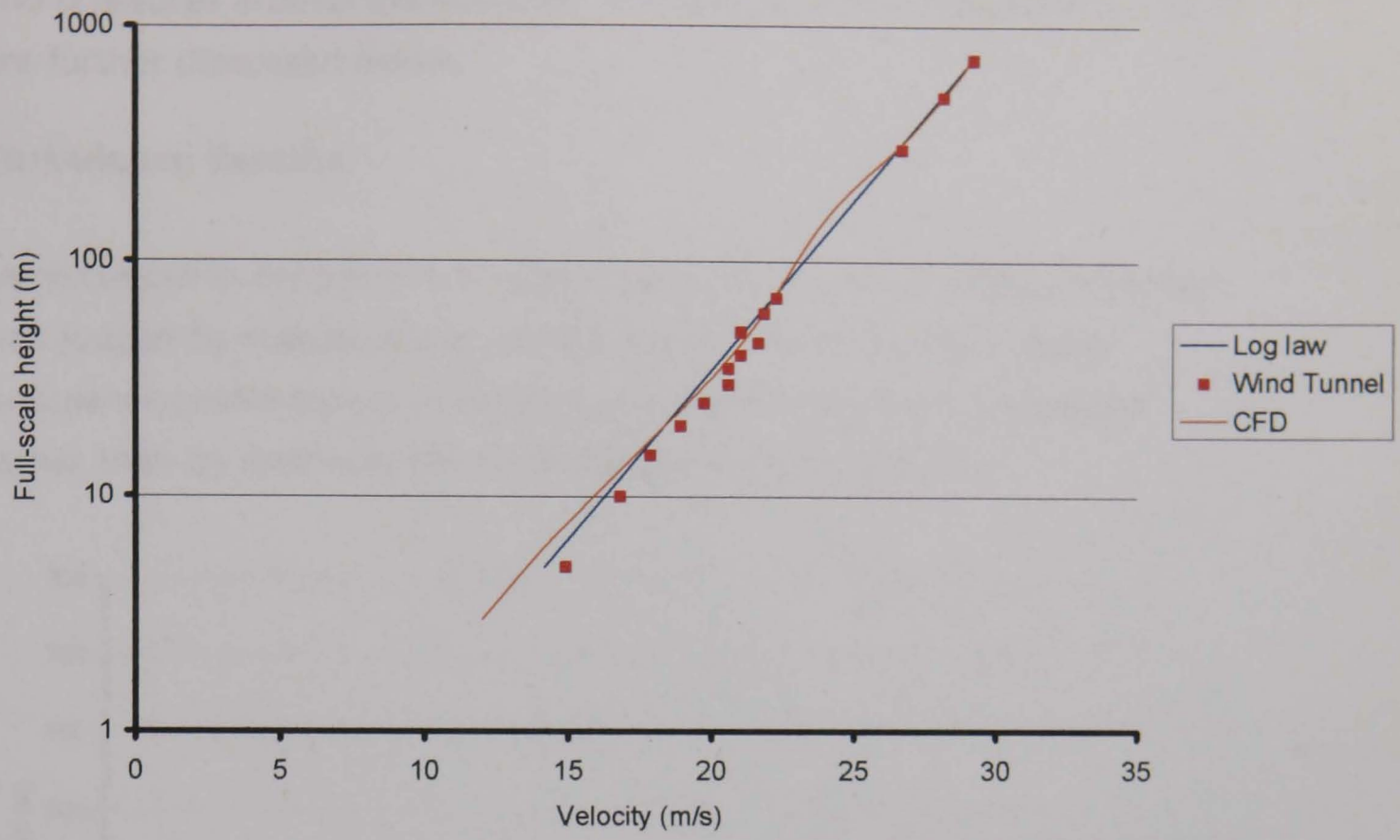

Figure 6-9: Velocity profile from RNG k-ε simulation compared with log law and wind tunnel profile (log scale)

As discussed in section 3.1.3, a stable velocity profile can be obtained for a sand grain roughness height of 7.5 times the aerodynamic roughness z_0. As shown in Figure 6-8 and Figure 6-9 this is a good match for the experimental velocity profile in the upper regions of the boundary layer, although there is an error of approximately 5-10% in velocity within 40m of the ground. Comparison with the target velocity profile shows that the error lies in the experimental velocity profile, where low-level accuracy appears to have been sacrificed in order to maintain a close match to the target profile at higher level.

This is probably due to the relatively short upstream fetch in the wind tunnel making precise profile matching hard to achieve. Its height may be related to the vertical barrier designed to trigger boundary layer development and seen in the background of Figure 6-2, as similar effects have been seen in other wind tunnel simulations (Holmes and Osonphasop, 1983). The building height is approximately 40m at full scale so it is expected that this higher velocity will directly affect velocities

and pressures around the building. The effects of this difference in profile are further discussed below.

Turbulence Results

As discussed in section 6.4.1, adequacy of the boundary layer simulation was judged by matching the velocity profile and achieving a stable turbulence profile that is in equilibrium with the boundary conditions rather than by matching the full-scale turbulence intensity.

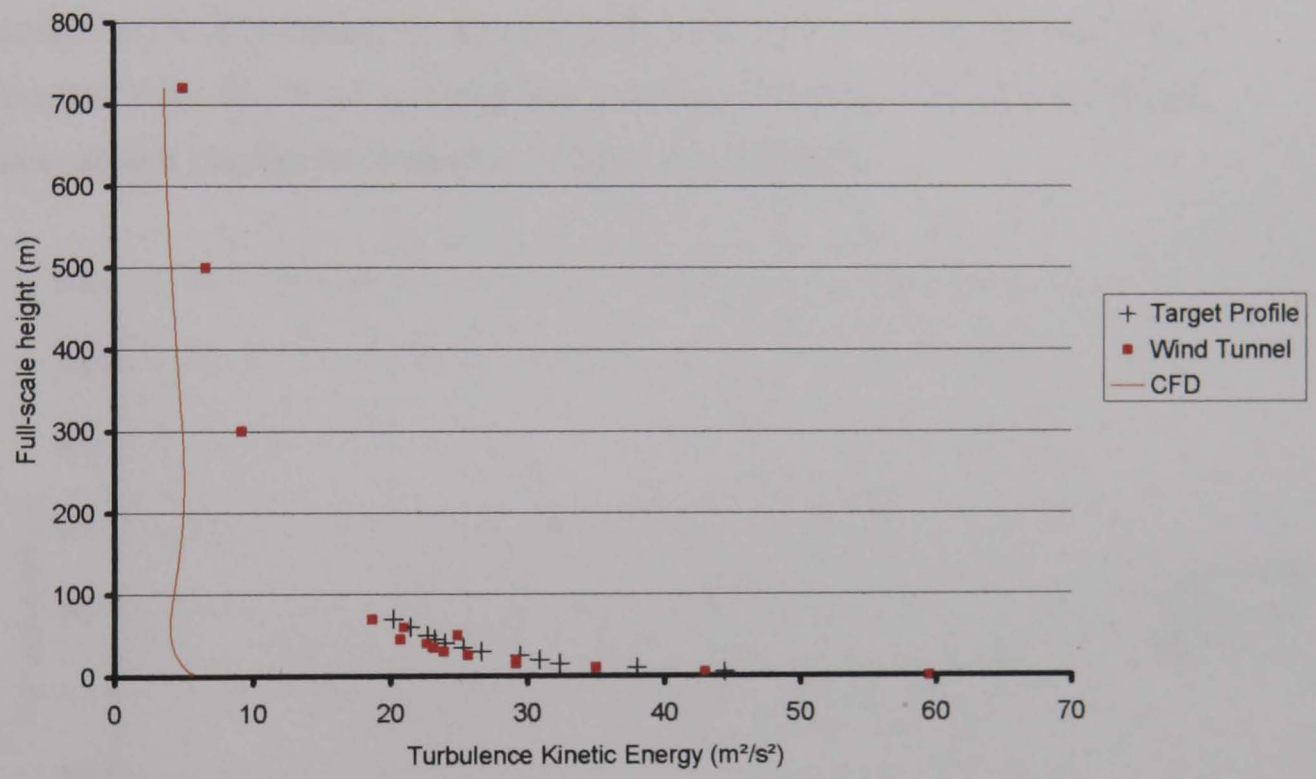

Figure 6-10: Turbulence kinetic energy profile from RNG k-ε empty tunnel simulation compared with target and wind tunnel profile

The flow achieved in CFX had a significantly lower turbulence intensity than that found in the wind tunnel as seen in Figure 6-10. However, the profile was stable and represented a fully developed boundary layer.

The reduced turbulence values in the oncoming flow may result in increased instability in the CFD result. It will certainly mean that local turbulence values from the CFD simulation cannot be used to estimate local turbulent fluctuations in velocity and pressure.

These velocity and turbulence profiles were used in the inlet boundary condition as well as the sides and roof of the computational domain. Once the profiles had been tested for steady state simulations they were then used in unsteady simulations. The profile was found to be stable in the unsteady case as well.

SST k-ω Simulations

The standard SST k-ω implementation requires very fine resolution of the wall region, impractical for the large complex flow cases considered here. However, it is possible to combine the SST k-ω model with wall laws designed for k-ε type turbulence models. This can result in a stable turbulence profile as shown in Figure 6-11 below.

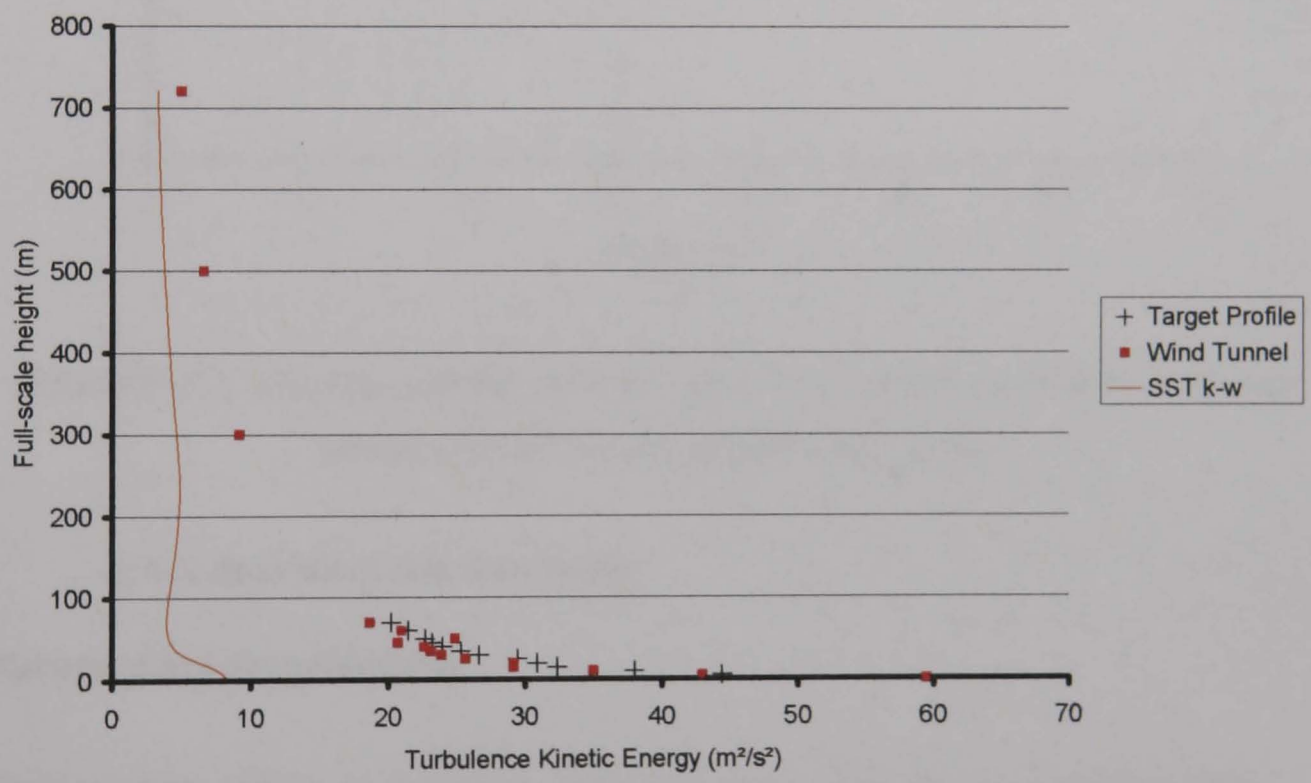

Figure 6-11: Turbulence profile with the SST k-ω model compared with target and wind tunnel profile

The velocity profile achieved with this model (Figure 6-9) was not such a close match to the log law or the experimental results, particularly in the first few cells above the rough floor. This may be due to inconsistencies in the wall treatment, as noted by CFX (2003) and Franke et al. (2004). This slightly lower velocity near floor level is likely to result in a small change in the predicted pressure and velocity upwind of the building. This

is likely to result in reduced stagnation pressure on the upwind face and the reduced intensity of separation as there is less momentum in the oncoming flow.

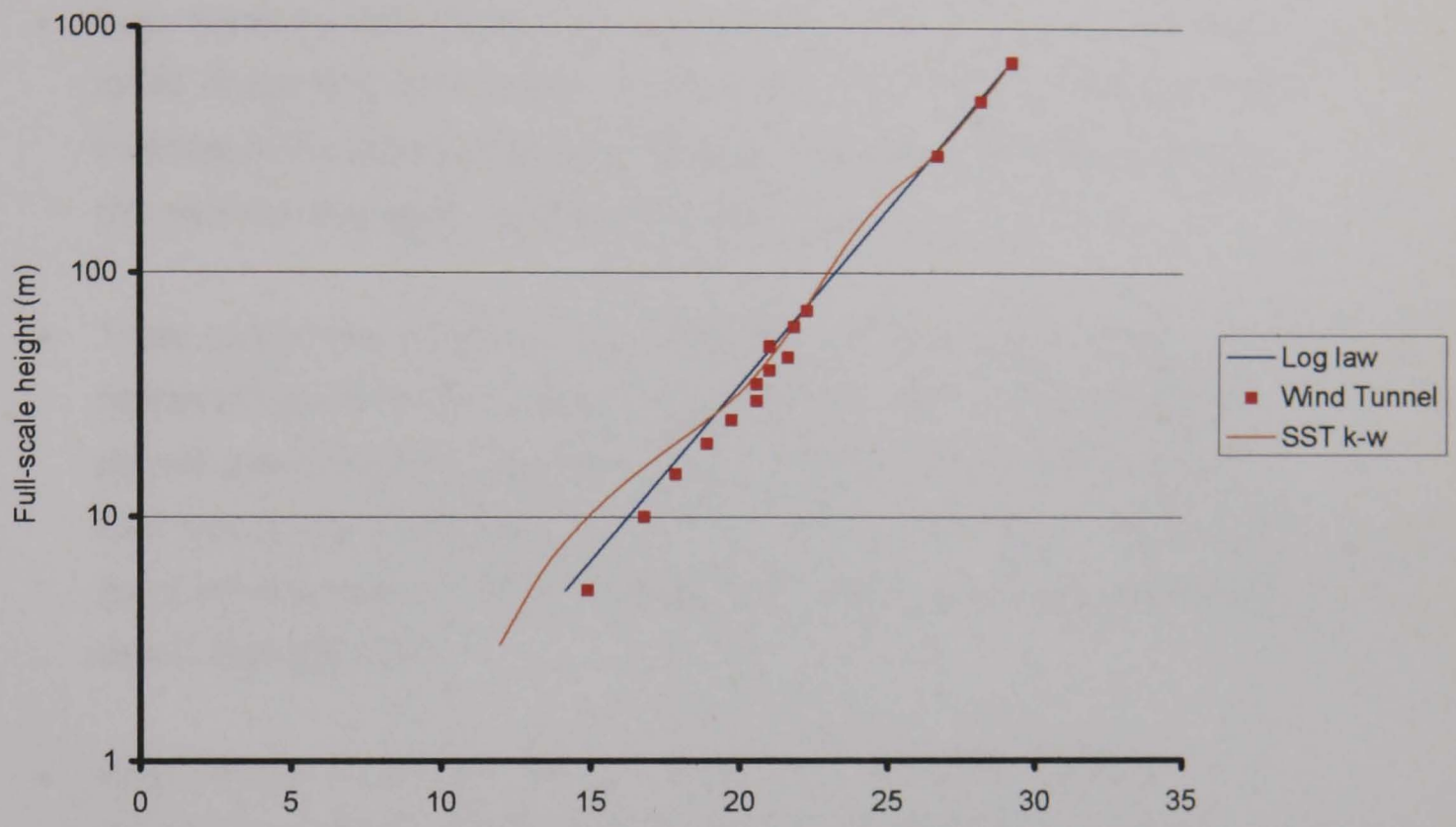

Figure 6-12: Velocity profile with the SST k-ω model compared with log law and wind tunnel profile (log scale)

6.4.2. Building Simulations

Parameters Considered

The key simulation parameters required were point pressures and area loads. Additionally, velocity and turbulence profiles were monitored to describe the mean and time varying flow properties.

The loaded areas considered in the CFD studies were chosen to match those of interest to structural engineers and for comparison with the wind tunnel results.

- Point pressures, not used directly but needed to derive structural design loads. Point pressures were monitored at points

corresponding to the roof apexes and at chosen points corresponding to pressure taps on the monitored panels below. These were widely distributed across the entire surface of the roof.

- Area loads (single triangular roof panel), corresponding to cladding loads or loading on a small structural element. Sample panels were investigated towards the leading edge, middle and trailing edge of the roof for the west, centre and east roofs.

- Truss Loads (set of panels contributing to a single roof truss), representing loads on a large structural element. Linear strips of panels were chosen, corresponding to the structural bays used in examining the 'twist' load case in the wind tunnel study. Four such bays were chosen, two in the west roof, one in the very centre and one in the east roof.

- Roof Section (West, centre or East thirds), corresponding to structural stability system or foundations. These were further subdivided into the internal sections of roof and overhanging sections.

The mean and variance of each load was considered. Spatial correlation (or lack of it) is significant for the effect it has on the mean and variance of the area loads, and was therefore evaluated solely in these terms and not calculated directly.

6.4.3.Steady state Studies

Studies were run to examine the effect on structural loading of choosing different convergence targets. A smaller selection of building regions was chosen to compare the results of the simulations in these initial studies: force on the central portion of roof was taken as representative of load on a full building section. Two roof panels, one near the front edge and one near the rear were taken as representative of member forces and point pressures on the front and rear edge of the roof were taken as extreme

case point pressures. The results of this investigation are shown in Table 6-4.

Steady state RANS simulations were attempted using the RNG k-ε model, monitoring overall building forces and point pressures. While the lower order solutions converged, it was not possible to obtain a satisfactory level of convergence with the second order discretisation and the residuals were seen to fluctuate at a level of around 10^{-3} in a similar manner to that seen for the Silsoe cube (see Figure 5-7).

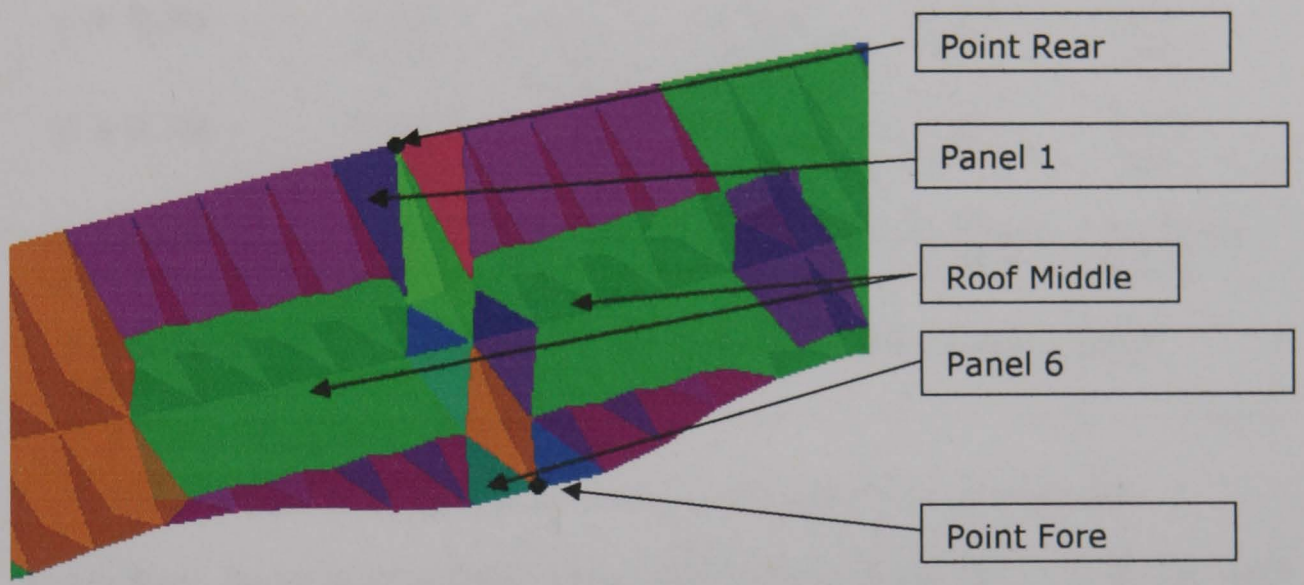

Figure 6-13: Central portion of grandstand roof: key to Table 6-4 and Table 6-5

Discretisation	Normal Force on Roof Middle (N)	Panel Force (N)		Point Pressure Coefficient	
		Panel 1 (rear)	Panel 6 (front)	Fore	Rear
Wind tunnel	.882	0.0210	0.0479	-1.36	-0.39
Upwind ($\beta = 0$)	0.77 -13%	0.023 +10%	0.052 +9%	-1.75 +29%	-0.846 +117%
β = 0.25	0.836 -5%	0.022 +5%	0.052 +9%	-1.567 +15%	-0.691 +77%
β = 0.50	0.901 +2%	0.02 -5%	0.047 -2%	-1.274 -6%	-0.52 +33%
β = 0.75	0.87 -1%	0.018 -14%	0.034 -29%	-0.896 -34%	-0.337 -14%
2nd Order ($\beta = 1$)*	0.55 approx	0.01	0.015 to 0.028	-0.109 to -0.546	-0.153 to -0.175
Automatic adjustment*	All variables failed to settle towards a mean value				

β = Blend factor

* = Did not converge satisfactorily – see discussion in main text

Table 6-4: Force and pressure for different discretisation schemes, with percentage difference from wind tunnel results

As the 1st order solution was blended towards the 2nd order solutions, the results appeared to approach the wind tunnel values for overall load on the central roof area and for wake pressures and forces. Pressures and forces near the leading edge were initially too high but descended as the discretisation accuracy was increased, becoming too low at a blend factor of 0.75.

For the blend factor of 0.75, a convergence target of 1×10^{-5} was required to obtain settled pressure values at all points. This is an order of magnitude lower than that generally used in industrial CFD.

Mesh dependence studies were run at this point, automatically refining the mesh at areas of high local velocity gradient and maintaining a blend factor of 0.75. These resulted in a failure to converge to a satisfactory

degree, however, with solution instability increasing as the mesh was refined.

For the full second order solution (blend factor = 1.0), convergence could not be achieved. All important parameters including overall structural loads were fluctuating very greatly from iteration to iteration during the failed solution process, indicating that the failure to converge was due to instability in the flow as modelled. Total loads integrated across large sections of the roof were seen to vary by a factor of 2. Loads on individual truss sections varied by a factor of 3 and point loads varied by up to a factor of 10 near the leading edge of the roof. The implications of this are discussed in section6.5.2, however it clearly indicates areas where pressures and forces cannot be confidently predicted using steady state simulations.

Similarly the software was unable to achieve convergence by automatic adjustment: progressively reducing values of blend factor at areas of poor convergence.

Table 6-4 shows that the greatest variation and uncertainty comes in the point pressure values and particularly towards the rear of the roof where the suction pressure was overpredicted by a factor of 2 in the upwind discretisation compared with 29% at the leading edge. For the poorly converged 2^{nd} order solution however instantaneous pressure values at the leading edge on occasion exceeded four times the value from wind tunnel testing. This could suggest that this separation area is the primary source of instability in the flow.

Once these point pressures are integrated across a finite area to generate surface loads for use in design the variability in the results reduces significantly. In each case the percentage variation in prediction of panel loading is lower or equal to the error in the respective point pressure relative to the wind tunnel value.

Similarly to the Silsoe cube results, this suggests that it is not possible to consistently achieve satisfactorily converged solutions for all structural loading parameters using steady RANS simulations. The unsteady flow

simulations for the cube showed the importance of performing transient simulations to obtain settled predictions of structural load across the building. Similarly here the progression was made to unsteady RANS and DES simulations.

6.4.4. Transient RANS and DES Studies

Following the poor convergence behaviour of steady state simulations, transient simulations were run with decreasing timesteps until convergence was achieved. Convergence was found to be highly dependent on mesh design, and very hard to achieve with coarse meshes. This is presumably because it was not possible to fully resolve the instability present in the flow. Convergence was easier to obtain with meshes which adequately refine the wake flow but smaller timesteps were needed as the mesh was refined.

There are no clear guidelines on timestep selection for unsteady RANS simulation. Timesteps were therefore tested on a trial and error basis until a satisfactory level of convergence was achieved, generally for RMS residuals between 1×10^{-5} and 5×10^{-5}. The previous work on the Silsoe cube suggests that timestep choice in unsteady RANS simulations does not significantly alter the results in the way it does for LES simulations, where the timestep and mesh size act as an explicit filter on the turbulent scales.

The mesh was generated from a steady state run with automatic mesh refinement in areas of high velocity gradient. A series of refinement steps was initiated and meshes saved with approximately 3.7 million and 5.7 million cells, shown in Figure 6-14 and Figure 6-15 respectively, with detailed views in Figure 6-16 to Figure 6-21. These were steps 3 and 5 respectively in the sequence of mesh refinement steps.

These refinement steps resulted in a general mesh refinement in the wake of the building and a much finer mesh at the leading edge and in the separation region above the roof. The use of multiple refinement steps allowed broader regions to be refined as the flow responded to earlier

refinements before being refined again. This improved convergence behaviour for the subsequent transient simulations. Due to the very fine mesh refinement, especially near the leading edge, both meshes achieve y^+ values of less than 50 across the roof and less than 10 near the leading edge. Some areas along the leading edge for mesh 1 approach y^+ values of 20. A timestep of 0.01s was required for convergence with both meshes.

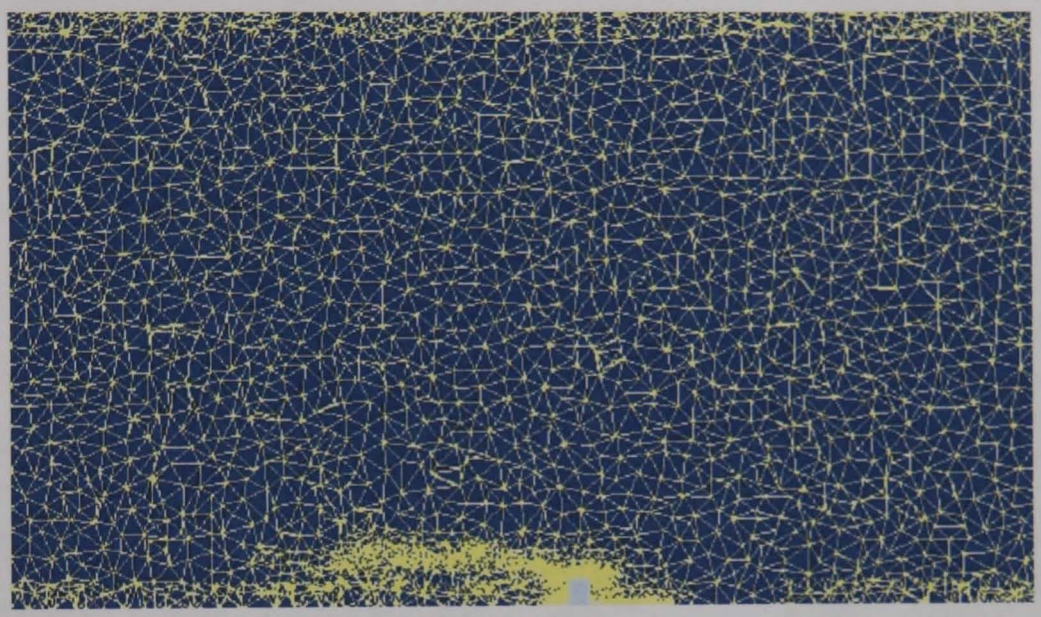

Figure 6-14: Transient RANS Mesh 1

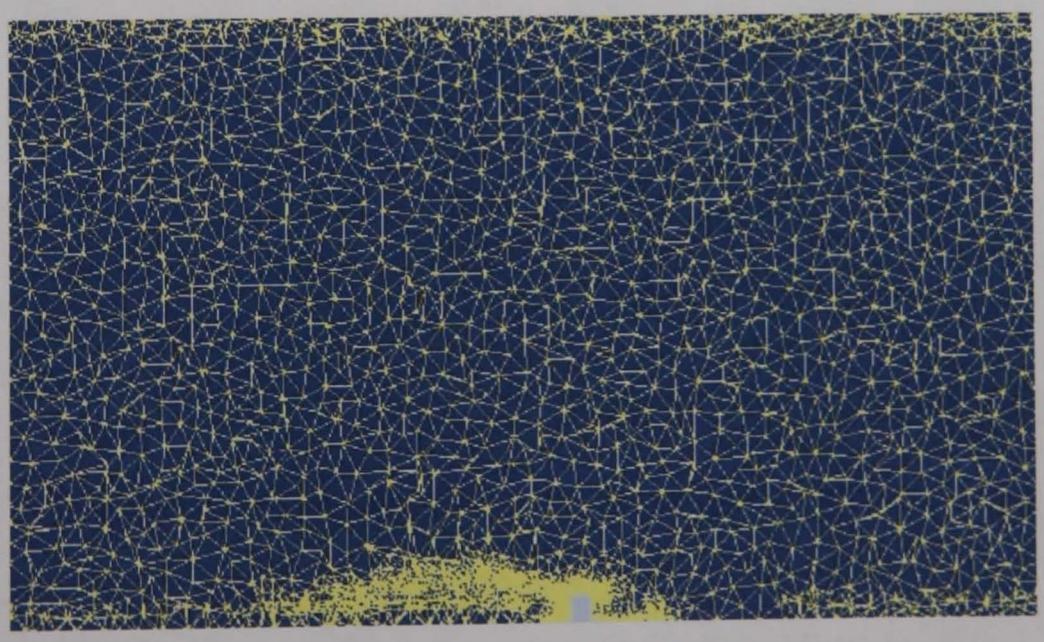

Figure 6-15: Transient RANS Mesh 2

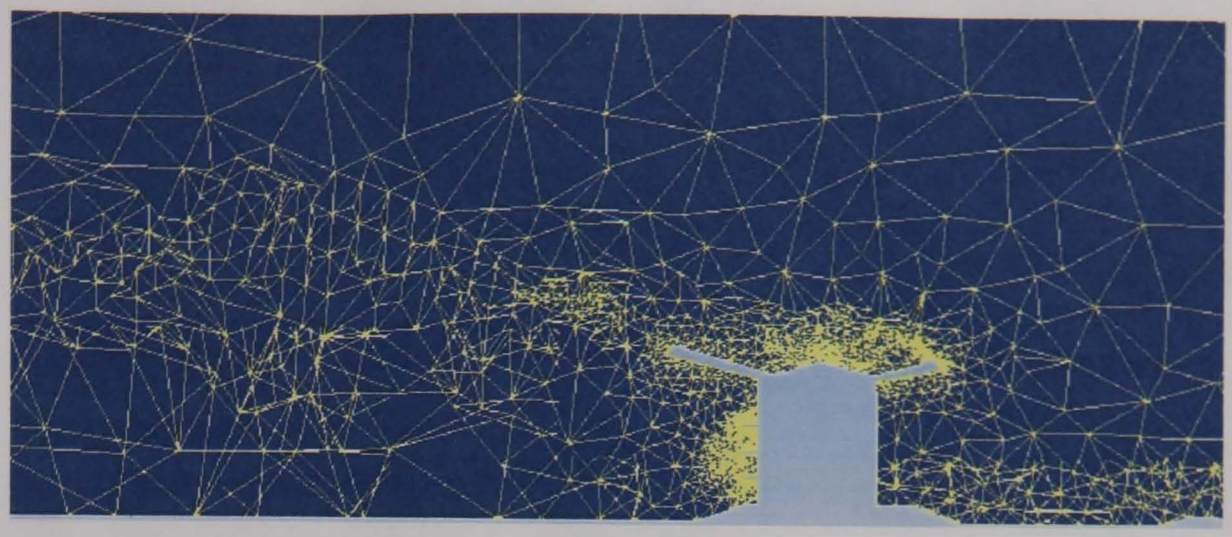

Figure 6-16: Transient RANS Mesh 1: building and wake

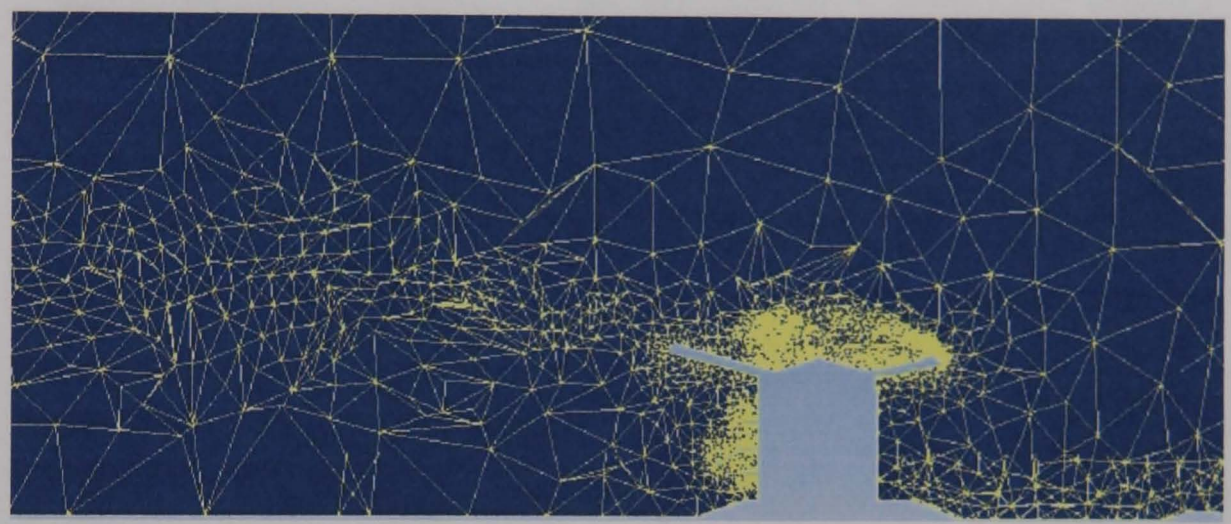

Figure 6-17: Transient RANS Mesh 2: building and wake

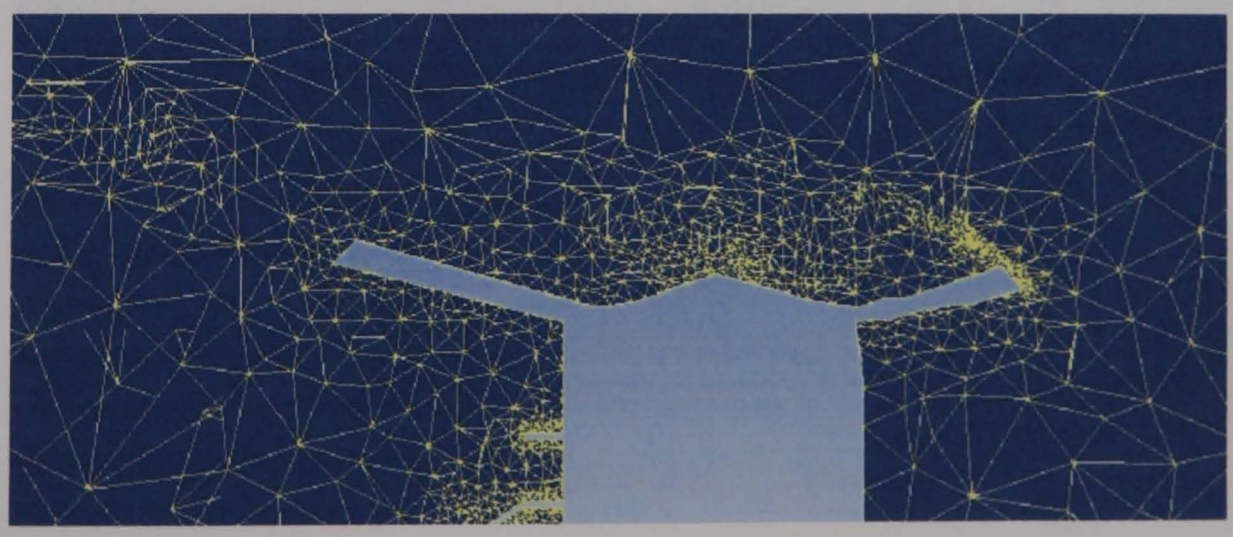

Figure 6-18: Transient RANS Mesh 1: detail on building

Figure 6-19: Transient RANS Mesh 2: detail on building

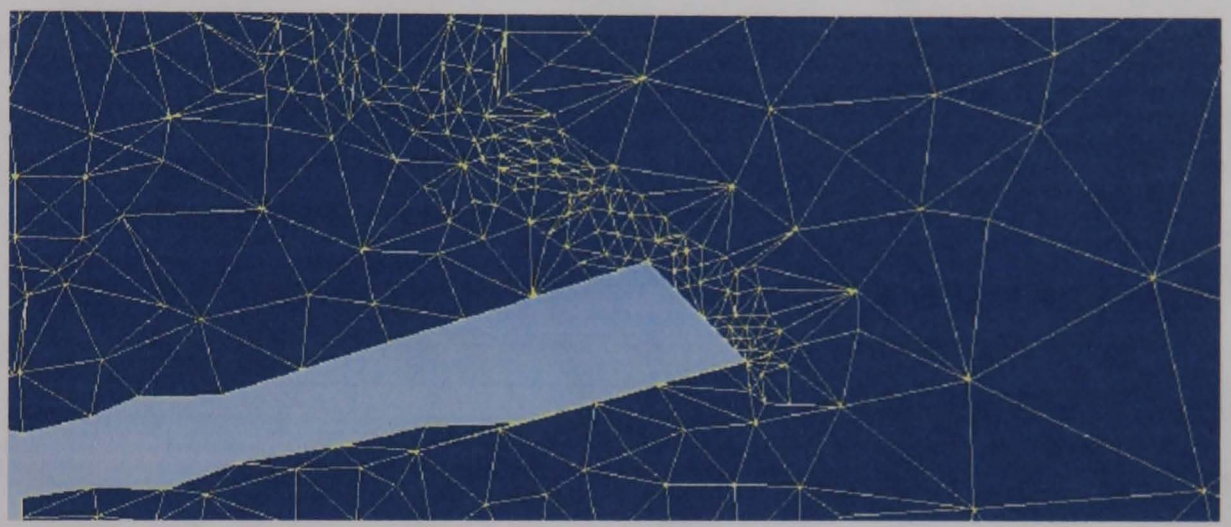

Figure 6-20: Transient RANS Mesh 1: detail on leading edge

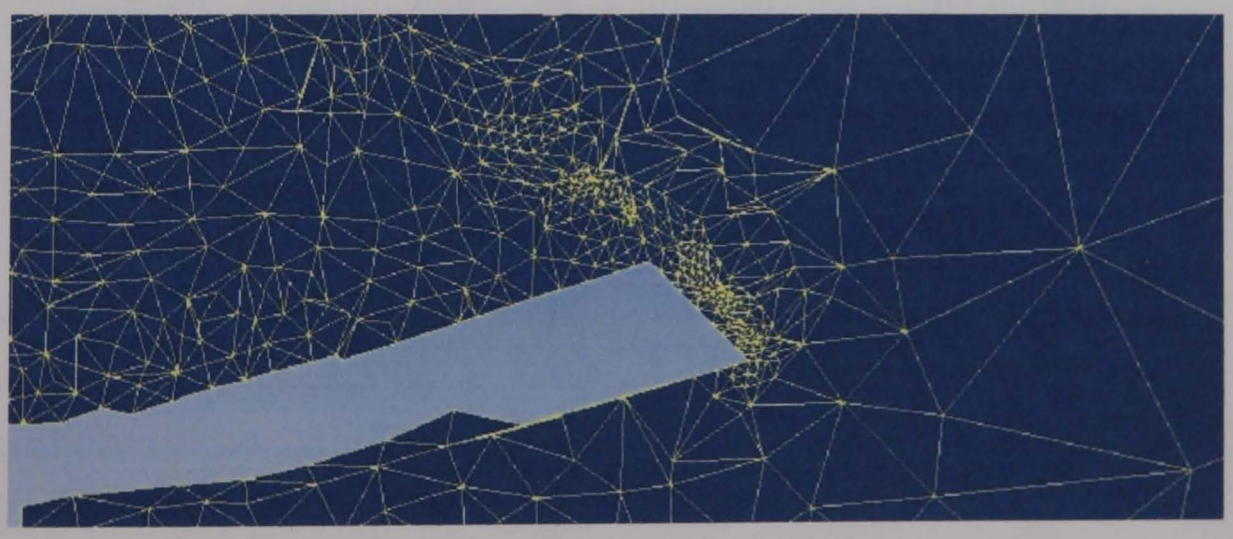

Figure 6-21: Transient RANS Mesh 2: detail on leading edge

The refinement seen near the wall of the building around the overhanging ledges in Figure 6-18 and Figure 6-19 was present in the initial mesh and was required to adequately represent these thin features. It was not a product of the mesh refinement process. The mesh refinement clearly

resulted in very large changes in mesh size from the refined building surface into the free stream. The large changes in mesh design from the building surface to the free stream mean that higher frequencies of turbulence will tend to be damped out in the free stream and possibly also near the buildings surface.

Transient results were tested for stationarity with the run test described in section 3.1.6 prior to calculating mean or variance values in order to ensure that sufficient transient data had been obtained to produce meaningful averaged parameters.

The transient simulations resulted in an underprediction of uplift across the entire roof and particularly at the leading edge, as shown in Table 6-5 below.

For comparison with the unsteady RANS simulations, the DES turbulence model was applied to this problem. The major requirement of a RANS grid is to sufficiently resolve the local flow component and automatic grid refinement is well suited to this. Grid requirements for DES simulations are rather different to those for RANS simulations so a new grid was built as described under "turbulence models" in section 6.3.1 above and shown in Figure 6-22 to Figure 6-29. The emphasis was on resolving the turbulent motions in the wake and avoiding sudden changes in grid size in any one area, as the grid size acts as a filter on the local turbulence scales. A timestep of 0.001s was used in the DES simulations.

The first DES grid (Figure 6-22) was intended to refine only the area in the immediate wake of the building while the second DES grid (Figure 6-23) allowed a much longer turbulent wake to develop. An expanded boundary layer was also used in the second DES run.

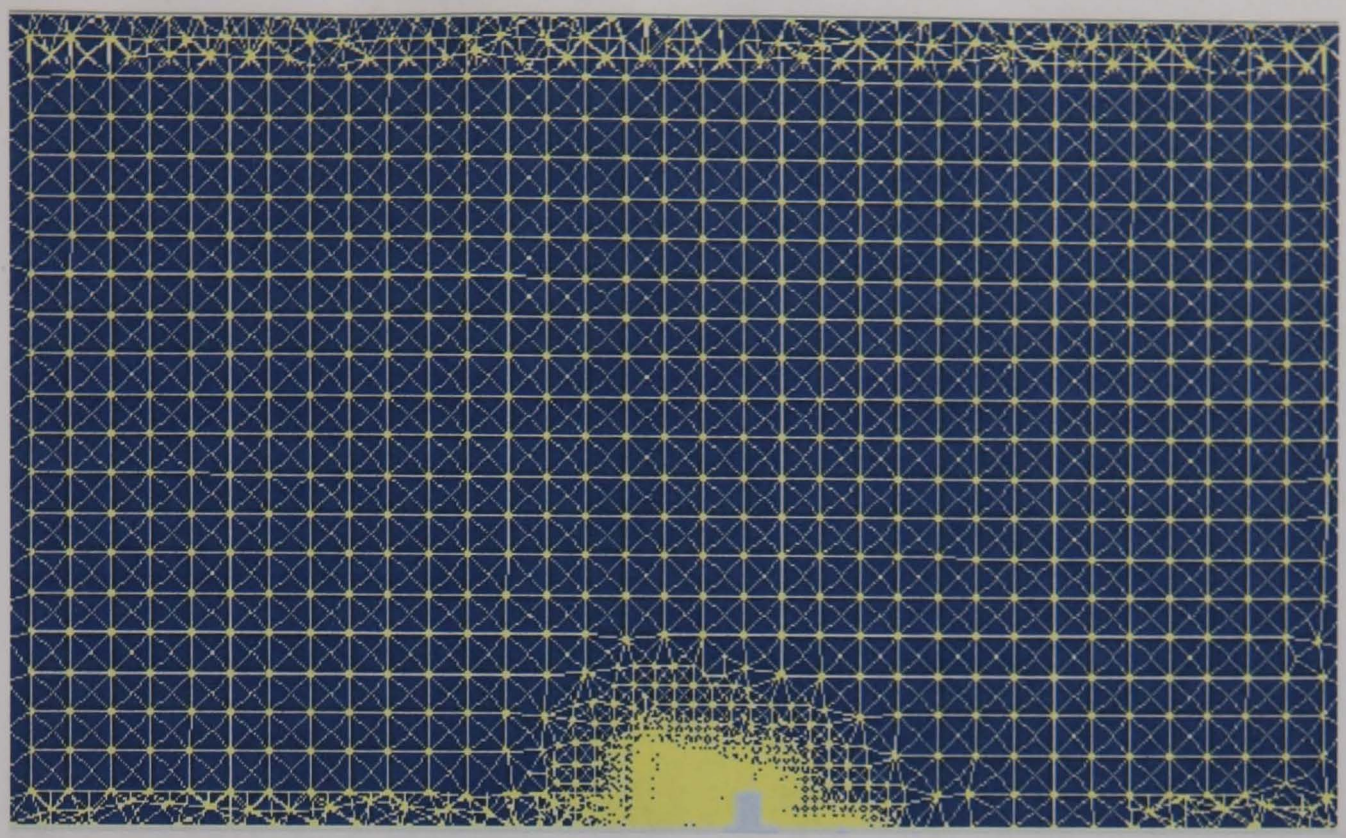

Figure 6-22: DES Mesh 1

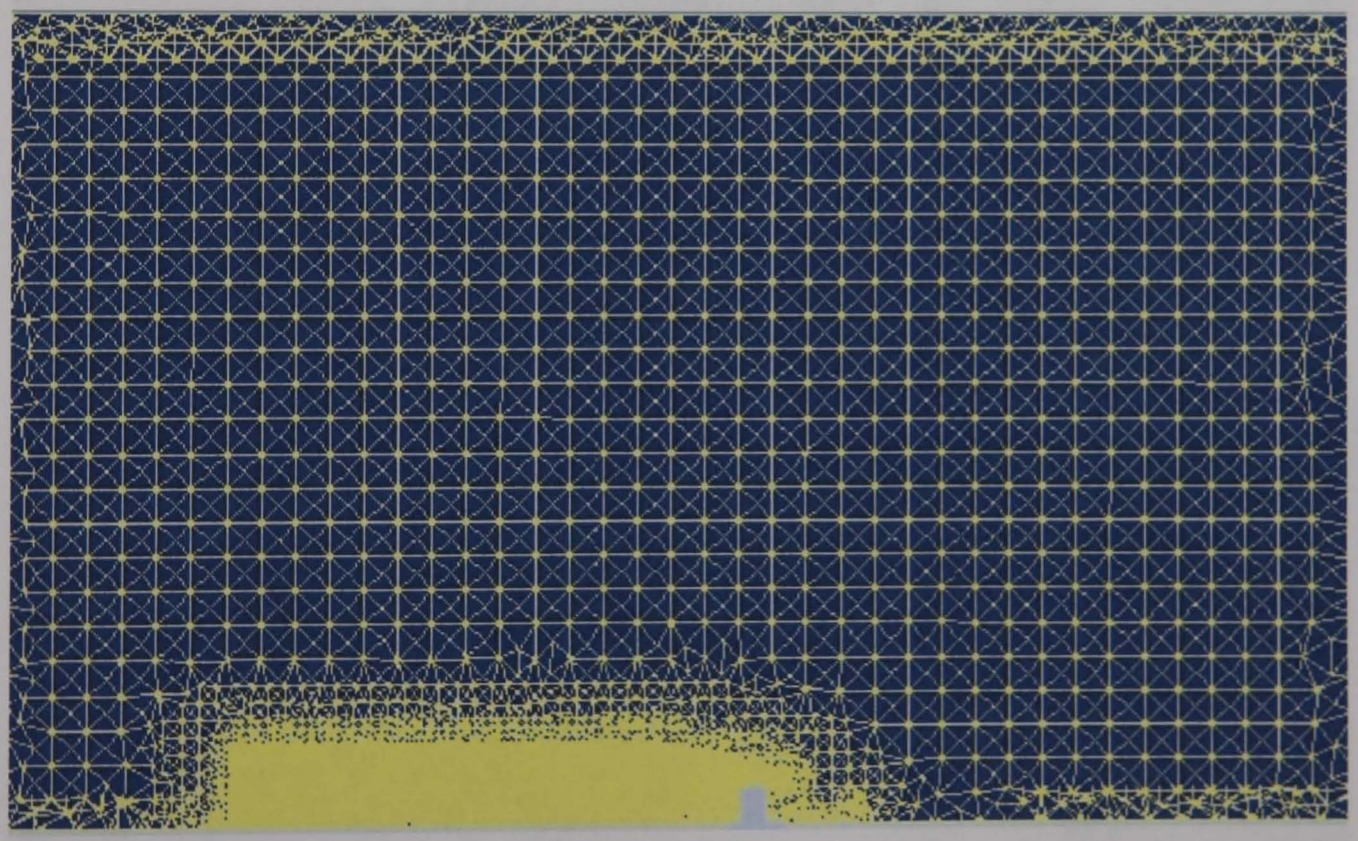

Figure 6-23: DES Mesh 2

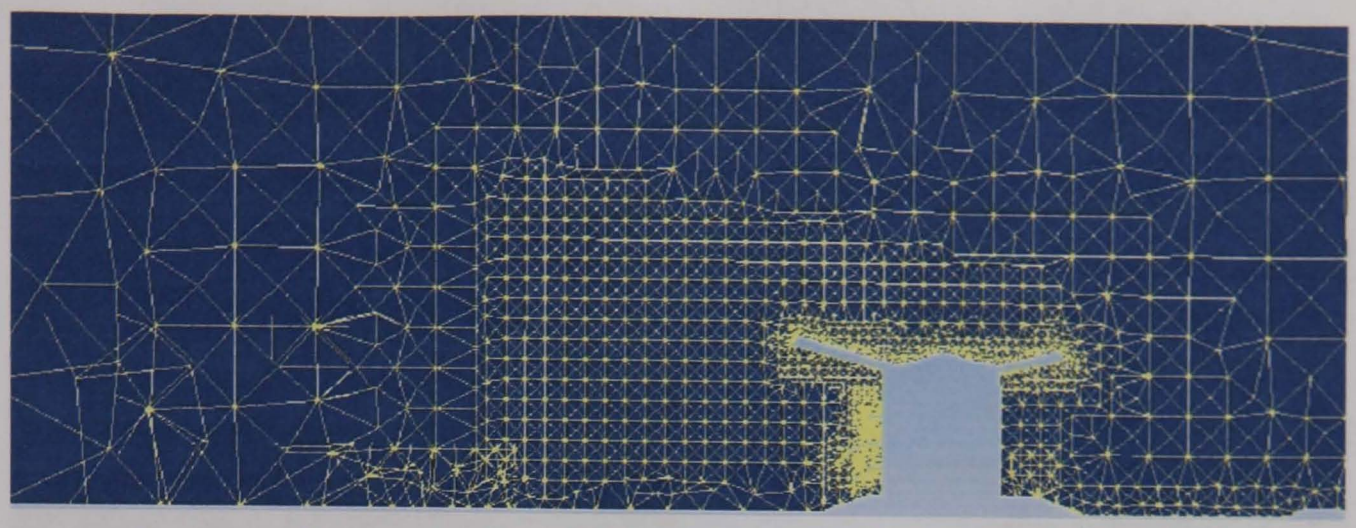

Figure 6-24: DES Mesh 1: side view on building and wake

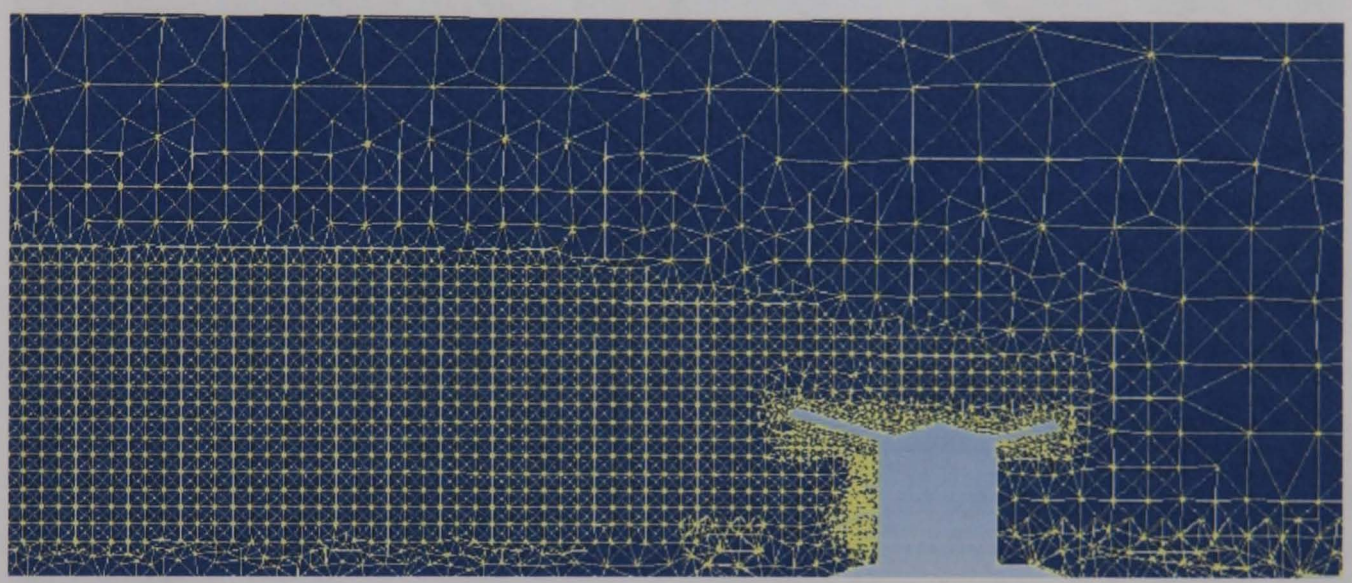

Figure 6-25: DES mesh 2 - side view on building

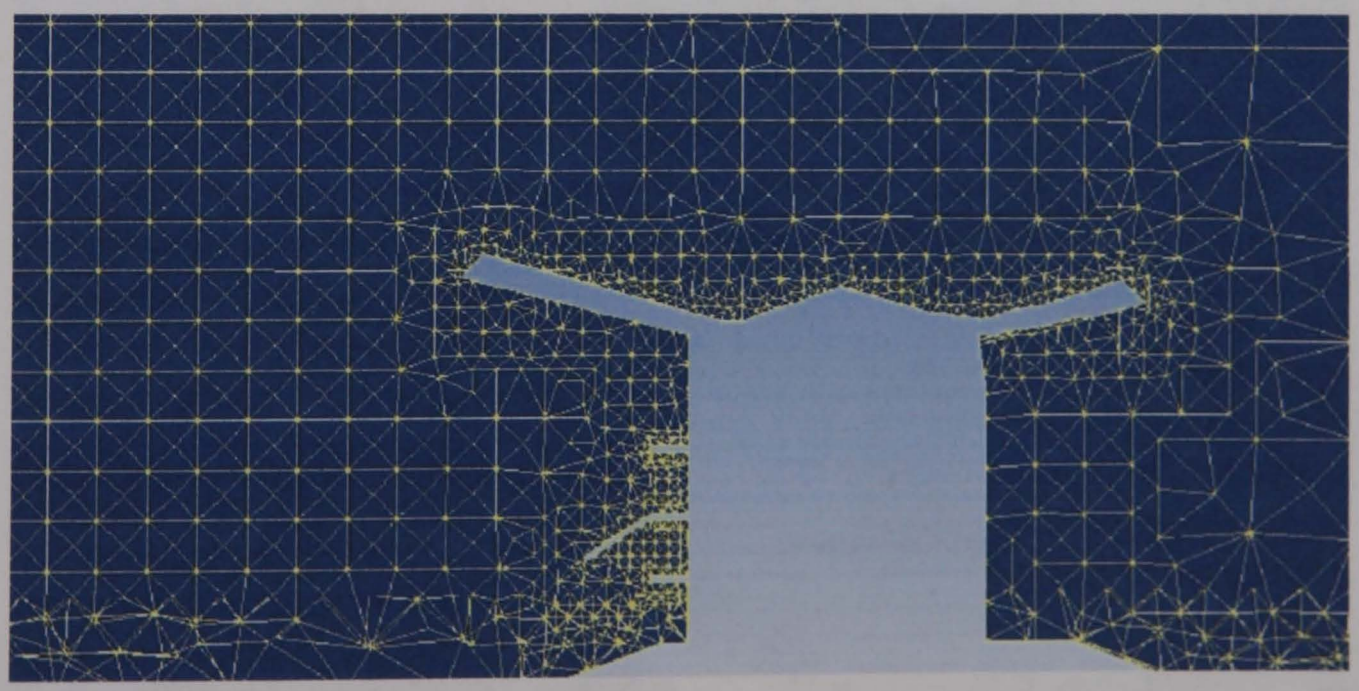

Figure 6-26: DES Mesh 1: mesh near building

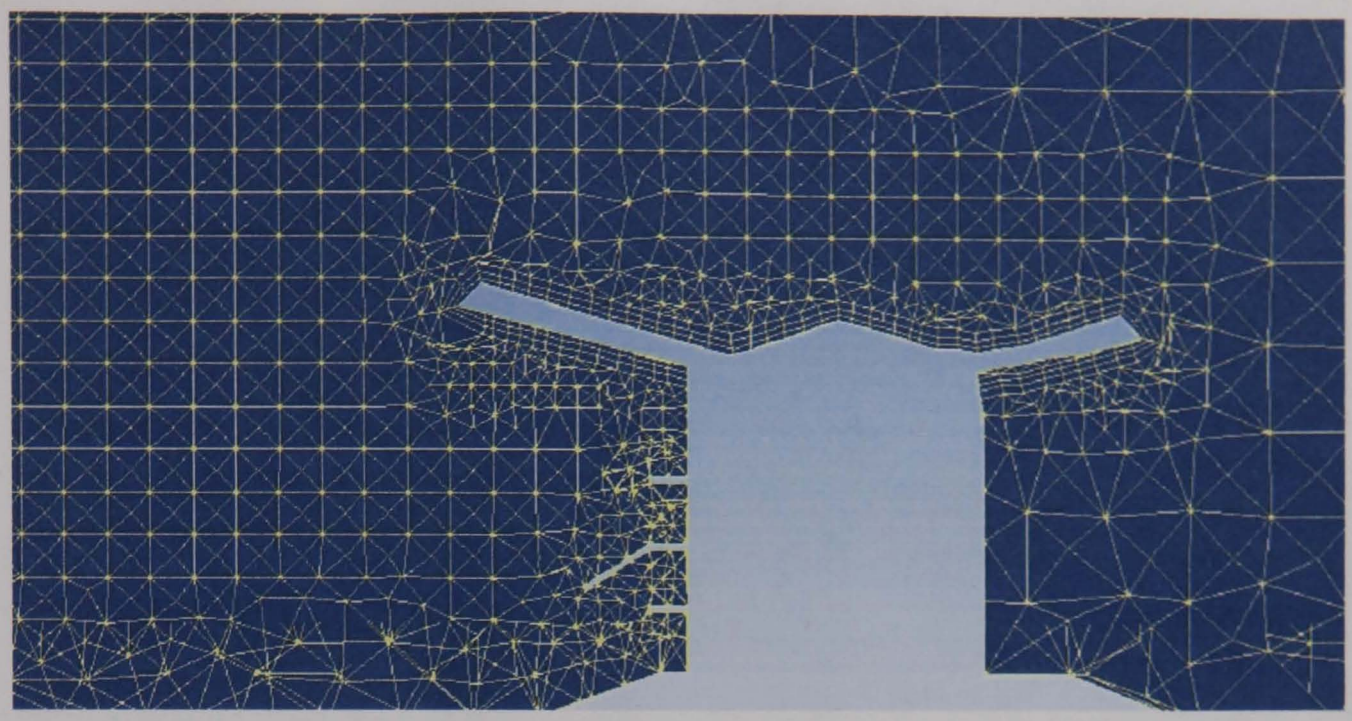

Figure 6-27: DES mesh 2: detail on building

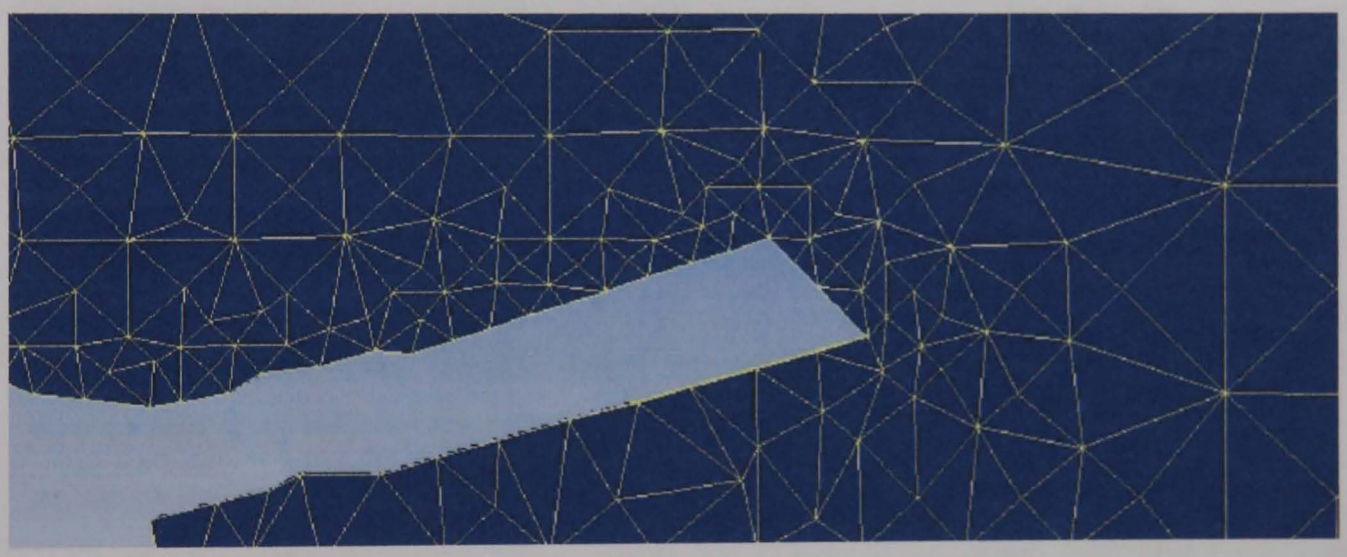

Figure 6-28: DES Mesh 1: detail on front eaves

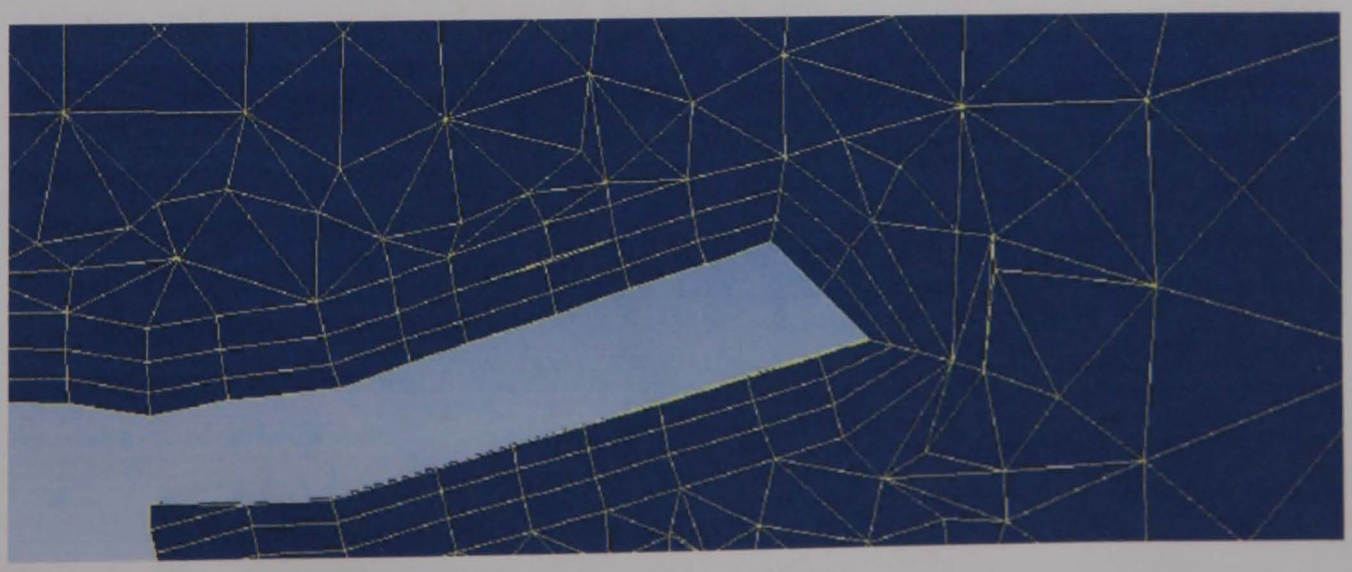

Figure 6-29: DES mesh 2: detail on leading edge

High resolution spatial discretisation and second order backwards Euler transient scheme where used. Again, convergence was hard to achieve, partly because of the challenges in producing a good quality mesh with such complex geometry. Significant amounts of time were put into building the mesh and then choosing an appropriate timestep. Once suitable convergence behaviour had been achieved the simulation had to be left to settle to an equilibrium state and then a sufficient number of simulations run to provide settled long term statistics. This required several thousand time steps, as opposed to several hundred for the unsteady RANS simulations.

y^+ values of less than 50 were achieved throughout with mesh 1, and generally less than 10 apart from the leading edge. y^+ values of less than 100 were achieved across the roof for mesh 2. These values are consistent with the use of wall laws but stretch the limits of applicability of the SST k-ω model used in the RANS portion of the flow.

Velocity Results

Experimental velocity results were only available for the empty wind tunnel but it is interesting to examine the spectrum of turbulence in the wake velocities for the transient RANS and DES cases (Figure 6-30). In both cases a complex spectrum of frequencies is present with the DES run showing some higher frequency content at more than 10Hz. The longest significant periods are near the length of the simulation time, suggesting that there could be some longer wavelengths fluctuations involved as well, although these were not of sufficient magnitude to invalidate the test for stationarity.

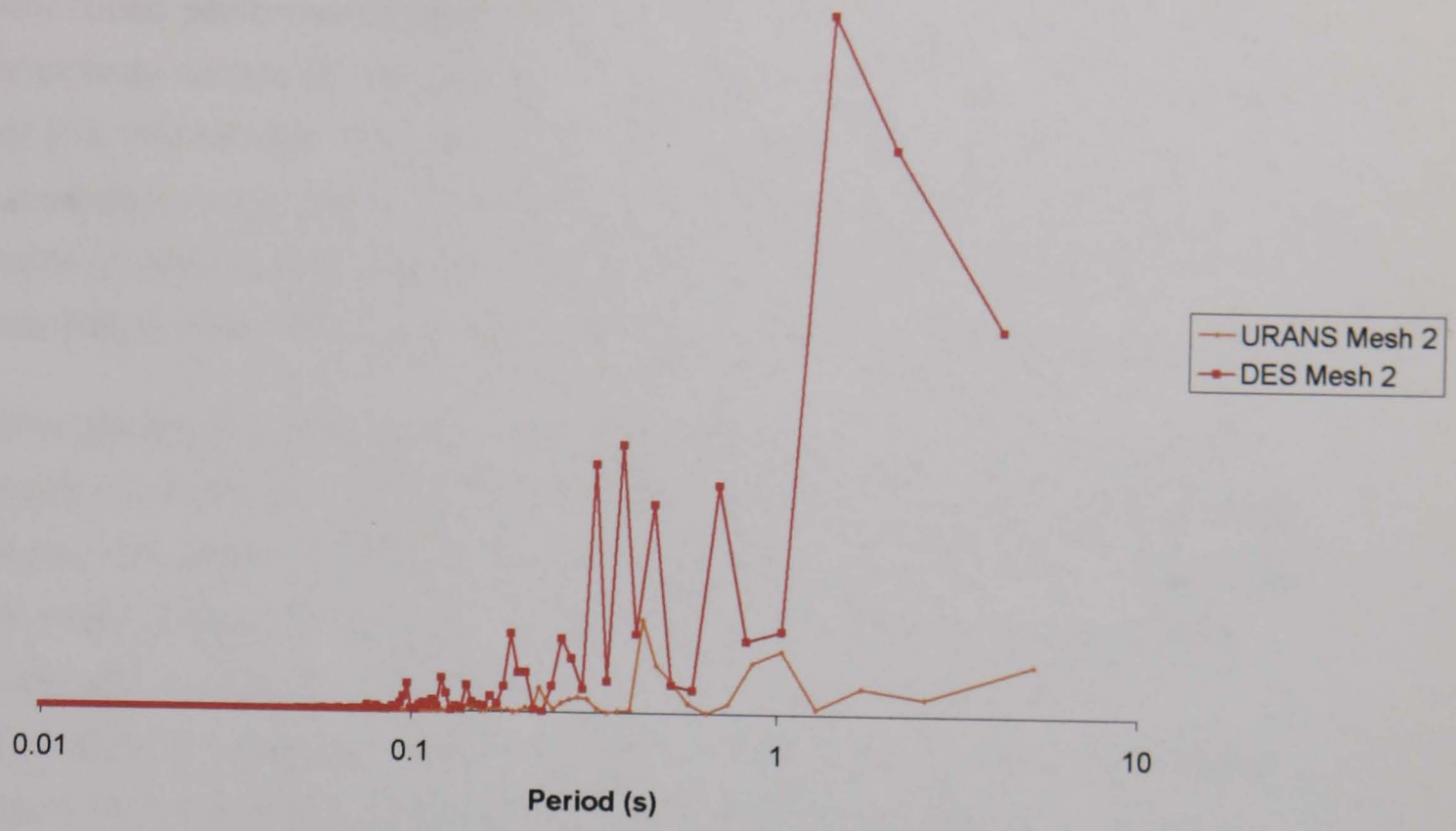

Figure 6-30, Spectral analysis of cross-stream velocities in the building wake from CFD simulations

Force on Large Sections of Roof

Simulation	Roof middle	Central bay
Wind Tunnel	0.88	0.384
Transient RANS: Mesh 1	0.39	0.188
Transient RANS: Mesh 2	0.36	0.170
DES Mesh 1	0.486	0.214
DES Mesh 2	0.502	0.221

Table 6-5: Force on roof sections in N (see Figure 6-13 for key)

Refinements in the unsteady RANS mesh resulted in some reduction in uplift force on the roof, increasing the underprediction.

Table 6-5 shows that the DES runs consistently produced stronger suction pressures over the roof than the Transient RANS simulations, possibly indicating a better separation prediction generally, as anticipated from the

improved performance of this model in predicting separation zones. The unsteady nature of the simulation may significantly increase entrainment of the free stream into the wake, increasing shear transfer into the separation zone and increasing suction pressures here. Enlarging the zone of mesh refinement in the wake and introducing an expanded boundary layer increased suction pressures on the roof by less than 5%.

The results are still significantly lower than those from the wind tunnel, showing a greater underprediction than that seen in the Silsoe Cube tests. Again the steady RANS solution (Table 6-4) can produce better predictions of mean pressures on the roof than the DES solution or unsteady RANS solutions (Table 6-5 and Table 6-6). However the steady RANS predictions have been shown to be highly dependent on CFD parameters such as mesh design, turbulence model and discretisation.

The wind tunnel measurements were performed such that force fluctuations on these large areas could be inferred by integration of the fluctuating pressure results. This method takes into account both the oncoming turbulence and building generated turbulence. The CFD results only allow building generated turbulence by vortex shedding to be included. The interaction between this local turbulence production and the large scale turbulence in the flow is not modelled.

Force on Panels: Central Bay

Although the DES model improves upon the unsteady RANS predictions, the pressure predictions are still far lower than those seen in the wind tunnel. Forces near the leading edge in particular are far lower than seen in the experiment, while results near the wake improve in accuracy.

A series of numbered panels along the roof centreline was chosen to represent loaded areas in the separation and reattachment zones, as shown in Figure 6-31.

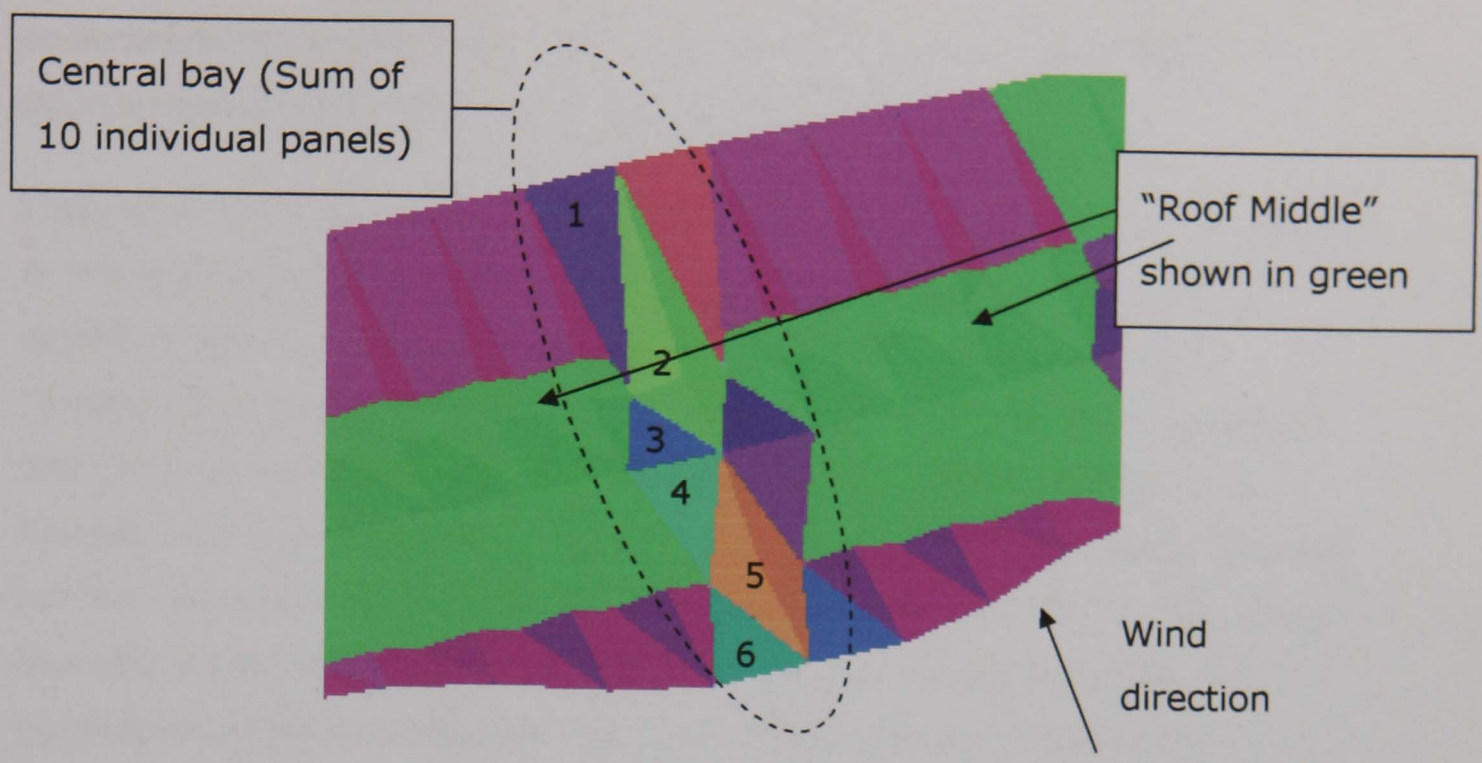

Figure 6-31: Central portion of grandstand roof: key to Table 6-6

	Panel 1	Panel 2	Panel 3	Panel 4	Panel 5	Panel 6
Wind Tunnel	0.021	0.049	0.018	0.03	0.092	0.048
Transient RANS: Mesh 1	0.027 +29%	0.038 -22%	0.01 -45%	0.013 -58%	0.025 -73%	0.013 -73%
Transient RANS: Mesh 2	0.024 +14%	0.032 -34%	0.009 -49%	0.011 -62%	0.022 -76%	0.012 -76%
DES: Mesh 1	0.026 +24%	0.041 -48%	0.013 -29%	0.016 -46%	0.029 -68%	0.016 -67%
DES: Mesh 2	0.025 +19%	0.040 -18%	0.012 -32%	0.017 -44%	0.033 -64%	0.019 -60%

Table 6-6: Mean force in N on individual roof panels near the roof centreline with percentage difference from wind tunnel results (see Figure 6-31 for key to panels)

Examining results for individual roof panels along the roof centreline (Table 6-6) shows that the results are much more accurate towards the rear of the roof than towards the leading edge. Results for panel 1 are overpredicted by 14-29% while results for panels 3 and 5 are

underpredicted by 60-76%. There is an average underprediction of approximately 40% relative to the wind tunnel results.

Looking at point loads for the second DES grid, point pressure fluctuations at the leading edge contain strong high frequency components with a period of around 0.34s with some lower frequencies (Figure 6-32). Trailing edge pressure fluctuations are dominated by lower frequencies of the order of 1 to 2 seconds, with some higher frequency components. Comparison with Figure 6-32 shows that the wake velocity fluctuations are further dominated by these lower vortex shedding frequencies, indicating that the higher frequency fluctuations formed at the leading edge separation point are being damped out moving back into the wake.

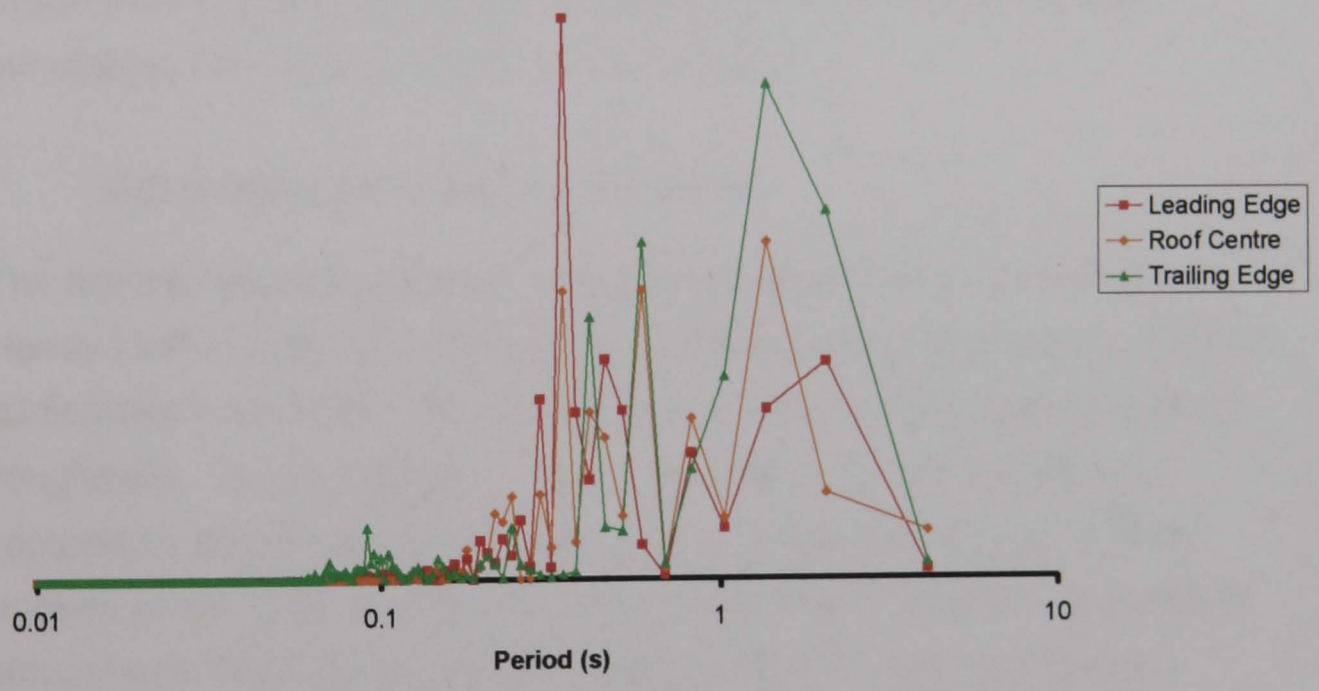

Figure 6-32: Spectral analysis for point pressures on the roof centreline from DES simulation

6.5. Discussion

The wind tunnel tests provide simulations of pressure loading under natural velocity and turbulence conditions. They account for non-correlation of forces across the building, requiring simulations of approximately 5 minutes for each wind direction. Pressures are provided

at discrete points on the building surface and then summed to calculate design loads. Typically, several hundred point pressures can be economically calculated for a building, limiting the extent of a single test. In this case it was only possible to instrument the roof of the building and one third of the building had to be separately tested. The complexity of the oncoming turbulent flow requires of the order of 10^5-10^6 instantaneous pressure readings for each tap.

In comparison, the CFD simulations reproduce natural mean velocity conditions and use turbulence models to represent the fluctuating component. Pressures can be calculated at a very large number of points but computational limitations mean that much shorter runs of the order 10^3-10^4 time steps may be the limit of what is currently practical. This has been shown to be sufficient to capture instability due to the flow around the building but is one of a number of barriers to directly simulating full-scale atmospheric turbulence.

6.5.1. Boundary Layer Simulation

The atmospheric boundary layer profile as described by Richards and Hoxey (1993) was not stable when combined with the standard RNG k-ε turbulence model and realistic approximations to the full-scale surface roughness. It was necessary to run the empty tunnel simulation repeatedly and iteratively to develop a stable profile which could be applied at the inlet for the simulations involving a building. A series of simulations must be run, typically requiring 5-10 well converged simulations of an empty domain. This process requires a significant amount of time and has a noticeable cost in computing time.

It was possible to generate a stable velocity and turbulence profile in the simulation domain. The velocity profile in particular was highly stable and when comparing the inlet boundary profile with the profile at the target location, the profiles were identical to within 2% from one building height upwards and within 5% from a third of a building height.

The turbulence profile was also highly stable with a change of less than 7% in turbulence kinetic energy values from the inlet to the target site.

6.5.2.Steady State Studies

As described above, the steady RANS calculations failed to converge to a satisfactory degree for a blend factor above 0.75. Up to that point, however, increasing discretisation accuracy resulted in steadily improving predictions of mean pressure coefficients and area forces. As the more accurate solutions result in more instability, a failure to converge and rapidly changing forces and pressures, clearly these steady RANS simulations do not represent a satisfactory solution to this flow problem.

The failure of the steady simulations suggests that significant vortex shedding instability exists in the flow on a scale which can be resolved by the computational grid. As the grid is refined the convergence problem increases as ever smaller instabilities fall into the realm of direct simulation.

6.5.3.Unsteady RANS and DES

Running an unsteady RANS simulation revealed complex large-scale fluctuations about a mean value but taking the mean of the time varying solution does not improve pressure predictions on the roof relative to the steady RANS predictions. On the contrary, the unsteady simulations systematically underpredict pressure in separation regions in a similar manner to that seen for the Silsoe cube.

Refining the mesh at this stage results in significant changes in local point pressure predictions, showing that a fully grid-independent solution has not been reached. Force predictions across the roof are consistent to within approximately 30% (Table 6-5 and Table 6-6) but are consistently lower than those predicted through wind tunnel testing. In most cases this underprediction increased as the transient RANS mesh was refined.

This suggests that further refining unsteady RANS simulations will not allow improved pressure predictions for such areas. DES simulation

appears to give a significant improvement in the prediction of mean forces but again a mesh-independent solution could not be obtained with current computer resources. Indeed, mesh independence cannot be achieved with LES and DES simulations as the mesh size acts as an explicit filter on the turbulent length scales resolved in the LES portion of the flow.

The DES results show slightly more complex unsteady behaviour with some higher frequencies involved. They show a slight improvement over unsteady RANS predictions but based on these results they do not appear to warrant the huge increase in computational power required.

Typically, higher frequencies were observed in the pressure fluctuations near the leading edge of the roof than near the wake. As the mesh size for this DES grid was deliberately kept constant across the building roof, this suggests that high frequency turbulence is being generated in the leading edge separation zone and then transmitted downstream where it excites lower frequency instabilities in the wake separation zone.

6.6. Conclusions

Moving up in complexity to the Ascot grandstand allows us to draw a number of additional detailed conclusions about the use of CFD in structural engineering as well as addressing some broader concerns.

6.6.1. Detailed Conclusions

- As with the Silsoe cube, steady RANS simulations do not converge sufficiently to give settled results for structural loading.
- Working at model scale results in a more uniform boundary layer as well as allowing sufficient refinement of the near-wall grid to meet the y^+ requirements of standard industrial turbulence models.
- Unsteady RANS solutions generally show reduced accuracy in pressure predictions from finer mesh resolution. Refining the RANS mesh appears to decrease suction pressures in the separation

region, possibly due to reduced numerical dispersion and therefore less entrainment of the free stream into the separation region.

- DES solutions appear to improve pressure predictions in the separation region, however further computational resources will be required if more detailed DES solutions are to be obtained. These results suggest that suction pressures are still underpredicted with DES simulations.

6.6.2. General Conclusions

The geometry and meshing capabilities of standard CFD software mean it is possible to attempt structural load predictions even for unusual building forms such as this. However there are a number of practical barriers to implementation as well as areas where the results are not sufficiently accurate for design, both of which are discussed below.

- Current software requires considerable time and effort to be placed into the early stages of geometry definition and mesh building. Mesh building in particular is an iterative process requiring convergence studies, and needing adjustment for the flow patterns found. Considerable improvements in automatic meshing will be required if CFD methods are to become competitive with wind tunnel testing and see wider use in structural engineering practice.

- Additional time is required for the selection of appropriate convergence criteria for the flow problem considered. More advanced convergence criteria based on point variable values would be a useful addition to standard CFD software.

7. Discussion and Conclusions

The Ascot building results highlight a number of limitations of CFD relative to wind tunnel testing for structural wind engineering. Given these results it is useful to return to the previous work on cubes and examine the extent to which CFD currently has a place in structural design and what developments will be needed if it is to take a more central role.

7.1. CFD Simulation for Bluff Bodies

The Silsoe cube chapter shows that the levels of convergence combined with relatively coarse meshes as used in many other engineering flow applications are not sufficient to predict the full range of pressures and forces required by structural engineers for the design of static bluff-bodies. A high degree of convergence is required with a carefully refined mesh and any relaxation of these requirements can result in very large changes in the results, possibly by a factor of 2 to 3.

Mesh refinement studies showed significant mesh dependence in some significant variables. Detailed pressure distributions were found to be highly dependent on the mesh design and degree of refinement. This means that mesh dependence studies must be performed for key variables in each new flow case and an assessment made of whether a sufficient degree of mesh independence can be achieved. For overall building loads and some local member forces this may be achieved with relatively coarse meshes while local pressure distributions may prove highly sensitive to meshing. Mesh refinement studies should be performed progressively, looking at the far-field to obtain a settled velocity and turbulence profile before going on to develop the mesh across the building surface and in the wake. This will necessarily result in a range of grid sizes within the domain, from fine meshes in areas of separation to coarser meshes in the wake and far field. LES and DES solutions present special grid resolution challenges discussed below.

If these requirements are met then net forces across the building can be predicted with an acceptable degree of accuracy, as can mean pressure

loads on some areas of a building. Notably the detailed pressure distribution on the front of the building is well predicted. Fluctuating pressure values and local forces in some areas cannot be accurately predicted.

Turbulence modelling is advancing rapidly but it is clearly not appropriate to model all of the turbulent length scales in these flows with a steady state simulation using a local turbulence model. Neither is it possible to directly represent all of the turbulent length scales in the flow through DNS so a proportion of the turbulence must be directly simulated and some accounted for in the local turbulence model.

Some portion of the local turbulence spectrum must therefore be filtered out and represented in the local turbulence model. However, LES methods use the grid size as the filter on local turbulence scale so the turbulent scales directly represented in the flow will vary with grid size through the domain. As discussed above, the grid size will vary considerably through the domain, resulting in a varying filter size and possible inconsistencies in the turbulence modelling.

The uniformity of the oncoming flow conditions used in these simulations can be seen to directly influence the results, giving rise to vortex shedding oscillations which are not damped out by the simulated turbulence. The lack of spectral information in the turbulence model means that there is insufficient interaction between modelled turbulence and directly simulated flow instabilities.

The use of time varying boundary conditions would allow some of these effects to be directly simulated. If all significant turbulent eddies could be resolved in the simulation then the remaining scales could be simulated through the turbulence model. This would certainly reduce the vortex shedding seen in these simulations, improving the mean and time-varying velocity and pressure predictions. This is expected to require detailed research work in how to best produce these boundary conditions and how to ensure the required flow statistics are maintained through the flow up to the building.

7.2. Prediction of Structural Loads

Previous work on the use of CFD in building aerodynamics has concentrated on the reproduction of experimental point pressure coefficients. This new work relates these values to the parameters used in structural design. Overall body forces, local member forces and point pressures are each considered in turn.

7.2.1. Overall Body Force

Steady RANS simulations have here been shown to be sufficiently accurate in the prediction of mean overall downwind forces for simple isolated structures. The error that does exist is mainly due to poor prediction of mean pressures on the rear face and as these are generally less than half of the pressures on the front face, this is within acceptable margins of error. For more complex or more streamlined bodies presenting a smaller face directly to the wind, net body forces are likely to be more strongly governed by the wake pressure. Mesh sensitivity studies will then be required to confirm the validity of the results.

The variation of body force with time can be predicted quasi-statically and codified methods used to account for non-simultaneous action of gusts across the building faces and between the front and back faces. This will result in an error in overall building force on the conservative (safe) side.

Time-varying simulations with non-steady boundary conditions would allow these effects to be simulated directly for the larger 2D turbulence, leaving codified methods to account for the smaller homogenous turbulence. However, there are many challenges in producing unsteady boundary conditions for CFD simulations which are stable through the domain and across multiple changes in grid scale.

Where the flow fields around multiple buildings interact, errors in wake and separation prediction from one building could significantly affect CFD results for the downstream buildings. Unsteady simulations with their improved prediction of wake separation would be required in these cases

and further validation work is needed to confirm the simulation requirements in such cases.

7.2.2. Force on Structural Members

Mean forces on individual structural members in the upwind stagnation region of the building can be calculated with an acceptable degree of accuracy. Again, the peak load can be calculated quasi-statically from mean results.

In the wake region, errors of up to 50% in pressure coefficient prediction are seen. These are typically present in conjunction with asymmetry and instability in the flow which is easily spotted with a symmetrical building but harder to discern for more unusual building types. Wake pressures are rarely critical to local member design as wind from another direction will typically generate stronger positive or negative pressures on the members in question but this could be a source of error for some flow conditions. This means that a detailed understanding of both the underlying flow patterns and the structural design requirements is required if CFD results are to be safely interpreted for structural design.

Peak member forces in the wake and to the sides can be calculated quasi-statically but building generated turbulence may have a significant effect near the leading edge and this is not adequately predicted by current methods. The magnitude and spectrum of turbulence fluctuations are both required if good design values are to be obtained.

7.2.3. Local Pressure Coefficients

Local pressure coefficients are again harder to predict accurately, particularly in regions of intense separation and high turbulence production. Better prediction of separation in turbulent flows and improved mathematical models of turbulence production are required if these effects are to be adequately resolved in CFD.

Until that time it is hard to see how CFD can be used to predict detailed cladding pressures for structures. Time-varying simulations for the Silsoe

Cube are shown to improve mean pressure predictions in some areas. Through quasi-static analysis these could take account of the upstream turbulence. However a significance formulation dependence has been found in mean and RMS suction pressures at the leading edge of a bluff body.

For simple buildings, it is possible to combine code of practice methods with CFD to predict local pressures but then may be little advantage to having performed the CFD simulation. For more complex buildings of the type generally considered in specialist wind engineering studies, code of practice methods are not so readily applicable. The CFD simulation can identify approximate zones of separation for simple buildings but where flow from one area interacts with another area of the building there would be insufficient confidence in the results.

7.3. Conclusions

This work shows that current CFD techniques can have a place in structural wind engineering if used with caution and with a thorough understanding of the limitations. CFD is not able to replace wind tunnels for general use in structural wind engineering and is not likely to do so in the foreseeable future. Until a method has been developed and validated for a variety of large-scale flow problems, the place of CFD in structural engineering may be in performing early design studies, visualising flow effects and possibly in examining detailed design issues in combination with wind tunnel testing. Within this broad conclusion, a number of specific conclusions can be drawn about individual CFD methods.

7.3.1. Detailed Conclusions

RANS Methods

- Steady RANS calculations underpredict turbulence generation on the cube boundary, resulting in an overly large recirculation region behind the cube. This has been shown to lead to an incorrect prediction of velocity, turbulence and mean pressure coefficients in the wake region.

Where one or more buildings are in the wake of another, this is likely to lead to errors in the oncoming flow for the downstream building(s).

- SST k-ω models give better predictions than k-ε models where the mesh can be sufficiently refined to allow convergence. However, this work has highlighted how the range of scales involved in structural wind engineering puts limits on the mesh design. This can make it impossible to achieve sufficient mesh resolution on all wall regions. The widespread use of this model in built environment applications would require the development and validation of improved wall treatments to allow coarser meshes or huge increases in computational power.

- Convergence can be hard to achieve with steady RANS calculations due to the inherent unsteadiness in bluff body flow. Use of low-order discretisation or coarse meshes can reduce this effect but non-physical asymmetry is still seen in the results.

- Unsteady RANS calculations improve the mean flow results, reducing asymmetry and reducing the overprediction of wake length, although the overprediction is still typically at least 100%.

LES and DES Methods

- DES solutions appear give generally improved pressure predictions in the separation region than RANS methods, however further computational resources will be required if more detailed DES solutions are to be obtained and the effects of grid resolution fully investigated. These results suggest that suction pressures are still underpredicted with DES simulations with steady boundary conditions

- This underprediction may be due to lack of entrainment of the free stream into the separation region. Transient simulation of the turbulent wake does not remove this underprediction.

7.3.2. Calculation of Structural Loads

Overall Building Loads

- CFD has been shown to accurately predict overall mean building forces for some isolated buildings, within the bounds of accuracy expected in structural wind engineering.

- Where there is significant interference from surrounding buildings, the uncertainties in predicting wake flow would result in errors in predicting the flow around downstream buildings. However for most structural engineering applications the direct effect of neighbouring buildings is neglected to allow for future changes in building layout. This effect would only be relevant where a large neighbouring building was likely to cause an increase in loading on the building studied.

Structural Member Forces

- Mean forces on structural members in the stagnation and wake region of an isolated building can be accurately calculated using RANS methods. For structural members located in separation regions such as the leading edge of the roof and side walls, errors in calculating the area and intensity of separation will result in significant errors in calculating member forces. The lack of accurate representation of the intensity and spectrum of turbulence production means that dynamic loading in these areas cannot be adequately assessed using current CFD techniques.

- Lack of detailed simulation of the spectrum and correlation of oncoming turbulence in the CFD results means that other methods must be used to calculate the attenuation of peak pressures in the stagnation and separation regions around the building. For instance, code of practice methods may be used to reduce the net force on large members due to non-correlation of gusts or to increase the response due to resonant effects.

Local Cladding Pressures

- CFD simulations allow qualitative prediction of separation and reattachment regions in a way that is easy to convey to the structural engineer. This can be useful in helping to understand the broad flow features around a building and understanding the locations of key separation regions and therefore high cladding loads.

- A significant formulation dependence has been found for peak cladding pressures. CFD methods are therefore not currently recommended for the calculation of peak structural cladding loads.

7.3.3. General Conclusions

Reviewing CFD methods by category:

- For an isolated building structure where the overall load is significantly affected by the oncoming wind conditions but not by surrounding buildings, RANS methods have been shown to give a reasonable approximation of the overall flow around the building. This can be used by experienced practitioners to inform design development and examine the effect of large scale changes in geometry.

- Steady RANS methods can predict mean flow features around an isolated cube in a qualitative sense, showing the recirculation region upstream of the cube leading to a horseshoe vortex around the base and the recirculation regions in the wake. Quantitatively the results are not of sufficient accuracy for structural wind engineering so CFD should not be relied upon as the sole design method.

- Further problems will be experienced for multiple buildings where errors in predicting the wake of one building will impact on the next building downstream. Unsteady flow features are clearly highly important both in their effect on the mean flow and in terms of peak pressures in separation regions.

- Unsteady RANS methods slightly improve on the mean flow prediction of steady state calculations but do not sufficiently capture the range of turbulence scales present in turbulent wakes and separation regions. While these methods may be of use in predicting mean flows and therefore estimating overall loads on isolated buildings, it is unlikely that RANS methods will ever produce accurate predictions of detailed structural loads for an arbitrary building shape.

- Until these key shortcomings are addressed, CFD should not be used in lieu of wind tunnel testing as the primary load calculation tool for structural engineering.

8. Recommendations for Future Work

Turbulence modelling is continuously developing but improved DES type turbulence models are needed for external flows, allowing for the transport of turbulence across different scale grids to represent the transmission of turbulence from the free stream into the area around the building and out into the separation region and the wake.

Further work is required in developing stable turbulence profiles for use in steady and unsteady RANS models. Current wall laws and turbulence model formulations do not provide stable boundary layers with full-scale turbulence values.

Improved modelling of separation is required including spectral information on turbulence generation, transport and destruction. This will require improved understanding of the physical processes involved in turbulence generation.

Coupled with this is the need for a better understanding of the physical structure of turbulent eddies and how this changes in the stagnation and separation regions of a bluff body. This will affect the levels of turbulence in these regions as well as the coherence of turbulent fluctuations.

Additional validation cases are needed for external bluff body flows, reducing the uncertainty in trying to match experimental results. At the small scale, good quality highly bounded cases such as the Martinuzzi cube should be produced giving mean and fluctuating pressure across the building. Recent advances in pressure tapping technology should make this easier and cheaper than in the past while digital storage and distribution should allow more comprehensive results to be published.

At full scale, testing methods should allow for the calculation of structural forces and overall building loads and these values should be presented in the published data. Pressure measurements should not be restricted to small areas as the correlation of pressures and therefore forces across the building is of great significance in calculating structural loads.

Similarly, CFD comparisons should look beyond mean pressure coefficients to examine peak structural load effects. This may be performed through gust factors predicted from mean and RMS values or may be calculated directly from longer time histories. Both of these present significant challenges as discussed previously in this document.

Future developments in CFD methods should aim for improved accuracy in predicting overall building loads, member forces and local pressures. Targeting the detailed prediction of mean pressure coefficients in particular areas may obstruct the development of useful design tools for industry. This may require greater input from the structural engineering industry in identifying the key design parameters and the degree of accuracy required. It is almost certain to require ongoing collaboration with the wind tunnel community where a great deal of practical wind engineering experience lies. However the complexity of the task means it is likely to require significant academic resources and experience covering both computational and experimental methods.

9. References

AIAA (1998). Guide for the Verification and Validation of Computational Fluid Dynamics Simulations. AIAA Pamphlet TB42 AIA, AIAA.

Alfonsi, G., C. Restano and L. Primavera. (2003). "Coherent structures of the flow around a surface-mounted cubic obstacle in turbulent channel flow." Journal of Wind Engineering and Industrial Aerodynamics 91: 495-511.

Baker, B. (1884). "The Forth Bridge." Engineering 38: 213-215, 223-225.

Bendat, J. S. and A. G. Piersol (1971). Random data: analysis and measurement procedures. New York, Wiley-Interscience.

Bilah, K. Y. and R. H. Scanlan (1991). "Resonance, Tacoma Narrows bridge failure, and undergraduate physics textbooks." American Journal of Physics 59(2): 118-124.

Blackmore, P. A. (1997). "The Role of wind tunnel testing in the design of building structures." Proc. Instn Civ. Engrs Structs & Bldgs 122: 253-265.

BMT (2003a). New Ascot Grand Stand Roof Load Alleviation Studies, BMT. commercial report (not published).

BMT (2003b). New Ascot Grand Stand Wind Tunnel Tests, BMT commercial report (not published).

BMT (2003c). New Ascot Grand Stand Wind Tunnel Tests – Cladding Studies, BMT commercial report (not published).

BMT (2003d). New Ascot Grand Stand Wind Tunnel Tests (Phase II), BMT commercial report (not published).

BRE (1994). BRE Digest 390: Wind Around Tall Buildings, BRE.

Browning (2004), 'Sting Jet': source of the most damaging winds in extra tropical cyclones, 6th UK conference on wind engineering, Cranfield University.

BSI (1972). Code of basic data for the design of buildings. CP3 Chapter V, Loading, Part 2 Wind loads.

BSI (2002). BS 6399-2:1997. Loading for Buildings - Part 2: Code of practice for wind loads, BSI.

BSI (2005), Eurocode 1: Actions on structures - Part 1-4: General actions - Wind actions. BS EN 1991-1-4:2005.

Castro, I. P. (2003). "CFD for External Aerodynamics in the Built Environment." The QNET-CFD Network Newsletter 2(2).

Castro, I.P.(2004) "Urban CFD – Single Building Issues and Implications", ERCOFTAC SIG.5 2nd European Workshop, University of Nottingham, September 9th-11th 2004.

CEN (2002). Draft prEN 1991-1-4.6:2002(E). Eurocode 1: Actions on structures, European Committee for Standardisation.

Cermak, J. E. (2003). "Wind-tunnel development and trends in applications to civil engineering." Journal of Wind Engineering and Industrial Aerodynamics 91: 355-370.

CFX (2003). CFX-5 User Documentation, version 5.6, Ansys CFX.

Chartered Institute of Building Services Engineers (CIBSE) (1999). Guide A: Environmental Design, London, CIBSE.

CIBSE (1998). Building Energy and Environmental Modelling, CIBSE.

Cook, M. J. and K. J. Lomas (1997). Guidance On The Use Of Computational Fluid Dynamics For Modelling Buoyancy Driven Flows. Building Simulation '97.

Cook, N. J. (1985). The designer's guide to wind loading of building structures Part 1: Background, Wind Data and Structural Classification, Thomas Telford.

Cook, N. J. (1990). The designer's guide to wind loading of building structures Volume 2: Static Structures, BRE, Butterworths.

Cremona, C. and Amandolese (2005). "Wind effect on structures: Numerical analysis of flow loading on bluff bodies" Structural Engineering International 15, no4: 252-257.

Deaves, D. M. and R. L. A. Harris (1978). A mathematical model of the structure of strong winds, CIRIA report 76. London, CIRIA.

Easom, G. (2000). Improved Turbulence models for Computational Wind Engineering. PhD Thesis. School of Civil Engineering, University of Nottingham.

Easom, G. and N. G. Wright (2001). "Development and Validation of a Non-linear k-e Model for Flow over a Full-scale Building." Journal of Wind and Structures 4(3): 177-196.

Eiffel, G. (1900). Travaux scientifiques exécutés à la tour de trois cents mètres de 1890 - 1900, Maretheux.

ENV1991-1-4 :2005. Eurocode 1: Actions on structures — Part 1-4: General actions — Wind actions, BSI.

ERCOFTAC (2000). Special Interest Group on "Quality and Trust in Industrial CFD": Best Practice Guidelines Version 1.0, ERCOFTAC SIG.

ESDU (1993) Data Item 84011 - Wind Speed Profiles over Terrain with Roughness Changes, Engineering Sciences Data Unit.

Fawcett, N. S. J. (1991). Getting started with CFD. Computational Fluid Dynamics - Tool or Toy? Institution of Mechanical Engineers, IMechE.

Ferziger, J. H. (1993). Simulation of complex turbulent flows: recent advances and prospects in wind engineering. Computational Wind Engineering I. S. Murakami. Amsterdam, Elsevier: 195-212.

Ferziger, J.H. and M. Peric, Computational Methods for Fluid Dynamics, 3rd revised edition, Springer-Verlaq.

Fothergill, C. E., P. T. Roberts and A.R.Packwood. (2002). "Flow and dispersion around storage tanks. A comparison between numerical and wind tunnel simulations." Wind and Structures 5(2-4): 89-100.

Franke, J., C. Hirsch, A.G.Jenson, H.W.Krus, M.Schatzmann, P.S.Westbury, S.D.Miles, J.A.Wisse and N.G.Wright. (2004). Recommendations on the use of CFD in wind engineering. COST Action C14: Urban wind engineering and industrial aerodynamics, Rhode-St-Genese, Belgium.

Hansford, M. (2002). "Wind of Change." New Civil Engineer.

Holmes, J. D. (2002). "Effective static load distributions in wind engineering." Journal of Wind Engineering and Industrial Aerodynamics 90: 91-109.

Holmes, J.D. and C. Osonphasop (1983). "Flow behind two-dimensional barriers on a roughened ground plane, and applications for atmospheric boundary layer modelling". Proc. 8th Australasian Fluid Mechanics Conference, 1983.

Hoxey, R.P. and P. Moran "Full scale wind pressure and load experiments - single span 7.0 x 22.6 m glasshouse.", AFRC. Institute of Engineering Research. Process Engineering Division.

Hoxey, R. P. and P. J. Richards. (1993). "Appropriate boundary conditions for computational wind engineering models using the k- epsilon turbulence model." Journal of Wind Engineering and Industrial Aerodynamics. 46-47: 145-153.

Hoxey, R. P., P. J. Richards, et al. (2002). "A 6m cube in an atmospheric boundary layer flow Part 1. Full-Scale and wind tunnel results." Wind and Structures 5 No.2: 165-176.

IStructE (2002). Guidelines for the use of computers for engineering calculations, IStructE.

Jensen, M. (1958). "The model law for phenomena in natural wind." IngeniØren 2: 121-128.

JFE (1993). Journal of Fluids Engineering Databank entry DB93-085.

Jiang, Y., D. Alexander, et al. (2003). "Natural ventilation in buildings: measurement in a wind tunnel and numerical simulation with large-eddy simulation." Journal of Wind Engineering and Industrial Aerodynamics 91: 331-353.

Kasperski, M. and H.-J. Niemann (1992). "The LRC (load-response-correlation) method: a general method of estimating unfavourable wind distributions for linear and nonlinear structural behaviour." Journal of Wind Engineering and Industrial Aerodynamics 43: 1753-1763.

Knapp, G. A., N. G. Wright, et al. (2003). Comparison of Full-Scale and CFD Results for the Silsoe 6m Cube. Eleventh International Conference of Wind Engineering, Lubbock, Texas.

Lakehal, D and W. Rodi (1997). "Calculation of the flow past a surface-mounted cube with two-layer turbulence models". Journal of Wind Engineering and Industrial Aerodynamics 67&68: 65-78.

Laveville, A. and C.D. Williams (1979). "The effect of intensity and large-scale turbulence on the mean pressure and drag coefficients of 2D rectangular cylinders." Wind engineering: proceedings of the fifth international conference, Fort Collins, Colorado, USA, July 1979: 397-404.

Larousse, A., R. Martinuzzi, et al. (1991). Flow Around Surface-Mounted, Three-Dimensional Obstacles. Proc. 8th Symposium on Turbulent Shear Flows, Munich.

Layton, W. J. (2002). "A Mathematical Introduction to Large Eddy Simulation. Pittsburgh", Computational Fluid Dynamics – Multiscale Methods (H.Deconinck, editor), Von Karman Institute for Fluid Dynamics, Belgium, 2002.

Lyn, D., Einav, S., Rodi, W., Park, J.H., 1995. "A laser-Doppler velocimetry study of ensemble averaged characteristics of the turbulent near wake of a square cylinder". Journal of Fluid Mechanics 304: 285–319.

Martin, T. J. and I. A. MacLeod (1995). "The Tay rail bridge disaster - A reappraisal based on modern analysis methods." Proc. Instn Cv. Engrs 108: 77-83.

Martinuzzi, R. and C. Tropea (1993). "The flow around a surface-mounted prismatic obstacle placed in a fully-developed channel flow." Journal of Fluids Engineering 115: 85-92.

Melbourne, W. H. (1978). "Criteria for Environmental Wind Conditions." Journal of Industrial Aerodynamics 3: 241-249.

Meinders, E. (1998). Experimental study of heat transfer in turbulent flows over wall-mounted cubes. Ph.D. Thesis, Delft University of Technology.

Menter, F.R. (1993) Zonal Two Equation k-ω Turbulence Models for Aerodynamic Flows, AIAA paper 93-2906.

Menter, F. R. and M. Kuntz (2003). Development and application of a zonal DES model for CFX-5, CFX Ltd.

Meroney, R. N., D. E. Neff, et al. (2002). Computational Fluid dynamics and physical model comparisons of wind loads and pedestrian comfort around a high rise building. Proceedings of the 2002 structures congress, AMCE.

Miles, S. D. and P. S. Westbury (2002). Assessing CFD as a Tool for Practical Wind Engineering Applications. 5th UK Conference on Wind Engineering, University of Nottingham, WES.

Montavon, C., Y. L. Sinai, et al. (2000). Review of applications of the CFX software to environmental flows - Case studies. 93rd Annual Meeting of the Air & Waste Management Association, Salt Lake City, AWMA.

Moran, P. and R. P. Hoxey (1979). "A probe for sensing static pressure in two-dimensional flow." J. Phs. E: Sci. Instrum. 12: 752-753.

Morgenthal, G. and A. McRobie (2002). "A comparative study of numerical methods for fluid structure interaction analysis in long-span bridge design." Wind and Structures 5(2-4): 101-114.

Morteza, A. M., P. E. Torkamani, et al. (2002). Modeling tall buildings for wind excitation. Proceedings of the 2002 structures congress.

Morvan, H. (2005). "Automating CFD for non-experts." Journal of Hydroinformatics 7: 17-29.

Morvan, H., P. Stangroom et al. (2007). Automated CFD Analysis for Multiple Directions of Wind Flow over Terrain. Wind and Structures 10 (2).

Newberry, C. W., K. J. Eaton, et al. (1968). Wind loading of a tall building in an urban environment. BRS paper, BRS.

Oliveira, P.J. and B.A. Younis (2000). "On the prediction of turbulent flows around full-scale buildings" Journal of Wind Engineering and Industrial Aerodynamics 86 (2000): 203-220.

Prevezer, T. and J. Holding (2002). "Bluff body asymmetric flow phenomenon - real effect or solver artefact?" Wind and Structures 5(2-4): 359-368.

QNET (2002). UFR3-14 Surface Mounted Cube in a Channel, QNET.

Richards, P. J., B. D. Connell, et al. (2004). Separating 2D and 3D turbulence - Implications for wind tunnel and CFD modelling. 6th UK conference on wind engineering, Cranfield University.

Richards, P. J. and R.P. Hoxey (1993) "Appropriate boundary conditions for computational wind engineering models using the k-ε turbulence model", Journal of Wind Engineering and Industrial Aerodynamics, Volumes 46-47, August 1993: 145-153.

Richards, P. J., A. D. Quinn, et al. (2002). "A 6m cube in an atmospheric boundary layer flow Part 2. Computational solutions." Wind and Structures 5 No.2: 177-192.

Roach, P.J. Verification and Validation in Computational Science and Engineering, Hermosa Publishers, 1998

Robins, A. G. and I. P. Castro (1977a). "A wind tunnel investigation of plume dispersion in the vicinity of a surface mounted cube - I. The flow field." Atmospheric Environment 11: 291-297.

Robins, A. G. and I. P. Castro (1977b). "A wind tunnel investigation of plume dispersion in the vicinity of a surface mounted cube - II. The concentration field." Atmospheric Environment 11: 299-311.

Rodi, W. (1997). "Comparison of LES and RANS Calculations of the Flow around Bluff Bodies." Journal of Wind Engineering and Industrial Aerodynamics 69-71: 55-75.

Scanlon, T. J. (1997). A Numerical Analysis of Flow and Dispersion around a Cube. Fifth International Conference of the International Building Performance Simulation Association, September 8-10 1997, Prague, Czech Republic.

Schmidt, S. and F. Thiele (2002). "Comparison of numerical methods applied to the flow over wall-mounted cubes." International Journal of Heat and Fluid Flow 23: 330-339.

SCI (1995). Modelling of Steel Structures for Computer Analysis, SCI.

Setrakian, A. A., D. J. McLean, et al. (1991). Applications of Computational Fluid Dynamics in Building Services Engineering. Computational Fluid Dynamics - Tool or Toy? Institution of Mechanical Engineers, IMechE.

Sharma, R. N. and P. J. Richards (2004). "The multi-stage process of windward wall pressure admittance." Journal of Wind Engineering and Industrial Aerodynamics 92: 1191-1218.

Simiu, E. and R. H. Scanlan (1996). Chapter 7: Wind Tunnels. Wind Effects on Structures. Fundamentals and Application to Design, Wiley-Interscience.

Solari, G. (2002). "The role of analytical methods for evaluating the wind-induced response of structures." Journal of Wind Engineering and Industrial Aerodynamics 90: 1453–1477.

Spalart, P. R. (2001). Young-Person's Guide to Detached-Eddy Simulation Grids, NASA.

Spalart, P. R., W.-H. Jou, et al. (1997). Comments on the feasibility of LES for wings, and on a hybrid RANS/LES approach. Advances in DNS/LES. C. Liu, Liu, Z., Greyden Press.

SRI (2000), CWE 2000 Competition CD, CD ROM, 25/01/2000 V3.2 Silsoe Research Institute.

Stangroom, P. and N. G. Wright (2003). CFD modelling of the Askervein Hill. 11th International Conference of Wind Engineering, Lubbock, Texas.

Stangroom, Paul (2004). CFD modelling of wind flow over terrain. PhD thesis, University of Nottingham.

Staples, C and Penrose (2000). Fluid-structure interactions: coupling of CFD and FE stress analysis. CFX Update No 19, Autumn 2000.

Stathopoulos, T. (1997). "Computational Wind Engineering: Past Achievments and Future Challenges." Journal of Wind Engineering and Industrial Aerodynamics 67&68: 509-532.

Stathopoulos, T. (2002). "The numerical wind tunnel for industrial aerodynamics: real or virtual in the new millennium?" Wind and Structures 5(2-4): 193-208.

Sterling, M., C.J.Baker et al.(2005). "Pressure and Velocity Fluctuations in the Atmospheric Boundary Layer." Wind and Structures 8(1): 13-34.

Straw, M.P. (2000) Computation and Measurement of Wind Induced Ventilation, PhD Thesis, University of Nottingham.

Strelets, M. (2001). Detached eddy simulation of massively separated flows, AIAA.

Sun, D., N. G. Wright, et al. (2005). Identification of 18 flutter derivatives using CFD turbulence modelling. EACWE, Prague.

Thomas, T. G. and J. J. R. Williams (1999). "Simulation of Skewed Turbulent Flow Past a Surface Mounted Cube." Journal of Wind Engineering and Industrial Aerodynamics 81: 347-360.

Versteeg and Malalaskera (1995). An Introduction to Computational Fluid Dynamics: The Finite Volume Method, Prentice Hall.

Wright, N. G. (2004). Appropriate use of computational wind engineering. Proc. 2004 Structures Congress, May 22-26, 2004, Nashville, Tennessee.

Yang, T. (2004. CFD and Field Testing of a Naturally Ventilated Full-Scale Building. PhD Thesis, University of Nottingham.

Appendix A: Wind Load Calculations to BS 6299 Part 2:1997

	The University of Nottingham		
	The 6m Cube at Silsoe Research Institute		
	Wind Load Calculations to BS 6399 Part 2	*GAK*	*September-05*
	Wind Normal to a face		

Wind Load Calculations to BS6399-2:1997, incl. Amendment 1 and Corrigendum 1

Pressure Coefficients

The directional method is used to determine the pressure coefficients for greater accuracy

Walls

B	*6 m*	*Crosswind breadth*	*fig 2*
D	*6 m*	*Inward Depth*	*fig 2*
b	*6 m*	*scaling length*	*3.3.1.1.2*
Gap to nearest building is greater than b, therefore no funnelling			*3.3.1.1.3*
D/H	*1*		
Windward Face		*θ = 0*	
Zone A	*0.7*	*extends 1.2m from either side of the building*	*Table 26*
Zone B	*0.83*	*elsewhere*	
Side faces		*θ = 90*	
Zone A	*-1.3*	*extends 1.2m from the front face of the building*	*Table 26*
Zone B	*-0.8*	*elsewhere*	
Rear Face		*θ = 180*	
Zone A	*-0.34*	*extends 1.2m from either side of the building*	*Table 26*
Zone B	*-0.24*	*elsewhere*	

Roof	*bw=bl=6*	*3.3.3.2.1*
Zone A	*-1.47*	*Table 30*
Zone B	*-1.25*	
Zone C	*-1.15*	
Zone D	*n/a*	
Zone E	*-0.69*	
Zone F	*n/a*	
Zone G	*±0.2*	

Appendix B: Wind Load Calculations to Draft prEN 1991-1-4.6:2002(E)

The University of Nottingham		
The 6m Cube at Silsoe Research Institute		
Wind Load Calculations to Eurocode 1 part 1.4	*GAK*	*September-02*
Wind Normal to a face		

Pressure Coefficients

The directional method is used to determine the pressure coefficients for greater accuracy

Walls

h	*6 m*	*height*
d	*6 m*	*depth*
b	*6 m*	*breadth*

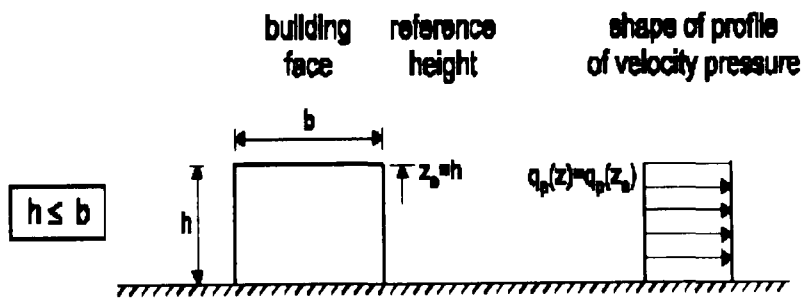

z	*6*	*reference height*	
e	*6*	*m*	*lesser of b or 2h*

Windward Face $\theta = 0$

	Cpe10	*Cpe1*	
everywhere	*0.8*	*1*	

Side faces $\theta = 90$

	Cpe10	*Cpe1*	
Zone A	*-1.2*	*-1.4*	*1.2m from front face c*
Zone B	*-0.8*	*-1.1*	*elsewhere*

Rear Face $\theta = 180$

	Cpe10	*Cpe1*
everywhere	*-0.5*	*-0.5*

Roof

	Cpe10	*Cpe1*
Zone F	*-1.8*	*-2.5*
Zone G	*-1.2*	*-2*
Zone H	*-0.7*	*-1.2*
Zone I	*±0.2*	*±0.2*